THE ANTI-PROLIFERATIVE ACTIVITY OF *DRIMIA ALTISSIMA* AND A NOVEL ISOLATED FLAVONOID GLYCOSIDE AGAINST HELA CERVICAL CANCER CELLS

M.N. NYAMBE

April 2019

NELSON MANDELA UNIVERSITY

THE ANTI-PROLIFERATIVE ACTIVITY OF *DRIMIA ALTISSIMA* AND A NOVEL ISOLATED FLAVONOID GLYCOSIDE AGAINST HELA CERVICAL CANCER CELLS

By

Mutenta Nsokolo, Nyambe

Submitted in fulfilment of the requirements for the degree of *Philosophiae Doctor* in the Faculty of Health Sciences at the Nelson Mandela University

April 2019

Supervisor: Prof. Maryna van de Venter
Co-Supervisor: Dr. Buyiswa Hlangothi
Co-Supervisor: Prof. Nanette Smith

DECLARATION

I, Mutenta Nsokolo Nyambe (s214232840), hereby declare that the thesis for *Philosophiae Doctor* (General Health Sciences) to be awarded is my own work and that it has not previously been submitted for assessment or completion of any postgraduate qualification to another University or for another qualification.

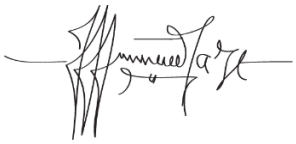

.....

Mutenta Nsokolo Nyambe

Official use:

In accordance with Rule G5.6.3,

5.6.3 A treatise/dissertation/thesis must be accompanied by a written declaration on the part of the candidate to the effect that it is his/her own work and that it has not previously been submitted for assessment to another University or for another qualification. However, material from publications by the candidate may be embodied in a treatise/dissertation/thesis.

Dedication

To my Beloved Wife, Chembo Mwape Nyambe

for always sticking by my side through thick and thin

Acknowledgements

To my first and only, Lord, Saviour and friend, Jesus Christ: I am so grateful to you for walking with me through the meandering and often painful process of my PhD and miraculously coming through for me during my 'just give-up' moments. Because of your absolute perfection all things have worked out for my good.

To my supervisor, Prof. Maryna van de Venter: I am truly indebted to you for being more than just my promoter. It is through your kindness, understanding, encouragement and steadfast belief in me that this work has come to fruition. Your motherliness has taught me lessons way beyond science.

To my co-supervisor, Dr. Buyiswa Hlangothi: Thank you for your impeccable guidance and for exercising patience during my bouts of stubbornness. I am grateful to you for teaching me the ropes of natural products research and for being a source of spiritual motivation.

To my wife, Chex: Oh what would I do without you? God knew it when He paired a procrastinator (me) with a perfectionist (you). Thank you so much for being strong for me and for being so understanding during my long and unbearable absence. You will always be my source of inner strength and the reason why I get up and fight. I love you!

To Prof. Denzil R. Beukes, Associate Professor at the University of the Western Cape: Thank you for assisting me with NMR structural characterization and for showing me that you will always be the chemistry 'boss'.

To the African Laser Center (ALC) for funding the research.

To the Nelson Mandela University Postgraduate Research Scholarship (PGRS) and HA Taylor Will Trust for funding.

To Prof. Sekazi K. Mtingwa, co-founder, African Laser Center (ALC), for giving me a great assistance at a dire point of my research.

To Dr. Abimbola Sowemimo, Associate Professor from the Department of Pharmacognosy, University of Lagos, for donating plant extracts for screening.

To the Central Analytical Facility (CAF) at the University of Stellenbosch for performing LC/MS spectrometry and Circular Dichroism (CD) spectroscopy experiments.

To Mr. Anthony P. Dold, a curator and taxonomist at Selmar Schonland Herbarium (GRA) in Makhanda, Eastern Cape, South Africa for plant authentication.

To Mr. Bresler Swanepoel for assistance with High Content Analysis (HCA) experiments.

To Mr. William Fewell for assistance with *in silico* molecular docking studies.

To Mr. Kenneth Oosthuizen for assistance with laboratory supplies.

To Mr. Mofo Setloboko, Senior analytical Chemist at InnoVenton for assistance with sample freeze drying.

To Prof. Vaughan Oosthuizen, Associate Professor, Department of Biochemistry and Microbiology, Nelson Mandela University for assistance with HPLC.

To Mr. Jean Ngororabanga (JMV) for assistance with melting point experiments.

To my chemistry lab mates: Mondeli Mngoma, Nehemiah Latolla (Nemo) and Lungelwa Mahanjana for adding a humorous touch to a rather serious learning environment.

To my MNRG lab mates for teaching me cell culture techniques and for selflessly donating their precious HeLa cells when I had so frequently contaminated mine.

To my dear friends: Mrs. Kina Muller for emotional and moral support; my mischievous mate Sendibitiyosi Gandidzanwa for companionship and helping me to distress with FIFA, though we often overdid it; my roommate Asane Talla for sharing with me a brotherhood that defies religious and international boundaries; and my confidant Disang Lekutlane for being there when I needed a friend and for sharing with me the hope that there is an even brighter life beyond our struggles.

To my family members for constant belief and prayers.

Table of Contents

List of Figures

List of Schemes

List of Tables

List of Abbreviations

ΔΨm	change in mitochondrial membrane potential
µg/mL	micrograms per milliliter
µM	micromolar
^{13}C NMR	Carbon Nuclear Magnetic Resonance Spectroscopy
^{1}H NMR	Proton Nuclear Magnetic Resonance Spectroscopy
ABTS	2,2′-Azinobis-(3-ethylbenzthiazoline-6-sulfonic acid)
ADP	adenosine diphosphate
Apaf-1	apoptosis proteinase activating factor-1
Bcl-2	B cell lymphoma 2
bp	base pair
BuOH	butanol
CADD	computer aided drug design
CAM	Compound Activity Mapping
CARD	N-terminal caspase recruitment domain
CD	Circular Dichroism
CD_3OD	deuterated methanol
Cdc	Cell division control protein
cdc25C	cell division cycle 25C
CDK 1 (Cdc2)	Cyclin-dependent kinase 1
CDK	Cyclin-dependent kinase
CED	cell-death defective worm mutants
CIN	cervical intraepithelial neoplasia
CKI	cyclin-dependent kinase inhibitors
CO_2	carbon dioxide
Cyto C	cytochrome *c*

d	Doublet
Da	Daltons
DAPI	4′,6-diamidino-2-phenylindole
dATP	deoxyadenosine triphosphate
dd	doublet doublet
DMSO	dimethyl sulfoxide
DNA	deoxyribonucleic acid
EtOAc	ethyl acetate
EtOH	ethanol
FBS	Fetal Bovine Serum
FLIP	FLICE-like inhibitory protein
FT-IR	Fourier-Transform Infrared
GLOBOCAN	Global Cancer Incidence, Mortality and Prevalence
h	hour(s)
H_2O	water
hAR	Human aldose reductase
HCA	High Content Analysis
HeLa	Cervical carcinoma cell line obtained from Henrietta Lacks
Hex	hexane
HIV	Human Immunodeficiency Virus
HMBC	Heteronuclear Multiple Bond Correlation
Hoechst 33342	bisBenzamide H 33342 trihydrochloride
HPV	Human Papilloma virus
HR-MS	high resolution mass spectrometry
HSQC	heteronuclear single quantum coherence
HTS	High-Throughput-Screening

Hz	hertz
IARC	International Agency for Research on Cancer
IC_{50}	50% Inhibitory Concentration
ICC	invasive cervical cancer
INDELs	insertions and deletions
J	Spin-spin Coupling Constant
kDa	KiloDalton
LC	Liquid Chromatography
LEEP	loop electrosurgical excision procedure
m	multiplet
m/z	mass to charge ratio
MDM2	Mouse double minute 2 homolog
MeOH	methanol
MHz	Megahertz
MS	Mass Spectrometry
MTT	3-(4,5-dimethylthiazol-2-yl)-2,5-diphenyl tetrazolium
Mult	multiplicity
n.d.	not determined
nm	nanometers
NMR	Nuclear Magnetic Resonance spectroscopy
NP	natural product
NucRed	NucRed™ Live 647
ºC	Degrees Celsius
PCD	Programmed Cell Death
PI	propidium iodide
ppm	Parts per million

pRb	Retinoblastoma protein
q	Quartet
RNA	ribonucleic acid
RPMI 1640	Roswell Park Memorial Institute 1640
s	singlet
SD	standard deviation
SEA	Similarity Ensemble Approach
Smac/DIABLO	second mitochondria-derived activator of caspases
TLC	Thin Layer Chromatography
TMRE	tetramethylrhodamine ethyl ester
TNF	Tumor necrosis factor
TOCSY	Total Correlated Spectroscopy
TRAIL	Tumor necrosis factor related apoptosis-inducing ligand
UV	ultraviolet
WHO	World Health Organization
δ	Chemical shift (ppm)
λ	Lambda

Abstract

Cancer is one of the leading causes of mortality worldwide. About 44% of all cancer morbidity and 53% of all cancer mortality occur in countries with a low to medium Human Development Index (HDI). Thus, cancer is rapidly emerging as a serious threat to public health in Africa and most especially, sub-Saharan Africa. The International Agency for Research on Cancer (IARC) projects that there will be 1.28 million new cancer cases and 970 000 cancer deaths in Africa by the year 2030 owing to the increase in economic development associated lifestyles. The dominant types of cancer in Africa are those related to infectious diseases such as Kaposi's sarcoma and cervical, hepatic and urinary bladder carcinomas. The main challenge to cancer treatment in Africa is the unavailability of efficacious anticancer drugs. This is because most developing countries can only afford to procure the most basic anticancer drugs, which are also frequently unavailable due to intermittent supplies. This results in patients progressing to more advanced cancer states. One way of combating this African problem is to focus on research that aims at discovering efficacious and cost effective cancer therapies from available natural resources within the African continent.

This study investigated the potential anti-proliferative activity (against HeLa cervical cancer cells) of four plants (*Adansonia digitata*, *Ceiba pentandra*, *Maytenus senegalensis* and *Drimia altissima*) commonly used in the African traditional treatment of malignancies. After *in vitro* bio-assay screening using the 3-(4,5-dimethylthiazol-2-yl)-2,5-diphenyl tetrazolium bromide (MTT) assay, *M. senegalensis* root extract (**MS-R**) and *D. altissima* bulb extract (**DA-B**) showed anti-proliferative activity against HeLa cervical cancer cells with IC_{50} values of 25 µg/mL and 1.1 µg/mL respectively. By possessing the strongest anti-proliferative activity among the tested extracts, *D. altissima* was selected for further studies. Liquid-liquid partitioning of the *Drimia altissima* bulb extract with *n*-hexane, ethyl acetate, and *n*-butanol, yielded partitions **79a** – **d**, with the *n*-butanol fraction, **79d**, exhibiting the strongest cytotoxic activity (IC_{50} = 0.497 µg/mL). Through High Content Analysis (HCA) screening, fraction **79d** was found to induce marked early mitotic cell cycle arrest.

Fractionation of **79d** using Diaion® HP-20 open column chromatography and a stepwise gradient of reducing polarity (water-methanol-ethanol-ethyl acetate) yielded cytotoxic fractions **82b**, **82c**, **82d** and **82e**, all with significant anti-proliferative activities at the tested concentrations of 0.1, 1.0 and 10 µg/mL. Bio-assay guided fractionation of **82c** (the most

effective fraction at the lowest tested concentration of 0.1 μg/mL) using Sephadex® LH-20 open column chromatography and 50% MeOH led to the isolation of compound **3.17**. After structural elucidation using 1D and 2D Nuclear Magnetic Resonance spectroscopy (NMR), High resolution Mass spectrometry (HRMS), Fourier-Transform Infrared spectroscopy (FT-IR), ultraviolet spectroscopy (UV) and Circular Dichroism (CD), compound **3.17** was identified as a novel *C*-glucosylflavonoid-*O*-glucoside, 6-C-[-apio-α-D-furanosyl-(1→6)-β-glucopyranosyl]-4′, 5, 7-trihydroxyflavone (Altissimin, **3.17**). Compound **3.17** exhibited a dose dependant anti-proliferative activity with an IC_{50} of 2.44 μM. The mechanism of action for compound **3.17** was investigated through cell cycle arrest, phosphatidylserine translocation (PS), caspase activation and mitochondrial membrane depolarization. The mechanism of cell death elicited by compound **3.17** in HeLa cells was found to involve the induction of M phase cell cycle arrest with consequent activation of apoptotic cell death which was evident from annexin V staining, mitochondrial membrane potential (ΔΨm) collapse and the activation of caspases -8 and -3.

In silico computational techniques were employed to virtually determine potential biological targets of compound **3.17**. Target fishing using the Similarity Ensemble Approach (SEA) target prediction gave human aldose reductase (hAR, AKR1B1) the highest ranking with a p value of 2.85×10^{-24}, a max Tc of 0.35 and a Z-score of 41.8217. Using AutoDock4 and the AutoDock tools suite (ADT), molecular docking of compound **3.17** in the hAR binding pocket was successfully achieved with a lower ΔG free energy binding (-9.4 kcal/mol) than that of positive control ligand 393 (-8.7 kcal/mol).

In conclusion, this study identified the genus *Drimia* and particularly *D. altissima* as a potential source for novel cytotoxic compounds. The discovery of altissimin (**3.17**), the first flavonoid glycoside to be isolated from *D. altissima*, enquires into the possible existence of similar compounds within the species. In addition to the observed *in vitro* cytotoxic activity against HeLa cells, the potential of altissimin (**3.17**) as a hAR enzyme inhibitor opens up the possibility of its use as an adjunct to increase cancer cell sensitivity to chemotherapy. Thus, altissimin (**3.17**) shows promise as a potential anticancer agent.

Chapter 1

Literature Review

1.1 Cell signaling: The cell cycle

In multicellular organisms, the reproduction of cells (cell proliferation) is an elaborate process which is achieved by a cascade of events called the 'cell cycle' in which chromosomes and other cellular components are copied and supplied into two daughter cells (Morgan 2007). Proliferating cells are faced with the choice of whether to participate in the cell cycle or to enter into a quiescent state and similarly, quiescent cells must choose to either remain quiescent or to re-enter the cell cycle (Smith 2005). During the embryonic stage of foetal development, cells are in a state of rapid division. However, with the exception of haematopoietic cells and those in the gastrointestinal lumen, most cells in an adult are in a quiescent state (Walkley et al. 2005). Cell division involves biochemical events whose sole purpose is to assure the resulting daughter cells of having an accurate and equal segregation of genetic material for normal biological function in the absence of which malignant conditions can arise (Meadows et al. 2011).

The normal mammalian cell cycle is divided into interphase and mitosis (M phase) (Figure 1.1). Interphase is further divided into G_0, G_1 (Gap1), S and G_2 (Gap2) phases while mitosis is divided into prophase, metaphase, anaphase and telophase (Israels and Israels 2009). During the four phases of the mammalian interphase which last between 12 to 24 hours, cells synthesize RNA leading to the translation of proteins for cell growth. The G_0 phase is occupied by cells which, after leaving the cell cycle, enter into quiescence and cease to divide. In the G_1 phase cells grow in size due to an increased production of proteins resulting from the translation of RNA. Replication of DNA occurs in the S phase while cell growth and protein manufacturing continue in the G_2 phase. In M phase (lasting about one to two hours) cell growth and protein synthesis is ceased and cells are each divided into two identical daughter cells (Mohan 2009). The determination of cell populations in each phase of the cell cycle (cell cycle analysis) is achieved by measuring the DNA content, also known as ploidy, which is the number of chromosomes that each cell contains (Crissman and Tobey 1974). Cells in phases

G_0 and G_1 have a diploid DNA content (2N), those in phases G_2 and M have a tetraploid DNA content (4N) and those in S phase have an intermediate DNA content.

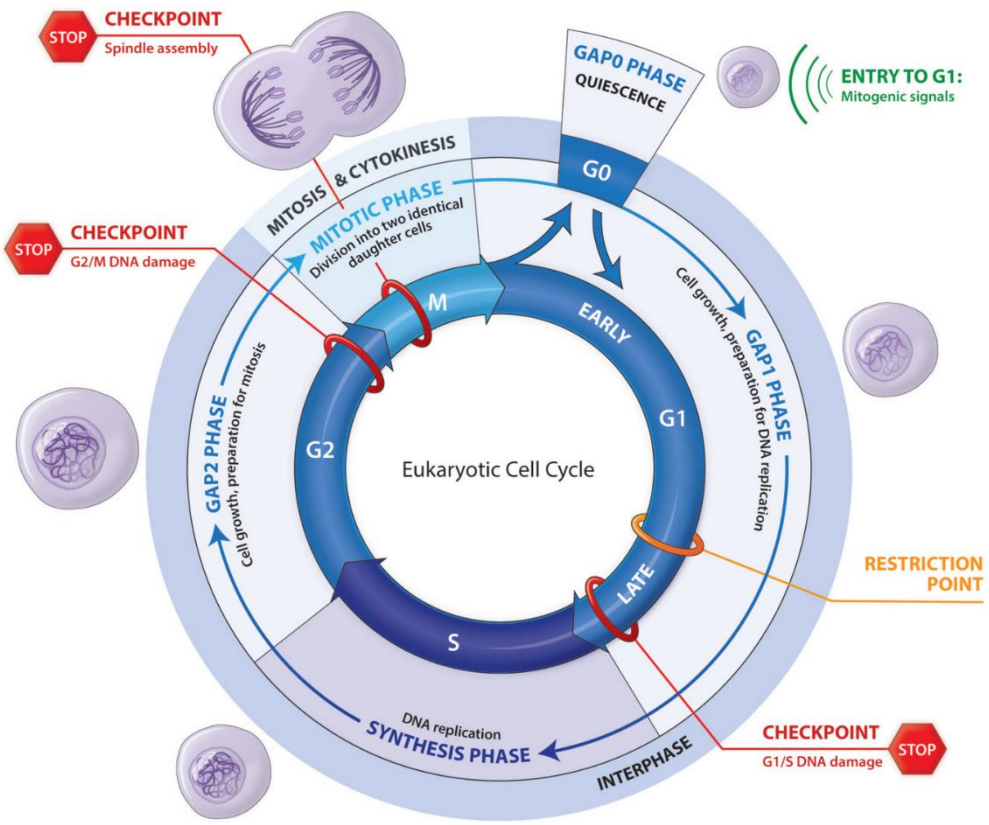

Figure 1.1 A schematic representation of the mammalian cell cycle with indicated checkpoints (Krumholtz 2018)

1.1.1 Cyclins and cyclin dependent kinases (CDKs)

The two main types of cell cycle control systems are intrinsic mechanisms and checkpoints. Intrinsic mechanisms are effected in each and every cell whereas checkpoints are only effected when anomalies are detected within the cell cycle. For progression through the cell cycle to be granted, it is important that a cell satisfies all the requirements at each checkpoint. Checkpoint mechanisms are regulated by the activation and consequent deactivation of cyclin dependent kinases (CDK) and cyclins (Obaya and Sedivy 2002). The activation of CDK2, CDK4, and CDK6 is required for cells to progress from G_1 to S phase, with CDK4 and CDK6 being involved in early G_1 and CDK2 in late G_1 for G_1/S phase transition (Neganova and Lako 2008). CDK4 and CDK6 interact and form active complexes with D-type cyclins (D1, D2 and D3)

whereas CDK2 forms activate complexes with E-type cyclins (E1 and E2). Progression through S phase requires the activity of CDK2 and cyclins A1 and A2, with cyclin A-CDK2 active complexes occurring in late S phase for DNA replication (Tannoch et al. 2002). The activated complexes of CDK4/6 and CDK2 with cyclins D and E respectively are essential for the hyperphosphorylation of the retinoblastoma protein (pRb) (Lundberg and Weinberg 1998). Following the phosphorylation of pRb, the release of S phase promoting transcription factors commits the cells to proliferate without any further need for mitogenic (external growth factor) signals. This point of the cell cycle is known as the restriction point (R) and its deregulation, often characterised by overexpression of cyclin D, mutation of the CDK4/6 inhibitor, p16 and consequent elevation of cyclin D-CDK activity and pRb phosphorylation, results in the development of cancer (Blagosklonny and Pardee 2002). Cell proliferation is dependent on the presence of activated cyclin-CDK complexes, which are regulated by oscillating cyclin levels throughout the different phases of the cell cycle (Figure 1.2) (Hochegger et al. 2008).

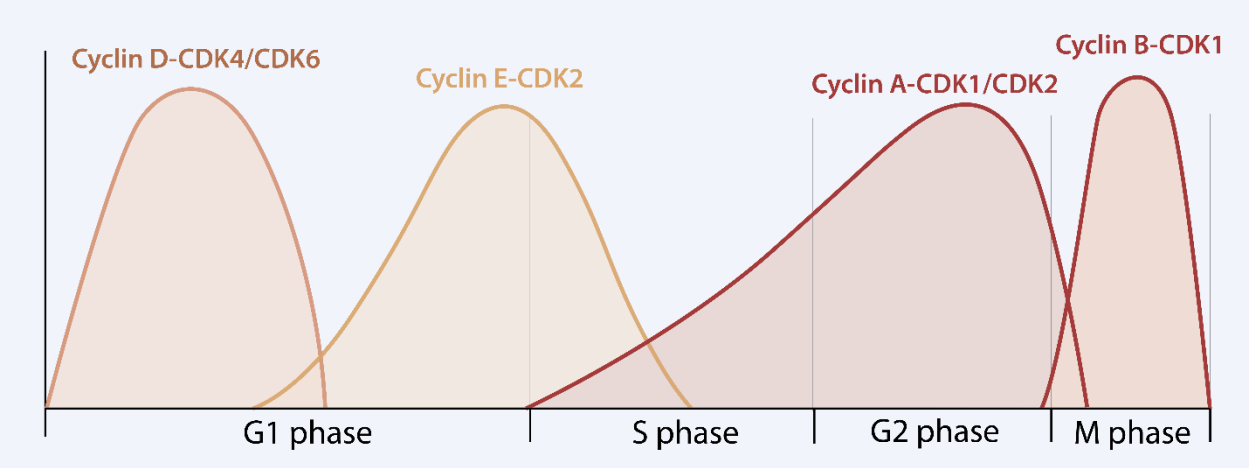

Figure 1.2 Transient activity of cyclin-CDK complexes regulating cell cycle progression (Adapted from: Hochegger et al. 2008)

Thus, cyclins act as regulators of CDK and cell proliferation. The degradation of cyclin D (ubiquitination) is a mitogenic signal-independent process which is performed by the ubiquitin proteasome pathway. Phosphorylation of cyclin D1 at Thr-286 through the action of glycogen synthase kinase 3β (GSK-3β) increases the ubiquitination of the protein (Alt et al. 2000). A family of cyclin-dependent kinase inhibitors called Cip/Kip (particularly p27/Kip1, p57 Kip2 and p21 Waf1/Cip1) form heterodimeric cyclin-CDK complexes whose actions result in the arrest of cells in G_1 and prevent progression to S phase (Figure 1.3) (Nakayama and Nakayama 1999). Over-expression of the p21 protein induces G_1 cell cycle arrest. Over-expression of p27

is a common feature of G_0 quiescent cells (Albrecht et al. 1998; Xiong et al. 1993). Comprising of $p16^{INK4a}$, $p15^{INK4b}$, $p18^{INK4c}$, $p19^{INK4d}$, the **IN**hibitors of CD**K4** (INK4) are a family of cyclin-dependent kinase inhibitors (CKIs) that selectively antagonise CDK4 and CDK6 with consequent inhibition of cell proliferation (Ortega et al. 2002).

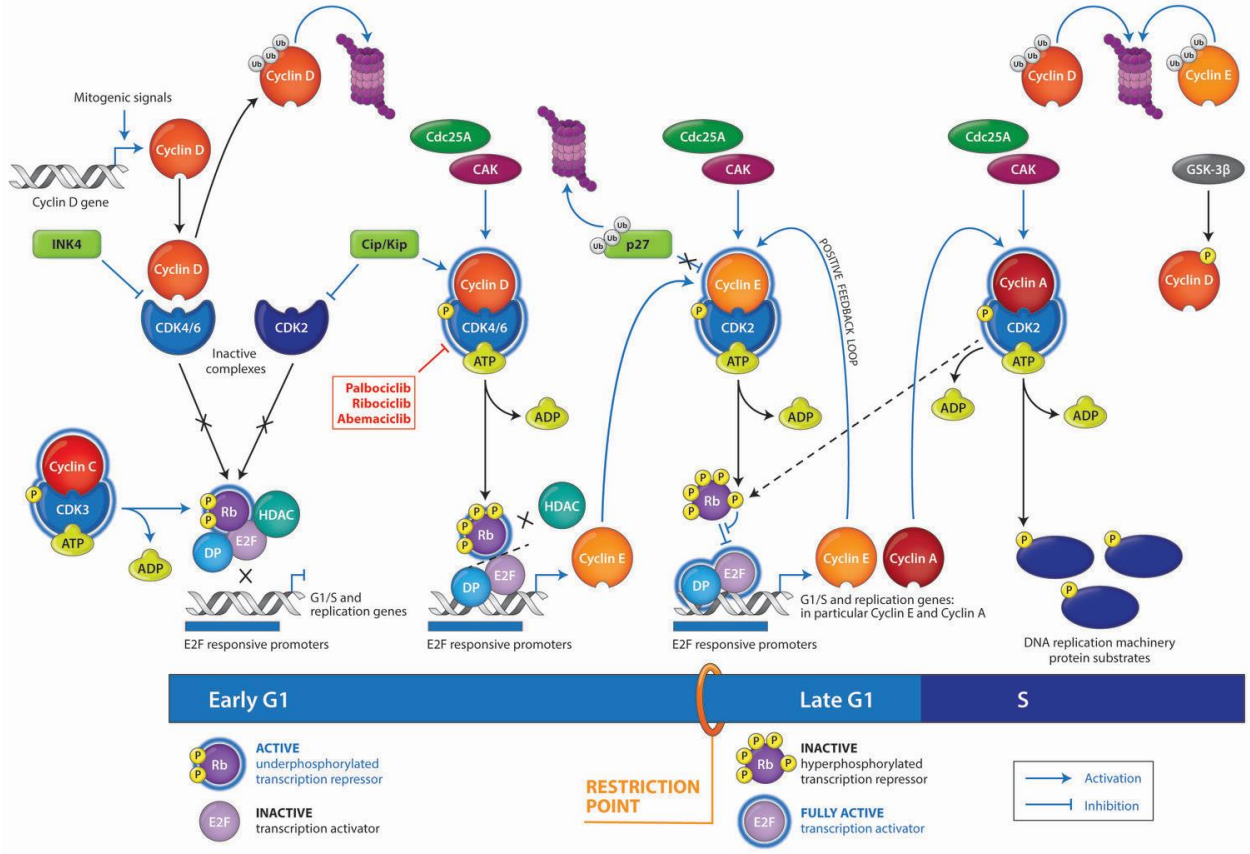

Figure 1.3 An illustration of early G_1, late G_1 and S phase cell signaling showing CDK/cyclin interactions and other regulators of G_1/S transition (Krumholtz 2018)

1.1.2 Retinoblastoma protein (pRb)

G_1/S progression of cells requires passage through the restriction point which is regulated by a member of the pocket protein family known as the retinoblastoma tumour suppressor protein (pRb). Harbouring multiple binding sites, pRb is able to interact with important regulatory proteins such as E2F transcription factors, the proto-oncoprotein c-Abl tyrosine kinase and proteins with conserved LXCXE motifs (Welsh and Wang 1995; Dahiya et al. 2000; Nevins 2001). Cell cycle-mediated phosphorylation of pRb by CDKs results in the inhibition of targeted pRb binding and thereby permits the progression of cells within the cell cycle. The inactivation of pRb first begins with phosphorylation by cyclin D-CDK4/6 followed with hyperphosphorylation by cyclin E-CDK2 (Figure 1.3) (Moser et al. 2018).

1.1.3 Tumour suppressor protein p53

Cancer is typically a result of an amalgamation of genomic aberrations such as point mutations, small insertions and deletions (INDELs) and large copy number variations (CNV) (Mullaney et al. 2010; Dayton and Piccolo 2017). The tumour suppressor protein p53 plays a cardinal role in the cellular response to genomic aberrations such as DNA damage. The detection of damaged DNA stimulates the activation of p53 by initiating its phosphorylation at Ser15 and Ser20 (Chehab et al. 1999; Loughery et al. 2014). The phosphorylation of p53 reduces its binding to the oncoprotein Mouse double minute 2 homolog (MDM2), a negative regulator that targets p53 for destruction by ubiquitination and proteosomal degradation (Figure 1.4) (Nag et al. 2013). Also, p53 can be phosphorylated at Ser15 and Ser37 by A-T mutated (ATM) gene, ATM-Rad3-related protein (ATR) and DNA-dependent protein kinase (DNA-PK) (Blackford and Jackson 2017). The activation of p53 by phosphorylation either results in cell cycle arrest and the repairing of DNA or induction of apoptotic cell death (regulated *via* phosphorylation at Ser46) (Speidel 2010). In the presence of DNA damage, p53 undergoes acetylation at Lys382 which results in increased p53 binding to DNA (Brooks and Gu 2003). The deacetylation of p53 is achieved through interaction with the enzyme sirtuin (silent mating type information regulation 2 homolog) 1 (*S. cerevisiae*) (SIRT1) (Lee and Gu 2013).

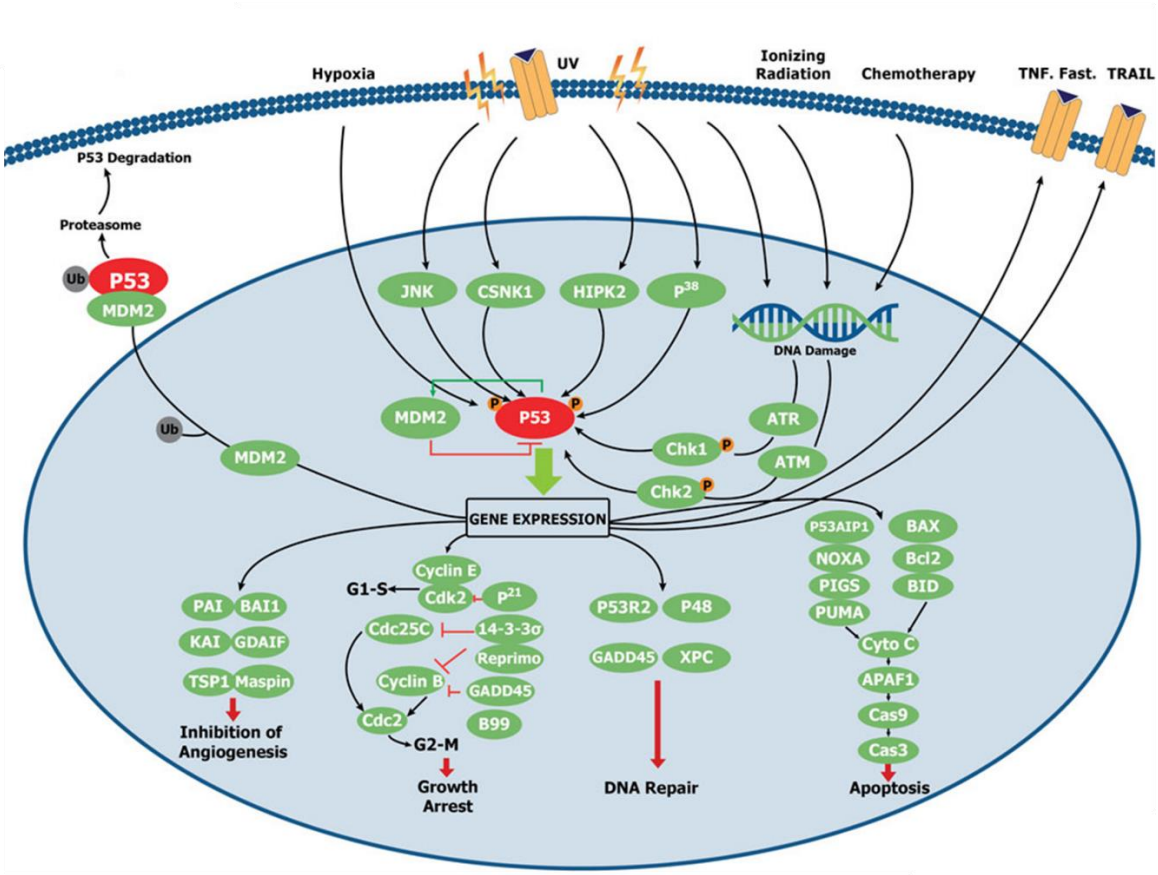

Figure 1.4 The p53 response to DNA damage and p53 regulation by MDM2 (Rockland 2018)

p53 binds and activates MDM2 transcription via promoter region, elevated levels of MDM2 bind to p53 and inhibits its ability to act as a transcription factor, MDM2 targets p53 for ubiquitination and proteolytic damage and targeted p53 undergoes proteosomal degradation

1.1.4 Histone H3

In eukaryotic cells, DNA is packed within the nucleus in the form of chromatin which consists of positively charged histone protein units and two ~80 base pair (bp) superhelical turns of DNA (Figure 1.5) (Li et al. 2007). Modulating the structure of chromatin is cardinal for the regulation of cellular transcription. The four core histones that form the nucleosome are H2A, H2B, H3 and H4 (Annunziato 2008). The histone structure consists of globular portions and unstructured N-terminal "tails" which, upon stimulation, can undergo posttranslational modifications (PTM) such as acetylation, lysine and arginine methylation, phosphorylation, ubiquitination, sumoylation, ADP ribosylation, deamination and proline isomerization (Kouzarides 2007). Modifications on the histone tail alters chromatin interaction with transcription factors and gene expression.

The acetylation of histone H2B primarily occurs at Lys5, 12, 15 and 20 while that of histone H3 primarily occurs at Lys9 (a key player in chromatin assembly), 14, 18 and 23. Additionally, phosphorylation of histone H3 at Ser10, Ser28 and Thr11 results in chromosome condensation during mitosis and meiosis. Inversely, cell cycle arrest in M phase is characterised by the dephosphorylation of histone H3 (Hans and Dimitrov 2001).

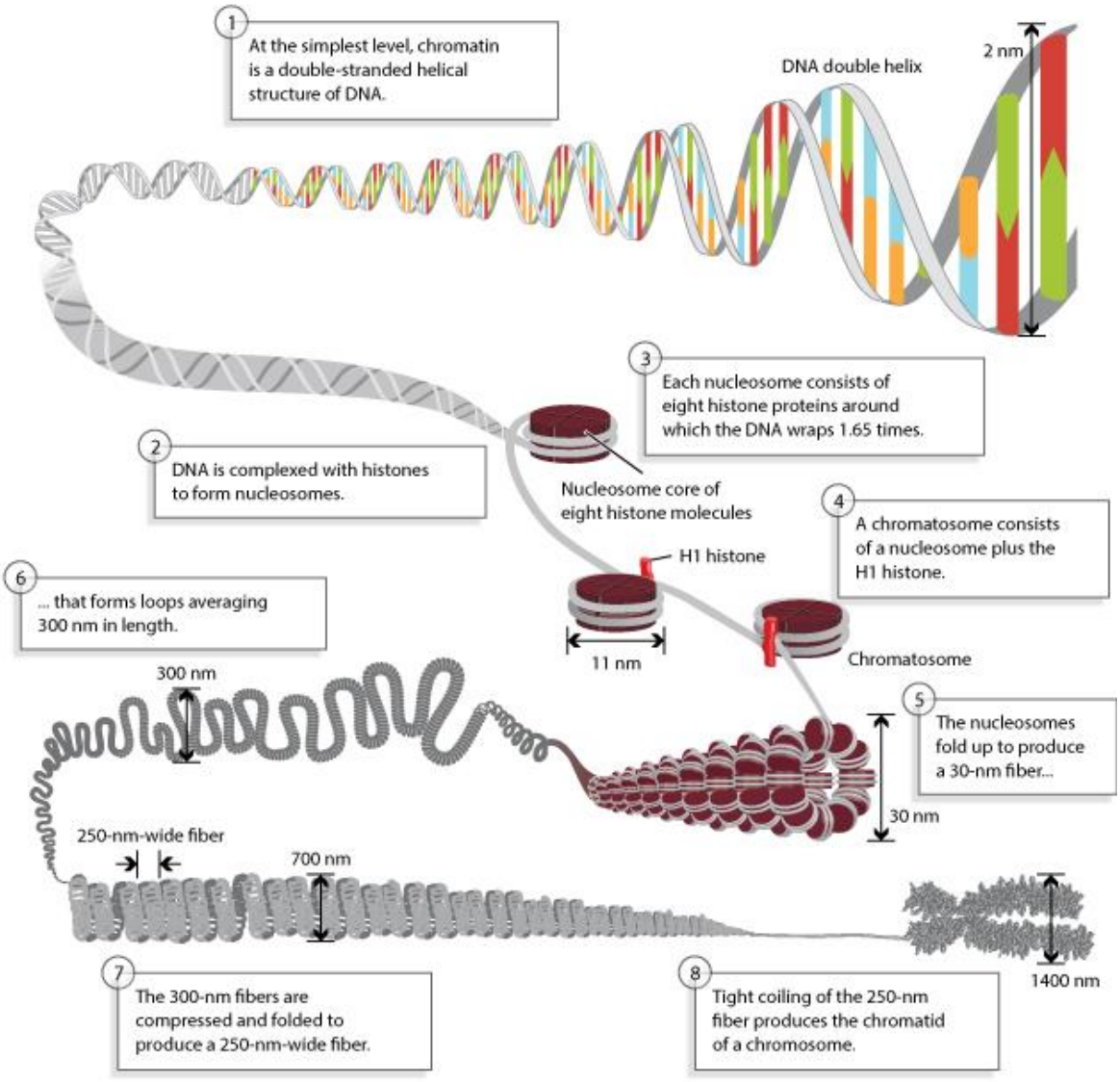

Figure 1.5 The structure of chromatin consisting of DNA packaged with repeating histone protein units[1] (Annunziato 2008)

[1] Chromosomal DNA packaging is achieved by complexation with histone units whose positive charge enables them to strongly bind to negatively charged DNA for the formation of nucleosomes

1.1.5 Cdc25C

The protein phosphatase **c**ell **d**ivision **c**ycle 25C (cdc25C) dephosphorylates and activates cdc2, also known as cyclin dependent kinase 1 (CDK1) at threonine 14 and tyrosine 15. The activation of cdc2 by cdc25C is considered as a critical step that is required for the entry of eukaryotic cells into mitosis (Hoffmann 2000). The constitutive phosphorylation of cdc25C by cdc25C associated protein kinase (c-TAK1) at Ser216 occurs throughout interphase as opposed to the G_2/M checkpoint where phosphorylation at this position only occurs when there is DNA damage (Peng et al. 1998). Phosphorylation of cdc25C at Ser216 causes it to bind to members of the 14-3-3 family resulting in cytoplasmic sequestration of cdc25C and consequent inhibition of premature mitosis (Krämer et al. 2004). In the event of DNA damage, checkpoint kinases Chk1 and Chk2 phosphorylate cdc25C at Ser216 (Bartek and Lukas 2003; Bahassi et al. 2008). In prophase, cdc25C phosphorylation by polo-like kinase 1 (PLK1) at Ser216 results in its translocation from the cytoplasm to the nucleus to enable interaction with cyclin B-CDK1 (also written as cyclin B-cdc2) and consequently permit the progression of cells through the rest of mitosis.

1.2 Programmed cell death (PCD)

In multicellular organisms, the quantity of cells is strictly controlled by regulating the rate at which cells divide as well as the rate at which they die. Cell death can be classified morphologically (apoptosis, autophagy and necrosis), enzymologically (involvement of either nucleases or proteases such as caspases, cathepsins and transglutaminases), functionally (programmed, accidental, physiological or pathological) and immunologically (immunogenic or non-immunogenic) (Kroemer et al. 2009). When cells are no longer needed, they commit 'suicide' by triggering intracellular death programs which are collectively known as 'programmed cell death' (Alberts et al. 2007). The term programmed cell death may refer to several phenomena including the loss of cells during the ageing process and the destruction of large cell populations during specific points of development (Lockshin and Beaulaton 1974). There is a marked morphological difference between cells undergoing programmed cell death and those undergoing pathological death. In pathological death such as trauma, cells swell, rupture and release their contents in a process known as necrosis (Leist and Nicotera 1997). Among the released intracellular components of necrotic cells are lysosomal enzymes which damage adjacent cells and stimulate inflammatory cascades with the involvement of macrophages and other immunological cells (Goodman 2008). On the other hand, cells undergoing programmed cell death do not release intracellular content, hence, the absence of inflammation. Among the different types of programmed cell death (apoptosis, autophagy and programmed necrosis), the most extensively studied and best understood is apoptosis (Ouyang et al. 2012).

1.2.1 Apoptosis

Coined in 1972 by the Australian pathologist John Kerr and his colleagues Andrew H. Wyllie and Alastair R. Currie, the word *apoptosis*, was derived from the Greek root words *apó* (away from) and *ptôsis* (falling) to mean "falling off", as applied to the seasonal falling off of leaves from trees (Lockshin and Zakeri 2001). During apoptosis, cells shrink in size and display nuclear and chromatin condensation. Morphologically, cells undergoing apoptosis appear as if they are 'boiling' (known as cell blebbing) as a result of cell membrane protrusion caused by transient membrane detachment or a rapture in the actin cortex (Charras 2008). This is followed after by cellular fragmentation into intact membrane-bound "apoptotic bodies" which are ultimately

engulfed by phagocytes in *in vivo* models without the release of intracellular material into the intestitium (Elmore 2007). In summary, apoptosis is characterised by cell rounding, reduced cell volume, chromatin condensation, nuclear fragmentation, cell blebbing with maintained membrane integrity and phagocytic engulfment. In the absence of phagocytic engulfment, apoptotic bodies undergo necrotic degradation as the second option in a process called secondary necrosis (Saraste and Pulkki 2000). Some of the biochemical features of apoptosis include regular length DNA fragmentation (~ 180 bp), mitochondrial release of factors such as cytochrome *c* and apoptosis inducing factor (AIF) into the cytoplasm, activation of caspases, phosphatidylserine translocation and early intracellular actin degradation (Becila et al. 2010).

1.2.1.1 Molecular mechanisms of apoptosis

As the first realised component of cell death, caspases were discovered through studies that were done on the nematode worm *Caenorhabditis elegans*. After the analysis of genes belonging to cell-death defective worm mutants (CED), it was realised that the product of the *ced-3* gene was a requirement for all developmental-related programmed cell deaths in the worm. In a breakthrough discovery, CED-3 was found to be a relative of the then newly discovered human protease, interleukin-lβ converting enzyme (ICE) (Yuan et al. 1993). This was followed after by the discovery of several 'ICE-like' proteases, 14 of which are mammalian, later to be renamed as 'caspases' and ICE becoming caspase-1. Caspases are now recognised as cardinal role players in the institution of cell death (Creagh and Martin 2001). Caspases are functionally divided into those that are activated through apoptosis (caspases-2, -3,-6, -7, -8, -9 and -10) and those that stimulate pro-inflammatory cytokines during immune response (caspases-1, -4, -5 and -11). Apoptotic caspases are further divided into initiator (upstream) and executioner (downstream) caspases. As their names state, initiator caspases (caspase-2, -8, -9 and -10) are the initiators of the caspase cascade while executioner caspases (caspase-3, -6 and -7) are responsible for executing apoptotic cell destruction (McArthur and Kile 2018). The executioner caspases are proteolytically activated by initiator caspases in order to perform their functions.

A modular protein known as apoptotic protease-activating factor 1 (Apaf-1) consisting of an N-terminal caspase recruitment domain (CARD), a CED-4 homologous domain and a C-terminus with 12 tryptophan/ aspartic acid (WD-40) repeats, combines with caspase-9 in the presence of

cytochrome *c* and deoxyadenosine triphosphate (dATP) to form 'the mitochondrial apoptosome' which initiates or amplifies apoptosis (Zou et al. 1999). Formation of the mitochondrial apoptosome requires first the release of cytochrome *c* from mitochondria, a process that is controlled by the B cell lymphoma 2 (Bcl-2) family of proteins (Ola et al. 2011). The Bcl-2 family can be divided into two (based on whether they are apoptotic or anti-apoptotic) or three sub-groups (based on the existing Bcl-2 homolog domain, BH). Members of the anti-apoptotic sub-group such as Bcl-2 and Bcl-X_L contain the BH4 domain while those of the apoptotic sub-group are either devoid of the BH4 domain (Bax, Bak and Bok) or having only the BH3 domain. In total, there are eight BH3-only members namely, hara-kiri (Hrk), BH3 interacting domain death agonist (Bid), Bcl-2 interacting mediator of cell death (Bim), Bcl-2 modifying factor (Bmf), p53, promoter-upregulated modulator of apoptosis (Puma), Noxa, Bcl-2 antagonist of cell death (Bad) and Bcl-2 interacting killer (Bik) (Ola et al. 2011). These are further divided into activators (active BID, BIM and PUMA) which activate effector proteins and derepressors (such as BAD and NOXA) which block anti-apoptotic effects. The anti-apoptotic Bcl-2 members inhibit the mitochondrial release of cytochrome *c* whereas the pro-apoptotic members promote its release. Activation of the BH3-only pro-apoptotic members result in the blockade of inhibitory effects from anti-apoptotic Bcl-2 members which causes AK-Bax to undergo oligomerisation (Chipuk and Green 2008). BH3-only members induce conformational changes in pro-apoptotic Bcl-2 members such as Bax and Bak, leading to their incorporation and/or oligomerisation into the outer mitochondrial membranes (OMM) and causing the formation of permeable channels through which cytochrome *c* can be escaped. The released cytochrome *c* enters the cytosol where it is then used for the creation of mitochondrial apoptosomes (Kalkavan and Green 2017).

1.2.1.1.1 Intrinsic apoptotic pathway

The intrinsic (mitochondrial) apoptotic pathway is initiated by Bcl-2 family members. Several pro-apoptotic signal transducing molecules and cytotoxicity inducers such as death, genomic and metabolic stresses and the presence of protein unfolding cause permeabilisation of the outer mitochondrial membrane (OMM) and consequent release of apoptotic material, including cytochrome *c*, second mitochondria-derived activator of caspases (Smac/DIABLO), Omi/HtrA2, AIF and endonuclease G, into the cytosol (Fulda and Debatin 2006). Released cytochrome *c* then binds to Apaf-1, causing an interaction with dATP that exposes the N-terminal CARD for

oligomerisation and activation of initiator procaspase-9 *via* a CARD-CARD interaction (Figure 1.6) (Adrain et al. 1999). This results in the recruitment of executioner caspase-3 to the apoptosome and its subsequent activation by the resident caspase-9. Activation of caspases can also take place through interactions with death receptors which oligomerise and activate initiator caspases (Contassot et al. 2007). Released smac/DIABLO and Omi/HtrA2 also activate caspases by silencing endogenous caspase inhibitors known as the inhibitor of apoptosis proteins (IAPs) (Liu et al. 2018).

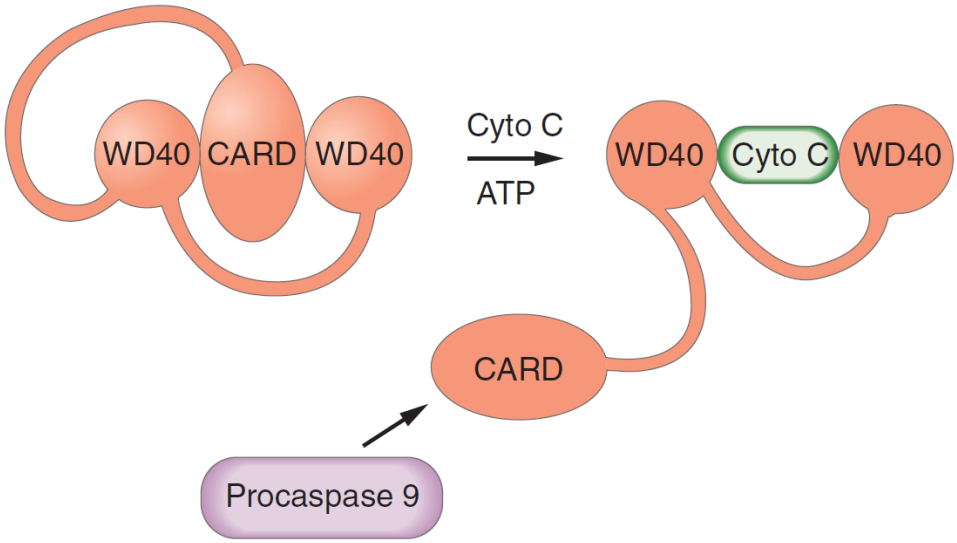

Figure 1.6 An illustration of procaspase-9 activation by Apaf-1 (Goodman 2008).

The caspase recruitment domain (CARD) is usually inaccessible to procaspase-9. In association with dATP, released mitochondrial cytochrome *c* binds to Apaf-1 on the WD40 repeats, causing a conformational change in Apaf-1 that exposes the CARD for procaspase-9 activation.

Since a large variety of cancers occur as a result of mutations in Bcl-2 regulation of the mitochondrial pathway, most of the developed anticancer drugs act as inducers of apoptosis through the activation of the intrinsic pathway. Examples of such drugs include regulators of Bcl-2 gene expression, drugs affecting Bcl-2 mRNA and drugs inhibiting Bcl-2 proteins. However, most of the apoptosis-inducing drugs destroy DNA or disrupt the cytoskeleton in cancer cells and normal cells alike (Alam 2003). Therefore, more ideal anticancer drugs would be those that selectively induce apoptosis in cancer cells. Over 30 years of research focused on the discovery of selective Bcl-2 modulating drugs has resulted in the development of small molecule compounds

called ‘BH3-mimetics’ as direct activators of apoptosis in malignant cells only through the selective targeting of pro-apoptotic Bcl-2 proteins (Delbridge et al. 2016). The first bonafide BH3-mimetic to show efficacy in cancer is navitoclax (**1.1**) (Figure 1.7), a dual Bcl-2 and Bcl-X_L antagonist (Zhu et al. 2015). Since navitoclax (**1.1**) acts on Bcl-X_L, its inhibitory activity on Bcl-X_L also results in thrombocytopenia. Following navitoclax (**1.1**), the first BH3-mimetic to be licensed for use in chronic lymphocytic leukaemia is venetoclax (**1.2**) (Figure 1.7) (Ashkenazi et al. 2017).

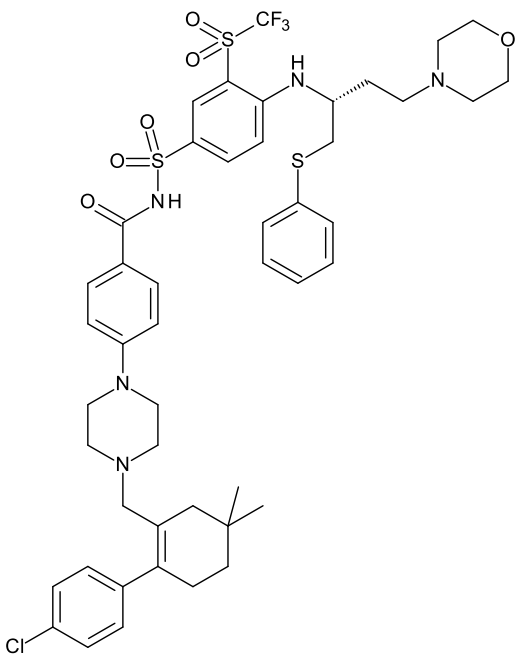

(1.1)

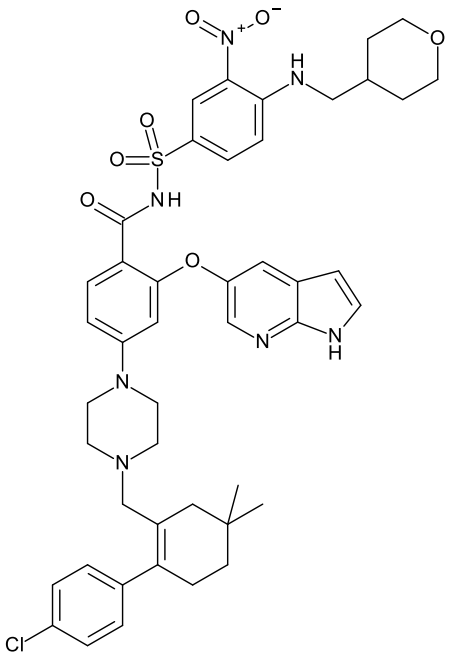

(1.2)

Figure 1.7 BH3-mimetics navitoclax (**1.1**) and venetoclax (**1.2**) as selective Bcl-2 antagonists

1.2.1.1.2 Extrinsic apoptotic pathway

The extrinsic apoptotic pathway is activated through extracellular signals arising from other cells. These extracellular ligands bind to receptor mediated transmembrane death receptors which are a member of the tumour necrosis factor (TNF) family of receptors consisting of over 20 proteins and characterised by the presence of 80 amino acids known as the ‘death domains’ (Peter et al. 1999). When extracellular ligands such as Fas-L and TNF-αL bind to their corresponding death receptors (in this case Fas and TNF-α respectively), the death domains transmit received extracellular death

signals to intracellular signaling pathways. To do this, the activated death receptors interact with adaptor proteins such as Fas associated protein with death domain (FADD) which then binds initiator procaspase-8 molecules (Ashkenazi 2002). The resulting receptor-ligand-initiator procaspase-8 or -10 complex is referred to as the death-inducing signaling complex (DISC) (Yang et al. 2005). The formed DISC then draws procaspase-8 molecules in close proximity to each other to facilitate for their autocatalytic cleaving and subsequent cytosolic release of initiator caspase-8. Cytosolic caspase-8 can then activate executioner caspase-3, -6 and/or -7 (Figure 1.8). Death receptor agonists under clinical trial include dulanermin and the monoclonal antibodies mapatumumab, lexatumumab and conatumumab.

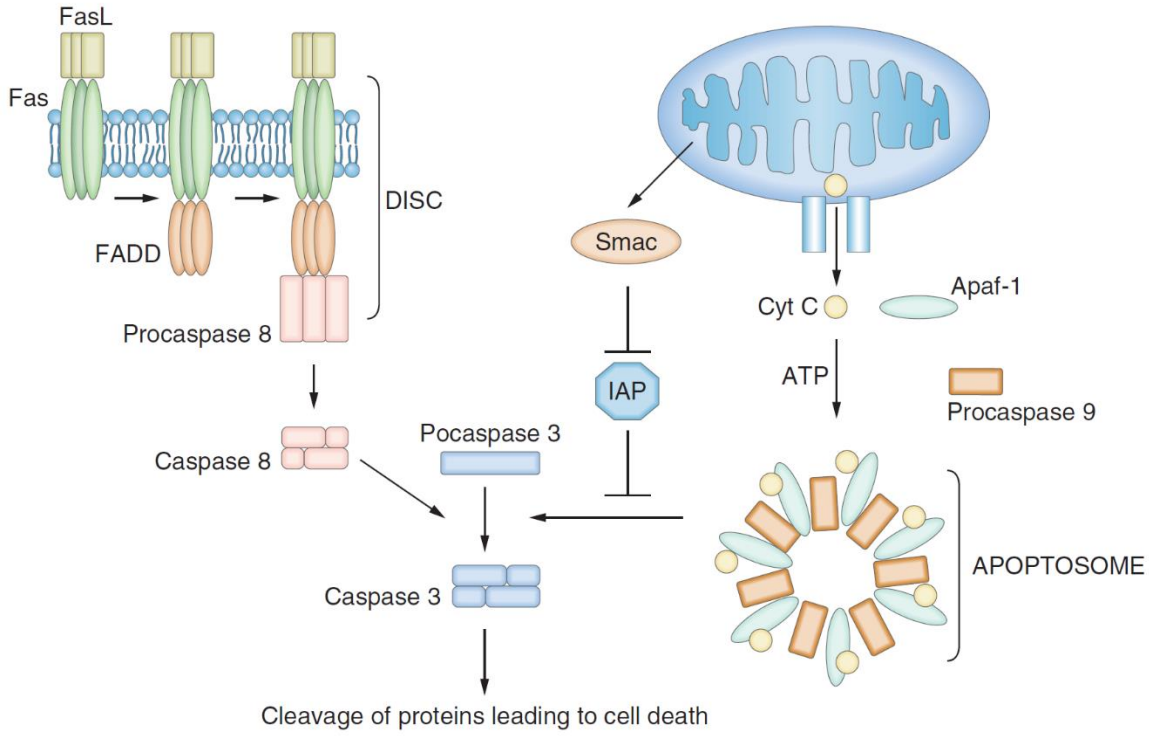

Figure 1.8 Molecular mechanisms of apoptosis showing the intrinsic and extrinsic pathways (Goodman 2008)

1.3 Cancer: A brief history

The word 'cancer' is derived from the Greek word *carcinos* meaning crab. This term was first used by Hippocrates (460-370 BC) to describe malignancies as having the characteristics of finger-like projections that, in a similar fashion to the claws of a crab, reach out to surrounding tissues (Stephens and Aigner, 2009). Celsius (28-50 BC) eventually translated *carcinos* into its Latin equivalent, cancer (American Cancer Society 2018a). The earliest documentation of malignancies is found in the Edwin Smith Surgical Papyrus (Figure 1.9A), an Egyptian paleographic scroll supposedly authored by the earliest known physician, Imhotep, whose votive statues are still in existence (Figure 1.9B) (Szépmuvészeti Múzeum 2017). The papyrus was discovered in a tomb in Thebes, Greece, dating between 3000 – 2500 B.C. (Lakhtakia 2014). The Edwin Smith Surgical Papyrus describes incurable cases of bulging afebrile tumours spreading on the breast (Breasted 1930). The oldest diagnosed case of cancer is that of a 2700 year old Scythian King from Arzhan, Russia, who suffered from a metastatic prostate cancer (Schultz et al. 2007), followed by a 2250 year old Egyptian Ptolemaic mummy only known as M1 (Figure 1.9C), who suffered from a prostate metastatic bone cancer (Prates et al. 2011).

Some of the early hypotheses about the cause of cancer include Hippocrates' humoral theory in which the body was believed to contain four *humors* or body fluids; blood, phlegm, yellow bile and black bile. An imbalance in the equilibrium between these four body fluids was believed to be the cause of disease, with cancer being caused by excess black bile. This was the accepted medical teaching through the middle ages for over 1,300 years (Sudhakar 2009). In the 17th Century, the humoral theory was replaced by Stahl and Hoffman's lymph theory in which cancer was believed to be caused by a fluid called lymph being discarded from the blood. In 1938, a German Pathologist called Johannes Muller developed the blastema theory which claimed that cancer cells did not arise from fluids but rather from budding (blastema) cells that did not share the same origin as normal cells (American Cancer Society 2018b). Rudolph Virchow, a student of Muller later proposed that cancers arise from chronic irritation and spread like fluids. This theory was corrected in the 1860's by the German surgeon, Karl Thiersch, who explained that cancers metastasize through malignant cells and not through an unknown fluid. Between 1800 to the 1920's, cancer was believed to be caused by trauma, even though experiments involving the injury of animals did not cause cancer.

Between 1649 and 1652, the doctors Zacutus Lusitani and Nicholas Tulp from Holland developed the contagion theory with the belief that cancer was a highly contagious disease. To implement this theory, cancer patients were isolated out of town to prevent the propagation of the disease (Bynum 1980). Though we now know that human cancers are not contagious, certain viral, bacterial and parasitic infections can create predispositions to cancer development.

Figure 1.9 (A) An excerpt from the Edwin Smith Surgical Papyrus (Levine 2015), (B) a statue of the earliest physician, Imhotep[2] (Szépmuvészeti Múzeum 2017) and (C) the Egyptian Ptolemaic wrapped human mummy, M1 (Prates et al. 2011)

[2] Several votive statues of Imhotep exist with this particular one being known as 'the budapest Imhotep'. The bronze statue consisting of arrays of gold, electrum and silver was dedicated to Imhotep (a high priest of Heliopolis often equated to the Greek god of medicine, Asklepios) to act as an intermediary between a man named Kham-Khonsu and the god Ta-tenen (Szépmuvészeti Múzeum 2017).

1.3.1 Hallmarks of cancer

A cancer can be defined as "a malignant growth that is characterised by a continuing, purposeless, unwanted, uncontrolled and damaging growth of cells that differ structurally and functionally from the normal cells from which they developed" (Stephens and Aigner 2009). The two main types of cancer are carcinomas (which are more common) and sarcomas. Carcinomas are cancers of the epithelial tissue whereas sarcomas are cancers of the connective tissue. Both types of cancer occur as a result of damages in the genetic make-up of a single cell caused by at least 6 mutations in specific proto-oncogenes and tumour suppressor genes (Stephens and Aigner, 2009). These mutations can be inherited, spontaneous, as a result of environmental factors such as ultra-violet radiation and chemical carcinogens or from a lifestyle of smoking, alcohol drinking, sedentary living and unhealthy eating habits.

The hallmarks of cancer were first introduced by Hanahan and Weinberg to detail the succession of capabilities acquired in the progressive development from a normal to a cancerous cell (Hanahan and Weinberg 2000). One of these hallmarks is the ability of cancerous cells to evade programmed cell death through dysregulations in Bcl-2 control of the intrinsic apoptotic pathway and by dampening Bcl-2 stress signals (Letai 2008). Cancerous cells are also able to proliferate continuously without control by increasing the levels of growth factors, stimulating surrounding cells to supply growth factors, upregulating surface receptors, modifying receptors to promote cancerous signaling and activating downstream proteins in the signaling pathway (Hanahan and Weinberg 2011). Cancer cells acquire the ability to disturb negative feedback loops that act as safety mechanisms in the event of a hyperactive mitogenic signal (Bardeesy and Sharpless 2006). The tumour microenvironment is often characterised by inflammation due to the infiltration of immunological cells. Cancerous cells benefit from this inflammatory state due to the associated increase in growth factors, survival factors, promotion of angiogenesis, invasion and metastasis and activation of epithelial-mesenchymal transition (EMT) (Grivennikov and Karin 2010). Cancerous cells are able to metastasize by interacting with the extracellular matrix through the invasion of tissues, intravasation, blood and lymphatic transition and tissue colonisation. These interactions require the active participation of surrounding tissues. To circumvent this, cancerous cells modify extracellular receptors that interact with external signals. For instance, cancerous cells promote their own migration by modifying receptors that participate in the paracrine loop with tumour associated macrophages

(TAM) involving CSF-1 and epidermal growth factor (EGF) resulting in the formation of elongated protrusions and cell invasion (Goswami et al. 2005).

Telomeres are portions of repeating nucleotide sequences at the ends of chromosomes which reduce in length with each cell division and hence, limit the number of times a cell can proliferate. Shortening telomeres ultimately reach the Hayflick limit which stimulates replicative senescence, apoptosis and tumour suppression *via* the p53 gene. The replenishing of telomeres is performed by the enzyme telomerase reverse transcriptase. Cancerous cells are able to immortalise themselves by overexpressing telomerase and dysregulating the p53 gene (Artandi and DePinho 2010). Normal cells limit uncontrolled cell proliferation through the release of anti-proliferative signals which can either induce G_0 or stimulate a postmitotic state during which cells are unable to undergo mitosis. Cancerous cells are able to circumvent this protective mechanism by dysregulating the tumour suppressors retinoblastoma protein (pRb) (which protects the restriction point) and p53 (which arrests the cell cycle in the event of DNA damage). Loss of pRb and p53 functions lead to uncontrolled cell proliferation despite DNA damage (Sherr 2004).

The immune system provides protection against cancer development through cancer immune-editing which involves the complete destruction of cancerous cells (elimination) as well as the control of cell growth in cancerous cells which cannot be eliminated (equilibrium). However, cancerous cells in the equilibrium phase can develop mechanisms to evade the immune system and continue proliferating (escape). Hence, the association between a weak immune system and poor cancer prognosis (Prendergast 2008). Cancerous cells can also utilise the existing gene alterations to promote further mutations and increase oncogenesis. This is achieved by increasing sensitivity to mutagens, altering DNA 'caretaker' genes and disrupting DNA repairing mechanisms (Venkitaraman 2001). Since vascular perfusion is essential for the supply of oxygen and nutrients, cancerous cells can activate an 'angiogenic switch' in which angiogenesis is promoted through the over-expression of pro-angiogenic factors such as vascular endothelial growth factor (VEGF) (Hicklin and Ellis 2005). In order for cancerous cells to maintain uncontrolled proliferation without experiencing resource shortage, they make adjustments to normal energy production by altering glucose production, increasing the expression of glucose transporters such as GLUT1 and utilising alternative metabolic pathways. This offers the cancerous cells the ability to divert glycolic intermediates to cell proliferation pathways (Marie and Shinjo 2011).

1.3.2 Cancer incidence in Africa

It has been estimated by Global Cancer Incidence, Mortality and Prevalence (GLOBOCAN) that there will be 18.1 million new cancer cases and 9.6 million cancer deaths worldwide in 2018 alone (Bray et al. 2018). Currently, cancer statistics in the high-income countries of North America and Western Europe are higher than those reported in Africa and Asia. However, it has been stated that cancer is soon to become a major cause of morbidity and mortality in all world regions regardless of economic status (Bray et al. 2012). The African continent has a complex sociodemographic picture resulting from religious, linguistic, cultural and economic differences that play a significant role in the incidence and prevalence of cancer (American Cancer Society 2011). Africa is demographically divided into Northern Africa and sub-Saharan Africa, with the former being populated by Arabs and the latter by indigenous black people. A huge economic disparity can be observed between the two African regions, with some sub-Saharan African countries like Zambia and Zimbabwe having a life expectancy ranging around 61 years while North African countries like Algeria and Tunisia range >75 years, which is almost par with Europe and the Americas (Statista 2018).

In Northern Africa, breast cancer (30%) followed by colorectal cancer are most common among women, whereas lung cancer followed by prostate, colorectal and liver cancers are most common among men (Figure 1.10) (IARC 2014). The high incidence of breast cancer in affluent Northern Africa can be attributed to increased economic development associated risk factors such as early menarche, low or late parity, obesity and increased exposure to xeno-chemical environmental pollutants (Luzzati et al. 2018). Prostate and liver cancer followed by Human Immunodeficiency Virus (HIV)-associated Kaposi's sarcoma are the most common cancers among sub-Saharan African men (Ferlay et al. 2014). Contrary to other world regions, cervical cancer (50 cases per 100,000) is the most common cancer among sub-Saharan African women owing to a combination of the high incidence in sexually transmitted Human Papillomavirus (HPV) infections (the aetiological cause of cervical cancer) and the unavailability of Papanicolaou (Pap) testing facilities. In 2012, the probability for a sub-Saharan African woman to develop cervical cancer was 3.8%, with a 2.5% chance that the cancer would eventually kill her (Cancer Atlas 2018).

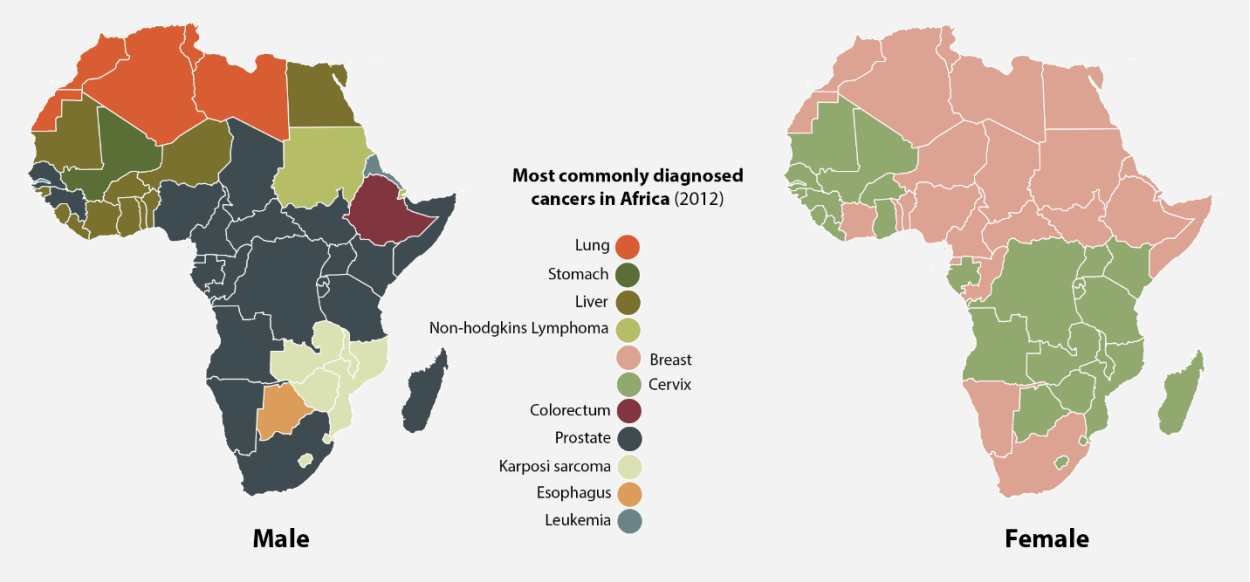

Figure 1.10 GLOBOCAN compilation of the most commonly diagnosed cancers in the African population in 2012 (Adapted from: Ferlay et al. 2014)

1.3.3 Cervical cancer

Cervical cancer is a sexually transmitted disease (STD) caused by infection with oncogenic high-risk strains of the Human Papillomavirus (HPV), a virus belonging to the *Pappilomaviradae* family (Burd 2003). Infection with HPV has been found to be essential but not sufficient for disease development and hence, the involvement of cofactors and molecular events. HPV is the cause of 99.7 % of all the cervical cancers worldwide with about 30 types of HPV known to primarily infect and cause cancers of the vagina, vulva, cervix, penis and anus (Clifford et al. 2003). The HPVs are small circular non-enveloped encapsulated DNA tumour viruses with ~ 8 kb genomes encoding eight genes E1, E2, E4, E5, E6, E7, L1 and L2 (Figure 1.11). The HPV has three functional regions with the first being the highly variable non-coding region consisting of 400 to 1000 bp which contain the p97 core promoter together with enhancer and silencer sequences for the control of DNA replication (Apt et al. 1996). The second is an early region consisting of open reading frames (ORFs) E1, E2, E4, E5, E6, and E7 which are implicated in the replication and oncogenic properties of the virus. The third is a late region containing the L1 and L2 genes that encode viral capsid structural proteins (IARC 2007).

Following viral exposure, HPV attacks the epithelial basal layer and gains entrance into the cell within several hours of viral internalisation with viral DNA released and sent to the host

nucleus (Woodman et al. 2007). Since basal epithelial cell differentiation is highly controlled and replication only permitted in suprabasal cells undergoing maturity or ageing, HPV encodes proteins E6 and E7 to stimulate cell proliferation, prolong the cell cycle progression and evade apoptosis (Ghittoni et al. 2010). The host cell is then manipulated to permit viral replication resulting in the production of thousands of HPV copies in each infected cell. Within 2 to 3 weeks the HPV completes its life cycle consisting of migration from the basal layer to the superficial epithelium, maturity, ageing and death of the cervical cancer cell (Crosbie et al. 2013).

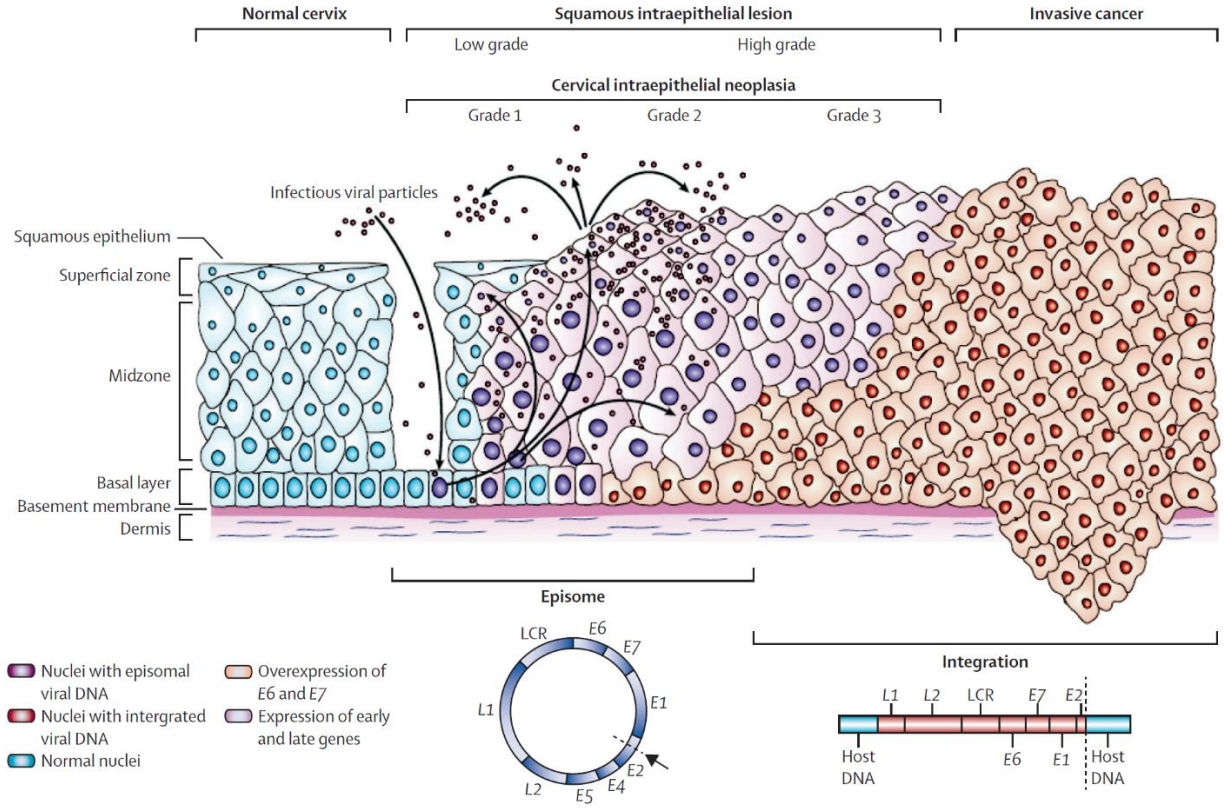

Figure 1.11 Human Papillomavirus (HPV) life cycle and genome (Crosbie et al. 2013)

HPV infects the basal layer of the cervical epithelium *via* microabrasions, expresses the early region HPV genes E1, E2, E4, E5, E6 and E7 and replicates episomal viral DNA. Further viral replication occurs in the mid and superficial epithelial zones with expression of late region HPV genes L1 and L2 and the early gene E4. Expressed L1 and L2 encapsulates progeny virions in the nucleus which are then released to infect new host cells. If unabated, the HPV infection ultimately results in high grade cervical cancer characterised by viral genome incorporation into the host chromosome, loss of E2 and increased expression of early genes E6 and E7

Infection with HPV results in the formation and appearance of precancerous lesions which may further develop into invasive cervical cancer (ICC) depending mainly on the strain of HPV causing the infection (Figure 1.12). The three recognised stages of cervical intraepithelial neoplasia (CIN) are: CIN1, exhibiting mild dysplasia; CIN2, exhibiting moderate dysplasia; and CIN3, exhibiting severe dysplasia and carcinoma in situ (Buckley et al. 1982). In this regard, high-grade squamous intraepithelial lesions (HGSIL, encompassing CIN2, CIN3 or CIN2 and CIN3) resulting from prolonged infection with high-risk HPV strains are likely to result in ICC (Khieu and Butler 2018). Low immune state diseases such as HIV/AIDS promote prolonged HPV infection and thus encourage the development of ICC by developing and maintaining CIN3.

Figure 1.12 Pictorial illustration of the progression from mild precancerous lesions to invasive cervical cancer (ICC) (Ibeanu 2011)

(A) Mild lesions extending into the endocervical canal, (B) mild lesions with skip patterns, (C) severe lesions with vascular punctation and mosaic features, and (D) invasive cervical carcinoma (ICC) in HIV immunocompromised patient

Invasive cervical cancer (ICC) is categorised into stages 0, 1A, 1B, 2A, 2B, 3A, 3B, 4A and 4B based on the progression of the lesions (Rambaldi 2014). Stage 0 corresponds to CIN3 and is characterised by the presence of cancerous cells in the innermost aspects of the cervical epithelium. In stage 1, the cancer is localised to the cervical tissue. Stage 1A is microscopically detected and presents with cancerous cells of 5 mm maximum depth and 7 mm maximum width. In stage 1B, the cancerous cells can be visualised without microscopic aid and are deeper than 5 mm and wider than 7 mm (Figure 1.13). Stage 2A presents with progression of cancer to the upper two thirds of the vagina but without the involvement of the uterus whereas stage 2B has uterine involvement. Stage 3A presents with the spread of cancer to the lower thirds of the vagina but without affecting the pelvis whereas stage 3B has pelvic involvement with possible spread to pelvic lymph nodes. In stage 4A, the cancer spreads to the bladder and rectum with pelvic lymph node involvement. In stage 4B, the cancer spreads beyond the pelvis to other parts of the body such as the abdominal cavity, gastro-intestinal tract, lungs, liver etc (Waggoner 2003).

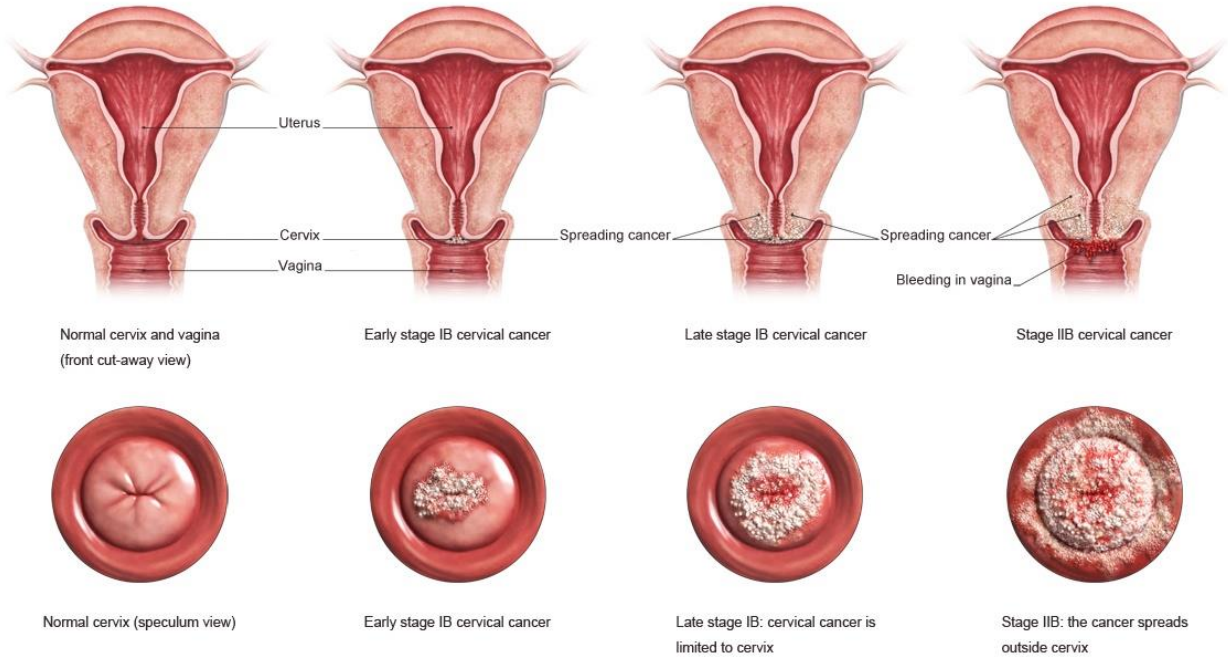

Figure 1.13 Illustration of cervical cancer progression from stages 1B to 2B (Everviz 2017)

1.3.3.1 Treatment of precancerous lesions and cervical cancer

Treatment of precancerous lesions depends on the stage of the lesions. In CIN1, the main treatment option is cryotherapy using liquid nitrogen to freeze the lesions. Apart from experiencing vaginal bleeding, discharge and pain, cryotherapy is usually well tolerated. In CIN2, cryotherapy can be used but surgery is advised for the purpose of excising the lower cervical epithelium. In places with poor medical facilities such as sub-Saharan Africa, the recommended surgical procedure in CIN2 is the loop electrosurgical excision procedure (LEEP) (Figure 1.14) (Odendal 2011).

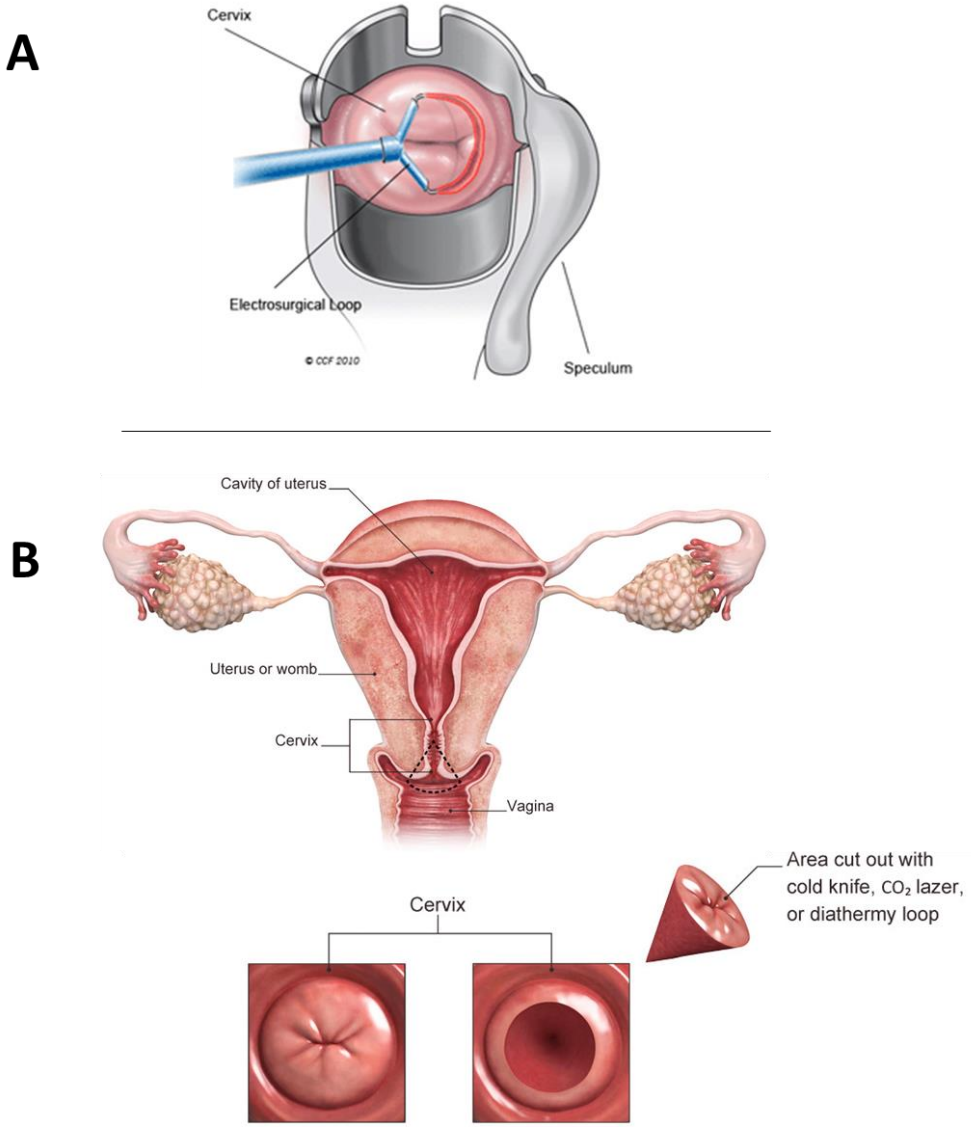

Figure 1.14 Illustrations showing the loop electrosurgical excision procedure (LEEP) (A) (Cleveland Clinic 2018) and conisation of the cervix (B) (Everviz 2017)

The LEEP method involves the excision of cervical tissue using a wire loop followed after by cauterisation and sealing with an electric current. As an alternative to LEEP, a cone of cervical tissue is removed in a process called conisation in order to eliminate precancerous cells underneath the epithelium (Landoni et al. 2007). In CIN3, the same methods in CIN1 and CIN2 can be employed except in severe or recurrent cases in which hysterectomy is ideal and most especially in post-menopausal women. The main options in the treatment of cervical cancer are surgery, radiotherapy and chemotherapy. In stages 1 and 2, treatment involves a combination of both internal and external radiotherapy, radical hysterectomy (Figure 1.15), pelvic lymphadenectomy and chemotherapy. Treatment for stages 3 and 4 involves the combination of internal and external radiotherapy, chemotherapy, radical hysterectomy, primary pelvic exenteration and palliative chemotherapy in distant metastases (Waggoner 2003). A major challenge in sub-Saharan Africa is the severe lack of access to radiation treatment. The preferred chemotherapy options for cervical cancer are those consisting of a cisplatin-based regimen (combined with either topotecan or paclitaxel in advanced cases) (Kamura and Ushijima 2013). However, due to cost implications, low income countries of sub-Saharan Africa are usually unable to adequately avail such combinations (Sitas et al. 2008; Martei et al. 2018).

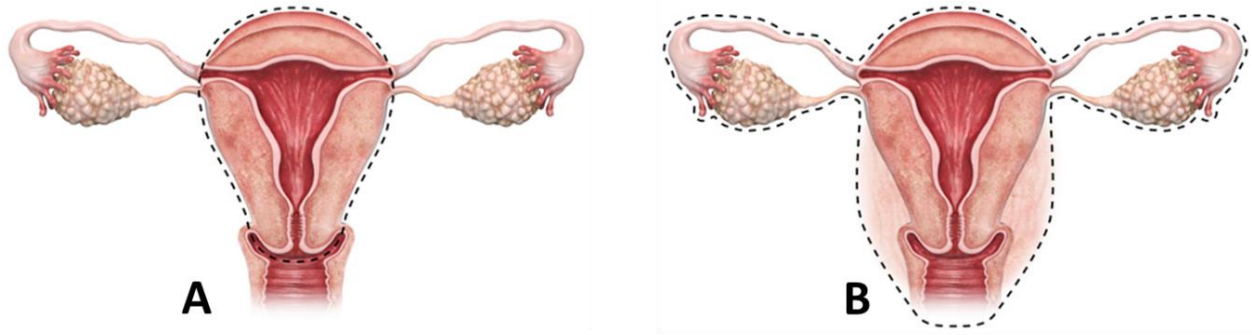

Figure 1.15 Illustrations showing total (A) and radical (B) hysterectomy (Everviz 2017)

1.3.3.2 The Henrietta Lacks (HeLa) cell line

The HeLa is an immortalised cervical cancer cell line obtained in 1951 by Dr. George Grey from the cervix of Ms. **He**nrietta **La**cks, a 30 year old patient with an aggressive adenocarcinoma of the cervix (Faussadier 2017). Though Ms. Henrietta Lacks passed on that very year, her cells have become the first successfully cultured immortal human cell line and are still being used today for scientific research (Lucey et al. 2009). Some of the breakthrough discoveries in science that have been achieved through the use of HeLa cells include the effects

of zero gravity in outer space, development of the polio vaccine, a Nobel Prize winning discovery of the link between HPV and cervical cancer with subsequent development of the HPV vaccine, the first human and animal hybrid cells, chromosome counting and major contributions in the understanding of leukaemia, the HIV virus and cancer (John Hopkins medicine 2018;MacDonald 2018). However, in the 1960's, a PhD student named Stanley Gartler discovered through a technique of isoenzyme analysis of glucose-6-phosphate dehydrogenase (G6PD) and phosphoglucomutase (PGM) electrophoretic polymorphisms that HeLa cells had in fact contaminated 19 other human cell lines with the same G6PD type A and PGM type 1 phenotypes (Gartler 1967; Gartler 1968; Masters 2002). This controversy sparked worldwide debates which ultimately led to the development of improved cell culture techniques. HeLa cells have since been found to contain Human Papillomavirus HPV-18 DNA with observed changes in microRNA expression (Meissner 1999).

1.3.3.3 Insights into African traditional healers' perceptions and practices on cervical cancer

It has been stated that about 80% of the African population rely on traditional medicines and practices as their primary source of health care (Mulaudzi 2003). Being the custodians of traditional African religion, customs and culture, the role played by traditional healers in the treatment and management of diseases among the African population cannot be ignored (Mokgobi 2014). It is therefore of paramount importance for scientific researchers to find out and be aware of the collective perceptions of traditional health givers towards the diagnosis and treatment of highly prevalent life-threatening diseases such as cervical cancer and to make strong attempts at harmonizing the two knowledge frontiers where possible.

In South Africa, traditional healers give the presented 'cancer' a diagnostic name based on its physical manifestations. For instance, the common terminologies used to describe cervical cancer among traditional healers in Limpopo are *Sesepidi*, meaning 'something that moves' and *Tlhagala*, a Sesotho word meaning 'to be worn out' (Mokgadi and Fhumulani 2008). Interestingly, these traditional terms are very similar in meaning to modern patho-physiological descriptions of cervical cancer such as 'metastasis' (*Sesepidi*) and tumour necrosis with foul vaginal discharge (*Tlhagala*). Other general terms for cancer in South Africa are *sefola, umdlavuza, lethala, thosola, seso, nyamakazi, fokozani, emfokozane, umhlavosi* and *imvelase,* most of which have similar or related meanings. The etiology of cervical cancer among African traditional beliefs is attributed to various factors such as inadequate intake of herbal medicines,

blasphemy towards ancestral spirits and as a form of retribution (Giger and Davidhizar 1995). Among the traditional healers of the Igbo tribe of Nigeria, cancer is generally believed to be caused by magic spells, bad blood, infections, bad air, incestuous behaviour and adultery. In these premises, cancer diagnosis incorporates the dual use of organic and spiritual methods with prescribed treatments including the use of plants, divinations, magic and psychotherapy (Dein 2004;Nwoha 1994). Among the traditional healers of Ga-Mothapo in South Africa, cervical cancer is believed to be caused by chain smoking, multiple sexual partners (*Ge mosadi a kitima le sekwata sa banna*), poor nutrition, early engagement in sexual activity, sexually transmitted infections (STIs) (*sekgalaka*) and genetic predispositions (Mokgadi and Fhumulani 2008). Though conventional science concedes that the precise etiological cause of cervical cancer is still unknown, some of the earlier identified risk factors include multiple sexual partners, early sexual practice, STIs, HIV/AIDS, smoking and intake of oral contraceptive pills (Brinton et al. 1987). By comparison, there is a striking resemblance between the perspectives of traditional African practices and conventional science on the risk factors of cervical cancer.

African traditional healers often mention irregular per vaginal bleeding, painful coitus, post-coital bleeding, dysmenorrhoea, lower abdominal pains, abnormal or foul smelling vaginal discharge, cervical lesions, pyrexia, polyuria, painful uterine growth (polyps) and feeling as if the 'womb is moving' as signs and symptoms of cervical cancer (Steyn and Muller 2000). In modern science, some of the reported early symptoms of cervical cancer are trans-vaginal hemorrhage, foul smelling vaginal discharge, post-coital discharge or bleeding and postmenopausal vaginal bleeding. If left untreated, the cervical cancer metastasises and symptoms progress with increased per vaginal bleeding, inguinal and/or supraclavicular lymphadenitis and the appearance of a continuous serosanguinous vaginal discharge which darkens and develops a foul necrotizing smell (López-Arias et al. 2017).

The African traditional treatment of cervical cancer focuses not only on curing the disease but also on promoting spiritual wellness and this is thought to be achieved by 'extracting' or 'pulling' the *Sesepedi* out of the uterus. Traditional treatment regimen for cervical cancer normally incorporate oral administration of herbal decoctions, direct application of a crushed bluestone (*mbapani*) and *Pentanisia prunelloides* (*stema-mollo*) mixture onto the lesions, formulation and intra-vaginal insertion of herbal 'pessaries' (*lekoni sekgalaka*), steam inhalation and incisions (Steyn and Muller 2000). These traditional methods are similar to those

practiced in modern medicine such as oral administration of chemotherapy (herbal decoctions), surgical removal of tumours (incisions) and radiotherapy (steam treatment).

In-vitro studies have shown *P. prunelloides* to possess strong uterotonic (ecbolic) properties (Moteetee and Seleteng Kose 2016). This may provide the rationale for its traditional use in cervical cancer to 'pull' the *Sesepedi* out of the uterus and to reduce per vaginal bleeding. *P. prunelloides* has also been reported to possess *in-vitro* anti-inflammatory, antibacterial and antiviral properties, which are applicable to the amelioration of cervical cancer since it's a virally induced (HPV), inflammatory disease (Van Wyk et al. 2009). Phytochemical studies of *P. prunelloides* leaves, roots and rhizomes revealed the presence of oleanolic acid, palmitic acid, diosgenin, the flavonoids epigallocatechin gallate (EGCG), epicatechin, epicatechin gallate and their derivatives (Yff et al. 2002; Mpofu et al. 2014; Mpofu et al. 2015). Epigallocatechin gallate (EGCG), the major compound in *P. prunelloides* rhizomes, has been reported to possess anti-cancer activity against HeLa and CaSki cervical cancer cell lines *via* the induction of telomere fragmentation, cell cycle arrest, induction of apoptosis and modulation of gene expression (also see Section 5.2.2.1) (Ahn et al. 2003; Li et al. 2005). This shows that African traditional healers have, in their own terms, a concise understanding of cervical cancer pathophysiology, the knowledge to identify signs and symptoms of the disease, practical ethnomedicinal experience to provide sustainable care and adequate medicinal plant repositories to at least assist in the discovery of newer and more effective cervical cancer treatments. Dialogue between traditional health practitioners and scientific researchers must therefore be encouraged to promote the sharing of information.

1.4 Research rationale: aims and objectives

With about 44 % of all cancer morbidity and 53 % of all cancer mortality occurring in countries with a low to medium Human Development Index (HDI), cancer is rapidly emerging as a serious threat to public health in sub-Saharan Africa. According to the International Agency for Research on Cancer (IARC) there will be 1.28 million new cancer cases and 970 000 cancer deaths in Africa alone by the year 2030 (Ferlay et al. 2010). In sub-Saharan Africa, the few positive strides in cancer management are being constantly met with the unavailability of cancer screening measures and the inaccessibility of recommended chemoradiotherapy regimen (only 10 % of the African population has access to radiotherapy) due to cost implications and lack of proper infrastructure to implement established drug supply chain systems (Cazap et al. 2016). Most developing countries can only afford to procure the most basic anti-cancer drugs which are also frequently unavailable due to intermittent supplies (INCTR 2018). These factors, coupled with the heavy HIV/AIDS burden in the sub-Saharan African region, largely contribute to the poor prognosis in African cancer patients. Among the greater concerns is cervical cancer, which currently has the highest recordings within Africa coming from Central and Southern Africa, including the countries Zambia, Zimbabwe, Malawi, Namibia and Mozambique. To put it into perspective, the sub-Saharan African female has a 3.8% chance of developing cervical cancer and a 2.5% chance that if she does in fact contract cervical cancer, it will eventually be the cause of her death (Cancer Atlas 2018). The toxicity of conventional anti-cancer drugs at therapeutic dosages coupled with the additional costs for symptomatic treatment and palliative care can be a source of discouragement to health seeking cancer patients. With > 80 % of the African population resorting to African traditional medicine as their primary source of health care, there is a desperate need to bridge the gap between conventional and traditional health care both in knowledge and in practice. One way of doing this would be to increase scientific interest in the African methods of treatment, particularly African medicinal plants.

The aim of this study was to identify the frequently used, yet least studied, medicinal plants in African traditional medicine to treat ‘cancers’ and to further explore their anti-cancer potential with the purpose of discovering novel phyto-chemotherapeutics. The HeLa cervical cancer cell line was used for all bio-assay experiments to ensure that the study was relevant to the current cancer picture in the sub-Saharan and most especially Southern African region.

To achieve these aims, the following objectives were undertaken:

- Identification and selection of potential plant sources for novel cytotoxic natural compounds through a literature search for frequently used, but least studied, African medicinal plants.
- Determination of the *in vitro* cytotoxic activity of four selected African medicinal plant extracts against HeLa cervical cancer cells.
- Bio-assay guided fractionation and isolation of natural compound(s) from the active medicinal plant extract(s).
- Structural characterisation of the isolated natural compound(s).
- Evaluation of the *in vitro* cytotoxic activity of the isolated natural compound(s)
- Determination of the *in vitro* mechanism of cell death elicited by the cytotoxic natural compound(s).
- Identification of potential biological targets for the isolated cytotoxic compound(s) using *in silico* molecular docking.

1.5 Structure of thesis

This thesis is divided into six chapters, consisting of a literature review and five experimental chapters (2 – 6) in successive fashion. The literature review gives an overview of the subject matter with deliberate effort made to ensure that the reader is adequately prepared in understanding the experimental chapters that follow. Each experimental chapter contains a concise introduction with the aims clearly stated. This is followed by the results and discussion section. The experimental section is given after the discussion of the results with references appearing at the end of each chapter.

In Chapter 2, results are given for the *in vitro* cytotoxicity screening of four selected African medicinal plant extracts against the HeLa cell line. Chapter 3 discusses natural products as a powerful resource in anti-cancer drug discovery and details the isolation and structural characterisation of a novel flavonoid *C*-glycoside from the bulb extract of *Drimia altissima*. Chapter 4 introduces High Content Analysis (HCA) as an emerging tool in natural product-based early drug discovery and reports HCA results for the *in vitro* anti-cancer activity of *Drimia altissima* fractions and isolated flavonoid *C*-glycoside. Chapter 5 discusses flavonoids as nutraceuticals with promising anti-cancer effects and determines the mechanism of cell death induced by the isolated flavonoid *C*-glycoside. Chapter 6 identifies a potential biological target for the isolated flavonoid *C*-glycoside through *in silico* molecular docking. Finally, a conclusion is made and recommendations are given for future studies.

References

Adrain, C., Slee, E.A., Harte, M.T., & Martin, S.J. 1999. Regulation of Apoptotic Protease Activating Factor-1 Oligomerization and Apoptosis by the WD-40 Repeat Region. *Journal of Biological Chemistry*, 274, (30) 20855-20860 available from: http://www.jbc.org/content/274/30/20855.abstract

Ahn, W.S., Huh, S.W., Bae, S.M., Lee, I.P., Lee, J.M., Namkoong, S.E., Kim, C.K., & Sin, J.I. 2003. A Major Constituent of Green Tea, EGCG, Inhibits the Growth of a Human Cervical Cancer Cell Line, CaSki Cells, through Apoptosis, G1 Arrest, and Regulation of Gene Expression. *DNA and Cell Biology*, 22, (3) 217-224 available from: https://doi.org/10.1089/104454903321655846 Accessed 25 November 2018.

Alam, J.J. 2003. Apoptosis: target for novel drugs. *Trends in Biotechnology*, 21, (11) 479-483 available from: http://www.sciencedirect.com/science/article/pii/S0167779903002324

Alberts, B., Johnson, A., Lewis, J., Raff, M., Roberts, K., & Walter, P. 2007. *Molecular biology of the cell*, 5 ed. New York, Garland Science.

Albrecht, J.H., Poon, R.Y., Ahonen, C.L., Rieland, B.M., Deng, C., & Crary, G.S. 1998. Involvement of p21 and p27 in the regulation of CDK activity and cell cycle progression in the regenerating liver. *Oncogene*, 16, 2141 available from: https://doi.org/10.1038/sj.onc.1201728

Alt, J.R., Cleveland, J.L., Hannink, M., & Diehl, J.A. 2000. Phosphorylation-dependent regulation of cyclin D1 nuclear export and cyclin D1-dependent cellular transformation. *Genes & development*, 14, (24) 3102-3114 available from: https://www.ncbi.nlm.nih.gov/pubmed/11124803

American Cancer Society 2011, *Cancer in Africa* Atlanta.

American Cancer Society. Early History of Cancer. https://www.cancer.org/cancer/cancer-basics/history-of-cancer/what-is-cancer.html . 2018a.
Ref Type: Online Source

American Cancer Society. Early Theories about Cancer Causes. https://www.cancer.org/cancer/cancer-basics/history-of-cancer/cancer-causes-theories-throughout-history.html . 2018b. 12-3-2018b.
Ref Type: Online Source

Annunziato, T.A. 2008. DNA Packaging: Nucleosomes and Chromatin. *Nature Education*, 1, (1) 26

Apt, D., Watts, R.M., Suske, G., & Bernard, H.U. 1996. High Sp1/Sp3 Ratios in Epithelial Cells during Epithelial Differentiation and Cellular Transformation Correlate with the Activation of the HPV-16 Promoter. *Virology*, 224, (1) 281-291 available from: http://www.sciencedirect.com/science/article/pii/S0042682296905309

Artandi, S.E. & DePinho, R.A. 2010. Telomeres and telomerase in cancer. *Carcinogenesis*, 31, (1) 9-18 available from: http://dx.doi.org/10.1093/carcin/bgp268

Ashkenazi, A. 2002. Targeting death and decoy receptors of the tumour-necrosis factor superfamily. *Nature Reviews Cancer*, 2, 420 available from: https://doi.org/10.1038/nrc821

Ashkenazi, A., Fairbrother, W.J., Leverson, J.D., & Souers, A.J. 2017. From basic apoptosis discoveries to advanced selective BCL-2 family inhibitors. *Nature Reviews Drug Discovery*, 16, 273 available from: https://doi.org/10.1038/nrd.2016.253

Bahassi, E.M., Ovesen, J.L., Riesenberg, A.L., Bernstein, W.Z., Hasty, P.E., & Stambrook, P.J. 2008. The checkpoint kinases Chk1 and Chk2 regulate the functional associations between hBRCA2 and Rad51 in response to DNA damage. *Oncogene*, 27, 3977 available from: https://doi.org/10.1038/onc.2008.17

Bardeesy, N. & Sharpless, N.E. 2006. RAS unplugged: Negative feedback and oncogene-induced senescence. *Cancer Cell*, 10, (6) 451-453 available from: https://doi.org/10.1016/j.ccr.2006.11.015 Accessed 2 December 2018.

Bartek, J. & Lukas, J. 2003. Chk1 and Chk2 kinases in checkpoint control and cancer. *Cancer Cell*, 3, (5) 421-429 available from: http://www.sciencedirect.com/science/article/pii/S1535610803001107

Becila, S., Mendez, C., Coulis, G., Labas, R., Astruc, T., Picard, B., Boudjellal, A., Pelissier, P., Bremaud, L., & Ouali, A. 2010. *Postmortem muscle cells die through apoptosis*, 231 ed.

Blackford, A.N. & Jackson, S.P. 2017. ATM, ATR, and DNA-PK: The Trinity at the Heart of the DNA Damage Response. *Molecular Cell*, 66, (6) 801-817 available from: https://doi.org/10.1016/j.molcel.2017.05.015 Accessed 27 November 2018.

Blagosklonny, M.V. & Pardee, A.B. 2002. The Restriction Point of the Cell Cycle. *Cell Cycle*, 1, (2) 102-109 available from: https://doi.org/10.4161/cc.1.2.108

Bray, F., Ferlay, J., Soerjomataram, I., Siegel, R.L., Torre, L.A., & Jemal, A. 2018. Global cancer statistics 2018: GLOBOCAN estimates of incidence and mortality worldwide for 36 cancers in 185 countries. *CA: A Cancer Journal for Clinicians*, 68, (6) 394-424 available from: https://doi.org/10.3322/caac.21492 Accessed 23 November 2018.

Bray, F., Jemal, A., Grey, N., Ferlay, J., & Forman, D. 2012. Global cancer transitions according to the Human Development Index (2008 - 2030): a population-based study. *The Lancet Oncology*, 13, (8) 790-801 available from: https://doi.org/10.1016/S1470-2045(12)70211-5 Accessed 23 November 2018.

Breasted, J.H. 1930. *The Edwin Smith Surgical Papyrus*, 1 ed. Chicago, Illinois, The University of Chicago Press.

Brinton, L.A., Hamman, R.F., Huggins, G.R., Lehman, H.F., Levine, R.S., Mailin, K., & Fraumeni, J. 1987. Sexual and Reproductive Risk Factors for Invasive Squamous Cell Cervical Cancer. *JNCI: Journal of the National Cancer Institute*, 79, (1) 23-30 available from: http://dx.doi.org/10.1093/jnci/79.1.23

Brooks, C.L. & Gu, W. 2003. Ubiquitination, phosphorylation and acetylation: the molecular basis for p53 regulation. *Current Opinion in Cell Biology*, 15, (2) 164-171 available from: http://www.sciencedirect.com/science/article/pii/S0955067403000036

Buckley, C.H., Butler, E.B., & Fox, H. 1982. Cervical intraepithelial neoplasia. *Journal of Clinical Pathology*, 35, (1) 1 available from: http://jcp.bmj.com/content/35/1/1.abstract

Burd, E.M. 2003. Human Papillomavirus and Cervical Cancer. *Clinical Microbiology Reviews*, 16, (1) 1 available from: http://cmr.asm.org/content/16/1/1.abstract

Bynum, W.F. 1980. The genesis of cancer. A study in the history of ideas. *Medical History*, 24, (3) 360-361 available from: https://www.ncbi.nlm.nih.gov/pmc/articles/PMC1082669/

Cancer Atlas. Infection-related cancers predominate in many areas in sub-Saharan Africa. http://canceratlas.cancer.org/the-burden/cancer-in-sub-saharan-africa/ . 2018.
Ref Type: Online Source

Cazap, E., Magrath, I., Kingham, T.P., & Elzawawy, A. 2016. Structural Barriers to Diagnosis and Treatment of Cancer in Low- and Middle-Income Countries: The Urgent Need for Scaling Up. *Journal of clinical oncology : official journal of the American Society of Clinical Oncology*, 2015/11/17, (1) 14-19 available from: https://www.ncbi.nlm.nih.gov/pubmed/26578618

Charras, T.G. 2008. A short history of blebbing. *Journal of Microscopy*, 231, (3) 466-478 available from: https://doi.org/10.1111/j.1365-2818.2008.02059.x Accessed 29 November 2018.

Chehab, N.H., Malikzay, A., Stavridi, E.S., & Halazonetis, T.D. 1999. Phosphorylation of Ser-20 mediates stabilization of human p53 in response to DNA damage. *Proceedings of the National Academy of Sciences of the United States of America*, 96, (24) 13777-13782 available from: https://www.ncbi.nlm.nih.gov/pubmed/10570149

Chipuk, J.E. & Green, D.R. 2008. How do BCL-2 proteins induce mitochondrial outer membrane permeabilization? *Trends in Cell Biology*, 18, (4) 157-164 available from: http://www.sciencedirect.com/science/article/pii/S0962892408000664

Cleveland Clinic. Loop Electrosurgical Excision Procedure (LEEP). https://my.clevelandclinic.org/health/treatments/4711-loop-electrosurgical-excision-procedure-leep . 2018.
Ref Type: Online Source

Clifford, G.M., Smith, J.S., Plummer, M., Mu+¦oz, N., & Franceschi, S. 2003. Human papillomavirus types in invasive cervical cancer worldwide: a meta-analysis. *British journal of cancer*, 2003/01/28, (1) 63-73 available from: https://www.ncbi.nlm.nih.gov/pubmed/12556961

Contassot, E., Gaide, O., & French, L.E. 2007. Death Receptors and Apoptosis. *Dermatologic Clinics*, 25, (4) 487-501 available from: http://www.sciencedirect.com/science/article/pii/S073386350700068X

Creagh, E.M. & Martin, S.J. 2001. Caspases: cellular demolition experts. *Biochemical Society Transactions*, 29, (6) 696 available from: http://www.biochemsoctrans.org/content/29/6/696.abstract

Crissman, H.A. & Tobey, R.A. 1974. Cell-Cycle Analysis in 20 Minutes. *Science*, 184, (4143) 1297 available from: http://science.sciencemag.org/content/184/4143/1297.abstract

Crosbie, E.J., Einstein, M.H., Franceschi, S., & Kitchener, H.C. 2013. Human papillomavirus and cervical cancer. *The Lancet*, 382, (9895) 889-899 available from: https://doi.org/10.1016/S0140-6736(13)60022-7 Accessed 1 December 2018.

Dahiya, A., Gavin, M.R., Luo, R.X., & Dean, D.C. 2000. Role of the LXCXE binding site in Rb function. *Molecular and cellular biology*, 20, (18) 6799-6805 available from: https://www.ncbi.nlm.nih.gov/pubmed/10958676

Dayton, J.B. & Piccolo, S.R. 2017. Classifying cancer genome aberrations by their mutually exclusive effects on transcription. *BMC medical genomics*, 10, (Suppl 4) 66 available from: https://www.ncbi.nlm.nih.gov/pubmed/29322935

Dein, S. 2004. Explanatory models of and attitudes towards cancer in different cultures. *The Lancet Oncology*, 5, (2) 119-124 available from: https://doi.org/10.1016/S1470-2045(04)01386-5 Accessed 24 November 2018.

Delbridge, A.R.D., Grabow, S., Strasser, A., & Vaux, D.L. 2016. Thirty years of BCL-2: translating cell death discoveries into novel cancer therapies. *Nature Reviews Cancer*, 16, 99 available from: https://doi.org/10.1038/nrc.2015.17

Elmore, S. 2007. Apoptosis: a review of programmed cell death. *Toxicologic pathology*, 35, (4) 495-516 available from: https://www.ncbi.nlm.nih.gov/pubmed/17562483

Everviz. Medical Illustrations of the Uterus. https://www.behance.net/gallery/55206621/Medical-illustrations-of-the-Uterus . 2017.
Ref Type: Online Source

Faussadier, X. HeLa cells: Origin of this important cell line in life science research. https://www.tebu-bio.com/blog/2017/11/28/hela-cells-the-first-cell-line/ . 11-28-2017.
Ref Type: Online Source

Ferlay, J., Shin, H.R., Bray, F., Forman, D., Mathers, C., & Maxwell Parkin, D. 2010. Estimates of worldwide burden of cancer in 2008: GLOBOCAN. *International Journal of Cancer*, 127, 2893-2917

Ferlay, J., Soerjomataram, I., Dikshit, R., Eser, S., Mathers, C., Rebelo, M., Parkin, D.M., Forman, D., & Bray, F. 2014. Cancer incidence and mortality worldwide: Sources, methods and major patterns in GLOBOCAN 2012. *International Journal of Cancer*, 136, (5) E359-E386 available from: https://doi.org/10.1002/ijc.29210 Accessed 23 November 2018.

Fulda, S. & Debatin, K.M. 2006. Extrinsic versus intrinsic apoptosis pathways in anticancer chemotherapy. *Oncogene*, 25, 4798 available from: https://doi.org/10.1038/sj.onc.1209608

Gartler, M.S. 1968. Apparent HeLa Cell Contamination of Human Heteroploid Cell Lines. *Nature*, 217, 750 available from: https://doi.org/10.1038/217750a0

Gartler, S.M. 1967. Genetic markers as tracers in cell culture. *National Cancer Institute monograph*, 26, 167-195 available from: http://europepmc.org/abstract/MED/4864103

Ghittoni, R., Accardi, R., Hasan, U., Gheit, T., Sylla, B., & Tommasino, M. 2010. The biological properties of E6 and E7 oncoproteins from human papillomaviruses. *Virus Genes*, 40, (1) 1-13 available from: https://doi.org/10.1007/s11262-009-0412-8

Giger, J.N. & Davidhizar, R.E. 1995. *Transcultural nursing : assessment and intervention*, 2 ed. St.Louis, MO, Mosby-Year Book.

Goodman, R. S. 2008, "Chapter 10 - Programmed Cell Death," *In Medical Cell Biology*, 3 ed. S. R. Goodman, ed., San Diego: Academic Press, pp. 291-307.

Goswami, S., Sahai, E., Wyckoff, J.B., Cammer, M., Cox, D., Pixley, F.J., Stanley, E.R., Segall, J.E., & Condeelis, J.S. 2005. Macrophages Promote the Invasion of Breast Carcinoma Cells via a Colony-Stimulating Factor-1/Epidermal Growth Factor Paracrine Loop. *Cancer Research*, 65, (12) 5278 available from: http://cancerres.aacrjournals.org/content/65/12/5278.abstract

Grivennikov, S.I. & Karin, M. 2010. Inflammation and oncogenesis: a vicious connection. *Current Opinion in Genetics & Development*, 20, (1) 65-71 available from: http://www.sciencedirect.com/science/article/pii/S0959437X09001919

Hanahan, D. & Weinberg, R.A. 2000. The Hallmarks of Cancer. *Cell*, 100, (1) 57-70 available from: https://doi.org/10.1016/S0092-8674(00)81683-9 Accessed 2 December 2018.

Hanahan, D. & Weinberg, R. 2011. Hallmarks of Cancer: The Next Generation. *Cell*, 144, (5) 646-674 available from: https://doi.org/10.1016/j.cell.2011.02.013 Accessed 2 December 2018.

Hans, F. & Dimitrov, S. 2001. Histone H3 phosphorylation and cell division. *Oncogene*, 20, 3021 available from: https://doi.org/10.1038/sj.onc.1204326

Hicklin, D.J. & Ellis, L.M. 2005. Role of the Vascular Endothelial Growth Factor Pathway in Tumor Growth and Angiogenesis. *Journal of Clinical Oncology*, 23, (5) 1011-1027 available from: https://doi.org/10.1200/JCO.2005.06.081 Accessed 2 December 2018.

Hochegger, H., Takeda, S., & Hunt, T. 2008. Cyclin-dependent kinases and cell-cycle transitions: does one fit all? *Nature Reviews Molecular Cell Biology*, 9, 910 available from: https://doi.org/10.1038/nrm2510

Hoffmann, I. 2000. The role of Cdc25 phosphatases in cell cycle checkpoints. *Protoplasma*, 211, (1) 8-11 available from: https://doi.org/10.1007/BF01279894

IARC 2007. *IARC Monographs on the Evaluation of Carcinogenic Risks to Humans, No. 90.* Lyon, The International Agency for Research on Cancer.

IARC 2014, *World Cancer Report 2014*.

Ibeanu, O.A. 2011. Molecular pathogenesis of cervical cancer. *Cancer Biology & Therapy*, 11, (3) 295-306 available from: https://doi.org/10.4161/cbt.11.3.14686

INCTR. Cancer in low- and middle-income countries. Magrath, Ian. http://www.inctr.org/network-magazine/current-edition-93/presidents-message/cancer-in-low-and-middle-income-countries/ . 2018.
Ref Type: Online Source

Israels, E.D. & Israels, L.G. 2009. The Cell Cycle. *STEM CELLS*, 19, (1) 88-91 available from: https://doi.org/10.1634/stemcells.19-1-88 Accessed 26 November 2018.

John Hopkins medicine. The Legacy of Henrietta Lacks. https://www.hopkinsmedicine.org/henriettalacks/importance-of-hela-cells.html . 2018.
Ref Type: Online Source

Kalkavan, H. & Green, D.R. 2017. MOMP, cell suicide as a BCL-2 family business. *Cell death and differentiation*, 25, 46 available from: https://doi.org/10.1038/cdd.2017.179

Kamura, T. & Ushijima, K. 2013. Chemotherapy for advanced or recurrent cervical cancer. *Taiwanese Journal of Obstetrics and Gynecology*, 52, (2) 161-164 available from: http://www.sciencedirect.com/science/article/pii/S1028455913000594

Khieu, M. & Butler, L. S. Cancer, Squamous Cell, High Grade Squamous Intraepithelial Lesion (HGSIL). https://www.ncbi.nlm.nih.gov/books/NBK430728/ . 2018. Treasure Island, StatPearls Publishing.
Ref Type: Online Source

Kouzarides, T. 2007. Chromatin Modifications and Their Function. *Cell*, 128, (4) 693-705 available from: http://www.sciencedirect.com/science/article/pii/S0092867407001845

Krämer, A., Mailand, N., Lukas, C., Syljuåsen, R.G., Wilkinson, C.J., Nigg, E.A., Bartek, J., & Lukas, J. 2004. Centrosome-associated Chk1 prevents premature activation of cyclin-BGÇôCdk1 kinase. *Nature Cell Biology*, 6, 884 available from: https://doi.org/10.1038/ncb1165

Kroemer, G., Galluzzi, L., Vandenabeele, P., Abrams, J., Alnemri, E.S., Baehrecke, E.H., Blagosklonny, M.V., El-Deiry, W.S., Golstein, P., Green, D.R., Hengartner, M., Knight, R.A., Kumar, S., Lipton, S.A., Malorni, W., Nuñez, G., Peter, M.E., Tschopp, J., Yuan, J., Piacentini, M., Zhivotovsky, B., Melino, G., & Nomenclature Committee on Cell Death 2009. Classification of cell death: recommendations of the Nomenclature Committee on Cell Death 2009. *Cell death and differentiation*, 2008/10/10, (1) 3-11 available from: https://www.ncbi.nlm.nih.gov/pubmed/18846107

Krumholtz, S.-L. The Cell Eukaryotic Cycle. http://www.slk-art.com/#/new-page/ . 2018.

Ref Type: Online Source

Lakhtakia, R. 2014. A Brief History of Breast Cancer: Part I: Surgical domination reinvented. *Sultan Qaboos University Medical Journal*, 14, (2) e166-e169 available from: http://www.ncbi.nlm.nih.gov/pmc/articles/PMC3997531/

Landoni, F., Parma, G., Peiretti, M., Zanagnolo, V., Sideri, M., Colombo, N., & Maggioni, A. 2007. Chemo-conization in early cervical cancer. *Gynecologic Oncology*, 107, (1, Supplement) S125-S126 available from: http://www.sciencedirect.com/science/article/pii/S0090825807004830

Lee, J.T. & Gu, W. 2013. SIRT1: Regulator of p53 Deacetylation. *Genes & cancer*, 4, (3-4) 112-117 available from: https://www.ncbi.nlm.nih.gov/pubmed/24020002

Leist, M. & Nicotera, P. 1997. The Shape of Cell Death. *Biochemical and Biophysical Research Communications*, 236, (1) 1-9 available from: http://www.sciencedirect.com/science/article/pii/S0006291X9796890X

Letai, A.G. 2008. Diagnosing and exploiting cancer's addiction to blocks in apoptosis. *Nature Reviews Cancer*, 8, 121 available from: https://doi.org/10.1038/nrc2297

Levine, M. J. Recognizing the Incurable in Ancient Egypt. https://www.geripal.org/2015/11/recognizing-incurable-in-ancient-egypt.html . 2015.
Ref Type: Online Source

Li, B., Carey, M., & Workman, J.L. 2007. The Role of Chromatin during Transcription. *Cell*, 128, (4) 707-719 available from: http://www.sciencedirect.com/science/article/pii/S0092867407001092

Li, W.g., Li, Q.h., & Tan, Z. 2005. Epigallocatechin gallate induces telomere fragmentation in HeLa and 293 but not in MRC-5 cells. *Life Sciences*, 76, (15) 1735-1746 available from: http://www.sciencedirect.com/science/article/pii/S002432050401029X

Liu, D., Perfettini, J. L., & Brenner, C. 2018, "Mitochondrial Regulation of Cell Death," *In Mitochondrial Biology and Experimental Therapeutics*, P. J. Oliveira, ed., Cham: Springer International Publishing, pp. 75-90.

Lockshin, R.A. & Beaulaton, J. 1974. Programmed cell death. *Life Sciences*, 15, (9) 1549-1565 available from: http://www.sciencedirect.com/science/article/pii/002432057490321X

Lockshin, R.A. & Zakeri, Z. 2001. Programmed cell death and apoptosis: origins of the theory. *Nature Reviews Molecular Cell Biology*, 2, 545 available from: https://doi.org/10.1038/35080097

López-Arias, A., Isla-Ortiz, D., Barquet-Muñoz, S., & Cantú-de-León, F. D. 2017, "Cervical Cancer Staging," *In Cervical Cancer*, G. J. de la Garza-Salazar, F. Morales-Vásquez, & A. Meneses-Garcia, eds., Switzerland: Springer, pp. 117-132.

Loughery, J., Cox, M., Smith, L.M., & Meek, D.W. 2014. Critical role for p53-serine 15 phosphorylation in stimulating transactivation at p53-responsive promoters. *Nucleic acids research*, 2014/06/07, (12) 7666-7680 available from: https://www.ncbi.nlm.nih.gov/pubmed/24928858

Lucey, B.P., Nelson-Rees, W.A., & Hutchins, G.M. 2009. Henrietta Lacks, HeLa Cells, and Cell Culture Contamination. *Archives of Pathology & Laboratory Medicine*, 133, (9) 1463-1467 available from: http://www.archivesofpathology.org/doi/abs/10.1043/1543-2165-133.9.1463 Accessed 2 December 2018.

Lundberg, A.S. & Weinberg, R.A. 1998. Functional inactivation of the retinoblastoma protein requires sequential modification by at least two distinct cyclin-cdk complexes. *Molecular and cellular biology*, 18, (2) 753-761 available from: https://www.ncbi.nlm.nih.gov/pubmed/9447971

Luzzati, T., Parenti, A., & Rughi, T. 2018. Economic Growth and Cancer Incidence. *Ecological Economics*, 146, 381-396 available from: http://www.sciencedirect.com/science/article/pii/S0921800917304913

MacDonald, A. 5 Contributions HeLa Cells Have Made to Science. https://www.technologynetworks.com/cell-science/lists/5-contributions-hela-cells-have-made-to-science-305036 . 2018. Technology Networks.
Ref Type: Online Source

Marie, S.K.N. & Shinjo, S.M.O. 2011. Metabolism and brain cancer. *Clinics (Sao Paulo, Brazil)*, 66 Suppl 1, (Suppl 1) 33-43 available from: https://www.ncbi.nlm.nih.gov/pubmed/21779721

Martei, M.Y., Chiyapo, S., Grover, S., Ramogola-Masire, D., Dryden-Peterson, S., Shulman, N.L., & Tapela, N. 2018. Availability of WHO Essential Medicines for Cancer Treatment in Botswana. *Journal of Global Oncology* 1-8

Masters, J.R. 2002. HeLa cells 50 years on: the good, the bad and the ugly. *Nature Reviews Cancer*, 2, 315 available from: https://doi.org/10.1038/nrc775

McArthur, K. & Kile, B.T. 2018. Apoptotic Caspases: Multiple or Mistaken Identities? *Trends in Cell Biology*, 28, (6) 475-493 available from: http://www.sciencedirect.com/science/article/pii/S0962892418300278

Meadows, C.J., Shepperd, A.L., Vanoosthuyse, V., Lancaster, C.T., Sochaj, M.A., Buttrick, J.G., Hardwick, G.K., & Millar, B.J. 2011. Spindle Checkpoint Silencing Requires Association of PP1 to Both Spc7 and Kinesin-8 Motors. *Developmental Cell*, 20, (6) 739-750 available from: https://doi.org/10.1016/j.devcel.2011.05.008 Accessed 26 November 2018.

Meissner, D. 1999. *Nucleotide sequences and further characterization of human papillomavirus DNA present in the CaSki, SiHa and HeLa cervical carcinoma cell lines*, 80 (Pt 7) ed.

Mohan, C. 2009. *Signal Transduction - A Short Overview of its Role in Health and Disease* San Diego, CA, Merck.

Mokgadi, S.M. & Fhumulani, M.M. 2008. The Perceptions Of Traditional Healers Of Cervical Cancer Care At Ga Mothapo Village In Limpopo Province. *Indilinga*, 7, (1) 103-116

Mokgobi, M.G. 2014. Understanding traditional African healing. *African journal for physical health education, recreation, and dance*, 20, (Suppl 2) 24-34 available from: https://www.ncbi.nlm.nih.gov/pubmed/26594664

Morgan, O.D. 2007. *The Cell Cycle - Principles of Control* Singapore, New Science Press Ltd.

Moser, J., Miller, I., Carter, D., & Spencer, S.L. 2018. Control of the Restriction Point by Rb and p21. *Proceedings of the National Academy of Sciences*, 115, (35) E8219 available from: http://www.pnas.org/content/115/35/E8219.abstract

Moteetee, A. & Seleteng Kose, L. 2016. Medicinal plants used in Lesotho for treatment of reproductive and post reproductive problems. *Journal of Ethnopharmacology*, 194, 827-849 available from: http://www.sciencedirect.com/science/article/pii/S0378874116314611

Mpofu, J.S., Msagati, A.M.T., & Klause, R.W.M. 2014. Cytotoxicity, phytochemical analysis and antioxidant activity of crude extracts from rhizomes of *Elephantorrhiza elephantina* and *Pentanisia prunelloides*. *African journal of traditional, complementary, and alternative medicines*, 111, 34-52

Mpofu, J.S., Msagati, A.M.T., & Krause, R.W.M. 2015. Flavonoids from the rhizomes of *Elephantorrhiza elephantina* and *Pentanisia prunelloides*. *Journal of Medicinal Plants Research*, 9, (16) 531-549

Mulaudzi, F. 2003. *A tribute to traditional healers*, 27 ed.

Mullaney, J.M., Mills, R.E., Pittard, W.S., & Devine, S.E. 2010. Small insertions and deletions (INDELs) in human genomes. *Human Molecular Genetics*, 2010/09/21, (R2) R131-R136 available from: https://www.ncbi.nlm.nih.gov/pubmed/20858594

Nag, S., Qin, J., Srivenugopal, K.S., Wang, M., & Zhang, R. 2013. The MDM2-p53 pathway revisited. *Journal of biomedical research*, 2013/06/06, (4) 254-271 available from: https://www.ncbi.nlm.nih.gov/pubmed/23885265

Nakayama, K. & Nakayama, K. 1999. Cip/Kip cyclin-dependent kinase inhibitors: brakes of the cell cycle engine during development. *BioEssays*, 20, (12) 1020-1029 available from: https://doi.org/10.1002/(SICI)1521-1878(199812)20:12<1020::AID-BIES8>3.0.CO;2-D Accessed 27 November 2018.

Neganova, I. & Lako, M. 2008. G1 to S phase cell cycle transition in somatic and embryonic stem cells. *Journal of anatomy*, 213, (1) 30-44 available from: https://www.ncbi.nlm.nih.gov/pubmed/18638068

Nevins, J.R. 2001. The Rb/E2F pathway and cancer. *Human Molecular Genetics*, 10, (7) 699-703 available from: http://dx.doi.org/10.1093/hmg/10.7.699

Nwoha, I.A. 1994. Traditional healers and perceptions of the causes and treatment of cancer. *Cancer Nursing*, 17, (6) 470-478

Obaya, A.J. & Sedivy, J.M. 2002. Regulation of cyclin-Cdk activity in mammalian cells. *Cellular and Molecular Life Sciences CMLS*, 59, (1) 126-142

Odendal, L. Cervical Cancer in Women with HIV. http://www.aidsmap.com/Cervical-cancer-in-women-with-HIV/page/1669155/ . 2011. NAM Publications.
Ref Type: Online Source

Ola, M.S., Nawaz, M., & Ahsan, H. 2011. Role of Bcl-2 family proteins and caspases in the regulation of apoptosis. *Molecular and Cellular Biochemistry*, 351, (1) 41-58 available from: https://doi.org/10.1007/s11010-010-0709-x

Ortega, S., Malumbres, M., & Barbacid, M. 2002. Cyclin D-dependent kinases, INK4 inhibitors and cancer. *Biochimica et Biophysica Acta (BBA) - Reviews on Cancer*, 1602, (1) 73-87 available from: http://www.sciencedirect.com/science/article/pii/S0304419X02000379

Ouyang, L., Shi, Z., Zhao, S., Wang, F.T., Zhou, T.T., Liu, B., & Bao, J.K. 2012. *Programmed Cell Death Pathways in Cancer: A Review of Apoptosis, Autophagy and Programmed Necrosis*, 45 ed.

Peng, C.Y., Graves, P.R., Ogg, S., Thoma, R.S., Byrnes, M.J., III, Wu, Z., Stephenson, M.T., & Piwnica-Worms, H. 1998. C-TAK1 protein kinase phosphorylates human Cdc25C on serine 216 and promotes 14-3-3 protein binding. *Cell Growth Differentiation*, 9, (3) 197-208 available from: http://cgd.aacrjournals.org/cgi/content/abstract/9/3/197

Peter, M. E., Scaffidi, C., Medema, J. P., Kischkel, F., & Krammer, P. H. 1999, "The Death Receptors," *In Apoptosis: Biology and Mechanisms*, S. Kumar, ed., Berlin, Heidelberg: Springer Berlin Heidelberg, pp. 25-63.

Prates, C., Sousa, S., Oliveira, C., & Ikram, S. 2011. Prostate Metastatic Bone Cancer in an Egyptian Ptolemaic Mummy, A Proposed Radiological Diagnosis. *International Journal of*

Paleopathology, 1, (2) 98-103 available from: //www.sciencedirect.com/science/article/pii/S1879981711000271

Prendergast, G.C. 2008. Immune escape as a fundamental trait of cancer: focus on IDO. *Oncogene*, 27, 3889 available from: https://doi.org/10.1038/onc.2008.35

Rambaldi, P. F. 2014, "Cervical Cancer: Staging," *In Whole-Body FDG PET Imaging in Oncology: Clinical Reports*, P. F. Rambaldi, ed., Milano: Springer Milan, pp. 121-123.

Rockland. p53 Signaling Pathway Overview. https://rockland-inc.com/p53-pathway.aspx . 2018.
Ref Type: Online Source

Saraste, A. & Pulkki, K. 2000. Morphologic and biochemical hallmarks of apoptosis. *Cardiovascular Research*, 45, (3) 528-537 available from: http://dx.doi.org/10.1016/S0008-6363(99)00384-3

Schultz, M., Parzinger, H., Posdnjakov, D.V., Chikisheva, T.A., & Schmidt-Schultz, T.H. 2007. Oldest Known Case of Metastasizing Prostate Carcinoma Diagnosed in the Skeleton of a 2,700-year-old Scythian King from Arzhan (Siberia, Russia). *International Journal of Cancer*, 121, (12) 2591-2595 available from: http://dx.doi.org/10.1002/ijc.23073

Sherr, C.J. 2004. Principles of Tumor Suppression. *Cell*, 116, (2) 235-246 available from: https://doi.org/10.1016/S0092-8674(03)01075-4 Accessed 2 December 2018.

Sitas, F., Parkin, D.M., Chirenje, M., Stein, L., Abratt, R., & Wabinga, H. 2008. Part II: Cancer in Indigenous Africans-2014;causes and control. *The Lancet Oncology*, 9, (8) 786-795 available from: https://doi.org/10.1016/S1470-2045(08)70198-0 Accessed 1 December 2018.

Smith, K.A. 2005. Determining to divide: how do cells decide? *Journal of biological physics*, 31, (3-4) 261-272 available from: https://www.ncbi.nlm.nih.gov/pubmed/23345898

Speidel, D. 2010. Transcription-independent p53 apoptosis: an alternative route to death. *Trends in Cell Biology*, 20, (1) 14-24 available from: http://www.sciencedirect.com/science/article/pii/S0962892409002402

Statista. Average life expectancy* in Africa for those born in 2018, by gender and region (in years). https://www.statista.com/statistics/274511/life-expectancy-in-africa/ . 2018.
Ref Type: Online Source

Stephens, F. O. & Aigner, K. R. 2009, "The Cancer Problem," *In Basics of Oncology*, Springer, pp. 3-16.

Steyn, M. & Muller, A. 2000. Traditional healers and cancer prevention. *Curationis; Vol 23, No 3 (2000)DO - 10.4102/curationis.v23i3.675* available from: https://curationis.org.za/index.php/curationis/article/view/675/613

Sudhakar, A. 2009. History of Cancer, Ancient and Modern Treatment Methods. *Journal of cancer science & therapy*, 1, (2) 1-4 available from: https://www.ncbi.nlm.nih.gov/pubmed/20740081

Szépmuvészeti Múzeum. Votive Statue of Imhotep. https://hu.museum-digital.de/portal/index.php?t=objekt&oges=204754 . 2017.
Ref Type: Online Source

Tannoch, V. J., Hinds, P. W., & Tsai, L. H. 2002, "Cell Cycle Control," *In Cancer Gene Therapy: Past Achievements and Future Challenges*, N. A. Habib, ed., Boston, MA: Springer US, pp. 127-140.

Van Wyk, B.-E., Van Oudtshoorn, B., & Gericke, N. 2009. *Medicinal Plants of South Africa*, 2 ed. Pretoria, Briza Publications.

Venkitaraman, A.R. 2001. Functions of BRCA1 and BRCA2 in the biological response to DNA damage. *Journal of Cell Science*, 114, (20) 3591 available from: http://jcs.biologists.org/content/114/20/3591.abstract

Waggoner, S.E. 2003. Cervical cancer. *The Lancet*, 361, (9376) 2217-2225 available from: http://www.sciencedirect.com/science/article/pii/S0140673603137786

Walkley, R.C., McArthur, A.G., & Purton, E.L. 2005. Cell Division and Hematopoietic Stem Cells. *Cell Cycle*, 4, (7) 893-896

Welch, P.J. & Wang, J.Y. 1995. Abrogation of retinoblastoma protein function by c-Abl through tyrosine kinase-dependent and -independent mechanisms. *Molecular and cellular biology*, 15, (10) 5542-5551 available from: https://www.ncbi.nlm.nih.gov/pubmed/7565706

Woodman, C.B.J., Collins, S.I., & Young, L.S. 2007. The natural history of cervical HPV infection: unresolved issues. *Nature Reviews Cancer*, 7, 11 available from: https://doi.org/10.1038/nrc2050

Xiong, Y., Hannon, G.J., Zhang, H., Casso, D., Kobayashi, R., & Beach, D. 1993. p21 is a universal inhibitor of cyclin kinases. *Nature*, 366, 701 available from: https://doi.org/10.1038/366701a0

Yang, J.K., Wang, L., Zheng, L., Wan, F., Ahmed, M., Lenardo, M.J., & Wu, H. 2005. Crystal Structure of MC159 Reveals Molecular Mechanism of DISC Assembly and FLIP Inhibition. *Molecular Cell*, 20, (6) 939-949 available from: https://doi.org/10.1016/j.molcel.2005.10.023 Accessed 30 November 2018.

Yff, B.T.S., Lindsey, K.L., Taylor, M.B., Erasmus, D.G., & Jäger, A.K. 2002. The pharmacological screening of *Pentanisia prunelloides* and the isolation of the antibacterial compound palmitic acid. *Journal of Ethnopharmacology*, 79, (1) 101-107 available from: http://www.sciencedirect.com/science/article/pii/S0378874101003804

Yuan, J., Shaham, S., Ledoux, S., Ellis, H.M., & Horvitz, H.R. 1993. The *C. elegans* cell death gene *ced-3* encodes a protein similar to mammalian interleukin-1b-converting enzyme. *Cell*, 75, (4) 641-652 available from: http://www.sciencedirect.com/science/article/pii/0092867493904859

Zhu, Y., Tchkonia, T., Fuhrmann-Stroissnigg, H., Dai, H.M., Ling, Y.Y., Stout, M.B., Pirtskhalava, T., Giorgadze, N., Johnson, K.O., Giles, C.B., Wren, J.D., Niedernhofer, L.J., Robbins, P.D., & Kirkland, J.L. 2015. Identification of a novel senolytic agent, navitoclax, targeting the Bcl-2 family of anti-apoptotic factors. *Aging Cell*, 15, (3) 428-435 available from: https://doi.org/10.1111/acel.12445 Accessed 30 November 2018.

Zou, H., Li, Y., Liu, X., & Wang, X. 1999. An APAF-1·Cytochrome c Multimeric Complex Is a Functional Apoptosome That Activates Procaspase-9. *Journal of Biological Chemistry*, 274, (17) 11549-11556 available from: http://www.jbc.org/content/274/17/11549.abstract

Chapter 2

In vitro Cytotoxicity Screening of Selected Medicinal Plants

2.1 Introduction

In developing countries, (especially in Africa and Asia) about 80% of the population solely depend on the natural environment and chiefly plant extracts for treating diseases (Campbell-Tofte et al. 2012). Though nature has been the primary source of therapeutics for thousands of years, less than 15% of the available 250 000 higher plant species have been investigated for their potential bioactivity (Cragg and Newman 2005a). Plants have been used for a very long time in the traditional treatment of various malignant conditions, some of which were loosely defined as 'cancers' based on the evidence of abnormal swelling such as is present in abscesses, calluses, polyps and tumours. In actual fact, over 60% of conventional anti-cancer drugs have the natural environment as their primary resource (Cragg and Newman 2005b). The main advantage that plant derived compounds have over synthetic drugs in the treatment of cancer is their relative non-toxicity and better bioavailability profiles (Amin et al. 2009). By mechanism of action, most of the plant derived conventional anti-cancer drugs are methyltransferase inhibitors, DNA damaging/ pro-oxidants, histone deacetylase inhibitors (HDACi) and mitotic disruptors (Amin et al. 2009).

2.2 African medicinal plants as potential sources for new anti-cancer therapies

In order to discover novel anti-cancer phyto-therapies from the African setup, there is need to identify frequently used medicinal plants in the traditional treatment of cancers and to focus on those which have undergone little or no cancer-related biological studies. Through a thorough literature search, the following 14 medicinal plants traditionally used to treat cancers and cancer related conditions within the African continent were identified as potential sources for anti-cancer agents; *Neostenanthera gabonensis* (*Magnoliales, Annonaceae*), *Pachypodanthium staudtii* (*Magnoliales, Annonaceae*), *Bixa Orellana (Malvales, Bixaceae*), *Maytenus senegalensis* (*Celastrales, Celastraceae*), *Ceiba pentandra* (*Malvales, Malvaceae*), *Jatropha multifidi* (*Malpighiales, Euphorbiaceae*), *Verbesina encelioides* (*Asterales,*

Asteraceae), *Gloriosa superba* (*Liliales*, *Colchicaceae*), *Adansonia digitate* (*Malvales*, *Malvaceae*), *Capparis thonningii* (*Brassicales*, *Capparaceae*), *Margaritaria discoidea* (*Malpighiales*, *Phyllanthaceae*), *Pteris quadriaurita* (*Polypodiales*, *Pteridaceae*), *Drimia altissima* (*Asparagales*, *Asparagaceae*) and *Microdesmis puberula* (*Malpighiales*, *Pandaceae*) (Figure 2.1).

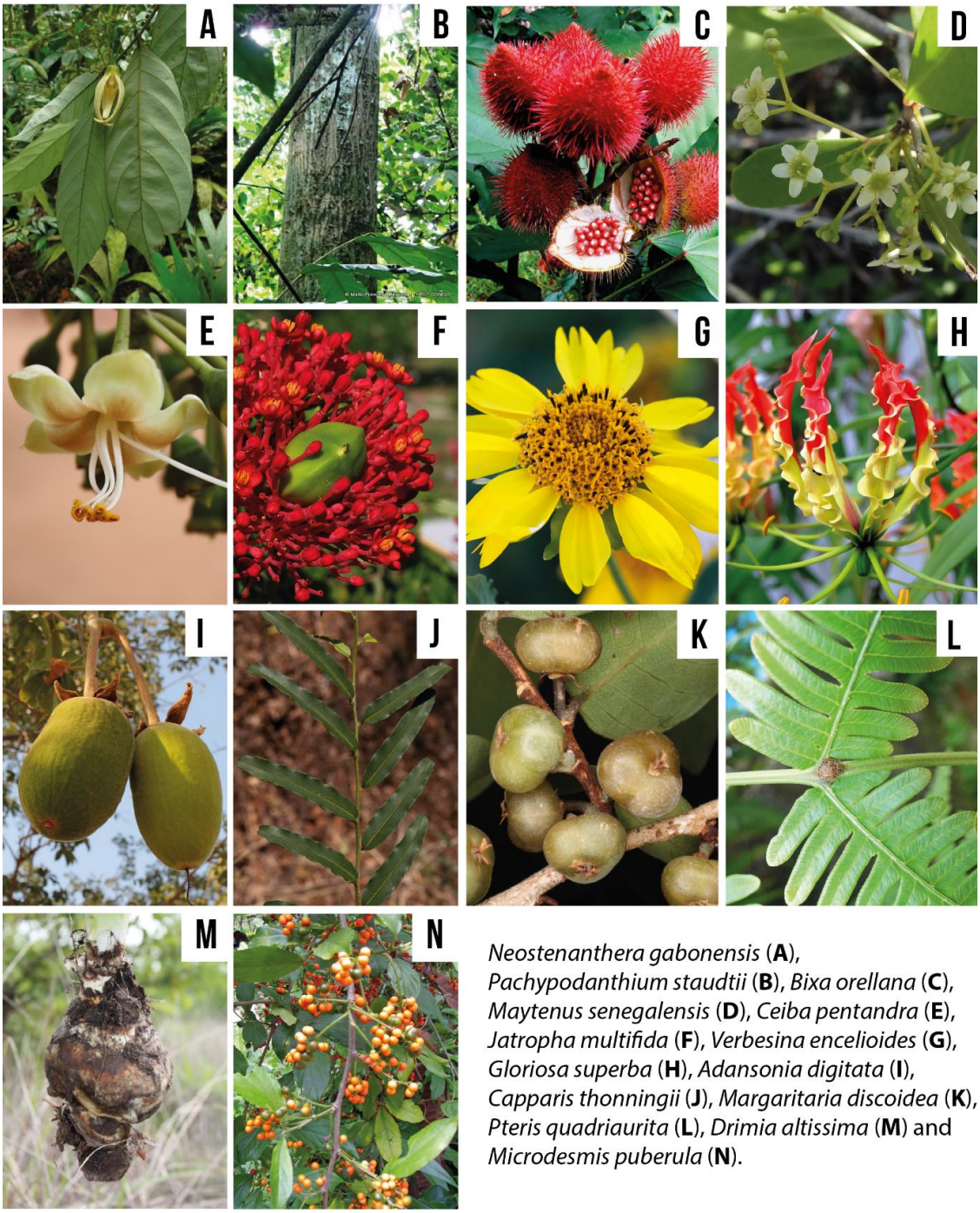

Figure 2.1 Selected African medicinal plants with potential anticancer activity

Images are not representative of whole plants. Image references are provided in-text

The leaves of *Neostenanthera gabonensis* (Figure 2.1a) (Fauna & Flora of Liberia 2015), popularly known as 'Anyi Afemi' in Ivory Coast, are used in West African traditional medicine to treat tumours and cancers (Global Plants 2018). However, no concrete literature evidence from biological studies currently exists to ascertain these claims. *N. gabonensis* comes from the *Annonaceae* family. Plants from the *Annonaceae* family are well known for yielding a variety of aporphinoid alkaloids with potent cytotoxic activity. Although the mechanisms of action by which these alkaloids cause cytotoxicity are not well understood, most of them target DNA manipulating enzymes such as polymerases and topoisomerases. An example of such compounds include liriodenine (**2.1**) (Figure 2.2), an oxoaporphine isolated from *Polyalthia longifolia*, with IC_{50} values of 3.6, 2.6, 2.5, 2.1 and 8.5 µM against KB, A-549, HCT-8, P-388 and L-1210 cell lines respectively (Stevigny et al. 2005). The first aporphine alkaloids to be isolated from *N. gabonensis* were (-)-stenantherine (**2.2**) and (-)-N-methylstenantherine (**2.3**) (Renner and Achembach 1988). Other aporphines isolated from *N. gabonensis* include (-)-caaverine (**2.4**) and lirinidine (**2.5**) (Guinaudeau 1994). The potential anticancer activity and mechanism of action for most of these compounds is yet to be known. The absence of literature evidence on the cytotoxic activity of *N. gabonensis* and its alkaloids provides an opportunity to investigate whether West African traditional use of this plant to treat tumours and cancers can be substantiated.

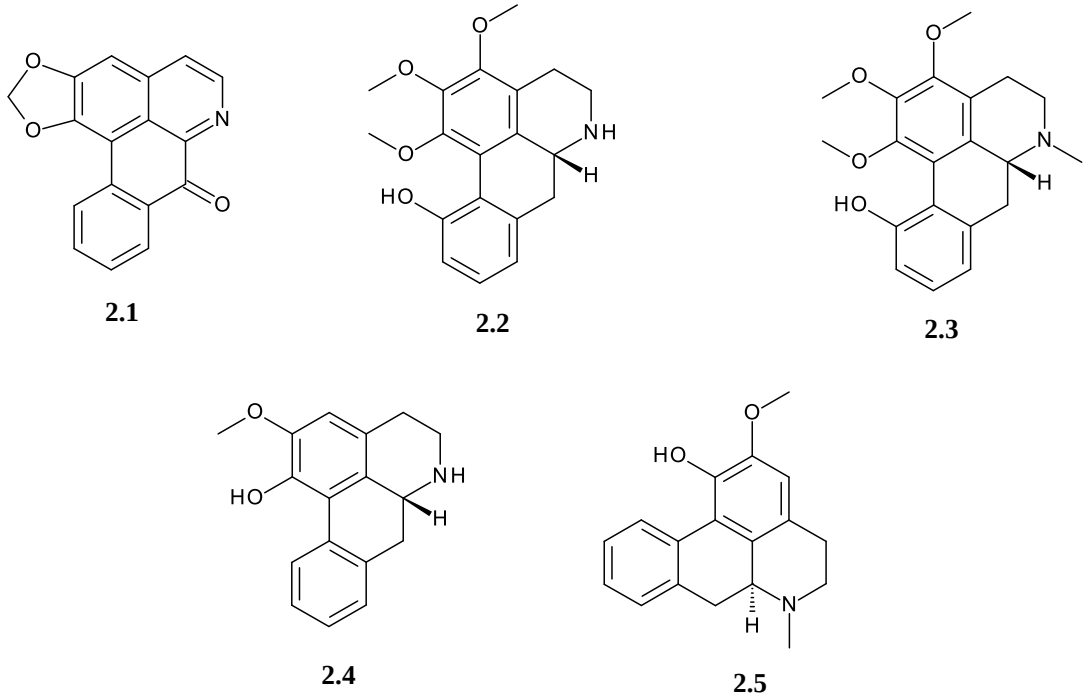

Figure 2.2 Aporphine alkaloids isolated from the *Annonaceae* family

The bark of *Pachypodanthium staudtii* (Figure 2.1b) (Help Congo 2018), known as 'Ntuen' in Cameroon, is used in African traditional medicine as a concoction with other ingredients to treat benign tumours (Sarpong et al. 1990; Focho et al. 2010). It is also widely used in the treatment of several other illnesses. For instance, in Ivory Coast the bark is pounded with *Ficus exasperata* (*Moraceae*) leaves, water and clay into a paste for topical treatment of oedemas, in Ghana and Gabon, the bark is used to eradicate body vermin, the Guere of Ivory Coast use the pulverized bark in arrow poisoning mixtures and in Libya they use it as a vermifuge (Global plants, 2014). Most of the studies undertaken on *P. staudtii* have focused on its anti-filarial activity (Attah et al. 2013) but no studies have been done to evaluate its potential cytotoxic activity. For instance, *P. staudtii* is known to possess flavonols. Flavonols are known to have antimutagenic activity by inhibiting Aryl hydrocarbon receptor (AHR) transformation. Among the flavonoids, flavonols possess the highest antimutagenic activity owing to the presence of a carbonyl functional group at the C-4 position (Lopez-Lazaro 2002). The flavonol pachypodol (**2.6**) (Figure 2.3), a potent antiviral agent, was once isolated from *P. staudtii* along with three *bisnor*lignans (Ngadjui et al. 1989). Pachypodol (**2.6**) was also isolated from the Indian shrub *Calycopteris floribunda* and shown to inhibit CaCo2 colon cancer cells (IC_{50} = 185.6 μM) in a Promega's CellTiter 96® non-radioactive cell proliferation assay (Ali et al. 2008). Another study reports pachypodol (**2.6**) isolated from the stem bark of East Asian *Acanthopanax brachypus* as having cytotoxic activity against HepG-2 cancer cells (IC_{50} = 4.5 μg/mL) (Hu et al. 2014). This shows that *P. staudtii* is a potential source for cytotoxic flavonoid compounds.

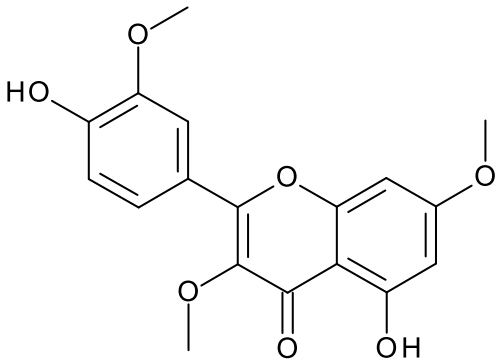

2.6

Figure 2.3 Structure for the cytotoxic flavonol pachypodol (**2.6**)

The seeds of *Bixa orellana* (Annatto seeds, Figure 2.1c) (Simran et al. 2017) are well known for their use in food colouring. Several phytochemical studies have confirmed the presence of carotenoid compounds in *B. orellana* seed extracts. Generally, carotenoids are known to exhibit

anti-carcinogenic effects by their ability to scavenge free radicals that cause DNA damage (Silva et al. 2001). Carotenoid compounds isolated from *B. orellana* include *cis*-bixin (**2.7**) and norbixin (**2.8**) (Figure 2.4) (Shilpi et al. 2006). The reported chemopreventive and antioxidant activity of *B. orellana* seed extracts is possibly due to the presence of these compounds. In particular, studies have shown that *cis*-bixin (**7**) possesses cytotoxic activity on various tumour cell lines with IC_{50} values ranging from 10 to 50 µM after 24 h exposure. According to a report by Tribodeau *et al*., 2010, *cis*-bixin (**7**) is selectively cytotoxic to highly drug-resistant multiple myeloma cell lines by inhibiting thioredoxin and thioredoxin reductase and hence, causing reactive oxygen species (ROS) mediated apoptosis (Tibodeau et al. 2010). Norbixin (**2.8**) has also been reported to have antimutagenic properties by causing an 87% inhibition of $H_2O_2^-$ induced mutagenic activity (Júnior et al. 2005). *B. orellana* has also been reported to contain vitamin E isomers called tocotrienols (T3), which have been reported to possess both *in vitro* and *in vivo* anti-cancer activity by delaying the development and metastasis of mammary tumours in HER-2/neu transgenic mice possibly *via* the induction of oxidative stress, senescent-like growth arrest and apoptosis (Pierpaoli et al. 2013).

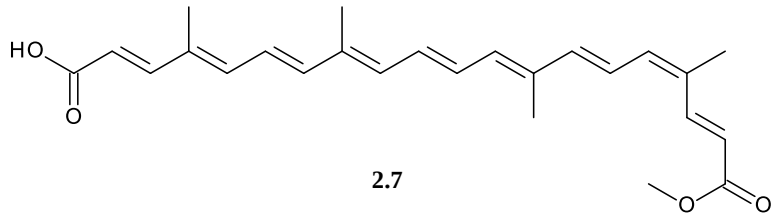

2.7

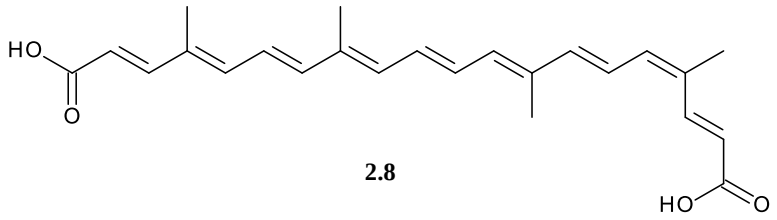

2.8

Figure 2.4 Structures for the cytotoxic carotenoids *cis*-bixin (**2.7**) and norbixin (**2.8**)

Species from the *Maytenus* Molina genus are widely used as traditional remedies for the treatment of various illnesses. Of these, the most frequently used in traditional African medicine are *M. senegalensis* (Lam) (Figure 2.1d) (Garcin 2018) and *M. heterophylla* (da Silva et al. 2011a). These two plants are traditionally used mainly for their anti-microbial and anti-inflammatory activities as well as for the relief of dysmenorrhoea and toothaches (da Silva et al. 2011a). The *Maytenus* genus has been a source of different types of compounds with cytotoxic activity. Maytansinoids, sesquiterpene polyesters and triterpenes isolated from this

genus have been found to possess antitumoral and cytotoxic activity (Shirota et al. 1994). For example, the aromatic triterpenes pristimerin (**2.9**) (also isolated from *M. senegalensis*), 6-oxotingenol (**2.10**), 6-oxopristimerol (**2.11**), 3-methyl-6-oxotingenol (**2.12**) and 3-methyl-22β, 23-diol-6-oxotingenol (**2.13**) (Figure 2.5) isolated from *M. ilicifolia* and *M. chuchuhuasca* exhibited cytotoxic activity against L-1210, P-388 and KB cell lines (Shirota *et al*., 1994). Another triterpene 30-hydroxy-11α-methoxy-18β-olean-12-en-3-one (HMO) (**2.14**) isolated from the acetonic/ethanolic extract of *M. procumbens* induced apoptosis in human cancerous HeLa cells (Momtaz et al. 2013). Maytenin (**2.15**), isolated from *M. boaria* is the main active constituent responsible for the plant's anticancer activity against basic cellular carcinoma, Kaposi's sarcoma and leukemia. Other species reported to have anti-cancer properties include *M. guangsiensis*, *M. ovatus*, *M. wallichiana*, *M. emarginata* and *M. senegalensis* (Kintzios et al. 2004). Despite the fact that most of the traditional uses of plant species from the *Maytenus* genus, and particularly *M. senegalensis*, have been confirmed by biological studies, very few studies have endeavoured to explore the potential anticancer activity of *M. senegalensis*.

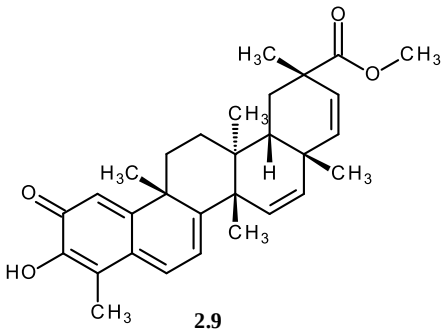

2.9

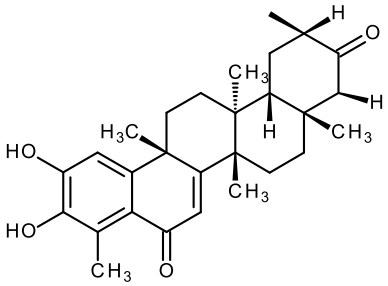

2.10

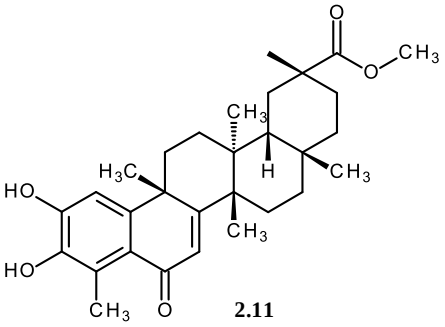

2.11

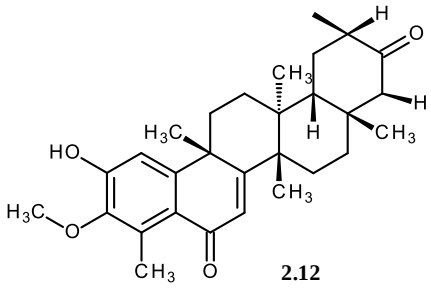

2.12

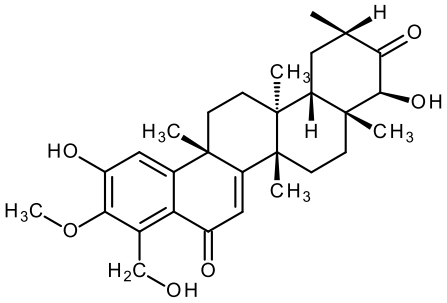

2.13

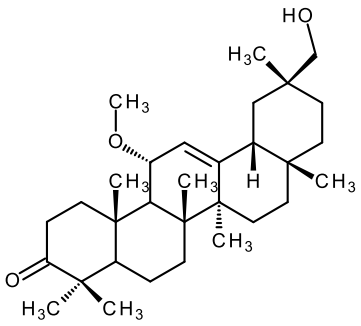

2.14

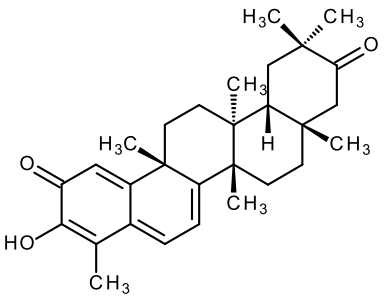

2.15

Figure 2.5 Structures for aromatic triterpenes isolated from the *Maytenus* Molina genus

Ceiba pentandra (Figure 2.1e) (Schmidt 2018) is one of several other plants commonly called 'mangroves' (Bandaranayake 1998). In Nigeria, the leaves of this plant are used as a vegetable cuisine (Igoli et al. 2005) while the stem bark is used by the Hausa and Fulani tribes as folk medicine for the treatment of fibrosis (Abubakur et al. 2007). The leaves and stem bark are also frequently used for the treatment of diarrhoea and stomach pain (Okoli et al. 2007). Several other traditional practices claim that *C. pentandra* stem bark is able to cure a myriad of diseases such as diabetes mellitus, hypertension, yellow fever, malaria, wounds and tumours (Asare 2012). Biological studies on *C. pentandra* have mainly focused on investigating its anti-diabetic, anti-diarrhoeal and wound healing (antibacterial) claims. A study by Ladeji *et al*. 2003 reporting the hypoglycaemic properties of the aqueous stem bark extract of *C. pentandra* in streptozotocin-induced diabetic mice confirms the anti-diabetic claims (Ladeji et al. 2003). In another study, a methanolic extract of *C. pentandra* stem bark significantly inhibited castor oil-induced diarrhoea (Sule et al. 2009) and hence, confirmed the anti-diarrhoeal claims. The *in vitro* antibacterial activity of extracts from the leaves and stem bark of *C. pentandra* has also been reported (Asare, 2012). Besides a study that reported the bark extract of *C. pentandra* to possess significant *in vitro* and *in vivo* antitumor activity (Kumar et al. 2016), no other biological studies have been done to investigate the traditional use of *C. pentandra* as an antitumour agent.

Jatropha is a created term from two Greek root words *iatrós* meaning 'doctor' and *trophé* meaning 'food'. From the term itself, medicinal properties of the *Jatropha* genus are well implied. The genus *Jatropha* consists of about 170 species with subgenera *Curcas* and *Jatropha*. Species from *Jatropha* have vast use in folklore medicine. *Jatropha* species are also known for their use in the traditional treatment of cancers. For instance, Nigerians use *J. gossypiifolia* to treat oral cancers and Mexicans use *J. gaumeri* to treat skin cancers (Sabandar et al. 2013). The cytotoxic and anti-tumour properties of *Jatropha* species are mainly attributed to the presence of diterpene metabolites. Several diterpenes with potential anti-cancer properties have been isolated from different species of *Jatropha*. Among these is the diterpene jatrophone (**2.16**) (Figure 2.6) isolated from *J. multifida* (Figure 2.1f) (Giardinaggio 2018), *J. gossypiifolia* and *J. elliptica* with anti-tumour activity and the diterpene 9β, 13α-dihydroxyisabellione (**2.17**) isolated from *J. isabelli* with cytotoxic properties (Devappa et al. 2011). The cytotoxic diterpenes curcusone C (**2.18**), curcusone D (**2.19**), multidione (**2.20**), 15-epi-4Z-jatrogrossidentadion (**2.21**) (also isolated from *J. multifida* and *J. grossidentata*), 4Z-jatrogrossidentadion (**2.22**), 4E-jatrogrossidentadion **(2.23)**, 2-hydroxyisojatrogrossidion

(**2.24**) and 2-epi-hydroxyisojatrogrossidion (**2.25**) isolated from *J. curcas* are responsible for the cytotoxic effects of *J. curcas* extracts against L5178y mouse lymphoma and HeLa human cervix carcinoma cell lines (Aiyelaagbe et al. 2011). A few cytotoxic compounds have also been isolated from *J. multifida*. Two macrocyclic diterpenoids, multifidanol (**2.26**) (structurally related to 15-epi-4Z-jatrogrossidentadion) and multifidenol (**2.27**), isolated from *J. multifida* showed significant cytotoxic activity against A-549, Neuro-2a , HeLa, MDA-231 and MCF-7 cell lines (Kanth et al. 2011). A lathyrane-type diterpene called multifidone (**2.28**) isolated from *J. multifida* showed *in-vitro* cytotoxic activity against THP-1 (IC_{50} = 45.63 ± 2.16 µM), HL-60 (IC_{50} = 120.70 ± 17.59 µM), A-375 (IC_{50} = 159.05 ± 24.33 µM) and A549 (IC_{50} = 127.12 ± 3.11 µM) cell lines (Das et al. 2009). These studies show that the *Jatropha* genus is a potential source for anti-cancer drugs. Despite these positive reports, few studies have embarked on investigating the mechanisms by which *Jatropha* species such as *J. multifida* cause their cytotoxic effects.

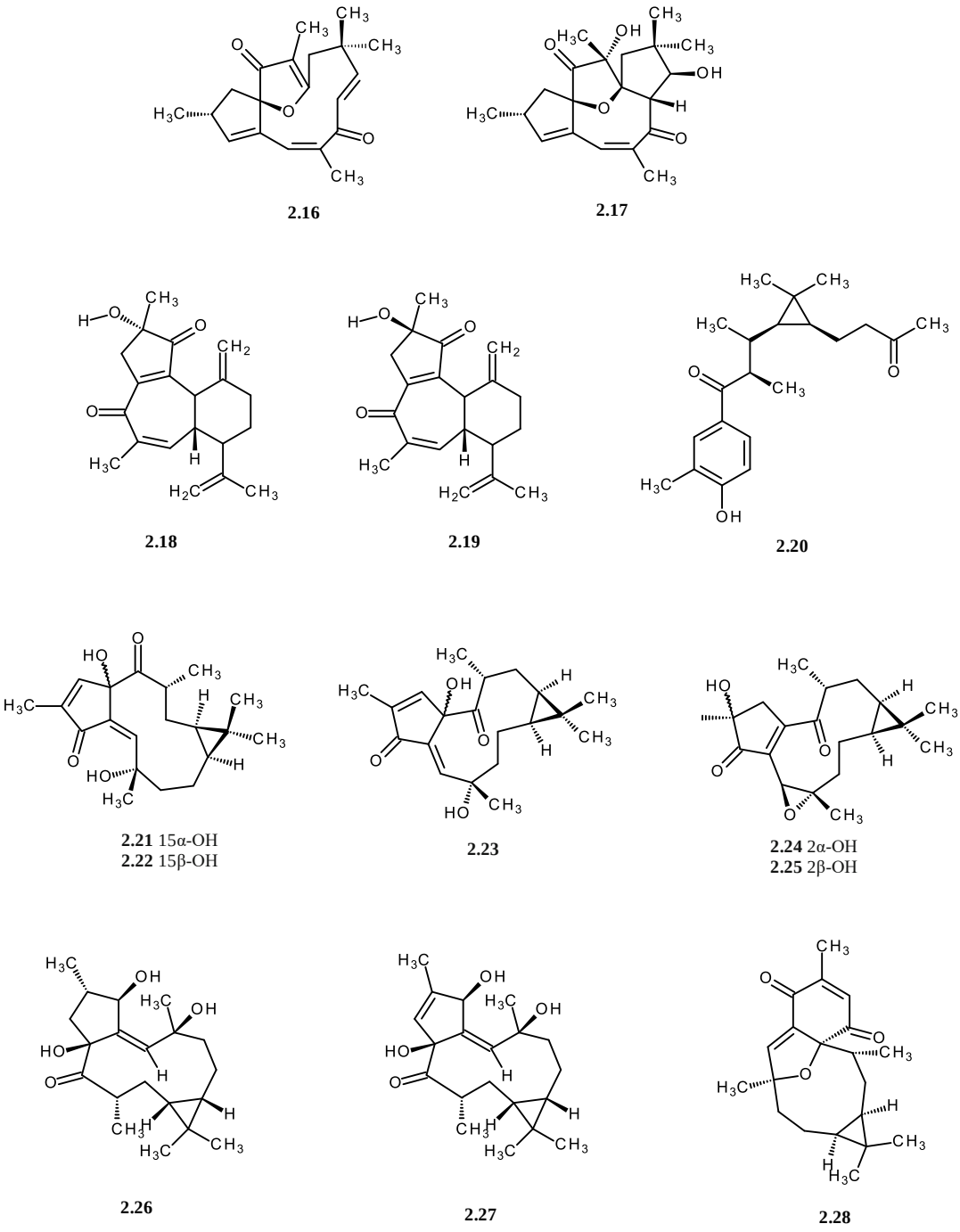

Figure 2.6 Selected cytotoxic diterpenes isolated from the *Jatropha* genus

Verbesina encelioides, commonly known as the 'Golden Crown Beard' (Figure 2.1g) (Bakali 2016), is a widely used weed in folk medicine for the treatment of cancers, gastro-intestinal diseases, dermatological abnormalities, snake bites, warts and haemorrhoids (Jain et al. 2008). *V. encelioides* is well known for being one of the sources of galegine (isoamylenegaunidine), a guanidine-based natural compound from which the anti-diabetic class of drugs called biguanides were derived (Malik et al. 2012). *V. encelioides* has been a subject of diabetes and

hyperlipidaemia associated studies because of this link. Due to the flexibility of the guanidine structural moiety and the ability of its three nitrogen atoms to interact with biological systems, guanidine-based compounds offer a wide spectrum of biological activity. A good number of natural/ synthetic anti-cancer and antimicrobial agents are guanidine functionalized (Said et al. 2013). Despite the fact that *V. encelioides* yields guanidine based compounds, very few biological studies have been done to investigate its anti-cancer potential. Among the few performed anti-cancer studies, those that focused on using extracts from aerial parts of *V. encelioides* failed to produce favourable results. In an *in-vitro* study undertaken by Kuete *et al*. 2012 to evaluate the cytotoxic and antimicrobial activity of *V. encelioides*, an 80% methanolic extract from the aerial part of the plant inhibited the growth of the micro-organisms *Enterobacter aerogenes* (EA27) and *Klebsiella pneumonia* (ATCC11296) at a minimum inhibitory concentration (MIC) of 1024 µg/ml but failed to show any cytotoxic activity against the human pancreatic cell lines, MiaPaCa-2, breast cancer cell line MCF-7, leukaemia cells CCRF-CEM and their multi-drug resistant sub-line CEM/ADR5000 (Kuete et al. 2012). In another study, a methanolic extract from the aerial parts of *V. encelioides* failed to display any cytotoxic activity against MCF-7, HepG2, HeLa and HFB4 cell lines (Almehdar et al. 2012). More recently, aerial parts of *V. encelioides* failed to show any anti-folate and antitumour activity against MCF-7, NCI-H460 and SF-268 cell lines (Albalawi et al. 2015). However, when Jain *et al*. performed a study using aqueous root infusions of *V. encelioides*, the extracts showed significant antitumoral activity (11-40% inhibition) (Jain *et al*., 2008). These results suggest that there could be cytotoxic compounds present in the root extracts of *V. encelioides* that may be absent in the aerial parts of the plant. Therefore, it would be of much interest to investigate the potential cytotoxic activity of the whole plant.

Gloriosa superba Linn, commonly called the 'Flame Lilly', Kembang Telang (Java, Indonesia) or Kalappaikkilangu (Tamil Nadu, India) (Figure 2.1h) (Plant valley 2018) is a widely used traditional remedy throughout the tropics of Africa and in Asia for treating a plethora of ailments such as abdominal pains, arthritis and dislocations, as an abortifacient, for wound healing, ascites, asthma and coughs, venereal diseases, gouts and tumours etc. (Maroyi and Van de Maesen 2011). *G. superba* has been listed in the IUCN Red Data Book as an over-exploited plant that is almost facing extinction due to high demands for the medicinal properties of its active compound colchicine (Ravindra and Mahendra 2009). Colchicine also possesses antimitotic properties that can be beneficial to cancer treatment (Dubey and Behera 2011). *In-vitro* studies have revealed colchicine cytotoxic activity against the cholangiocarcinoma cell

line with an IC_{50} of 0.02µg/ml (Mahidol et al. 2002). However, due to its high toxicity, colchicine cannot be pharmacologically used in its native form. For this reason, several researchers are working to discover new colchicine derivatives that circumvent toxic effects (Dubey and Behera, 2011). A colchicine related compound KL-4 **(2.29)** (Figure 2.7) isolated from an *Aspergillus* species endophytic fungus residing within the seeds of *G. superba* was found to possess antimicrobial and broad spectrum antitumoral activity (Budhiraja et al. 2013). In a study that evaluated different Thai medicinal recipes used for the treatment of cancer, a recipe consisting of *G. superba*, *Smilax glabra* and *Thunbergia laurifolia* showed high anti-proliferating activity against KB and HT29 cell lines (Manosroi et al. 2012). All this indicates that *G. superba* is a potential source for anticancer compounds.

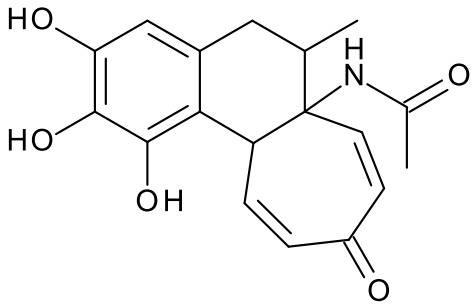

2.29

Figure 2.7 Structure for colchicine-like compound KL-4 (**2.29**)

Adansonia digitata L., commonly known as the 'Baobab Tree' (Figure 2.1i) (Tipdisease 2018), is a widely used plant in the African tradition. It is mainly used as a food, a beverage and a medicine for several ailments. The pulp of *A. digitata* is used as a febrifuge, for treating dysentery and as eye-drops in measles patients. The mashed dried powdered roots are used as a tonic for malarial patients while the semi-fluid gum exuded from the bark is used as treatment for sores (Gebauer et al. 2012; Inngjerdingen et al. 2004). The traditional use of *A. digitata* to treat infectious diseases was substantiated by results from a biological study showing its antibacterial, antifungal and anti-oxidant effects (Lagnika et al. 2012). In an anti-inflammatory assay, *A. digitata* showed a >70 % inhibition of COX-1 and COX-2 enzymes (Mulaudzi et al. 2013). The antiviral, anti-inflammatory, antipyretic, antimicrobial and anti-trypanosomal activities of *A. digitata* have already been extensively reported (De Caluwé et al. 2010) but no anticancer activity reports are currently available.

Capparis is a major genus of the *Capparaceae* family. Several species from this genus have been subjects of extensive biological studies due to their various biological activities ranging

from anti-inflammatory, anti-oxidant and anticancer to anti-diabetic, antiprotozoal and analgesic (Upadhyay 2011). In Southern Nigeria, the fruit of *C. thonningii* (Figure 2.1j) (Randt 2014), synonymous to *C. brassii*, is traditionally used as a vermifuge against tapeworms while its leaves are either orally ingested as an aphrodisiac or decocted and applied onto the skin to treat cancers and tumours. Several species from the genus *Capparis* have been found to possess significant anticancer activity. For example, a 38 kDa protein isolated from the seeds of *C. spinosa* inhibited the proliferation of HepG2, HT29 and MCF-7 cell lines with IC_{50} values of 1.0, 40 and 60 µM respectively (Lam and Ng 2009). One of the compounds isolated from *C. spinosa*, stachydrine (**2.30**) (Figure 2.8) has anti-metastatic effects attributed to its inhibition of CXCR3 and CXCR4 chemokine receptors in cancerous cells. The fact that stachydrine (**2.30**) has also been isolated from the fruits of *C. thonningii* (*C. moonii*) is suggestive of the potential anticancer activity of *C. thonningii* (Mishra et al. 2007).

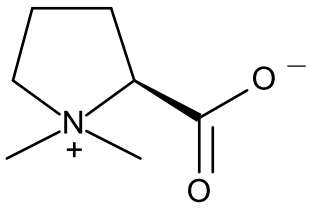

2.30

Figure 2.8 Structure for the CXCR3/CXCR4 inhibitor stachydrine (**2.30**)

The root bark of *Margaritaria discoidea* (Figure 2.1k) (Phillipson 2018) is frequently used to treat fevers, coughs and inflammatory conditions (Kamuhabwa et al. 2000). Methanolic extracts of *M. discoidea* have also shown cytotoxic activity by inhibiting the proliferation of HT29 (25-50% cell inhibition at 10 µg/mL) and A431 (50-75% cell inhibition at 10 µg/mL) cell lines (Kamuhabwa et al. 2000) but the mechanisms of action have not yet been reported. *M. discoidea* has been reported to contain securinane-type alkaloids (Diallo et al. 2015). A study reported that the cytotoxic activity of *M. discoidea* stem bark extracts against ovarian cancer cell lines OVCAR-8, A2780 and A2780cis is possibly due to the presence of the compounds securinine (**2.31**) and gallic acid (**2.32**) (Figure 2.9) (Johnson-Ajinwo et al. 2015). The anti-cancer activities of securinine (**2.31**) and gallic acid (**2.32**) are already well documented but there are no further reports of cytotoxic compounds isolated from *M. discoidea*.

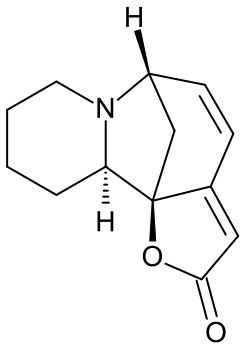

2.31

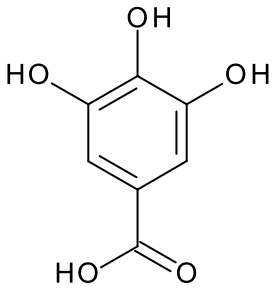

2.32

Figure 2.9 Structures for securinine (**2.31**) and gallic acid (**2.32**)

Pteris quadriaurita Retz. (Figure 2.1l) (Moran 2006), commonly known as the 'Stripped brake', is a fern that is frequently used to treat cancers in African traditional medicine. In Nigeria, the crushed rhizomes of *P. quadriaurita* are traditionally used as an emollient and an astringent (Nwosu 2002). In India, the juice extracted from *P. quadriaurita* leaves together with the sap of *Pheonix sylvestris* are traditionally used for the treatment of irregular menstruations by oral administration early in the morning on an empty stomach and at noon for two to three consecutive days (Rout et al. 2009). *P. quadriaurita* is also traditionally used as an anthelmintic and the freshly decocted rhizomes are used to treat visceral and spleen obstructions (Thomas 2011). Contrary to the negative results previously reported (Banerjee and Sen 1980), methanolic extracts from the fronds of *P. quadriaurita* have shown maximum antibacterial activity especially against *Pseudomonas aeruginosa* at an MIC of 25 mg/mL and a minimum bactericidal concentration of 50 mg/mL (Thomas, 2011). However, these results are questionable due to the extremely high concentrations that were used for the study. Currently, no studies have been undertaken to evaluate the ethnobotanical use of *P. quadriaurita* as an anticancer agent. The anticancer activity of ferns is usually attributed to the presence of flavonoids and their *O*-glycosides. Flavonoids with additional anti-oxidant activity exhibit slightly increased cytotoxic activity (Cao et al. 2013). However, a fern called *Pteridium aquilinum* (Bracken) is the only vascular plant known to cause cancer (Hirono et al. 1970) owing to the presence of an illudane type norsesquiterpene glucoside, ptaquiloside (**2.33**) and its analogues (Figure 2.10) (Hirono et al. 1984). *P. quadriaurita* was reported to contain either ptaquiloside (**2.33**) or its analogue pterosin B (**2.34**) (Tomšík 2014). Despite this, it would still be worthwhile to investigate if *P. quadriaurita* also possesses anti-oxidant flavonoids with potential anticancer activity.

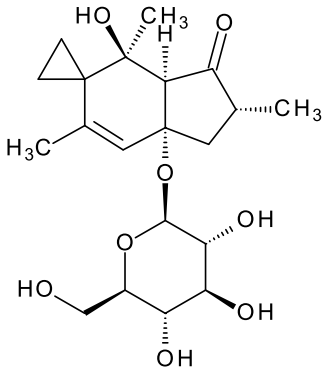

2.33

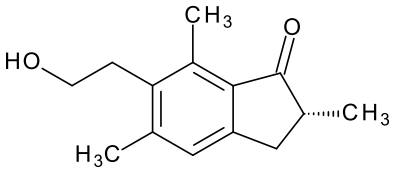

2.34

Figure 2.10 Structures for the norsesquiterpene glucoside ptaquiloside (**2.33**) and its analogue pterosin B (**2.34**)

Species from the genus *Drimia* have been used for over centuries as ethnomedicines for the treatment of various ailments such as dropsy, respiratory conditions, bone and articulation disorders, dermatological diseases, epileptic seizures and cancers (Bozorgi et al. 2017). The biological activities of species within *Drimia* have been attributed to the presence of bufadienolides which exist as the main plant constituents. Bufadienolides are well known for their anticancer properties though the mechanisms by which they elicit these actions are often unknown (Gao et al. 2011). Plants from *Drimia* with reported cytotoxic activity include *D. maritima*, *D. calcarata* (*D. riparia*) and *D. indica*. Among several others, the bufadienolide riparianin (**2.35**) (Figure 2.11), isolated from *D. calcarata*, has been found to possess antitumor activity (Moodley et al. 2007). However, the main challenge with bufadienolides is their narrow therapeutic index due to cardiotoxic side effects (Iizuka et al. 2001). This has created a need for the discovery of less toxic *Drimia* metabolites, possibly from the lesser studied species such as *D. altissima* (Figure 2.1m) (Schmidt 2009).

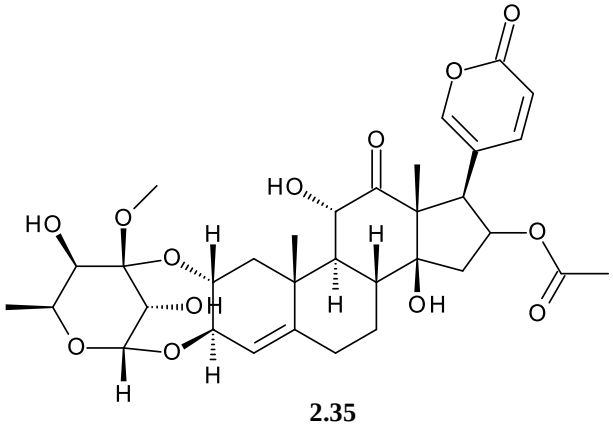

2.35

Figure 2.11 Structure for the cytotoxic bufadienolide riparianin (**2.35**)

Orally administered root decoctions of *Microdesmis puberula* (Figure 2.1n) (Scamperdale 2018) are used in South-Western Nigerian traditional medicine for the treatment of cancers (Ashidi et al. 2010). The Guineans also have a traditional practice of using the entire *M. puberula* plant to treat tumours (Graham et al. 2000). Analgesic and anti-stress effects of *M. puberula* methanolic stem wood extracts have been reported (Okany et al. 2012) but no biological studies have been performed to evaluate its anticancer and antitumor traditional claims.

2.3 Chapter aims

Key issues discussed in chapter 1 include the increasing prevalence of cancer in Africa, the limitations and safety concerns of current anticancer treatment modalities and the potential of African natural product-based research in the development of new phyto-therapies. After a literature search-driven identification of 14 African medicinal plants used in folklore medicine to treat cancers/ inflammatory conditions, four of the plants, *Maytenus senegalensis*, *Ceiba pentandra*, *Adansonia digitata* and *Drimia altissima*, were selected for *in vitro* cytotoxicity screening as potential sources for novel anticancer compounds. The selection of the four plant extracts was done by researchers at the University of Lagos as part of a collaboration. The aim of this chapter is to evaluate the anticancer potential of the four selected plants through *in vitro* cytotoxicity screening and to select the most active plant extract(s) for bio-assay guided isolation of anticancer compound(s).

2.4 Results and discussion

2.4.1 3-(4,5-dimethylthiazol-2-yl)-2,5-diphenyl tetrazolium bromide (MTT) assay

3-(4,5-dimethylthiazol-2-yl)-2,5-diphenyl tetrazolium bromide (MTT) (Figure 2.11) is a yellow tetrazolium salt which is converted by dehydrogenase enzymes in viable cells to an insoluble purple compound called formazan resulting from the cleavage of the tetrazolium ring (Stockert et al. 2012). The amount of purple formazan that is extracted from the cells is proportional to the number of viable cells. It is worth noting that since the MTT assay quantifies the number of viable cells at the end of the treatment period, it is not possible to distinguish between treatments that have cytotoxic (cell killing) from those that have cytostatic (cell growth inhibiting) effects.

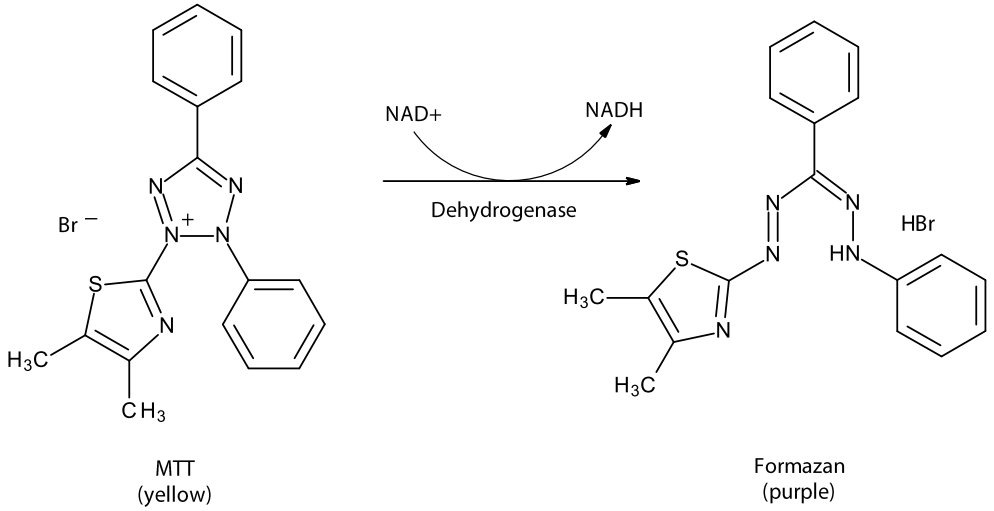

Figure 2.12 The conversion of 3-(4,5-dimethylthiazol-2-yl)-2,5-diphenyl tetrazolium bromide (MTT) to formazan (Stockert et al. 2012).

The cytotoxic activity of extracts from *M. senegalensis* (**MS-L** and **MS-R**), *C. pentandra* (**CP-L**), *A. digitata* (**AD-R**) and *D. altissima* (**DA-R**) was evaluated in HeLa cells using a modified MTT assay (Mosmann 1983). From the obtained results, the root extract of *M. senegalensis* (**MS-R**) showed strong cytotoxic activity (IC_{50} = 25 µg/mL) while the leaf extract (**MS-L**) was ineffective (IC_{50} = 264 µg/mL) (Figure 2.12).

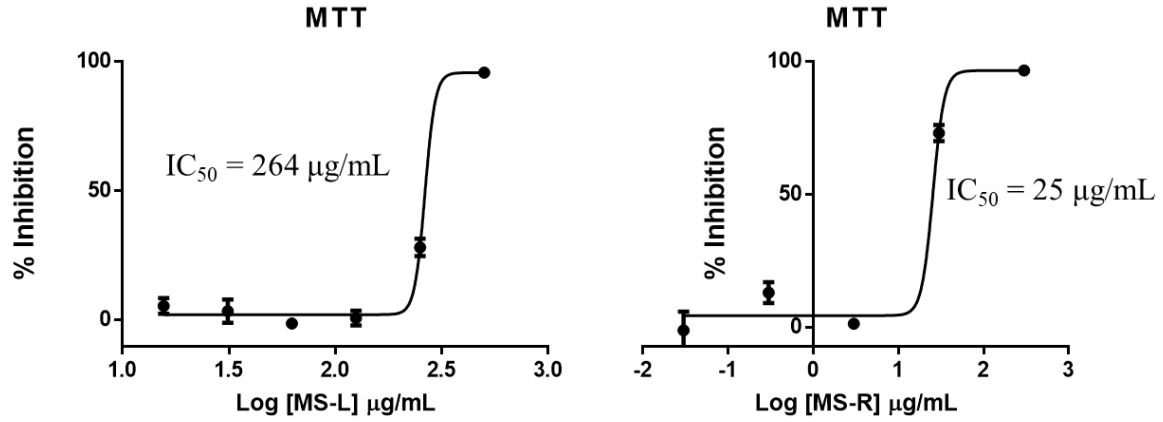

Figure 2.13 MTT dose response curves for *M. senegalensis* leaf (**MS-L**) and root (**MS-R**) extracts in HeLa cells

The leaf extract of *C. pentandra* (**CP-L**) was found to be ineffective (IC_{50} = 300 µg/mL) (Figure 2.13) while the root extract of *A. digitata* (**AD-R**) showed significant cytotoxic activity (IC_{50} = 48 µg/mL) (Figure 2.14). The bulb extract of *D. altissima* (**DA-B**) exhibited the strongest cytotoxic activity with an IC_{50} of 1.1 µg/mL (Figure 2.15).

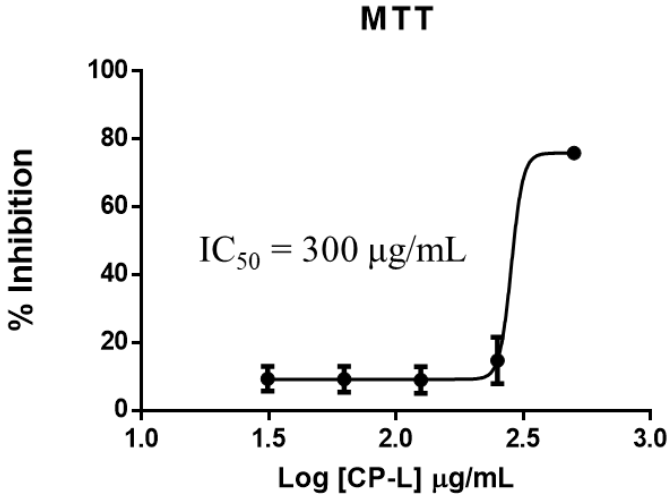

Figure 2.14 MTT dose response curve for *C. pentandra* leaf (**CP-L**) extract in HeLa cells

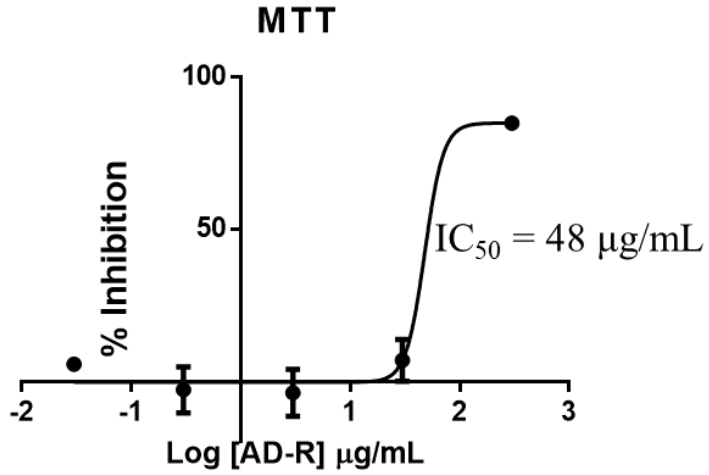

Figure 2.15 MTT dose response curve for *A. digitata* leaf root (**AD-R**) extract in HeLa cells

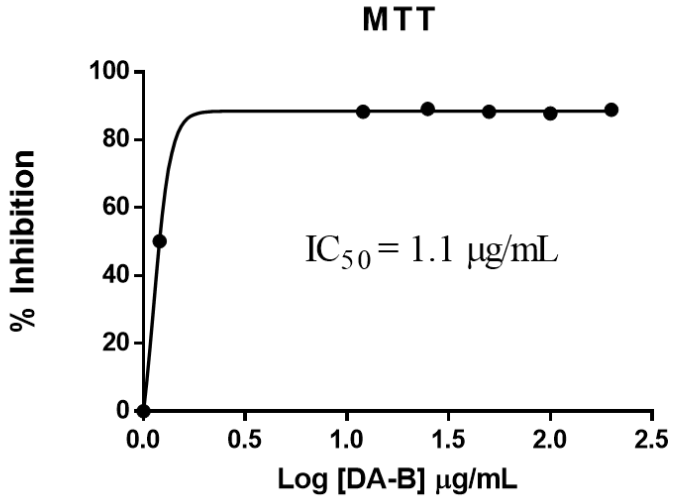

Figure 2.16 MTT dose response curve for *D. altissima* bulb (**DA-B**) extract in HeLa cells

In this chapter, African medicinal plants are highlighted as a great resource for the potential discovery of anti-cancer therapies owing to hundreds of years of African traditional use as treatments for cancerous/ inflammatory conditions. A literature search for African medicinal plants with potential to yield anticancer compounds led to the selection of four plants, *M. senegalensis*, *C. pentandra*, *A. digitata* and *D. altissima*, which underwent MTT *in vitro* cytotoxicity screening in HeLa cervical cancer cells.

From the results, the root extract of *M. senegalensis* (**MS-R**) possessed strong cytotoxic activity against HeLa cells with an IC_{50} of 25 µg/mL while the leaf extract (**MS-L**) was found to be ineffective. Interestingly, most biological studies on *M. senegalensis* focus on leaf extracts while neglecting the roots. An *in vitro* study found *M. senegalensis* leaf extracts to possess antimycobacterial activity against a resistant strain of *Mycobacterium tuberculosis* (da Silva et al. 2011b). Another *in vitro* study performed by Tahir *et al.* reported the antiplasmodial activity of *M. senegalensis* in which leaf and bark extracts showed activity against *Plasmodium falciparum* with IC_{50} values of 3.9 and 5.10 µg/mL for the 3D7 strain as well as 10.0 and 65.0 µg/mL for the Dd2 strain (Tahir et al. 1999). *M. senegalensis* leaf extracts have also been reported to possess *in vivo* anti-inflammatory properties (Da silva et al., 2011a). Based on this, a study of *M. senegalensis* roots is more likely to result in the discovery of new compounds. The root extract of *A. digitata* (**AD-R**) also exhibited cytotoxic activity with an IC_{50} of 48 µg/mL. The bulb extract of *D. altissima* (**DA-B**) was the most cytotoxic with an IC_{50} of 1.1 µg/mL. By exhibiting the most potent cytotoxic activity against HeLa cells, *D. altissima* (**DA-B**) had the greatest potential for the discovery of cytotoxic compounds and was thus selected for further studies.

2.5 Experimental

2.5.1 General experimental procedures

All extractions utilised LiChrosolv® (Merck, Germany) solvents. Samples were dried *in-vacuo* using a Buchi R-210 Rotavapor or freeze dried using a Virtis SP Scientific sentry 2.0 lyophilizer with an Alcatel Pascal vacuum pump. HeLa cervical cancer cells were obtained from Cellonex, South Africa and grown in Roswell Park Memorial Institute 1640 (RPMI 1640) medium from GE Healthcare Life Sciences (South Logan, Utah, USA) supplemented with gamma irradiated Fetal Bovine Serum (FBS) from Biowest (South America). Cells were cultured in BioFlow-II Labotec laminar flow cabinets and incubated in a ThermoForma CO_2 incubator. 3-(4,5-dimethyl-2-thiazolul)-2,5-diphenyl-2H-tetrazolium bromide (MTT) was obtained from Sigma® (St. Louis, MO, USA).

2.5.2 Plant material

The plant specimens of *Adansonia digitata*, *Ceiba pentandra* and *Maytenus senegalensis* were obtained from Osun State, Nigeria and identified at the Forest Research Institute (FRIN), Ibadan, Nigeria in November 2014. The plant specimen of *Drimia altissima* (L.F.) Ker Gawl was collected in Kwa-Nobuhle, (Uitenhage, Eastern Cape, South Africa) by Buyiswa Hlangothi in February, 2015. The plant material was transported to Nelson Mandela University, Chemistry Department and stored in the plant room until the time of extraction. Plant authentication was performed by Tony Dold, a curator and taxonomist at Selmar Schonland Herbarium (GRA) in Makhanda, Eastern Cape, South Africa, where a specimen of *Drimia altissima* (L.F.) Ker Gawl. with voucher number Hlangothi011(GRA) was deposited.

2.5.3 Extraction of plant biomasses

The roots and leaves of *Adansonia digitata*, *Ceiba pentandra* and *Maytenus senegalensis* were oven dried at 40 °C, pulverized to powder and extracted using 96% EtOH for 72 h. The filtrate was concentrated using a rotary evaporation (Buchi, Switzerland) at 40 °C. The extract was then stored at 4 °C until needed for studies. The bulbs of *D. altissima* were washed under running water, peeled and dried at 40 °C after which the plant material was shredded into smaller pieces and submerged in liquid nitrogen until brittle. The resulting biomass was crushed with a mortar and pestle to powder in readiness for soxhlet extraction. About 100 g of dry powdered biomass was loaded onto the soxhlet apparatus and extracted for 75 cycles (1

cycle = 16 min) at 65 °C under reflux using MeOH/CH_2Cl_2 (8:2, 150 mL). The resulting extract was dried *in vacuo* to yield 10.85 g of a brown crude extract designated as **DA-B**.

2.5.4 3-(4,5-dimethylthiazol-2-yl)-2,5-diphenyl tetrazolium bromide (MTT) assay

HeLa cells were seeded into 96-well culture plates at a density of 5 000 cells/well in RPMI 1640 supplemented with 10 % fetal bovine serum (FBS) and incubated for 24 h. Test concentrations for each extract were determined based on repeat experiments to achieve IC_{50} values from the dose response curves. Extracts **MS-L** (15.625, 31.25, 62.5, 125, 250 and 500 µg/mL), **MS-R** (0.03, 0.3, 3.0, 30 and 300 µg/mL), **CP-L** (15.625, 31.25, 62.5, 125, 250 and 500 µg/mL), **AD-R** (0.03, 0.3, 3.0, 30 and 300 µg/mL) and **DA-B** (1.2, 12, 25, 50, 100 and 200 µg/mL) were added to the cells with melphalan used as positive control. The treated cells were incubated for a further 48 h after which the medium was replaced with 100 µL MTT (Sigma®) (0.5 mg/mL in RPMI 1640). After 3 h of incubation at 37 °C, the MTT was aspirated and the purple formazan product dissolved in 100 µL DMSO. The absorbance was measured at 560 nm using a multi-well scanning spectrophotometer (Multiscan MS, Labsystems). All incubation steps were carried out in a 37 °C humidified incubator with 5% CO_2.

2.5.5 Data analysis

Each IC_{50} was performed once in quadruplicate and data was analysed using GraphPad Prism version 6. Data points on the log-dose response curves represent the mean ± standard deviation (SD) of quadruplicate values.

References

Abubakur, M.S., Musa, A.M., Ahmed, A., & Hussaini, I.M. 2007. The Perception and Practice of Traditional Medicine in the Treatment of Cancers and Inflammations by the Hausa and Fulani Tribes of Northern Nigeria. *Journal of ethnopharmacology*, 111, 625-629

Aiyelaagbe, O.O., Hamid, A.A., Fattorusso, E., Taglialatela-scafati, O., Schröder, H.C., & Müller, W.E.G. 2011. Cytotoxic Activity of Crude Extracts as well as of Pure Components from *Jatropha* Species, Plants Used Extensively in African Traditional Medicine. *Evidence-Based Complementary and Alternative Medicine* 1-7

Albalawi, M.A.Z., Bashir, N.A.O., & Tawfik, A. 2015. Anticancer and Antifolate Activities of Extracts of Six Saudi Arabian Wild Plants Used in Folk Medicine. *Journal of Life Sciences*, 9, 334-340

Ali, H.A., Chowdhury, A.K.A., Rahman, A.K.M., Borkowski, T., Nahar, L., & Sarker, S.D. 2008. Pachypodol, a Flavonol from the Leaves of *Calycopteris floribunda*, Inhibits the Growth of CaCo 2 Colon Cancer Cell Line *in vitro*. *Phytotherapy Research*, 22, (12) 1684-1687 available from: http://dx.doi.org/10.1002/ptr.2539

Almehdar, H., Abdallah, H.M., Osman, A.M., & Abdel-Sattar, E.A. 2012. *In vitro* Cytotoxic Screening of Selected Saudi Medicinal Plants. *Journal of Natural Medicine*, 66, 406-412

Amin, A., Gali-Muhtasib, H., Ocker, M., & Schneider-Stock, R. 2009. Overview of major classes of plant-derived anticancer drugs. *International Journal of Biomedical Science*, 5, (1) 1-11

Asare, P. 2012. Comparative Evaluation of *Ceiba pentandra* Ethanolic Leaf Extract, Stem Bark Extract and the Combination thereof for *in vitro* Bactria Growth Inhibition. *Journal of Natural Sciences Research*, 2, (5) 44-50

Ashidi, J.S., Houghton, P.J., Hylands, P.J., & Efferth, T. 2010. Ethnobotanical survey and cytotoxicity testing of plants of South-western Nigeria used to treat cancer, with isolation of cytotoxic constituents from Cajanus cajan Millsp. leaves. *Journal of ethnopharmacology*, 128, (2) 501-512 available from: http://www.sciencedirect.com/science/article/pii/S0378874110000267

Attah, S.K., Ayeh-Kumi, P.F., Sittie, A.A., Oppong, I.V., & Nyarko, A.K. 2013. Extracts of Euphorbia hirta Linn. (Euphorbiaceae) and Rauvolfia vomitoria Afzel (Apocynaceae) demonstrate activities against Onchocerca volvulus microfilariae in vitro. *BMC complementary and alternative medicine*, 13, 66 available from: http://europepmc.org/abstract/MED/23506674

Bakali, H. B. *Verbesina encelioides*. https://www.teline.fr/fr/photos/asteraceae/verbesina-encelioides#photo-2 . 2016.
Ref Type: Online Source

Bandaranayake, W.M. 1998. Traditional and Medicinal Uses of Mangroves. *Mangroves and Salt Marshes*, 2, 133-148

Banerjee, R.D. & Sen, S.P. 1980. Antibiotic Activity of Pteridophytes. *Economic Botany*, 34, (3) 284-298

Bozorgi, M., Amin, G., Shekarchi, M., & Rahimi, R. 2017. Traditional medical uses of *Drimia* species in terms of phytochemistry, pharmacology and toxicology. *Journal of Traditional Chinese Medicine*, 37, (1) 124-139 available from: http://www.sciencedirect.com/science/article/pii/S0254627217300365

Budhiraja, A., Nepali, K., Sapra, S., Gupta, S., Kumar, S., & Dhar, K.L. 2013. Bioactive Metabolites from an Endophytic Fungus of *Aspergillus* Species Isolated from Seeds of *Gloriosa superba Linn*. *Med Chem Res*, 22, 323-329

Campbell-Tofte, J.I.A., Mølgaard, P., & Winther, K. 2012. Harnessing The Potential Clinical Use of Medicinal Plants As Anti-Diabetic Agents. *Botanics: Targets and Therapy*, 2, 7-19

Cao, J., Xia, X., Chen, X., Xiao, J., & Wang, Q. 2013. Characterization of Flavonoids from *Dryopteris erythrosora* and Evaluation of their Antioxidant, Anticancer and Acetylcholinesterase Inhibition Activities. *Food and Chemical Toxicology*, 51, 242-250 available from: http://www.sciencedirect.com/science/article/pii/S0278691512007405

Cragg, G.M. & Newman, D.J. 2005a. Biodiversity: A continuing source of novel drug leads. *Pure Appl.Chem.*, 77, (1) 7-24

Cragg, G.M. & Newman, D.J. 2005b. Plants as a source of anti-cancer agents. *Journal of ethnopharmacology*, 100, (1GÇô2) 72-79 available from: http://www.sciencedirect.com/science/article/pii/S0378874105003259

da Silva, G., Serrano, R., & Silva, O. 2011a. Maytenus heterophylla and Maytenus senegalensis, two traditional herbal medicines. *Journal of natural science, biology, and medicine*, 2, (1) 59-65 available from: http://europepmc.org/abstract/MED/22470236

da Silva, G., Taniça, M., Rocha, J., Serrano, R., Gomes, E.T., Sepodes, B., & Silva, O. 2011b. *In vivo* anti-inflammatory effect and toxicological screening of *Maytenus heterophylla* and *Maytenus senegalensis* extracts. *Human & Experimental Toxicology*, 30, (7) 693-700 available from: http://het.sagepub.com/content/30/7/693.abstract

Das, B., Reddy, K.R., Ravikanth, B., Raju, T.V., Sridhar, B., Khan, P.U., & Rao, J.V. 2009. Multifidone: A Novel Cytotoxic Lathyrane-Type Diterpene Having an Unusual Six-membered A Ring from *Jatropha multifida*. *Bioorganic and Medicinal Chemistry Letters*, 19, 77-79

De Caluwé, E., Halamová, K., & Van Damme, P. 2010. *Adansonia digitata* L. - A Review of Traditional Uses, Phytochemistry and Pharmacology. *Afrika Focus*, 23, (1) 11-51

Devappa, R.K., Makkar, H.P.S., & Becker, K. 2011. *Jatropha* Diterpenes: A Review. *J Am Oil Chem Soc*, 88, 301-322

Diallo, M.S.T., Balde, A.M., Camara, A., Traore, M.S., Bah, M.L., Diallo, A.S., Camara, A.K., Laurent, S., Roch, A., Muller, R.N., Maes, L., Pieters, L., & Balde, M.A. 2015. Ethnobotanical, Phytochemical and Biological Investigations of *Margaritaria discoidea* (Baill.) Webster, A Plant Species Widely Used in Ghanaian Traditional Medicine. *Journal of Plant Sciences*, 3, (1-2) 40-46

Dubey, K.K. & Behera, B.K. 2011. Statistical Optimization of Process Variables for the Production of an Anticancer Drug (Colchicine Derivatives) through Fermentation: At Scale-up Level. *New Biotechnology*, 28, (1) 79-85

Fauna & Flora of Liberia. *Neostenanthera gabonensis*. http://www.liberianfaunaflora.org/liberian-flora/annonaceae/697-neostenanthera-gabonensis . 2015.

Ref Type: Online Source

Focho, D.A., Egbe, E.A., Chuyong, G.B., Fongod, A.G.N., Fonge, B.A., Ndam, W.T., & Youssoufa, B.M. 2010. An ethnobotanical investigation of the annonaceae on Mount Cameroon. *Journal of Medicinal Plants Research*, 4, (20) 2148-2158

Gao, H., Popescu, R., Kopp, B., & Wang, Z. 2011. Bufadienolides and their antitumor activity. *Natural Product Reports*, 28, (5) 953-969 available from: http://dx.doi.org/10.1039/C0NP00032A

Garcin, A. *Maytenus senegalensis*. https://www.teline.fr/en/photos/celastraceae/maytenus-senegalensis#photo-8 . 2018.
Ref Type: Online Source

Gebauer, J., El-Siddig, K., & Ebert, G. 2012. Baobab (*Adamsonia digitata* L.): A Review on a Multipurpose Tree with Promising Future in the Sudan. *Gartenbauwissenschaft*, 67, (4) 155-160

Giardinaggio. *Jatropha multifida*. https://www.giardinaggio.it/appartamento/singolepiante/jatropha/jatropha.asp . 2018.
Ref Type: Online Source

Global Plants. *Neostenanthera gabonensis* (Engl. & Diels) Exell [family *Annonaceae*]. https://plants.jstor.org/stable/10.5555/al.ap.upwta.1_270?searchUri=filter%3Dname%26so%3Dps_group_by_genus_species%2Basc%26Query%3Dneostenanthera%2Bgabonensis . 2018.
Ref Type: Online Source

Graham, J.G., Quinn, M.L., Fabricant, D.S., & Farnsworth, N.R. 2000. Plants used against cancer - an extension of the work of Jonathan Hartwell. *Journal of ethnopharmacology*, 73, (3) 347-377 available from: http://www.sciencedirect.com/science/article/pii/S037887410000341X

Guinaudeau, H. 1994. Aporphinoid Alkaloids, V. *Journal of Natural Products*, 57, (8) 1033-1135

Help Congo. *Pachypodanthium staudtii*. http://www.help-congo-stories.org/index.php/a-conkouati/la-foret-tropicale-de-conkouati/un-peu-de-botanique/les-arbres/246-pachypodanthium-staudtii . 2018.
Ref Type: Online Source

Hirono, I., Aiso, S., Yamaji, T., Mori, H., Yamada, K., Niwa, H., Ojika, M., Wakamatsu, K., Kigoshi, H., & Niiyama, K. 1984. Carcinogenicity in Rats of Ptaquiloside Isolated from Bracken. *Gan*, 75, (10) 833-836 available from: http://europepmc.org/abstract/MED/6510632

Hirono, I., Shibuya, C., Fushimi, K., & Haga, M. 1970. Studies on Carcinogenic Properties of Bracken, *Pteridium aquilinum*. *Journal of the National Cancer Institute*, 45, (1) 179-188 available from: http://jnci.oxfordjournals.org/content/45/1/179.abstract

Hu, H.b., Zhang, X.w., & Wu, Y. 2014. Antitumor Activity of Stilbenoids and Flavonoids Isolated from *Acanthopanax brachypus*. *Russian Journal of General Chemistry*, 84, (7) 1434-1441 available from: http://dx.doi.org/10.1134/S1070363214070329

Igoli, J.O., Ogaji, O.G., Tor-Anyiin, T.A., & Igoli, N.P. 2005. Traditional Medicine Practice Amongst The Igede People of Nigeria. Part II. *African Journal of Traditional, Complementary and Alternative Medicines*, 2, (2) 134-152

Iizuka , M., marashina, T., & Tadataka, N. 2001. Bufadienolides and a New Lignan from the Bulbs of *Urginea maritima*. *Chemical and Pharmaceutical Bulletin*, 49, (3) 282-286

Inngjerdingen, K., Nergård, C.S., Diallo, D., Mounkoro, P.P., & Paulsen, B.S. 2004. An Ethnopharmacological Survey of Plants Used for Wound Healing in Dogonland, Mali, West Africa. *Journal of ethnopharmacology*, 92, 233-244

Jain, S.C., Jain, R., & Menghani, E. 2008. *Verbesina encelioides*: Perspective and Potentials of a Noxious Plant. *Indian Journal of Traditional Knowledge*, 7, (3) 511-513

Johnson-Ajinwo, O.R., Richardson, A., & Li, W.W. 2015. Cytotoxic Effects of Stem Bark Extracts and Pure Compounds from *Margaritaria discoidea* on Human Ovarian Cancer Cell Lines. *Phytomedicine*, 22, (1) 1-4 available from: http://www.sciencedirect.com/science/article/pii/S094471131400347X

Júnior, A.C.T.S., Asad, L.M.B.O., de Oliveira, E.B., Kovary, K., Asad, N.R., & Felzenszwalb, I. 2005. Antigenotoxic and Antimutagenic Potential of an Annatto Pigment (Norbixin) Against Oxidative Stress. *Genetics and Molecular Research*, 4, (1) 94-99

Kamuhabwa, A., Nshimo, C., & de Witte, P. 2000. Cytotoxicity of some Medicinal Plant Extracts Used in Tanzanian Traditional Medicine. *Journal of ethnopharmacology*, 70, 143-149

Kanth, B.S., Kumar, A.S., Shinde, D.B., Babu, K.H., Raju, T.V., Kumar, C.G., Sujitha, P., & Das, B. 2011. New Bioactive Macrocyclic Diterpenoids from *Jatropha multifida*. *Bioorganic and Medicinal Chemistry Letters*, 21, 6808-6810

Kintzios, S. E., Barberaki, M. G., & Makri, O. G. 2004, "Terrestrial Plant species with Anticancer Activity: a presentation," *In Plants That Fight Cancer*, S. E. Kintzios & M. G. Barberaki, eds., CRC Press, pp. 35-194.

Kuete, V., Wiench, B., Hegazy, M.F., Mohamed, T.A., Fankam, A.G., Shahat, A.A., & Efferth, T. 2012. Antibacterial Activity and Cytotoxicity of Selected Egyptian Medicinal Plants. *Planta Med*, 78, 193-199

Kumar, R., Kumar, N., Ramalingayya, G.V., Setty, M.M., & Pai, K.S.R. 2016. Evaluation of *Ceiba pentandra* (L.) Gaertner bark extracts for *in vitro* cytotoxicity on cancer cells and in vivo antitumor activity in solid and liquid tumor models. *Cytotechnology*, 2016/07/25, (5) 1909-1923 available from: https://www.ncbi.nlm.nih.gov/pubmed/27456242

Ladeji, O., Omekarah, I., & Solomon, M. 2003. Hypoglycemic Properties of Aqueous Bark Extract of *Ceiba pentandra* in Streptozotocin-induced Diabetic Rats. *Journal of ethnopharmacology*, 84, 139-142

Lagnika, L., Amoussa, M., Adjovi, Y., & Sanni, A. 2012. Antifungal, Antibacterial and Antioxidant Properties of *Adansonia digitata* and *Vitex doniana* from Bénin Pharmacopeia. *Journal of Pharmacognosy and Phytotherapy*, 4, (4) 44-52

Lam, S.K. & Ng, T.B. 2009. A Protein with Antiproliferative, Antifungal and HIV-1 Reverse Transcriptase Inhibitory Activities from Caper (*Capparis spinosa*) Seeds. *Phytomedicine*, 16, (5) 444-450 available from: http://www.sciencedirect.com/science/article/pii/S0944711308001700

Lopez-Lazaro, M. Flavonoids as Anticancer Agents: Structure-Activity Relationship Study. Current Medicinal Chemistry - Anti-Cancer Agents 2[6], 691-714. 11-1-2002.
Ref Type: Abstract

Mahidol, C., Prawat, H., Prachyawarakorn, V., & Ruchirawat, S. 2002. Investigation of Some Bioactive Thai Medicinal Plants. *Phytochemistry Reviews*, 1, 287-297

Malik, C.P., Garg, P., Singh, Y., & Grover, S. 2012. Medicinal Uses, Chemical Constituents and Micro Propagation of Three Potential Medicinal Plants. *International Journal of Life Science and Pharma Research*, 2, (3) 57-76

Manosroi, J., Sainakham, M., Manosroi, W., & Manosroi, A. 2012. Anti-proliferative and Apoptosis Induction Activities of Extracts from Thai Medicinal Plant Recipes Selected from MANOSROI II Database. *Journal of ethnopharmacology*, 141, 451-459

Maroyi, A. & Van de Maesen, L.J.G. 2011. *Gloriosa superba* L. (Family Colchicaceae): Remedy or Poison? *Journal of Medicinal Plants Research*, 5, (26) 6112-6121

Mishra, S.N., Tomar, P.C., & Lakra, N. 2007. Medicinal and Food Value of *Capparis* - A Harsh Terrain Plant. *Indian Journal of Traditonal Knowledge*, 6, (1) 230-238

Momtaz, S., Hussein, A.A., Ostad, S.N., Abdollahi, M., & Lall, N. 2013. Growth inhibition and induction of apoptosis in human cancerous HeLa cells by *Maytenus procumbens*. *Food and chemical toxicology : an international journal published for the British Industrial Biological Research Association*, 51, 38-45 available from: http://europepmc.org/abstract/MED/22989702

Moodley, N., Crouch, N.R., & Mulholland, D.A. 2007. Bufadienolides from *Drimia macrocentra* and *Urginea riparia* (*Hyacinthaceae*: *Urgineoideae*). *Phytochemistry*, 68, (19) 2415-2419 available from: http://www.sciencedirect.com/science/article/pii/S003194220700338X

Moran, R. *Pteris quadriaurita*. http://www.plantsystematics.org/imgs/robbin/r/Pteridaceae_Pteris_quadriaurita_23180.html . 2006.
Ref Type: Online Source

Mosmann, T. 1983. Rapid colorimetric assay for cellular growth and survival: Application to proliferation and cytotoxicity assays. *Journal of Immunological Methods*, 65, (1) 55-63 available from: http://www.sciencedirect.com/science/article/pii/0022175983903034

Mulaudzi, R.B., Ndhlala, A.R., Kulkarni, M.G., Finnie, J.F., & Van Staden, J. 2013. Anti-inflammatory and Mutagenic Evaluation of Mediinal Plants Used by Venda People against Venereal and Related Diseases. *Journal of ethnopharmacology*, 146, 173-179

Ngadjui, B.T., Lontsi, D., Ayafor, J.F., & Sondengam, B.L. 1989. Pachypophyllin and Pachypostaudins A and B: Three Bisnorlignans from *Pachypodanthium staudtii*. *Phytochemistry*, 28, (1) 231-234 available from: http://www.sciencedirect.com/science/article/pii/0031942289850447

Nwosu, M.O. 2002. Ethnobotanical Studies on Some Pteridophytes of Southern Nigeria. *Economic Botany*, 56, (3) 255-259

Okany, C.C., Ishola, I., & Ashorobi, R.B. 2012. Evaluation of analgesic and antistress potential of methanolic stem wood extract of *Microdesmis puberula* Hook.f. ex Planch (Pandaceae) in mice. *International Journal of Applied Research in Natural Products; Vol 5, No 3 (2012)* available from: http://ijarnp.org/index.php/ijarnp/article/view/125

Okoli, R.I., Aigbe, O., Ohaju-Obodo, J.O., & Mensah, J.K. 2007. Medicinal Herbs Used for Managing Some Common Ailments among Esan People of Edo State, Nigeria. *Pakistan Journal of Nutrition*, 6, (5) 490-496

Phillipson, B. P. *Margaritaria discoidea*. http://tropical.theferns.info/plantimages/4/b/4b427cfed325bd67a7d732f55798f91a9a452722.jpg . 2018.
Ref Type: Online Source

Pierpaoli, E., Viola, V., Barucca, A., Orlando, F., Galli, F., & Provinciali, M. 2013. Effect of annatto-tocotrienols supplementation on the development of mammary tumors in HER-2/neu transgenic mice. *Carcinogenesis*, 34, (6) 1352-1360 available from: http://carcin.oxfordjournals.org/content/34/6/1352.abstract

Plant valley. *Gloriosa superba* (Flame Lilly). https://plantvalley.org/products/gloriosa-superba-flame-lily-10-seeds . 2018.
Ref Type: Online Source

Randt, d. F. *Capparis brassii* SED a 080913_edited-1. https://www.ispotnature.org/communities/southern-africa/view/observation/390389/capparis-brassii-sed-a-080913edited-1 . 2014.
Ref Type: Online Source

Ravindra, A. & Mahendra, K.R. 2009. Review: Current Advances in *Gloriosa superba* L. *Biodiversitas*, 10, (4) 210-214

Renner, C. & Achembach, H. 1988. Stenantherine and *N*-methylstenantherine, new aporphines from *Neostenanthera gabonensis*. *Journal of Natural Products*, 51, (5) 973-976

Rout, S.D., Panda, T., & Mishra, N. 2009. Ethnomedicinal Studies on Some Pteridophytes of Similipal Biosphere Reserve, Orissa, India. *International Journal of Medicine and Medicinal Sciences*, 1, (5) 192-197

Sabandar, C.W., Ahmat, N., Jaafar, F.M., & Sahidin, I. 2013. Medicinal Properties, Phytochemistry and Pharmacology of Several *Jatropha* Species (*Euphorbiaceae*): A Review. Phytochemistry, 85, 7-29

Said, M., Badshah, A., Shah, N.A., Khan, H., Murtaza, G., Vabre, B., Zargarian, D., & Khan, M.R. 2013. Antitumor, Antioxidant and Antimicrobial Studies of Substituted Pyridylguanidines. *Molecules*, 18, 10378-10396

Sarpong, K., Mensah, M.L.K., & Heymann, H. 1990. Some alkaloid constituents of the bark of *Pachypodanthium staudtii* Engl. and Diels. *Journal of University of Science and Technology*, 9, (1) 15-20

Scamperdale. *Microdesmis puberula*. http://tropical.theferns.info/image.php?id=Microdesmis+puberula . 2018.
Ref Type: Online Source

Schmidt, M. *Drimia altissima* (L.f.) Ker Gawl. http://www.africanplants.senckenberg.de/root/index.php?page_id=78&id=603#image=6336 . 2009.
Ref Type: Online Source

Schmidt, M. *Ceiba Pentandra*. http://tropical.theferns.info/plantimages/e/0/e0417d099720f47d9890fd2e1b0f3ee76fd7efac.jpg . 2018.
Ref Type: Online Source

Shilpi, J.A., Taufiq-Ur-Rahman, M., Uddin, S.J., Alam, M.S., Sadhu, S.K., & Seidel, V. 2006. Preliminary pharmacological screening of Bixa orellana L. leaves. *Journal of ethnopharmacology*, 108, (2) 264-271 available from: http://europepmc.org/abstract/MED/16963211

Shirota, O., Morita, H., Takeya, K., & Itokawa, H. 1994. Cytotoxic Aromatic Triterpenes from *Maytenus Ilicifolia* and *Maytenus Chuchuhuasca*. *Journal of Natural Products*, 57, (12) 1675-1681

Silva, C.R., Antunes, L.M.G., & Bianchi, M.D.P. 2001. Antioxidant Action of Bixin Against Cisplatin-Induced Chromosome Aberrations and Lipid Peroxidation in Rats. *Pharmacological Research*, 43, (6) 561-566

Simran, M., Singh, P.S., & Pathan, S. 2017. Protective Potential of Herbal Plants and their Constituents on the Clastogenicity Produced by Anticancer Treatments. *International Journal of Engineering Technology, Management and Applied Sciences*, 5, (7)

Stevigny, C., Bailly, C., & Quertin-Leclercq, J. 2005. Cytotoxic and Antitumor Potentialities of Aporphinoid Alkaloids. *Current Medicinal Chemistry*, 5, 173-182

Stockert, J.C., Bl+ízquez-Castro, A., Ca+¦ete, M., Horobin, R.W., & Villanueva, +. 2012. MTT assay for cell viability: Intracellular localization of the formazan product is in lipid droplets. *Acta Histochemica*, 114, (8) 785-796 available from: http://www.sciencedirect.com/science/article/pii/S0065128112000190

Sule, M.I., Njinga, N.S., Musa, A.M., Magaji, M.G., & Abdullahi, A. 2009. Phytochemical and Antidiarrhoeal Studies of the Stem Bark of *Ceiba pentandra* (Bombacaceae). *Nigerian Journal of Pharmaceutical Sciences*, 8, (1) 143-148

Tahir, A.E., Satti, G.M.H., & Khalid, S.A. 1999. Antiplasmodial Activity of Selected Sudanese Medicinal Plants with Emphasis on *Maytenus senegalensis* (Lam.) Exell. *Journal of ethnopharmacology*, 64, 227-233

Thomas, T. 2011. Preliminary Antibacterial Evaluation of Fronds of *Pteris quadriaurita* Retz. Towards Bacteria Involved in Dermatological Diseases. *Journal of Applied Pharmaceutical Science*, 1, (8) 214-216

Tibodeau, J.D., Isham, C.R., & Bible, K.C. 2010. Annatto Constituent Cis-Bixin Has Selective Antimyeloma Effects Mediated by Oxidative Stress and Associated with Inhibition of Thioredoxin and Thioredoxin Reductase. *Antioxidants and Redox Signaling*, 13, (7) 987-997

Tipdisease. Baobab (*Adansonia Digitata*) Overview, Health Benefits, Side effects. http://1.bp.blogspot.com/-Xf5ZvP-nb5s/VdF8NNHJ4PI/AAAAAAAA20o/0NKpGfbifxY/s1600/Baobab%2B%2528Adansonia%2BDigitata%2529%2BOverview%252C%2BHealth%2BBenefits%252C%2BSide%2Beffects%2B%25282%2529.jpg . 2018.
Ref Type: Online Source

Tomšík, P. 2014. Ferns and Lycopods - A Potential Treasury of Anticancer Agents but Also a Carcinogenic Hazard. *Phytotherapy Research*, 28, (6) 798-810 available from: http://dx.doi.org/10.1002/ptr.5070

Upadhyay, R.K. 2011. Kareel Plant: A Natural Source of Medicines and Nutrients. *International Journal of Green Pharmacy* 255-265

Chapter 3

Bio-activity Guided Isolation of a Novel Flavonoid *C*-glycoside from *Drimia altissima* (L.F.) Ker Gawl. (*Asparagaceae*)

3.1 Introduction

Drug discovery can be defined as the search for potential therapeutic agents through the screening of compound libraries, the isolation of natural bio-active metabolites and the design of synthetic compounds for specific pharmacological targets (Nature 2018). The process of drug discovery has been termed as a 'chemical beauty' contest because compounds cannot be eligible for drug development unless they are both biologically relevant and drug-like (Leeson 2012). Biological relevance is the ability of a compound to interact with pharmacological targets such as proteins (receptors, ion channels and carrier enzymes) and nucleic acids whereas drug-likeness pertains to the ability of such a compound to possess physicochemical properties that promote oral bioavailability (Deng et al. 2013).

The inception of medicinal and combinatorial chemistry has resulted in the generation of numerous compounds with poor physicochemical properties (non-drug-like) and hence, the introduction of the Lipinski rule of 5 (RO5) as a screening method to discriminate between drug-like and non-drug-like compounds (Lipinski 2004). RO5 restricts drug-like compounds to having a molecular weight less than 500 Da, not more than 5 hydrogen bond donors, not more than 10 hydrogen bond acceptors and lipophilicity (octanol-water partition coefficient log *P*) not greater than 5 (Benet et al. 2016). A virtual concept referred to as 'chemical space' has been defined as the total number of small carbon-based molecules that can be principally generated (Dobson 2004). Cheminformatics report that there are about 10^{60} drug-like organic molecules in the known chemical space (Reymond and Awale 2012). Despite this vast number of potential drug candidates, only 1 in 1000 synthetic compounds makes it through the clinical trials phase (Tamimi and Ellis 2009). This is because numerous drug development challenges are encountered before a concept drug can be turned into a marketed product.

3.1.1 Challenges to drug discovery and development

Drug discovery and development is a highly expensive and risky business process that takes a minimum of 10 – 15 years to accomplish (Tamimi and Ellis 2009). One of the key challenges faced by drug discovery enthusiasts is high cost rates. On estimate, discovering, developing and launching a single drug candidate costs as much as USD 0.8 - 1.8 billion (Khanna 2012). Another challenge is high failure rates associated with clinical trials. Only 1 in 10 clinical trial candidates is likely to succeed with most failures occurring during phase II as a result of lack of efficacy (51%), strategic reasons (29%) and safety concerns (19%). Also, the pharmaceutical industry is the most regulated industry in the world. Extensive global regulatory standards have to be met in order to prove a drug candidate's efficacy and safety across races, ethnicities and age groups. This is time consuming and leads to few new chemical entities (NCE's) being approved by the FDA.

3.1.2 Advantages of natural products over synthetic compounds

Chemical entities in drug discovery are either synthetic compounds or natural products (NP). Synthetic compounds are chemically derived whereas natural products are extracted from the natural environment such as from plants, animals, microbes and marine algae. These compounds can be further categorised as totally synthetic, totally synthetic with natural product pharmacophores (natural product inspired), totally natural, natural with semi-synthetic modifications and natural product mimics (Newman and Cragg 2016). However, for the scope of this chapter, the mention of synthetic compounds only implies chemical entities that are totally synthetic.

According to the ZINC database there are currently about 22 million commercially available synthetic compounds, of which only a relatively small number have biological relevance (Figure 3.1) (Irwin and Shoichet 2005; Harvey et al. 2015). On the other hand, the dictionary of natural products records 160, 000 compounds, all of which are biologically relevant and most of which are drug-like (130,000) (Harvey et al. 2015). Since the 1940's, about 74.8% of commercially available anti-cancer drugs are either natural product based or natural product inspired (Newman and Cragg 2012). In the quest for new therapeutic agents, one of the main advantages of pursuing natural products over synthetic compounds is that natural products have intrinsic biological relevance. This is because natural products are secondary metabolites synthesized by living organisms to target biological processes for biological purposes such as

adaptation to surrounding environments and as defence mechanisms against predators (Lahlou 2013). As mentioned above, one of the key drug development challenges is high failure rates associated with clinical trials, with 19% of these failures occurring as a result of toxicity. Owing to hundreds of years of ethnobotanical plant usage as natural remedies, natural products are relatively less toxic than synthetic compounds and hence, more likely to succeed as NCE's. For instance, ancient herbal formulations such as the Mesopotamian records (dated 2600 BC as the oldest existing pharmacopoeia) are still in use today (Ji et al. 2009). Natural products exhibit more chemical and structural diversity than synthetic compounds to the extent that over 40% of the natural product pharmacophores are absent from medicinal chemistry libraries, with some being too difficult and/ or too expensive to chemically synthesize. For instance, since 1996 there has been an ongoing attempt to chemically synthesize maitotoxin, a highly potent toxin isolated from the dinoflagellate *Gambierdiscus toxicus*, but success has not yet been reported (Krämer 2015).

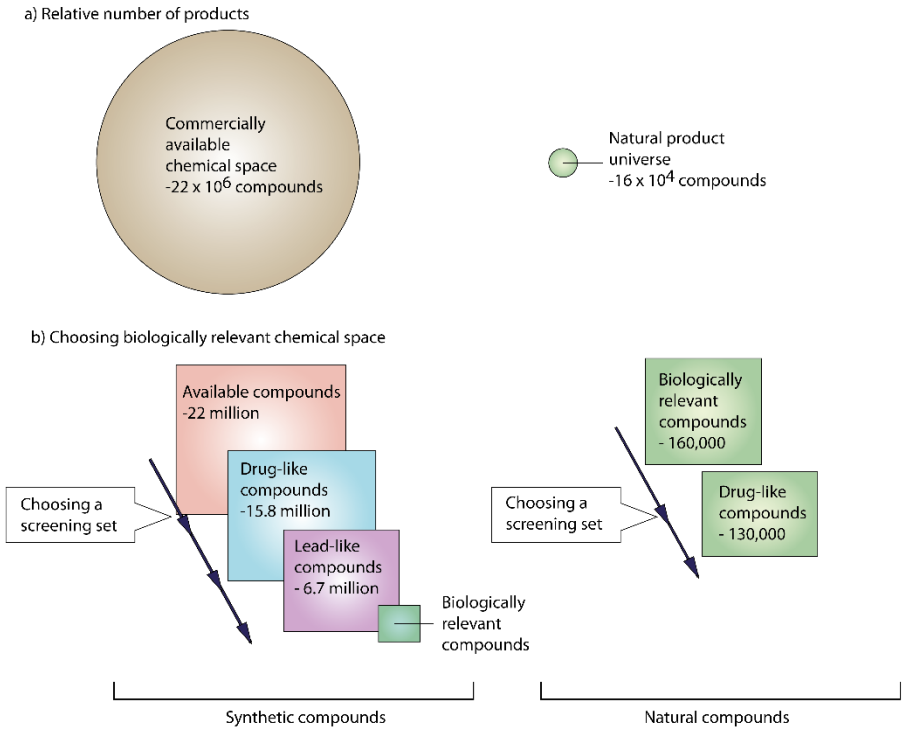

Figure 3.1 Biological relevance comparison between synthetic and natural compounds (Adapted from: Harvey et al. 2015)

3.1.3 Challenges to natural product drug discovery

In the past few decades, there has been a significant reduction in the approval of natural product-based drugs owing to current paradigms in the pharmaceutical industry and the challenges associated with the discovery of bio-active natural compounds. This has led to an explosive interest in combinatorial chemistry and high through-put screening (HTS) (Li and Vederas 2009). Natural product drug discovery faces challenges that are inherent to natural products and those that are specific to the African setting. Inherent challenges can be further classified into basic and practical problems (Guantai and Chibale 2012). One of these basic challenges is variations in the content of bioactive plant metabolites resulting from seasonal and environmental changes to the extent that even plants of the same cultivar and under the same agricultural conditions could have significant variations in their chemical compositions (Aires et al. 2011). This makes repetition of experiments very difficult and unreliable. In conventional early stage natural product drug discovery (Figure 3.2), extensive literature review and careful consideration of ethnobotanical practices is usually performed in order to identify and select medicinal plants for bio-activity screening. A basic challenge to this approach is that obtaining ethnobotanical information on certain natural product sources can be very difficult. For instance, it is a challenge to obtain ethnobotanical information on deep water marine algae since they are usually inaccessible to traditional practitioners. For this reason, some researchers choose to randomly select and screen plants for classes of compounds such as alkaloids, steroids, flavonoids etc. Even though this approach increases the chances of obtaining novel compounds, it provides no guarantee of efficacy. Other researchers randomly select large numbers of plants and perform biological assays. Except for a few successes such as the discovery of paclitaxel and camptothecin, this method is time consuming, expensive and has a very high failure rate (Katiyar et al. 2012). Natural products have no guarantee of supply since plant species can become extinct. It has been estimated that 15,000 out if 50,000 – 70,000 medicinal plants are faced with extinction (Brower 2008). Legislations can also prevent access to certain medicinal plants.

One of the practical challenges to natural product drug discovery is the high complexity of metabolic content in plant extracts which makes fractionation and purification of active metabolites a very tedious process. There is also a risk of losing bio-activity after fractionation and purification since some of the efficacies of plant extracts are a result of synergy between two or more chemical constituents. Another challenge usually encountered in natural product

research is that bio-active compounds are usually isolated in very minute quantities. This can be a limiting factor to compound characterisation as well as bio-activity testing as adequate amounts are required in these processes. In the African setting, the major challenges to natural product drug discovery include insufficient funding, unavailability of or poor infrastructure and absence of skilled researchers (Guantai and Chibale 2012).

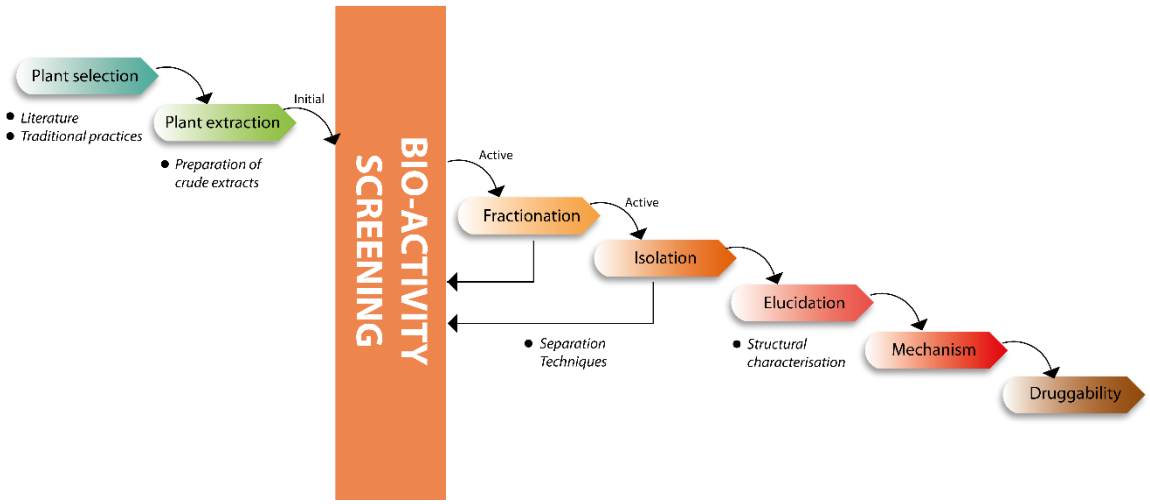

Figure 3.2 Conventional early stage natural product drug discovery (Adapted from: Guantai and Chibale 2012)

3.1.4 Bridging the gap between conventional and modern drug discovery paradigms

In order for natural products to reclaim their role in pharmaceutical drug development it is important to merge conventional natural product drug discovery methods with modern approaches. For instance, natural product databases and repositories would provide in-depth information on isolated compounds such as geographical source, structural elucidation and biological data. In Africa, the few available databases such as Natural Product Research Network for East and Central Africa (NAPRECA), Network for Analytical and Bioassay Services in Africa (NABSA) and South African National Biodiversity Institute (SANBI) only represent a very small fraction of the entire plant diversity of the continent. Natural products need to be applied to modern drug discovery techniques such as virtual screening, *in silico* docking and high throughput screening (HTS). Bio-informatics can be applied to perform ligand-based virtual screening to determine mechanisms of action and structural activity relationship studies (SAR) (Claus and Underwood 2002). This would assist in identifying previously unknown biological activities which could then be followed up with *in vitro* bio-assays. The absorption, distribution, metabolism and excretion (ADME) characteristics of a

potential drug candidate are a known challenge in early drug discovery. *In silico* software such as VolSurf and MetaSite can be used to predict ADME properties such as solubility, membrane permeability, bio-availability etc., thereby allowing for the selection of more druggable natural compounds (Scotti et al. 2010).

Since synergistic natural compounds are less effective when tested separately, natural product drug discovery can incorporate the design of dual drugs in which two synergistic natural pharmacophores are covalently linked together to create novel highly potent hybrid drugs. Such hybrid compounds have been found in natural existence. A good example is thiomarinol (**3.1**), an antimicrobial antibiotic isolated from the marine bacterium *Alteromonas rava* sp. nov. SANK 73390. Thiomarinol is a hydrid compound consisting of a pseudomonic acid C analogue (**3.2**) and holothin (**3.3**). Other examples include the naphthylisoquinoline alkaloid michellamine (**3.4**), a homo-dimer of the alkaloid korupensamine A (**3.5**) and korundamine A (**3.6**), a hetero-dimer of korupensamine A (**3.5**) and Yaoundamine A (**3.7**) (Figure 3.3) (Tietze et al. 2003). This hybrid approach has also led to the design of multi-target-directed ligands in which natural products are linked to synthetic compounds acting on different pharmacological targets. Examples of such compounds include the cytotoxic hybrid distamycin A/DC-81 (**3.8**) (K562 cells, IC_{50} = 0.04µM) formed by linking the natural antibiotic distamycin A (**3.9**) (K562 cells, IC_{50} = 12µM) isolated from *Streptomyces distallicus* with a synthetic antineoplastic antibiotic DC-81 (**3.10**) (K562 cells, IC_{50} = 1µM). Another semi-synthetic hybrid is paclitaxel/ α-tocopherol hybrid glycine ester (**3.11**) consisting of the natural anti-oxidant α-tocopherol (**3.12**) and the antimitotic agent paclitaxel (**3.13**) (isolated from the bark of *Taxus brevifolia*) linked together via a diester. Hybrid **3.11** exhibited an increased selectivity for A431 skin carcinoma cells (Decker 2011).

Apart from the exploration for natural lead compounds, natural products can also be used to identify novel protein targets through metabolic and activity based profiling. In these processes, the metabolic activity of an organism is evaluated upon exposure to biologically active compounds to determine the affected metabolic pathways. The identified target proteins or enzymes are then subjected to either classical or reverse pharmacology in which the targets are cloned and subjected to "ligand fishing" with various natural and/ or synthetic compounds (Takenaka 2001).

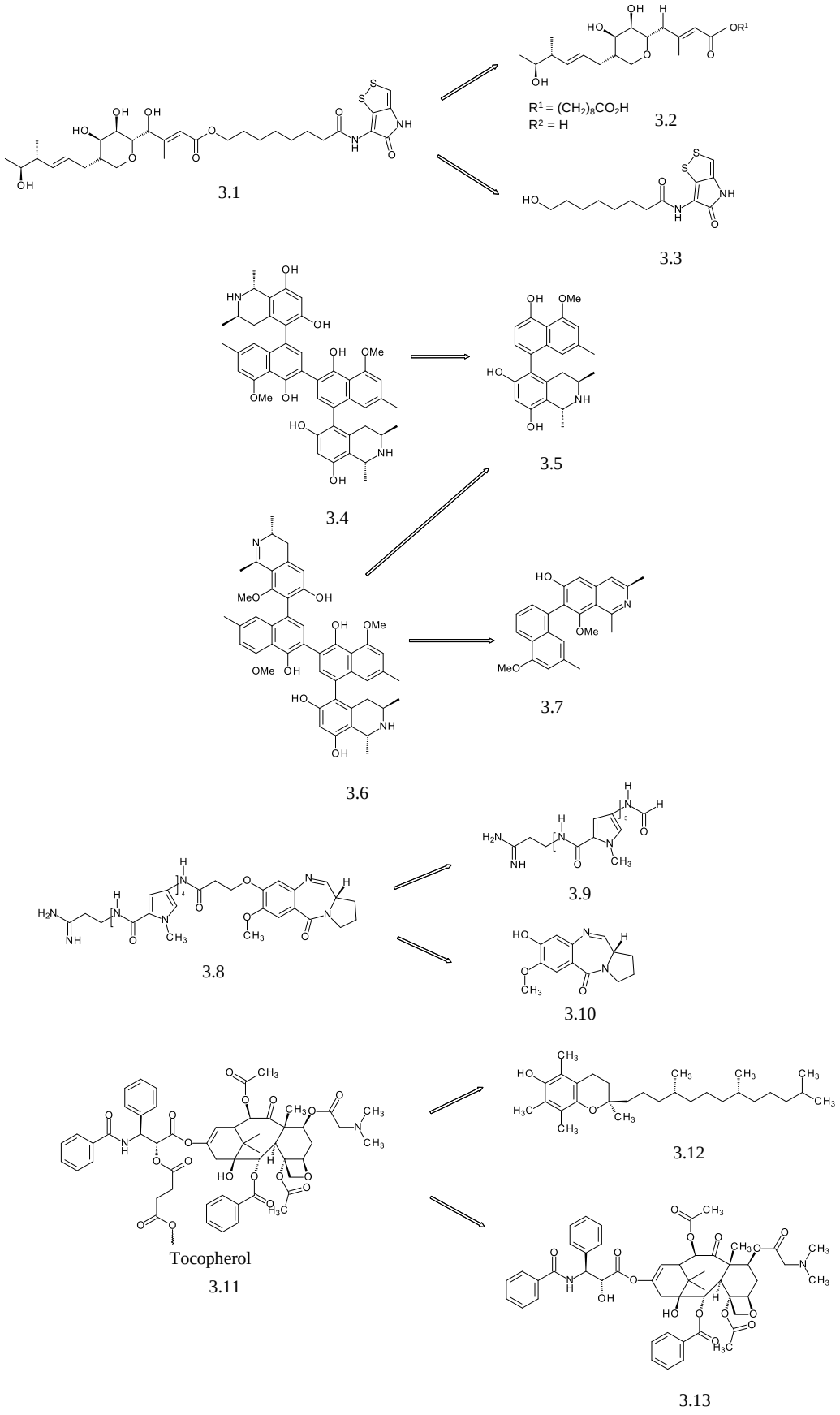

Figure 3.3 Natural and semi-synthetic bio-active hybrids and dimers (Tietze et al. 2003)

3.2 Pharmacognosy of *Drimia altissima* (L.F.) Ker Gawl.

Drimia altissima (Figure 3.4), commonly known as the "African Squill" or the "Tall White Squill", is a terrestrial bulbous plant that is widely distributed in tropical and southern Africa from Senegal all the way to South Africa (Williams et al. 2016). *D. altissima* is often referred to in isiZulu as *Umahlokoloza* (Crouch et al. 2010), or by its Afrikaans names; *Maerman*, *Jeukbol*, *Maermanbol*, *Maermanui* and *Slangkop* (Quattrocchi 2000) *D. altissima* was previously called *Urginea altissima* (L.F.) Baker before the genera *Drimia* and *Urginea* were combined under the *Hyacinthaceae* sub-family (Stedje 2000). Other *D. altissima* synonyms include *Scilla altissima*, *Idothea altissima* (L.F.) Kuntze and *Ornithogalum altissimum* L.F (Iwu 2014). The name *altissima* is derived from the Latin word *altus* (high) and the superlative suffix *issimus* (extremely) to mean "very tall".

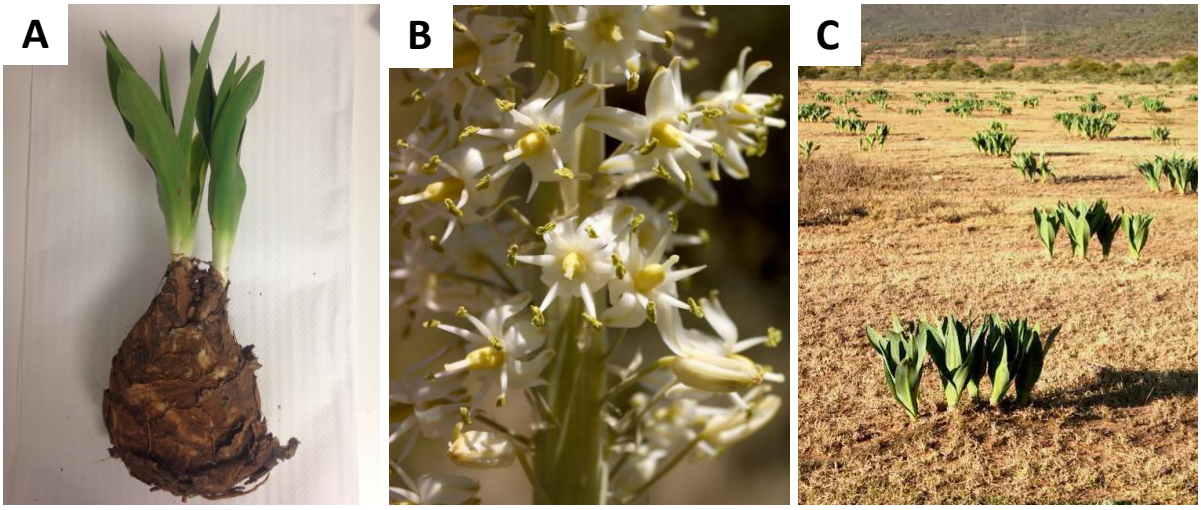

Figure 3.4 Images showing the bulb and leaves (A), inflorescence (B) and habitat (C) of *Drimia altissima* (L.F) Ker Gawl. (Dressler et al. 2014)[3]

The leaves of *D. altissima* (20 - 50 cm long, 2 - 7.5 cm wide) are shaped like a lance head and expand after the opening of the flowers. The long internode forming the peduncle is perpendicular with a diameter of about 1 cm. The inflorescence (about 80 cm) is a dense arrangement consisting of 700 flowers with intervals of spreading pedicels (8 – 30 mm long) on a common axis. The modified leaves seated on the pedicels reach up to 14 mm in length with associated tubular expansions reaching up to 3 mm. The external floral whorls (either white or greenish white with green or purple bands facing away from the stem) are either free

[3] Images courtesy of Dresser et al. 2014, except 3.4A which was photographed by Mr. Mutenta N. Nyambe at Nelson Mandela University, Chemistry Department, 2015

or united, up to 2 mm and having a length of between 5 - 11 mm. The filaments are either linear or slightly triangular, and may either be free (4 - 7 mm) or united with the external floral whorls. The ovaries are about 2 – 5 mm (equivalent to the length of the style) and take an oval shape. The capsule is almost spherical with a notched apex of 8 - 15 mm in height and 9 - 15 mm in diameter. The seeds are semi-orbicular and 5 - 8 mm long (Stedje 1987). Scanning electron microscopy (SEM) of the leaf surface in *Drimia* species shows striations with cells exhibiting a single central row of papillae and prominent stomata (Figure 3.5). The wax in *Drimia* species is devoid of crystalloids. The longitudinal leaf blades are almost cylindrical with tapering into elongated cones. The epidermis exhibits the outer periclinal wall and cuticle which are significantly thick while the inner periclinal walls are lobed. The mesophyll shows a single palisade layer of cells appearing underneath the epidermises. There is no lacunae, vascular bundles appear with 1 to 2 rings and vascular tissue consist of V-shaped xylems. Among cell inclusions are crystal fragments and raphid-styloid intermediate crystals which are present in idioblast cells (Lynch et al. 2006). The bulbs are half above ground with rough, overlapping scales.

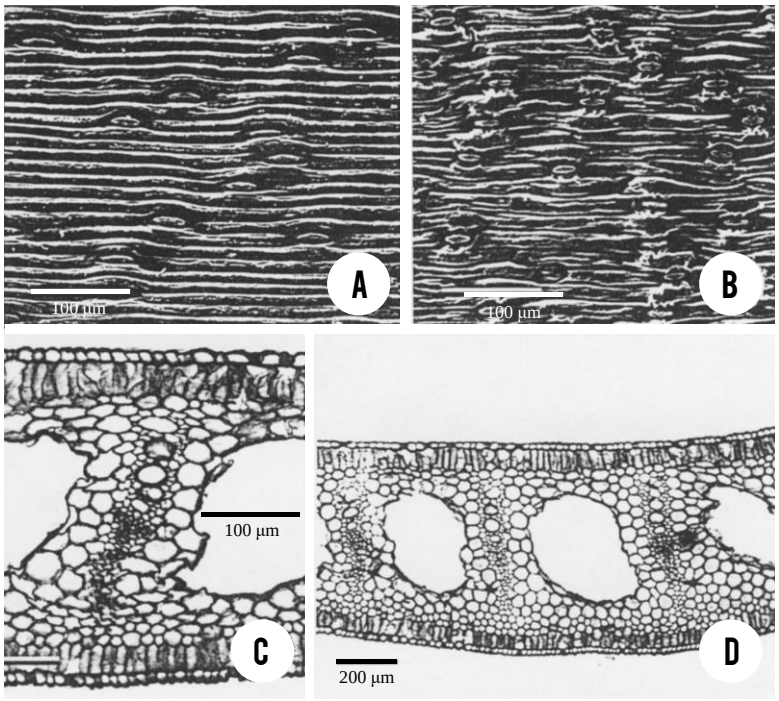

Figure 3.5 Microscopic (SEM) images of *D. altissima* leaves (Lynch et al. 2006)

(A) Abaxial leaf surface showing long and narrow epidermal cells, (B) abaxial leaf surface showing papillae on cells proximal to stomata, (C) transverse section of the leaf with single palisade layer underneath the epidermises, and (D) transverse section of the leaf with large lacunae between single rows of vascular bundles

3.2.1 Phylogenetic classification of the *Asparagaceae* family

Drimia altissima is a member of the *Asparagaceae* family. The *Asparagaceae* is a family of monocotyledonous flowering plants from the *Asparagales* order (APG III 2009). A recent study estimates that there are 114 genera and 2900 species in the *Asparagaceae* family (Christenhusz and Byng 2016). The *Asparagaceae* family can be further divided into seven sub-families; *Aphyllanthoidae*, *Agavoidae*, *Brodiaeoidae*, *Schilloidae*, *Lomandroidae*, *Asparagoidae* and *Nolinoidae* (Figure 3.6) (Chase et al. 2009).

Within *Asparagaceae*, *Drimia altissima* comes from the *Schilloidae* sub-family, which is sometimes considered as a separate family under the name *Hyacinthaceae*. *Hyacinthaceae* is an established monophyletic family with approximately 70 genera and between 700 - 1000 species (Pfosser and Speta 1999; Manning et al. 2003) which are mainly distributed around Europe, Africa and south-west Asia (APG II 2003). Taxonomic differentiation of genera and species within the *Hyacinthaceae* family has been a matter of contention since the time of Linnaeus (Stedje 2001). This controversy has continued in recent decades due to contradicting results from different phylogenetic studies. Based on results from analytical studies of plastid DNA *trnL-F*, phytochemistry as well as morphological and micro-structural data, the *Hyacinthaceae* family has been divided into four tribes; *Oziroëeae*, *Urgineeae*, *Hyacintheae* (which is further divided into sub-tribes *Pseudoprospero*, *Massoliinae* and *Hyacinthinae*) and *Ornithogaleae* (Figure 3.6) (Manning et al. 2003). A phylogenetic study showed the relationship between genera from *Hyacinthaceae* tribes and sub-tribes (Figure 3.7) (Goldblatt et al. 2012).

From the *Urgineeae* tribe arises the genera *Bowiea*, *Drimia*, *Schizobasis* and *Fusifilum*, with the latter two occasionally included in *Drimia*. Among these, species from *Drimia* have the most extensive use as medicinal plants (Nath et al. 2014). After a study of chloroplast DNA and morphological data, a suggestion has been made to combine the genera *Drimia*, *Urginea* and *Thuranthos* into one genus, with *Drimia* given a wide circumscription (Stedje 2000). The same study analysed the nucleotide sequence of the intergenic spacer between the chloroplast genes *trnL* (UAA), the *trnF* (GAA) and the *trnL* (UAA) intron to show the relationship between 11 species within *Drimia* (Figure 3.8).

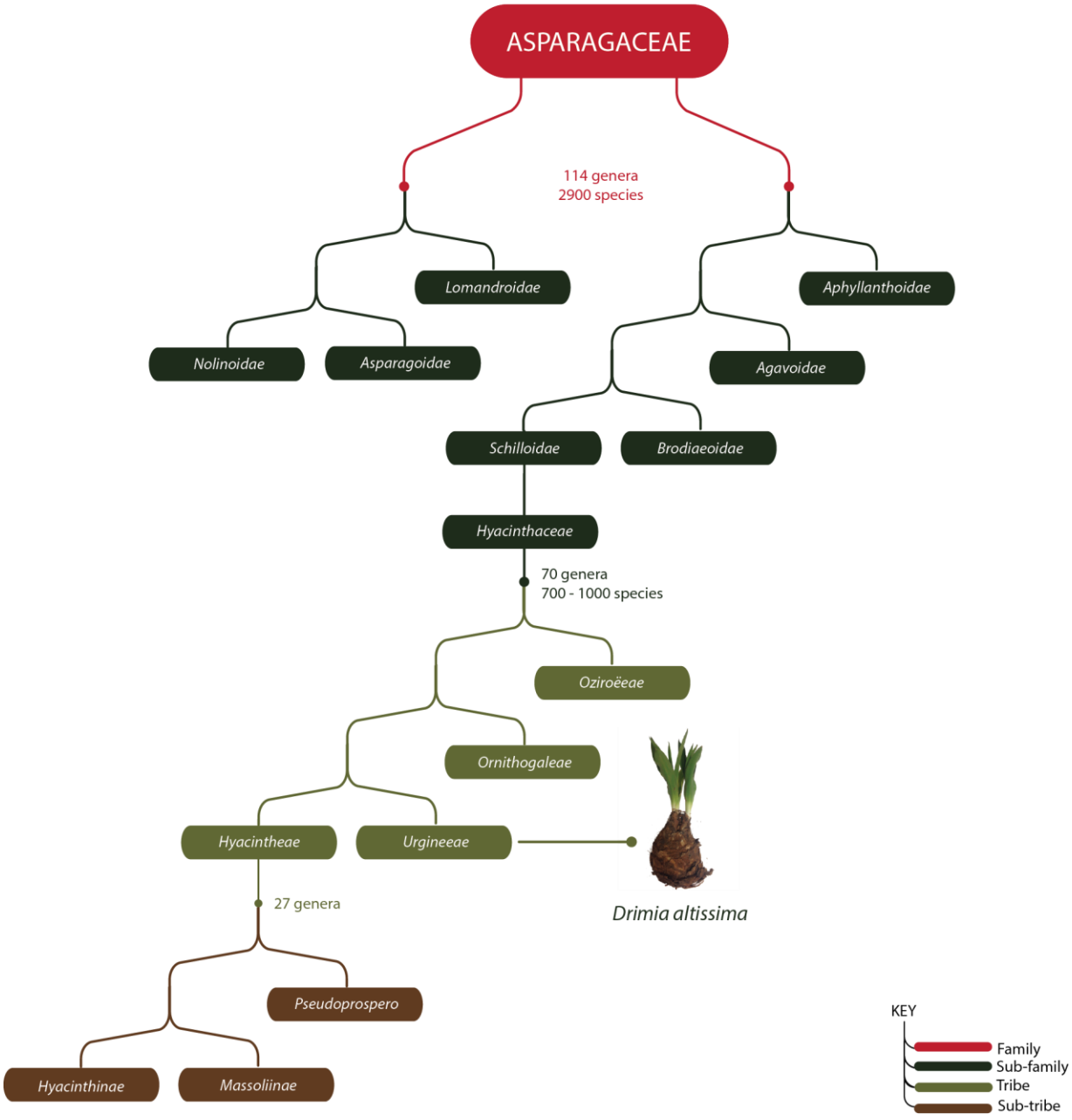

Figure 3.6 Cladogram of the *Asparagaceae* family showing separations between sub-families, tribes and sub-tribes (Adapted from: Manning et al. 2003; Chase et al. 2009)

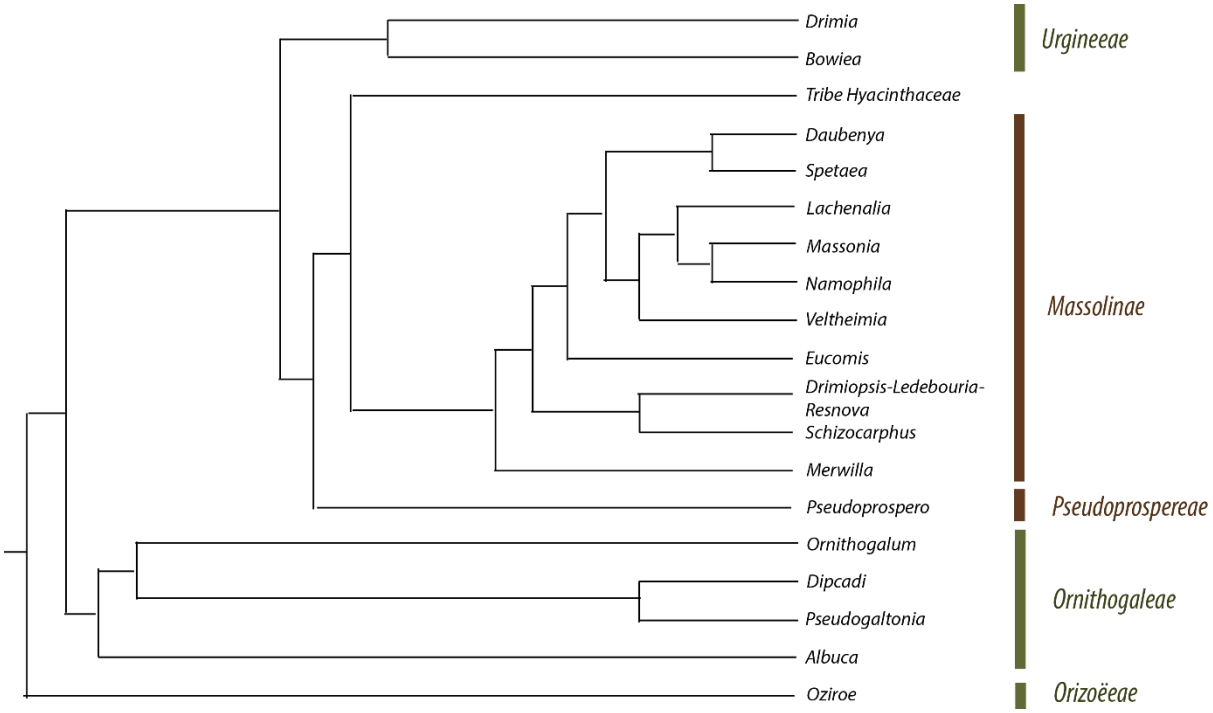

Figure 3.7 Phylogeny of *Hyacinthaceae* showing relationships between genera within tribes and sub-tribes (Goldblatt et al. 2012)

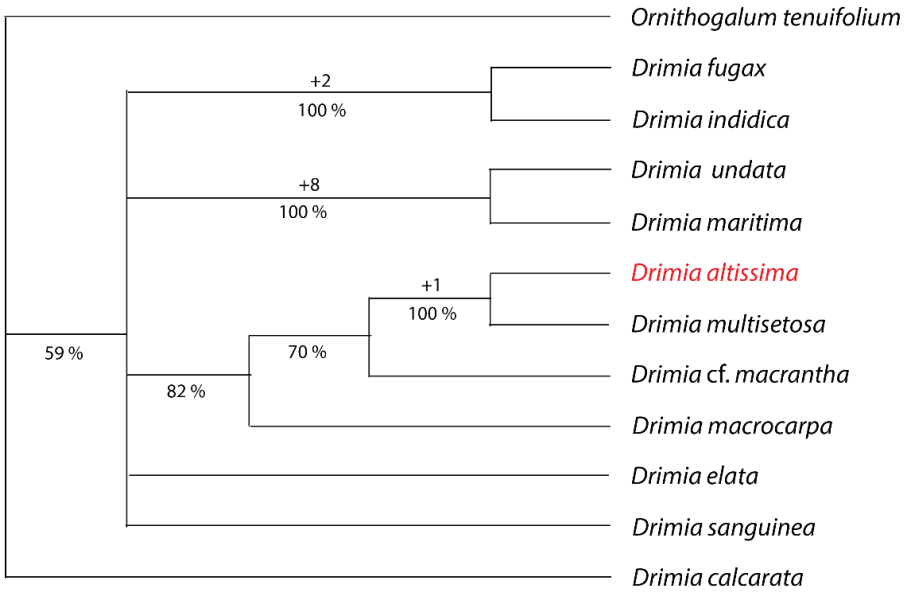

Figure 3.8 Cladogram of 11 *Drimia* species after analysis of the nucleotide sequence of the intergenic spacer between the chloroplast genes *trnL* (UAA), the *trnF* (GAA) and the *trnL* (UAA) intron (Stedje 2000)

Ornithogalum tenuifolium was used as outgroup. Numerical values above the branches show the number of extra steps required for node collapse while percentages are bootstrap values

3.2.2 *Drimia altissima* plant habitat and distribution

The genus *Drimia* is native to and present across the Mediterranean region and sub-Saharan Africa where it is widespread with several herbarium specimens accessible in Southern Africa (Figure 3.9A) (Conservatoire et Jardin Botaniques 2012). The genus *D. altissima* is widely distributed in Tropical, Eastern and Southern Africa (Figure 3.9B). East African countries reporting the presence of *D. altissima* include Eritrea, Ethiopia, Somalia and Djibouti. In Southern Africa *D. altissima* is widespread in South Africa, Namibia, Botswana, Zimbabwe, Mozambique, Malawi and Tanzania. *D. altissima* finds its habitat in Albany thickets, fynbos, bushlands, open woodlands, grasslands and savanna where it reaches a height of 35 - 200 cm at altitudes of up to 2,100 meters above sea level (Stedje 1987).

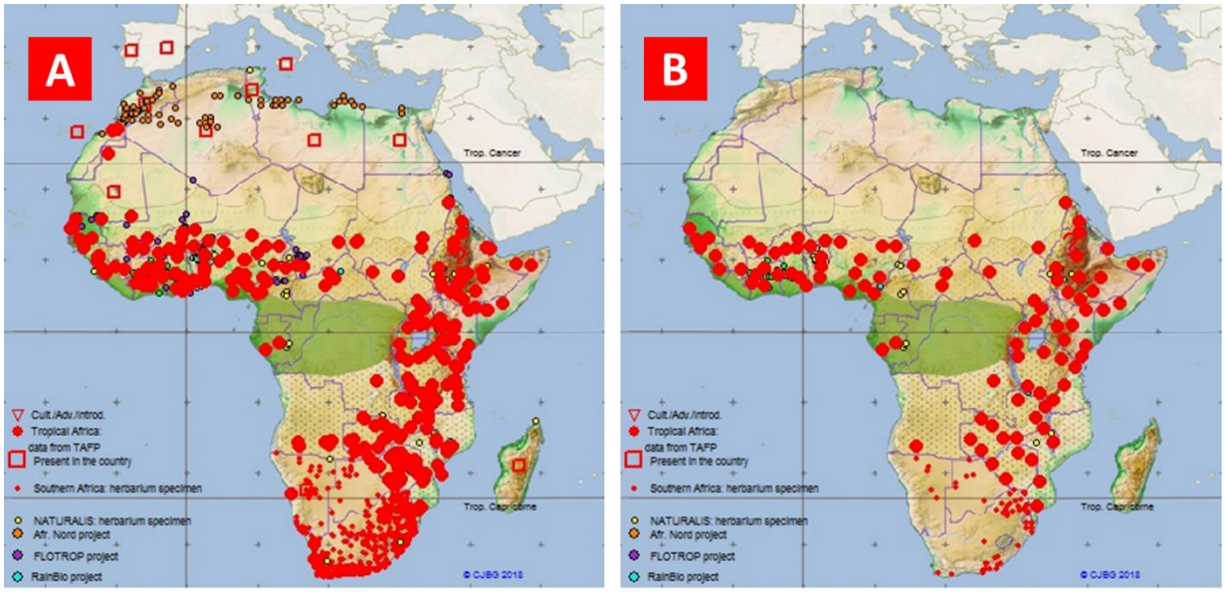

Figure 3.9 Plant distribution map for genus *Drimia* (A) and species *D. altissima* (B) (Conservatoire et Jardin Botaniques Ville De Genève 2012)

3.3 Phytochemistry of the *Urgineeae* tribe

The main types of compounds isolated from genera within *Urgineeae* are flavonoids and bufadienolides. Bufadienolides are considered as chemotaxonomic markers for the *Urgineeae* tribe (Pohl et al. 2000).

3.3.1 Commonly isolated compounds from genus *Drimia*

Phytochemical investigations of *Drimia* species have resulted in the isolation of several bio-active *C*-glycosylflavones and scillaridin-based cardiotonic glycosides. For instance, the *C*-glycosylflavones vitexin, isovitexin, orientin, isoorientin, scoparin, vicenin-2 and possibly an isovitexin-*O*-xyloside (Fernandez et al. 1975), as well as the bufadienolides proscillaridin A and Scillaren A have been isolated from *D. maritima* (Kedra and Kedrowa 1968; Iizuka et al. 2001). The ethnomedicinal and pharmacological use of extracts and compounds derived from plants belonging to the genus *Drimia* is well documented (See Chapter 2, Section 2.2).

3.3.2 Compounds previously isolated from *Drimia altissima*

Phytochemical studies involving *D. altissima* have so far only resulted in the isolation of bufadienolides. Bufadienolides that have been isolated from *D. altissima* include hellebrigenin (**3.14**), urginin (**3.15**) and arenobufagin-3-*O*-α-L-rhamnopyranoside (**3.16**) Figure 3.10) (Shimada et al. 1979; Ermias et al. 1994). A report claiming the isolation of the isoquinoline alkaloids lycorine and acetylcaranine from *D. altissima* (Miyakado et al. 1975) has since been identified as a mistake resulting from the misidentification of an Amaryllidaceous bulb (Pohl et al. 2001). Presently, there are no literature reports of flavonoids isolated from *D. altissima*.

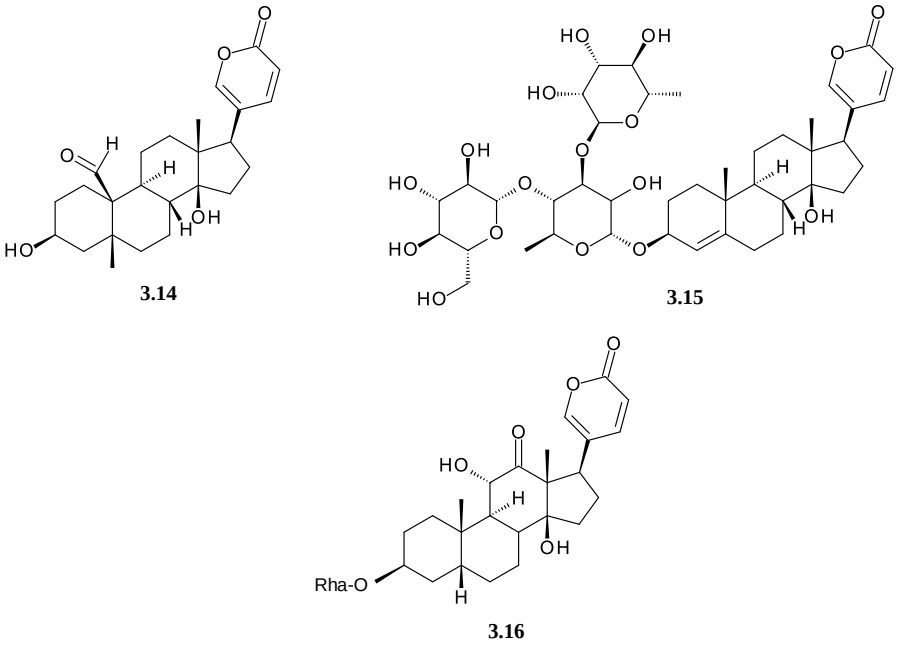

Figure 3.10 Selected bufadienolides isolated from *Drimia altissima*

3.4 Chapter aims

In chapter 2, after *in vitro* cytotoxicity screening of extracts from the four selected plants, it was discovered that the methanolic bulb extract of *Drimia altissima* possessed the highest anti-proliferative activity against HeLa cells. This chapter, gives a detailed description of the bio-activity guided isolation and structural characterisation of a novel natural compound from the methanolic bulb extract of *Drimia altissima* which is partly responsible for the cytotoxic activity of the extract.

3.5 Results and discussion

3.5.1 Soxhlet extraction and isolation of metabolite from *Drimia altissima*

Bulbs of *Drimia altissima* were collected from Kwa-Nobuhle (Uitenhage), South Africa. The plant biomass was extracted with MeOH:CH_2Cl_2 (8:2) using a soxhlet apparatus to afford crude extract **MN-14-79** (Scheme 3.1). Sufficient de-ionized water was then added to **MN-14-79** after which the aqueous mixture underwent a series of liquid-liquid partitioning with *n*-Hex, EtOAc, and *n*-BuOH respectively to give partitions **79a** (aqueous), **79b** (Hex), **79c** (EtOAc) and **79d** (*n*-butanol). ^{1}H NMR of partition **79d** (Figure 3.11) exhibited signals in the aliphatic region, in the sugar region δ_H 3 – 4 and in the aromatic region δ_H 6 – 8.5.

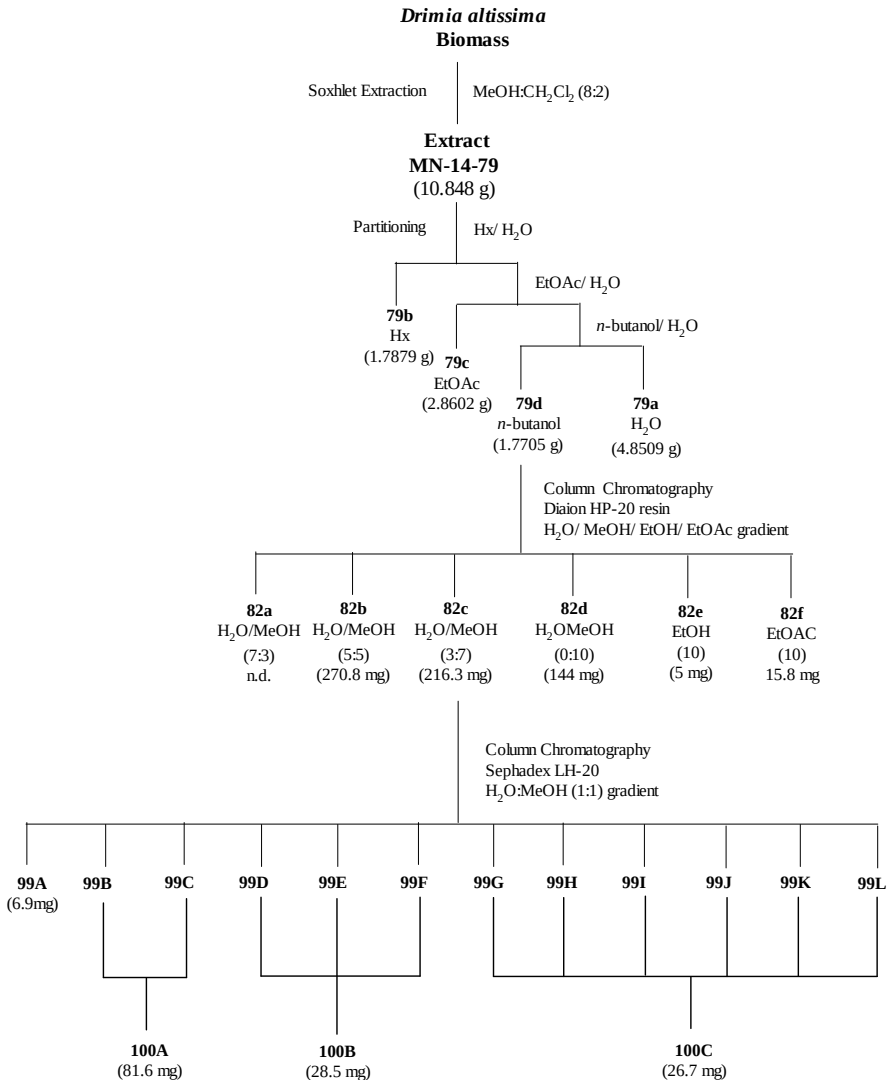

Scheme 3.1 Scheme showing the isolation of compound **100c** (**3.17**) from *Drimia altissima*

n.d. = Not determined

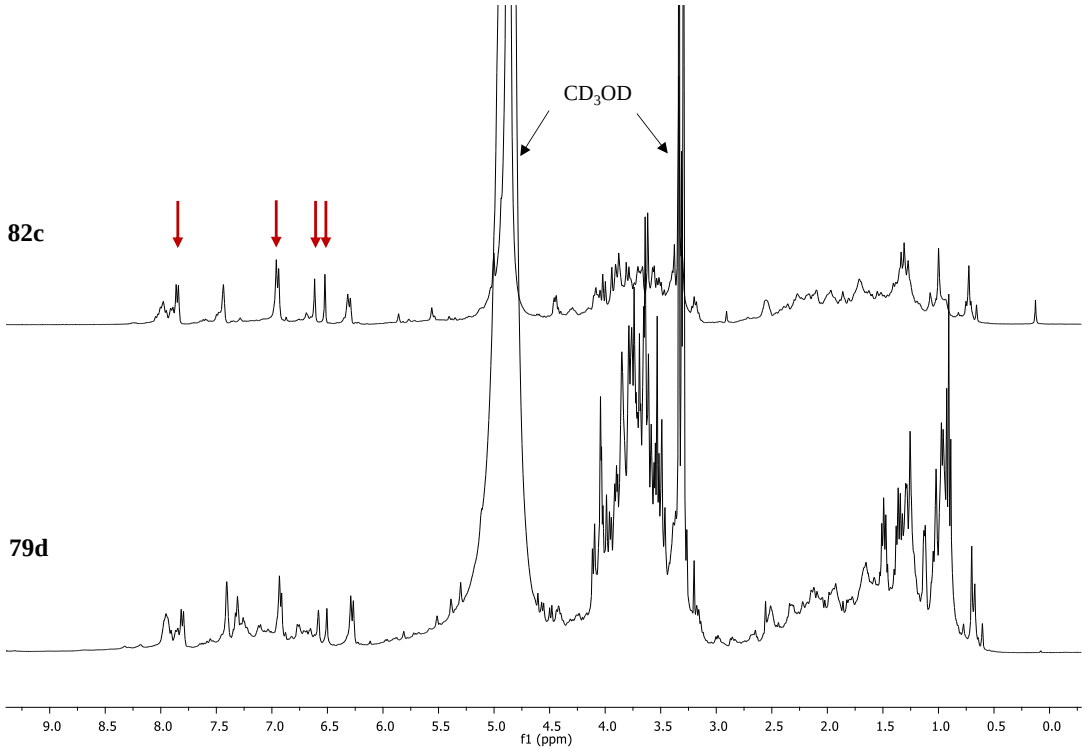

Figure 3.11 ^{1}H NMR spectra (CD_3OD, 400MHz) of *Drimia altissima* methanolic crude extract **79d** and fraction **82c**

The four red arrows indicate peaks of interest in the aromatic region

Based on bio-assay results (see Chapter 4, Section 4.3.1), partition **79d** was further selected for fractionation. Bio-assay guided fractionation of **79d** by Diaion® HP-20 resin open column chromatography using a stepwise gradient of reducing polarity (H_2O-MeOH-EtOH-EtOAc) yielded 6 fractions (**82a** – **f**), with fraction **82c** exhibiting peaks of interest in the aromatic region (Figure 3.11). Further purification of fraction **82c** by Sephadex® LH-20 open column chromatography using 50% MeOH yielded fractions **99a** – **l**. After Thin Layer Chromatography (TLC) profiling on silica gel using *n*-BuOH, glacial acetic acid and water (4:1:2 v/v) as mobile phase (Figure 3.12), fractions **99b** – **99c**, **99d** – **99f** and **99g** – **99l** were combined to form sub-fractions **100a**, **100b** and **100c** respectively (Scheme 3.1). Sub-fraction **100c** was found to be 99% pure using Liquid Chromatography/Mass Spectrometry (LC/MS) at 280nm (Figure 3.13) and hence, designated as compound **3.17**.

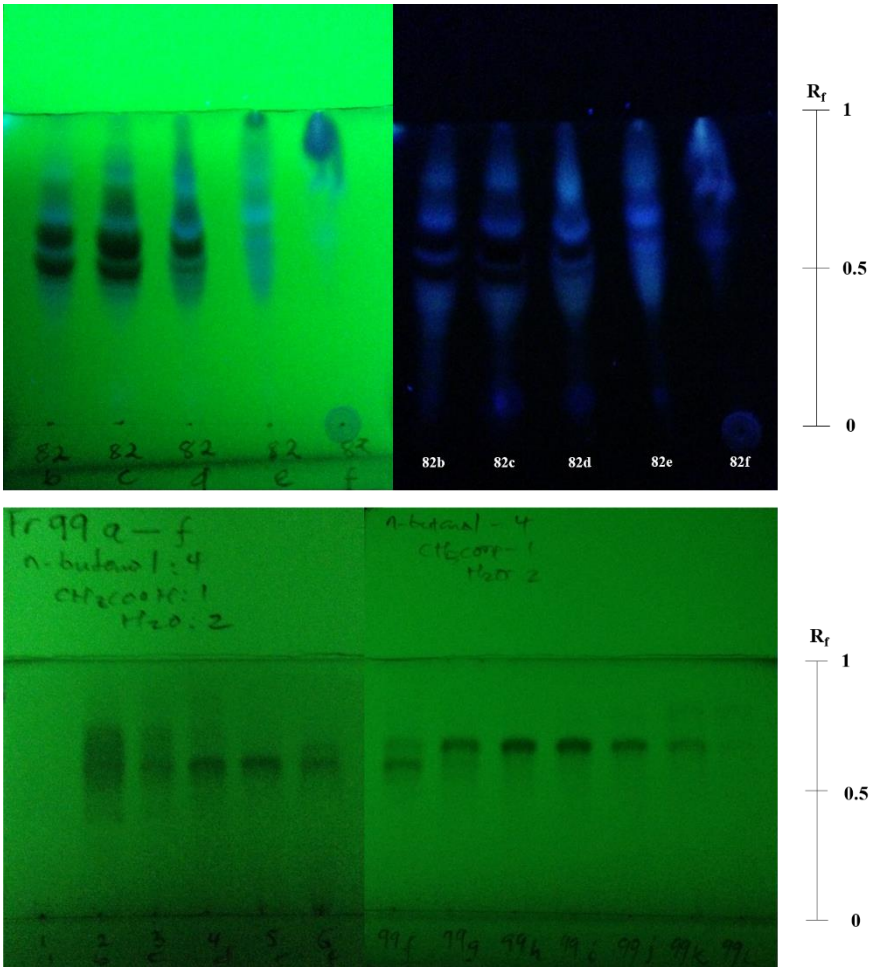

Figure 3.12 Silica gel TLC profiling of fractions **82b** – **f** (top) and **99a** – **l** (bottom) using *n*-BuOH, glacial acetic acid and water (4:1:2 v/v) as mobile phase.
UV lamp wavelengths: 254 nm (top right) and 365 nm (top left and bottom)

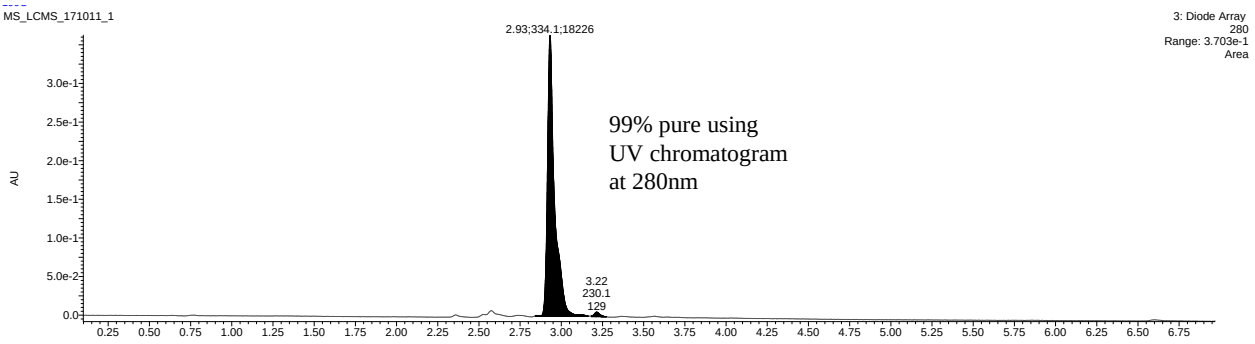

Figure 3.13 LC/MS chromatogram of compound **3.17** at 280 nm using water and acetonitrile (95:5 v/v) as mobile phase

3.5.2 Structural characterisation of compound 3.17

3.5.2.1 Mass spectrometry (MS)

The fragmentation pattern and nomenclature of fragment ions resulting from the ionization of flavonoid glycosides was developed in the 1970's and has undergone several alterations over the years (Pikulski and Brodbelt 2003). In the free aglycone, designations $^{i,j}A_0$ and $^{i,j}B_0$ are used in reference to fragments with intact A- and B- rings respectively, with superscripts *i* and *j* indicating cleaved bonds in the C-ring. Fragments of glycosides with retained charges on their sugar portions are labelled A_i, B_i and C_i, where *i* denotes cleaved bonds counted from the terminal sugar moiety (Cuyckens and Claeys 2004). Similarly, ionic fragments containing the aglycone are designated X_j, Y_j and Z_j, where *j* is the number of the cleaved interglycosidic bond from the aglycone. The glycosidic linkage between the aglycone and the sugar residue is designated as 0. For flavonoid-*C*-glycosides with *O*-interglycosidic linkages such as compound **3.17**, Y_0 and Y_1 represent aglycone-containing fragments with cleaved *C*- and *O*-glycosides respectively (Figure 3.14) (Vukics and Guttman 2010).

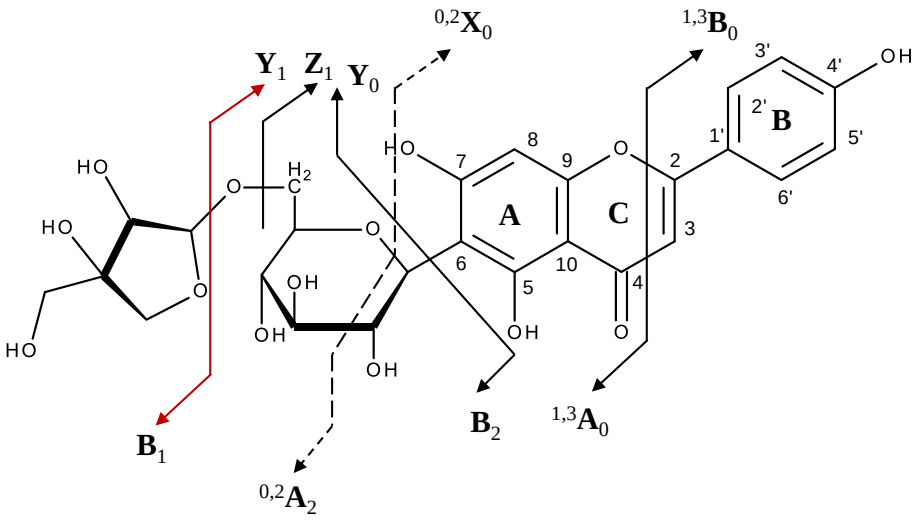

Figure 3.14 Fragmentation pattern and nomenclature for flavonoid *C*- and *C*-*O*-glycosides (Vukics and Guttman, 2010)

From LC/MS and HR-MS results, ESI-MS analysis in the positive mode (Figure 3.15) obtained pseudomolecular ions at *m/z* 565.15 $[M+H]^+$ (base peak) and *m/z* 584.13 $[M+H_2O]^+$, confirming the theoretical molecular weight of compound **3.17** ($C_{26}H_{28}O_{14}$, 564.54 Da). The

observed fragment at *m/z* 431 $[M+H-134]^+$ indicated a Y_1 fragmentation pattern (Figure 3.14) representing a flavonoid glycoside after departure of a sugar moiety.

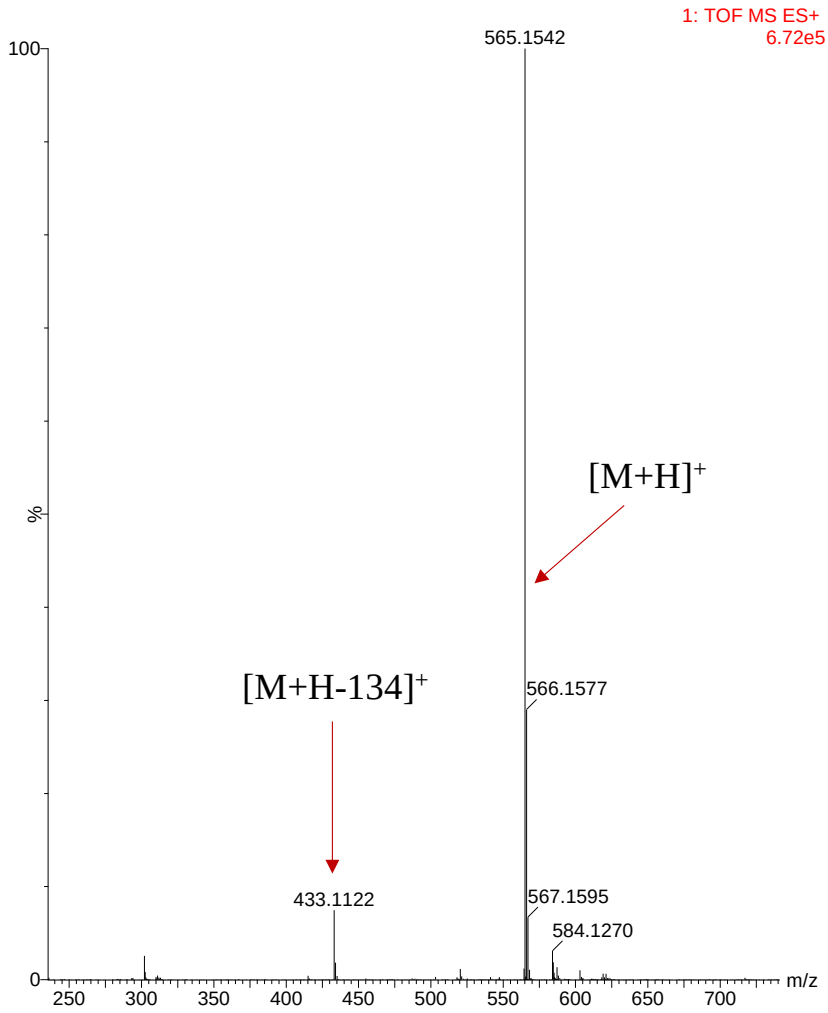

Figure 3.15 LC/ESI-MS spectrum of **3.17** in positive ionization mode

3.5.2.2 Ultraviolet spectroscopy (UV)

The UV absorption of flavonoid compounds in MeOH is characterised by the appearance of two absorption peaks designated as Band I (λ 300 – 380 nm) and Band II (λ 240 – 280 nm) as a result of absorption from the B-ring cinnamoyl and the A-ring benzoyl systems respectively. Flavones and flavonols with oxygenated A-rings but non-oxygenated B-rings tend to have more pronounced Band II absorption peaks whereas those which also have B-ring oxygenation have more pronounced Band I. Band I can be used to distinguish between flavones and flavonols containing an –OH substituent at position C-3, with Band I for flavones appearing

around λ 304 – 350 nm and that of flavonols appearing around 352 – 385 nm. However, this does not apply to flavonols in which the -OH at C-3 is either methylated or *O*-glycosylated as the Band I range (λ 328 – 357 nm) in this case tends to overlap that of flavones. Increased oxygenation of the B-ring results in a bathochromic shift of Band I with subsequent splitting of Band II into IIa and IIb (without shifting). Similarly, an increase in the hydroxylation of ring-A results in a significant bathochromic shift in Band II and a less conspicuous shift in Band I. For flavones, hydroxylation at C-5 has a marked effect on the absorption pattern of Bands I and II, with absence of hydroxylation causing both Bands to appear at shorter wavelengths (λ 3 – 10 nm in Band I and 6 – 17 nm in Band II) than in their hydroxylated forms. Glycosylation of the –OH groups in flavones and flavonols at positions C-3, C-5 and C-4′ cause hypsochromic shifts, most notably in Band I. However, glycosylation at all other positions has no effect on the UV absorption spectra of flavonoids in MeOH (Mabry et al. 1970).

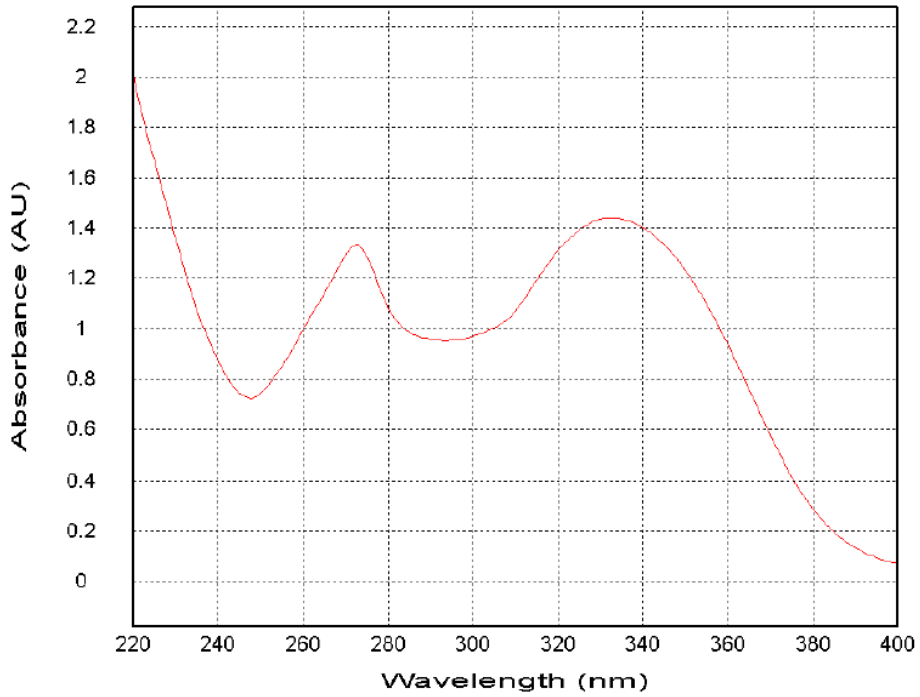

Figure 3.16 UV absorption spectrum of compound **3.17**

The UV spectrum of compound **3.17** (Figure 3.16) exhibited a typical two maxima flavonoid absorption pattern with a pronounced Band I at λ 333 nm indicating the presence of hydroxylation on the B-ring and a less pronounced Band II at λ 272 nm. The shorter wavelength of Band I confirmed the absence of an –OH substituent at position C-3 while the absence of a bathochromic shift in Band I and lack of splitting in Band II indicated a single –OH substituent

at C-4′ of the B-ring. Compared to the absorption patterns of non-hydroxylated A-rings, the 22 nm bathochromic shift observed in Band II of compound **3.17** confirmed the A-ring –OH substituents at positions C-5 and C-7.

3.5.2.3 Circular Dichroism (CD)

Flavonoid glycosides with chiral aglycones exhibit Cotton effects identical to their corresponding aglycones whereas those possessing racemic aglycones exhibit weak Cotton effects at λ 250 – 350 nm. Flavones have a single chiral centre at position C-2 while flavonols with an –OH substituent at C-3 have two chiral centres at positions C-2 and C-3. UV absorption maxima in the range λ 270 – 290 nm and 320 – 330 nm are a result of a π – π* and n – π* electronic transitions respectively, with the former being more helpful when determining the optical chirality of flavonoid glycosides. Flavones with a 2*S* configuration generally exhibit a positive Cotton effect in the range λ 245 – 270 nm accompanied by a negative Cotton effect in the range λ 225 – 240 nm (Gaffield 1970).

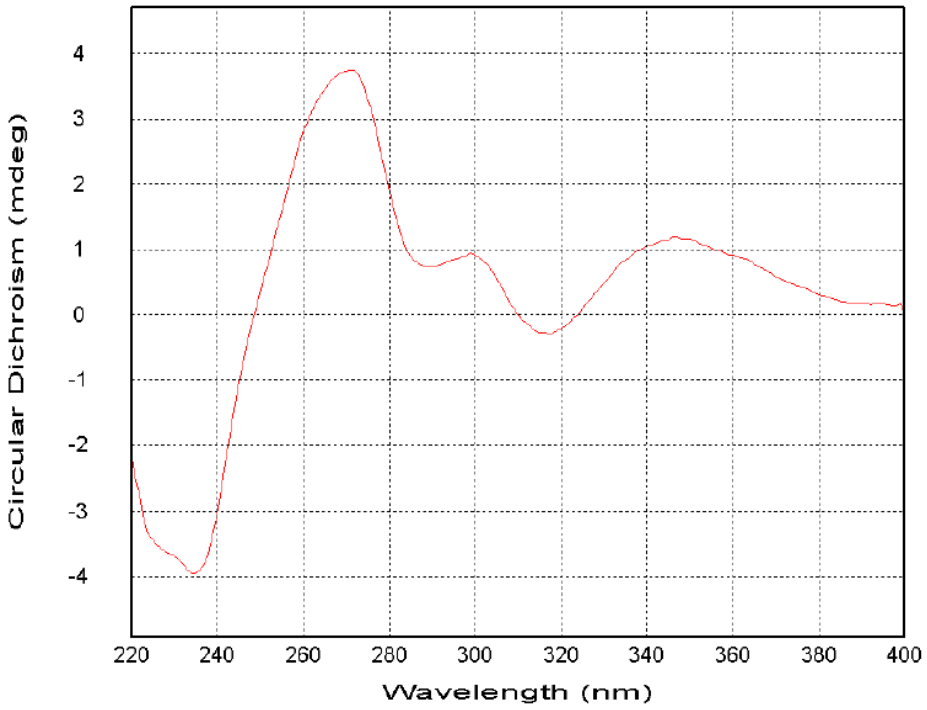

Figure 3.17 Circular Dichroism (CD) spectrum of compound **3.17**

The CD spectrum of compound **3.17** (Figure 3.17) exhibited a negative π – π* Cotton effect at λ 235 and a positive π – π* Cotton effect at 271 nm corresponding with a 2*S* configuration at chiral position C-2.

3.5.2.4 Fourier-Transform Infrared (FT-IR) spectroscopy

In the infrared analysis of flavonoid compounds, the most dominant bands are aromatic ring vibrations ranging from 1598 – 1612 cm^{-1}, 1560 - 1570 cm^{-1} and 1452 - 1488 cm^{-1} and phenolic -OH deformation vibrations ranging from 1308 - 1370 cm^{-1} (Heneczkowski et al. 2001). Other characteristic flavonoid bands include Phenolic -OH stretching vibrations ranging from 1112 - 1172 cm^{-1} and out-of-plane bending absorption of the 4′-substituted flavonoid B-ring ranging from 831 - 837 cm^{-1} (Wagner 1963).

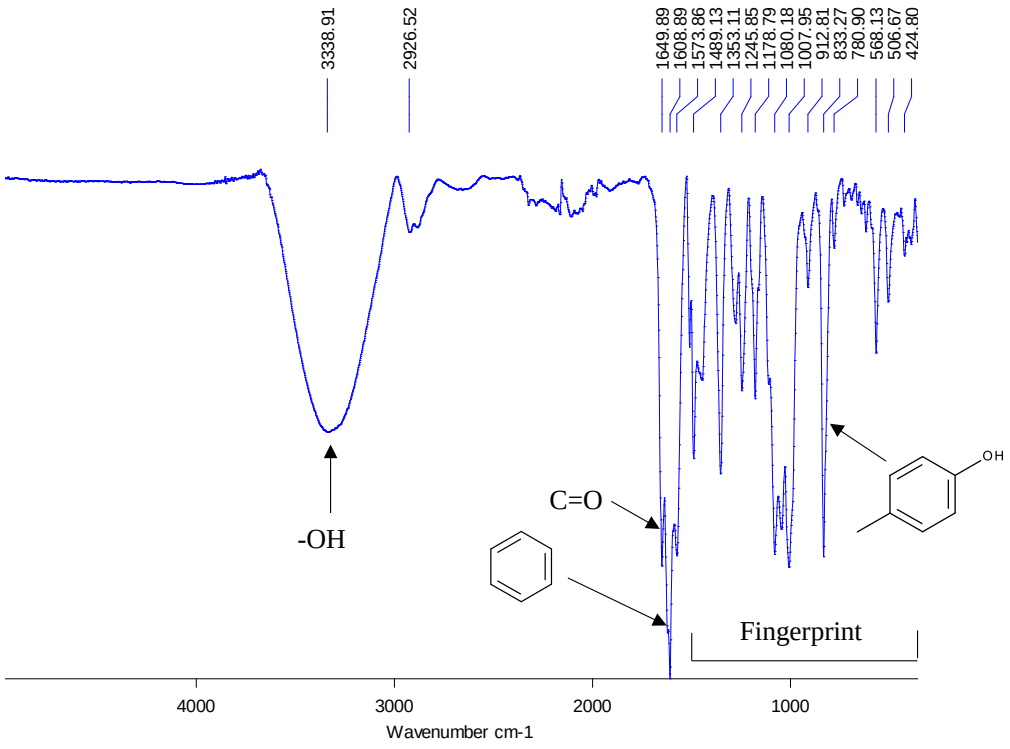

Figure 3.18 FT-IR spectrum of compound **3.17**

The FT-IR spectrum of **3.17** (Figure 3.18) presented a sharp carbonyl stretching vibration at 1649.89 cm^{-1}, confirming the flavonoid carbonyl functional group at C-4. The FT-IR spectrum also exhibited a broad hydroxyl stretching vibration at 3338.91 cm^{-1} and a sharp aromatic ring vibration at 1608.89 cm^{-1}. *Para*-substitution of the flavonoid B-ring was confirmed by a conspicuous out-of-plane deformation vibration at 833.27 cm^{-1}.

3.5.2.5 1D Nuclear Magnetic Resonance (NMR) spectroscopy

The ^{1}H NMR spectrum of **3.17** (Figure 3.19) showed overlapping signals in the sugar region (δ_H 3.0 – 4.0) with doublets at δ_H 4.93 and 5.0 (J = 10.2) suggestive of two anomeric protons. Within the aromatic region, there were two singlets at δ_H 6.55 and 6.64 and two doublets at δ_H 6.96 and 7.88, creating an AMX spin system characteristic of flavonoid compounds as previously observed in Figure 3.11 (Maltese et al. 2009). Unlike the ^{1}H NMR spectrum of **82c**, no up-field aliphatic protons were present. These results were suggestive of a flavonoid compound with two glycosidic moieties.

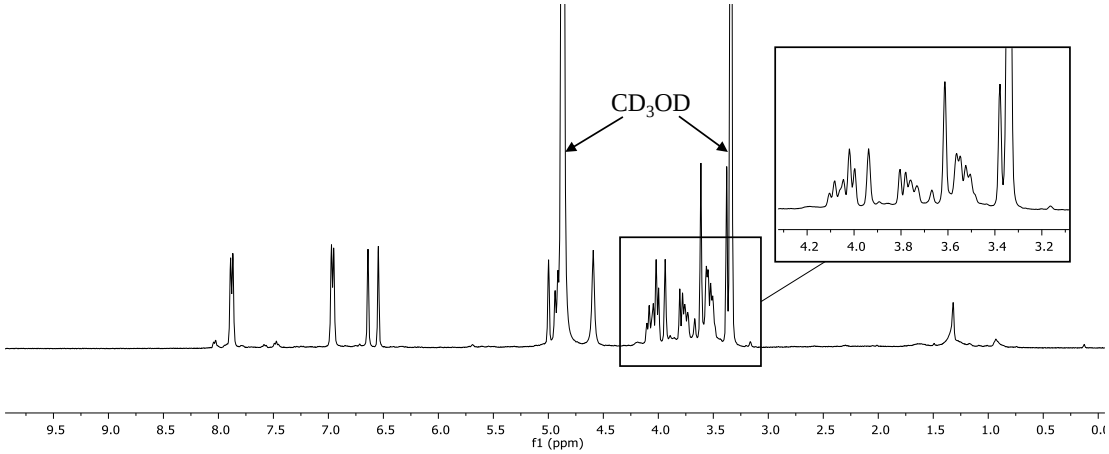

Figure 3.19 ^{1}H NMR spectrum (CD_3OD, 400MHz) of compound **3.17**

Comparison of ^{1}H and ^{13}C NMR spectroscopic data of **3.17** (Table 3.1) with that of isovitexin (**3.18**) from literature (Ramarathnam et al. 1989) allowed for the identification of the flavonoid aglycone as apigenin (**3.19**) (Figure 3.20). The ^{13}C NMR spectrum of **3.17** (Figure 3.21) had 24 carbon resonances with peak intensities at δ_C 117.1 and 129.5 showing the presence of symmetry in the aromatic region and a carbonyl signal at δ_C 184.1. The presence of sugars was confirmed by carbon signals in the region δ_C 60 – 85.

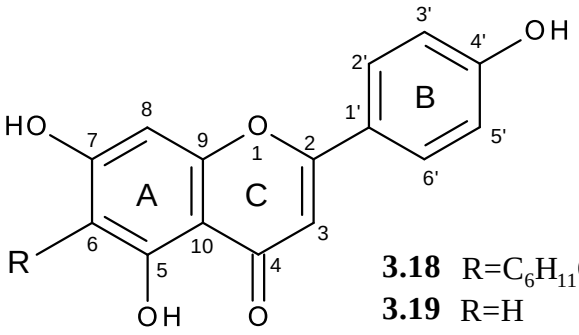

3.18 R=$C_6H_{11}O_6$
3.19 R=H

Figure 3.20 Structures for compounds **3.18** and **3.19** showing flavonoid rings A, B and C

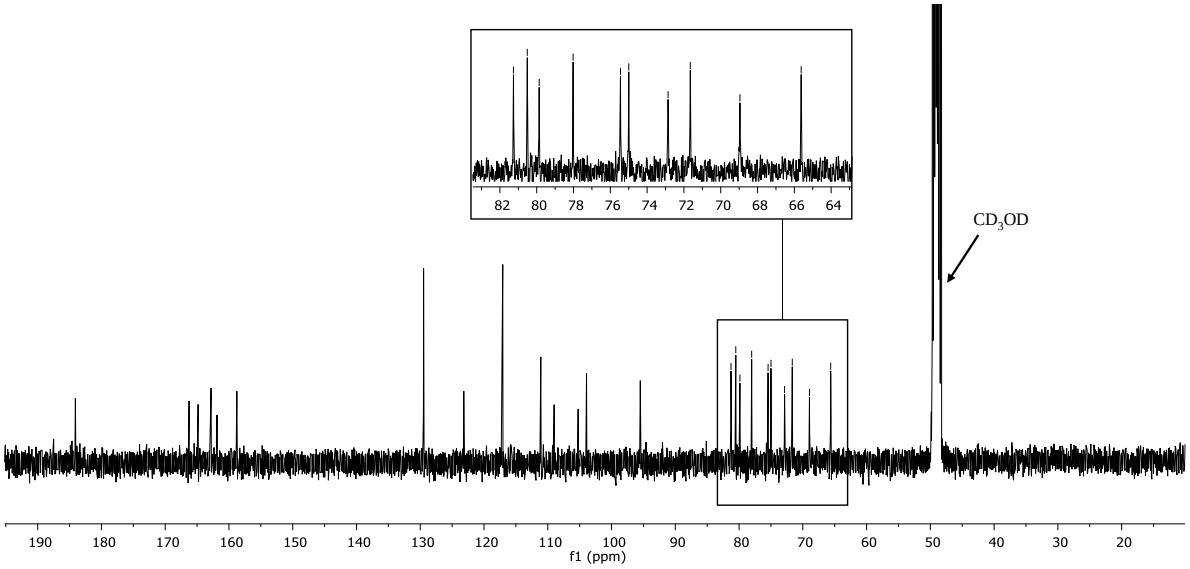

Figure 3.21 ^{13}C NMR spectrum (CD_3OD, 100MHz) of compound **3.17**

From the ^{13}C DEPT135 NMR spectrum (Figure 3.22), the presence of 11 methine, 3 methylene and 10 quaternary carbons were determined. Hetero-aromaticity of the flavonoid aglycone was indicated by 9 of the quaternary carbons signalling in the aromatic region.

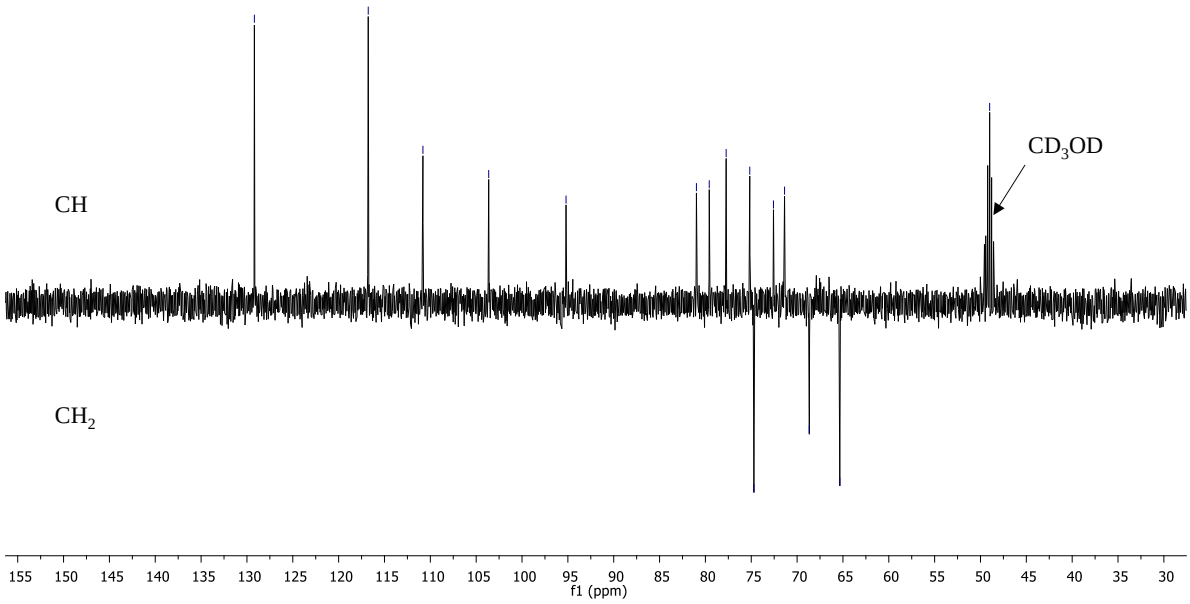

Figure 3.22 ^{13}C DEPT135 NMR spectrum (CD_3OD, 100MHz) of compound **3.17**

Table 3.1 ^{1}H (CD_3OD, 400MHz), ^{13}C (CD_3OD, 100MHz) and 2D NMR (^{1}H COSY and HMBC) spectroscopic data for compound **3.17**

Compound 3.17					
Carbon No.	**δ_C**	**δ_C, mult**	**δ_H, mult, J_{Hz}**	**COSY**	**HMBC**
Apigenin aglycone					
2	166.25	C			
3	103.92	CH	6.64, s		C-1′, C-2, C-4, C-10
4	184.09	C			
5	161.88	C			
6	109.00	C			
7	164.84	C			
8	95.49	CH	6.55, s		C-6, C-7, C-9, C-10
9	158.77	C			
10	105.23	C			
1′	123.17	C			
2′	129.48	CH	7.88, d (8.0)	H-3′	C-2, C-4′
3′	117.06	CH	6.96, d (7.9)	H-2′	
4′	162.80	C			
5′	117.06	CH	6.96, d (7.9)	H-6′	C-1′, C-4′
6′	129.48	CH	7.88, d (8.0)	H-5′	
6-C-Glucopyranosyl unit					
1″	75.45	CH	4.93, d (10.2)		C-2″, C-3″, C-5, C-6, C-7
2″	72.86	CH	4.08 *		
3″	79.9	CH	3.51 *		C-4″
4″	71.65	CH	3.56 *		
5″	81.26	CH	3.56 *	H-6″	
6″	68.95	CH_2	3.75 - 4.02	H-5″	
6″-Apio-D-Furanosyl unit					
1‴	111.09	CH	5.00, d (2.5)		C-4‴
2‴	78.02	CH	3.94, s		
3‴	80.51	C			
4‴	75.00	CH_2	3.79 - 4.0 *		C-1‴, C-3‴
5‴	65.63	CH_2	3.61, s		C-2‴, C-3‴, C-4‴

(*) Signal patterns unclear due to overlap

3.5.2.6 2D heteronuclear through-bond NMR correlations

HSQC-TOCSY NMR correlations were used to determine the arrangement of the two sugar moieties (Figure 3.23). From the HSQC-TOCSY results (Figure 3.24), a single spin system was observed in one of the sugar moieties. The anomeric proton H-1″ at δ_H 4.93 correlated with protons of carbons C-2″, C-3″, C-4″ and C-5″ at δ_C 72.86, 79.9, 71.65 and 81.26, respectively (Figure 3.24A). Further HSQC-TOCSY correlations were observed between H-5″ and the protons of carbons C-1″ and C-6″ at δ_C 75.45 and 68.95 respectively. Correlations in the aromatic region confirmed the apigenin aglycone (Figure 3.24B). These results, coupled with reported ^{1}H and ^{13}C NMR chemical shifts belonging to the *C*-glucose of isovitexin (**3.18**) helped to identify the sugar unit as glucopyranoside (Ramarathnam et al. 1989). Three separate spin systems where observed in the HSQC-TOCSY correlations of the second sugar (Figure 3.24A). The anomeric proton H-1‴ at δ_H 5.0 shared the same spin system with H-2‴ (δ_H 3.94) whereas H-4‴ (δ_H 3.79, 4.0) and H-5‴ (δ_H 3.61) geminal protons were in two separate spin systems. These results were characteristic of a furanose moiety and thus, led to the identification of the second sugar unit as apio-D-furanoside. From ^{1}H NMR results, the H-1‴ to H-2‴ coupling constant (J = 2.5 Hz) corresponded to an α- anomeric configuration.

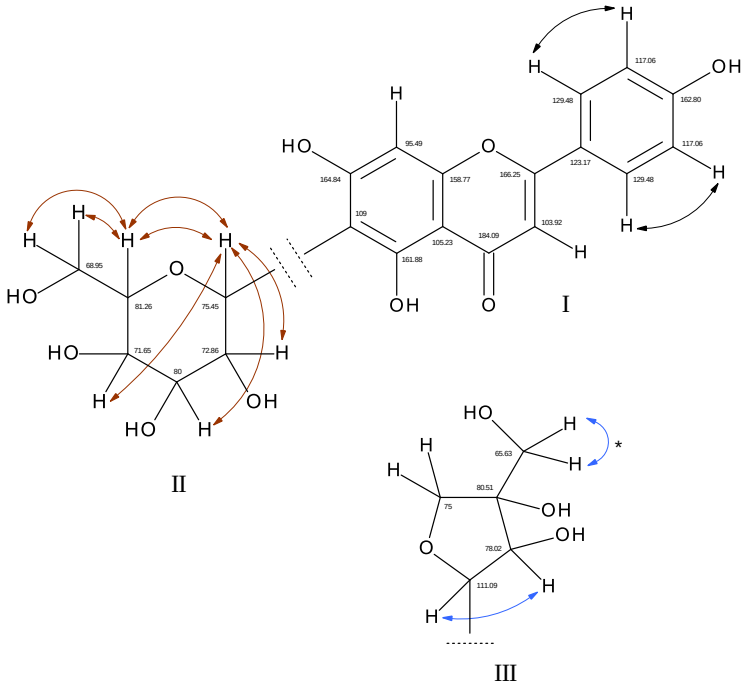

Figure 3.23 HSQC-TOCSY NMR correlations for compound **3.17**

(I) apigenin aglycone, (II) glucopyranosyl unit and (III) apio-D-furanosyl unit.

The black, brown and blue arrows indicate flavonoid, glucopyranose and furanose correlations respectively. (*) shows correlation determined by TOCSY NMR

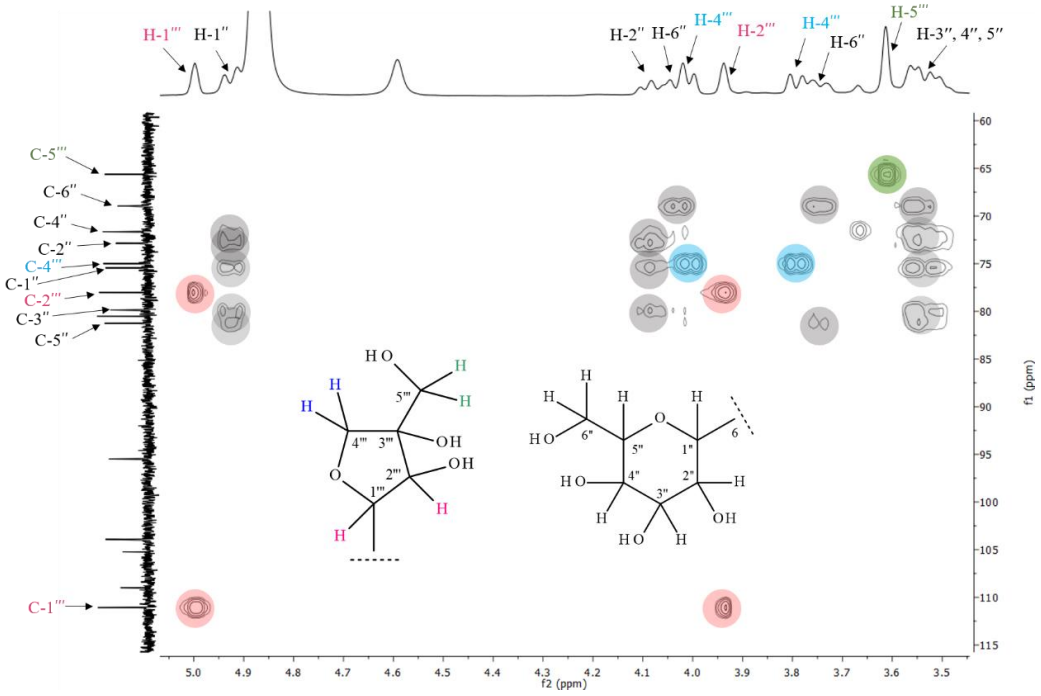

Figure 3.24a HSQC-TOCSY NMR spectrum (CD_3OD, 400MHz) of compound **3.17** showing resonances in the sugar and anomeric regions

The grey, pink, blue, and green dots represent coupling within the same spin system

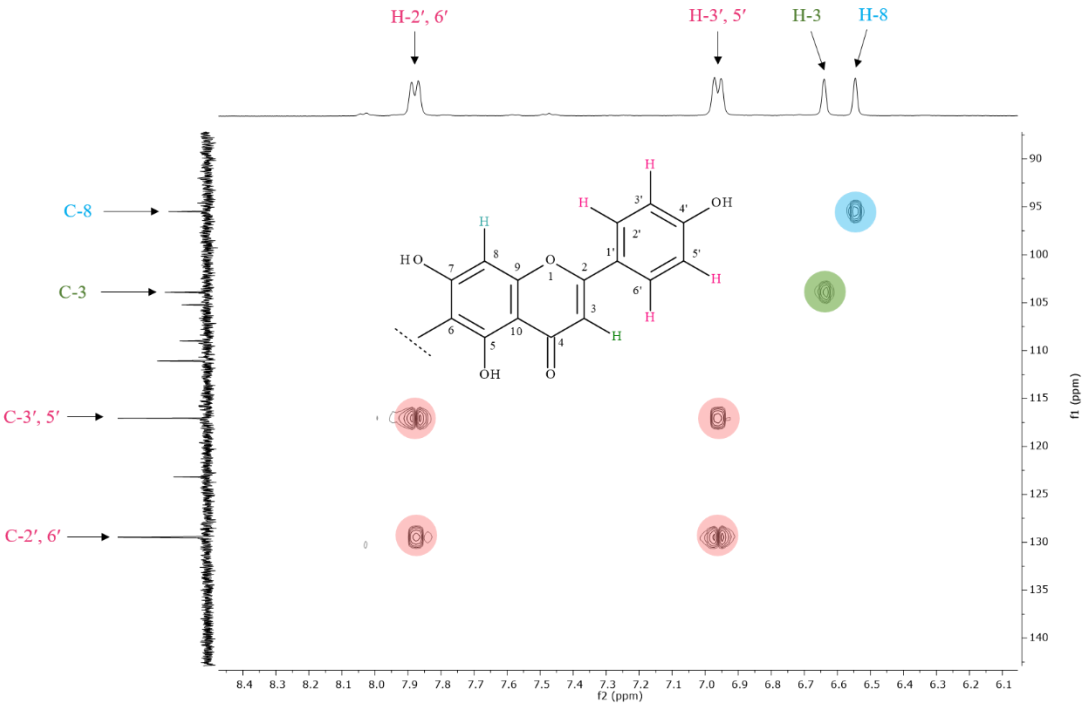

Figure 3.24b HSQC-TOCSY NMR spectrum (CD_3OD, 400MHz) of compound **3.17** showing resonances in the aromatic region

HMBC NMR correlations were used to determine the arrangement of the apigenin aglycone and the attachment of the glucopyranoside (Figure 3.25). From the HMBC NMR spectrum of **3.17** (Figure 3.26), attachment of the glucopyranoside to the aglycone *via* a *C*-glycosidic bond was determined through a correlation between C-6 at δ_C 109 and the anomeric proton H-1″ at δ_H 4.93 (Figure 3.26A). Compared to flavonoid 6-*C*-glycosides, anomeric protons belonging to flavonoid 6-*O*-glycosides are more deshielded and hence, appear around δ_H 5.1 (Ramarathnam et al. 1989). Furthermore, the correlations between H-1″ and carbons C-5 at δ_C 161.88 and C-7 at δ_C 164.84 would not be observable *via* an *O*-glycosidic linkage as this would exceed HMBC's 3-bond limitation. Unlike α- anomeric configurations which are at a 60° dihedral angle, β- anomeric configurations are at 180°, hence, their H-1″ - H-2″ coupling constants being much higher. Based on the high H-1″ to H-2″ coupling constant (J = 10.2 Hz) observed in the ^{1}H NMR, the anomeric configuration of the *C*-sugar was determined as β-glucopyranoside.

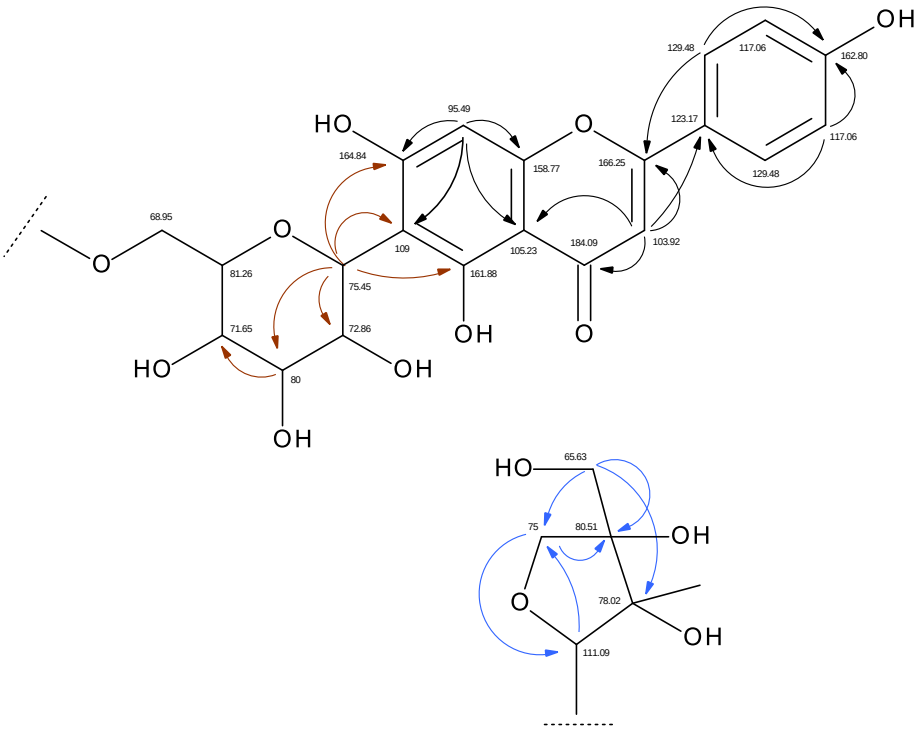

Figure 3.25 ^{1}H – ^{13}C HMBC NMR correlations for compound **3.17**

The black, brown and blue arrows indicate flavonoid, glucopyranose and furanose correlations respectively

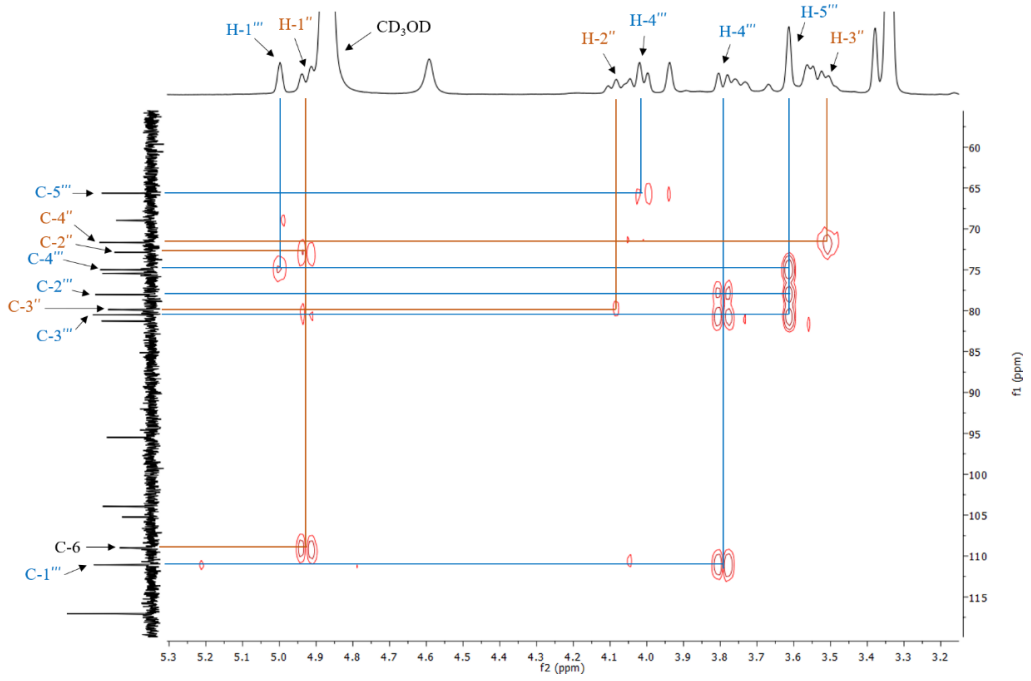

Figure 3.26a ^{1}H – ^{13}C HMBC NMR spectrum (CD_3OD, 400MHz) of compound **3.17** showing resonances in the sugar and anomeric regions

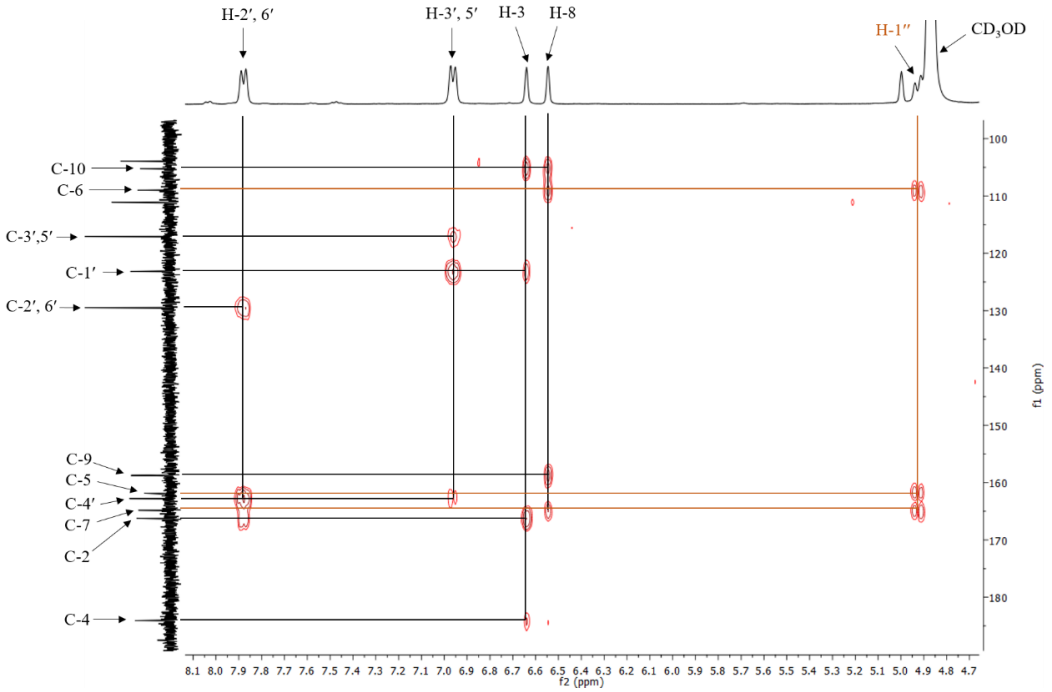

Figure 3.26b ^{1}H – ^{13}C HMBC NMR spectrum (CD_3OD, 400MHz) of compound **3.17** showing resonances in the anomeric and aromatic regions

The fact that no HMBC correlations were observed between the aglycone and the furanose anomeric proton H-1‴ was suggestive of a glycosidic linkage between the β-glucopyranoside and the apio-α-D-furanoside. The ^{13}C NMR chemical shift of C-6″ in the unsubstituted *C*-glucopyranoside of isovitexin was reported at δ_C 62.9. In compound **3.17**, C-6″ had a significantly higher chemical shift, resonating at δ_C 68.95 resulting from the deshielding effect of a proximal electron withdrawing group. It was therefore concluded that in compound **3.17**, the apio-α-D-furanoside is linked to the *C*-β-glucopyranoside at C-6″ *via* an *O*-glycosidic bond. The structure of **3.17** was thus established as 6-*C*-[-apio-α-D-furanosyl-(1→6)-β-glucopyranosyl]-4′, 5, 7-trihydroxyflavone or simply 6″-*O*-α-apio-D-furanosylisovitexin (Figure 3.27). Compound **3.17** has been named 'altissimin', derived from the specie name, *altissima*. Several flavonoids with *C*-glucopyranosyl and furanosyl residues have been previously reported in literature. However, altissimin (**3.17**) presents a unique structural arrangement of the two sugar residues to the apigenin aglycone. Altissimin (**3.17**) is also the first *C*-glycosylflavone to be isolated from *D. altissima*. A similar compound consisting of *C*-β-D-glucopyranosyl and apio-β-D-furanosyl residue attachments to an 8-hydroxyapigenin aglycone was isolated from the aerial parts of *Gaillardia grandiflora* (Moharram et al. 2017).

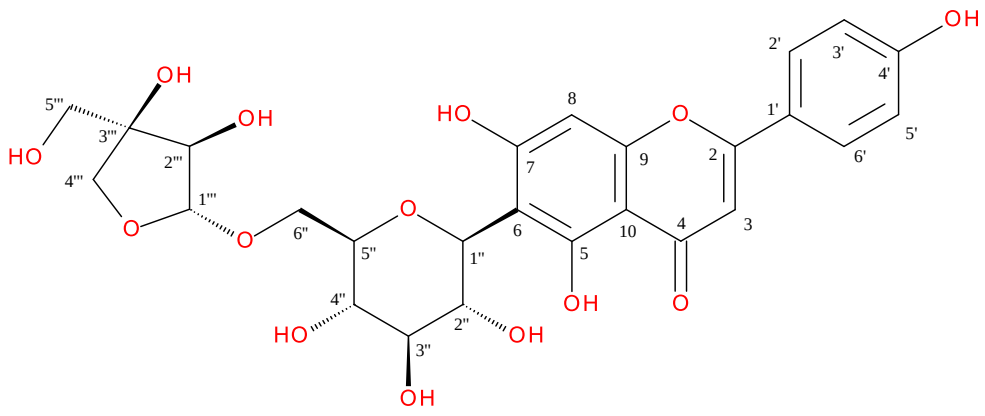

Figure 3.27 Proposed structure of compound **3.17**

3.5.2.7 2D through-space NMR correlations

Through NOESY, determination of spacial relationships within the compound confirmed the proposed structural arrangement of **3.17** (Figure 3.28). In the sugar region, there was a correlation between the furanose anomeric proton H-1‴ and the glucopyranose geminal protons at H-6″ (Figure 3.29A), thereby confirming *O*-inter-glycosidic attachment between the furanose and the *C*-glucose. A correlation between the geminal protons at H-4‴ was also observed. In the aromatic region there were correlations between the vicinal protons H-2″, 6″ and H-3″, 5″ (confirming a *para* substitution of the flavonoid B-ring) as well as between H-3 and H-6′ (Figure 3.29B).

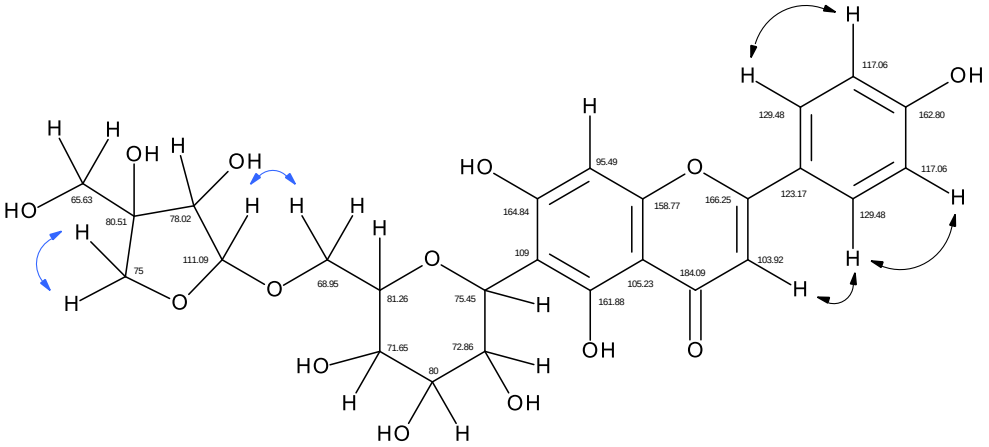

Figure 3.28 $^{1}H - {}^{1}H$ NOESY NMR correlations for compound **3.17**

The black and blue arrows indicate flavonoid and furanose correlations respectively

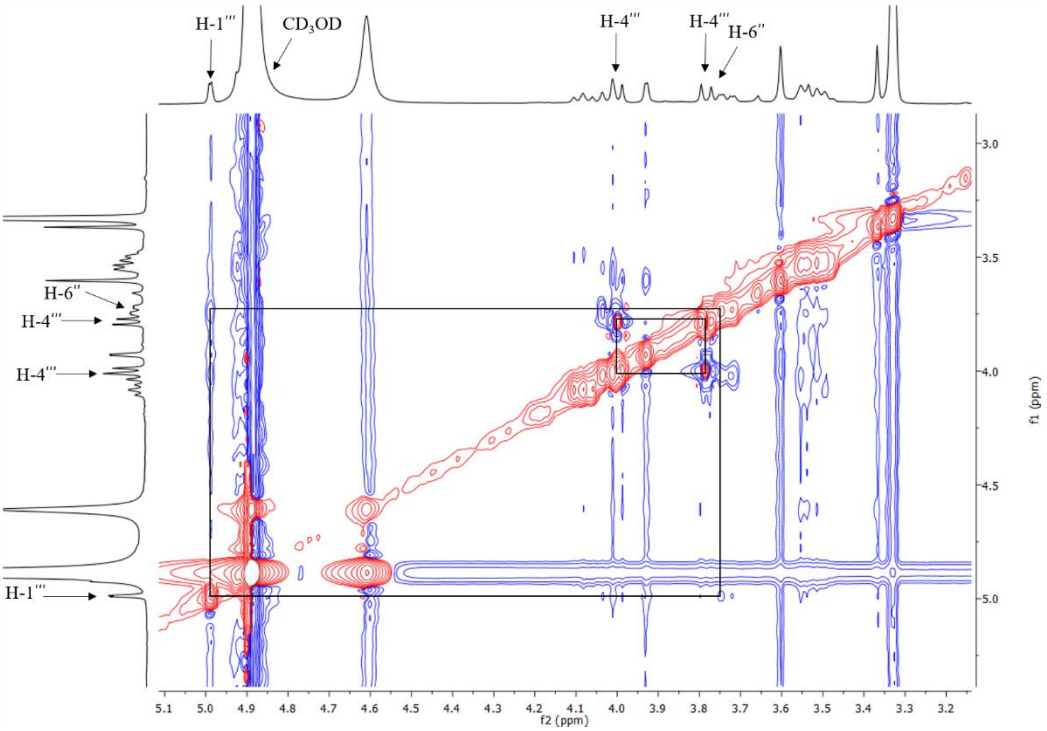

Figure 3.29a ^{1}H – ^{1}H NOESY NMR spectrum (CD_3OD, 400MHz) of compound **3.17** showing resonances in the sugar and anomeric regions

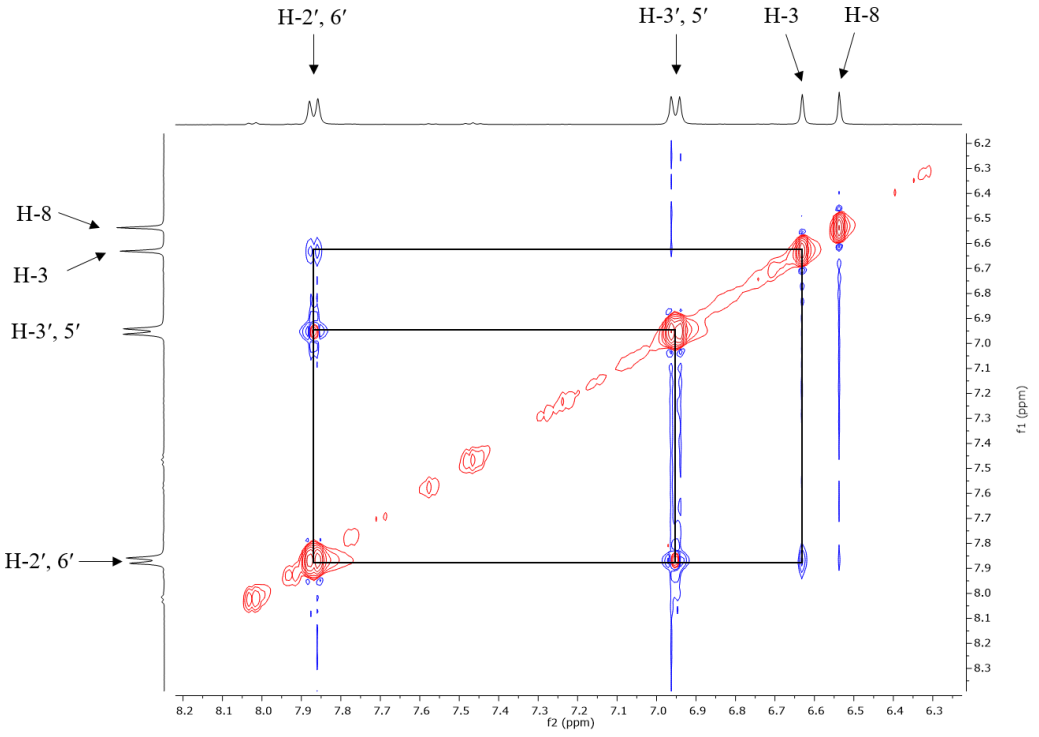

Figure 3.29b ^{1}H – ^{1}H NOESY NMR spectrum (CD_3OD, 400MHz) of compound **3.17** showing resonances in the aromatic regions

3.6 Biosynthesis of flavonoid *C*-glycosides

In the biosynthesis of flavonoids, enzymatic formation of naringenin chalcone by chalcone synthase is considered the most important step. During this process, acetate units from malonyl-CoA undergo three successive condensation reactions resulting in the 6-carbon elongation of 4-coumarate followed by cyclization to form flavonoid ring A (Figure 3.30). Since neither naringenin nor chalcone is a *C*-glycosyl acceptor, the ring is further opened to form a dibenzoylmethane isomer which then accepts *C*-glycosylation. The glycosylation of flavonoid metabolites serves as a storage mechanism and a preventer of cytoplasmic damage in plants because flavonoid glycosides are more hydrophilic and less reactive than their aglycones (Harborne and Williams 1982). The favoured positions for glycosylation in flavones are C-6 and C-8 for *C*-glycosides and C-7 for *O*-glycosides (Vukics and Guttman 2010). Flavonoid *C*-glycosides are further categorised into mono-*C*-glycosylflavonoids, di-*C*-glycosylflavonoids and *C*-glycosylflavonoid-*O*-glycosides, with the last category having inter-glycosidic bonds via the -OH groups of the *C*-sugars (Cuyckens and Claeys 2004).

Flavonoid *C*-glycosides are formed through the enzymatic transference of a sugar unit from uridine diphosphate-glucose (UDP-glucose) to the C-6 or C-8 position of a flavone aglycone. In this process, *C*-glucosyltransferase mediates the transfer of a glucose unit with subsequent release of UDP (Kerscher and Franz 1987). The biosynthetic formation of a (1→2) *O*-inter-glycosidic linkage between a furanose moiety and a *C*-glucoside on the C-8 position of the flavone has been reported (Hahlbrock et al. 1971). In the case of compound **3.17**, in addition to *C*-glycosylation of the apigenin aglycone, it is proposed that a furanose moiety is subsequently added to the –OH at carbon C-6″ by uridine diphosphate-apiose (UDP-apiose) through the enzymatic activity of apiofuranosyltransferase to form a (1→6) *O*-inter-glycosidic linkage between the furanose and the *C*-glucoside (Figure 3.27).

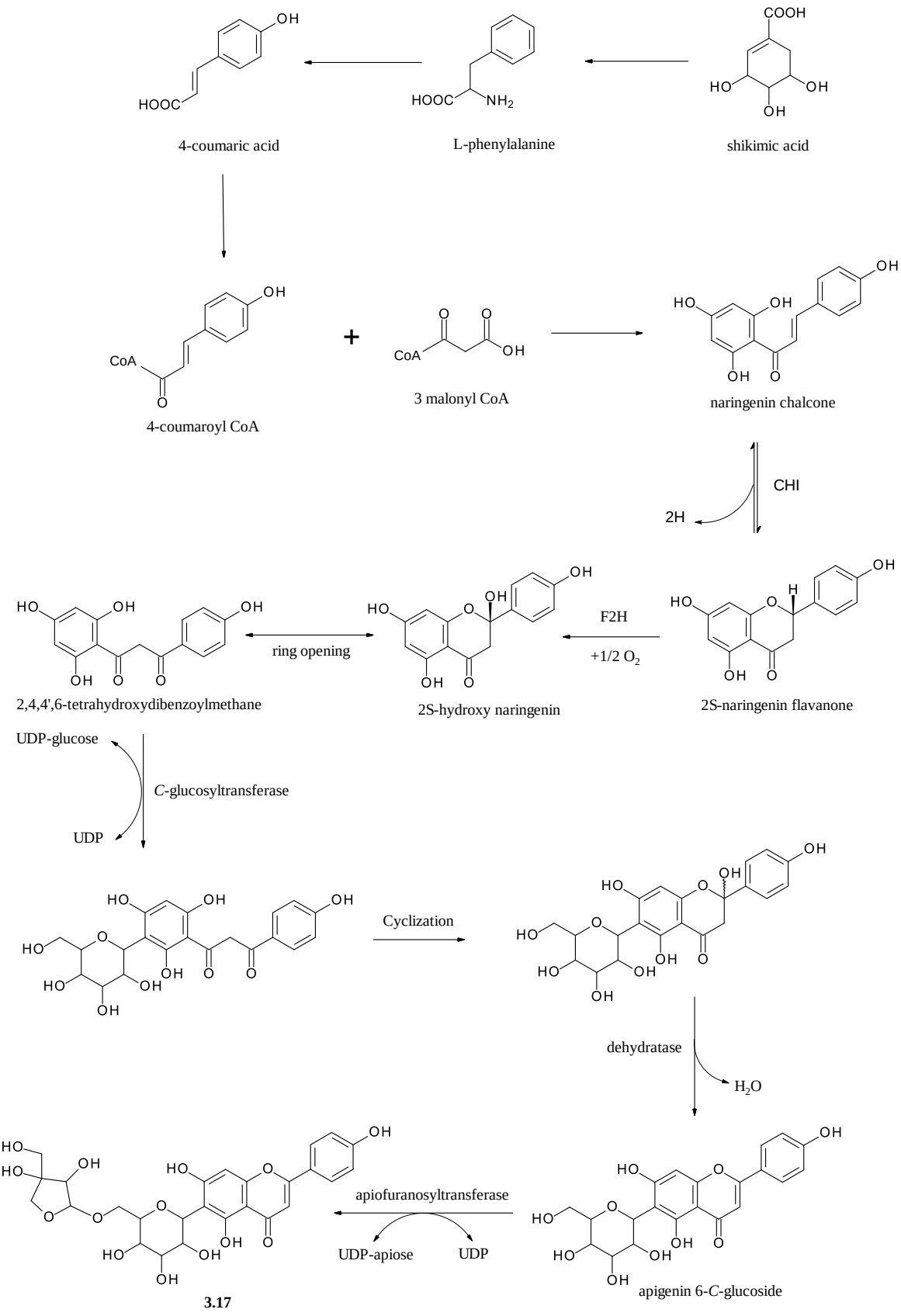

Figure 3.30 Proposed biosynthesis of compound **3.17**

3.7 Experimental

3.7.1 General experimental procedures

All extractions and chromatography utilised LiChrosolv® (Merck, Germany) solvents. Open column reverse phase chromatography techniques were carried out using Diaion® HP-20 (Supelco, USA) and Sephadex® LH-20 resins (Merck, South Africa). Samples were freeze dried using a Virtis SP Scientific sentry 2.0 lyophilizer with an Alcatel Pascal vacuum pump and/ or dried *in vacuo* using a Buchi R-210 Rotavapor. NMR experiments were performed with an Ultrashield Plus Bruker Avance III 400 MHz NMR spectrometer using standard pulse sequences. FT-IR results were obtained using a Bruker Tensor 27 FT-IR spectrometer and analysed using Opus data collection program. LC/MS and HR-MS results were obtained on a Waters Synapt G2 quadrupole time-of-flight mass spectrometer (detected by an ESI positive source with a 15 V cone voltage) from the Central Analytical Facilities (CAF) at Stellenbosch University, South Africa. The UV and Circular Dichroism (CD) results were recorded on a Chirascan Plus Spectrapolarimeter.

3.7.2 Plant material

Bulbs of *Drimia altissima* (L.F.) Ker Gawl were collected in Kwa-Nobuhle, (Uitenhage, Eastern Cape, South Africa) by Buyiswa Hlangothi in February, 2015. The plant material was transported to Nelson Mandela University, Chemistry Department and stored in the plant room until the time of extraction. Plant authentication was performed by Tony Dold, a curator and taxonomist at Selmar Schonland Herbarium (GRA) in Makhanda, Eastern Cape, South Africa, where a specimen of *Drimia altissima* (L.F.) Ker Gawl. with voucher number Hlangothi011(GRA) was deposited.

3.7.3 Soxhlet extraction and isolation of compound 3.17

The bulbs of *Drimia altissima* were washed under running water, peeled and dried at 40 °C after which the plant material was shredded into smaller pieces and submerged in liquid nitrogen until brittle. The resulting biomass was then crushed with a mortar and pestle to powder in readiness for soxhlet extraction. About 100 g of dry powdered biomass was loaded onto the soxhlet apparatus and extracted at 65 °C under reflux using MeOH/CH_2Cl_2 (8:2, 150 mL) for 75 cycles (1 cycle = 16 min). The resulting extract was then dried *in vacuo* to yield a brown crude extract (**MN-14-79**, 10.85 g). **MN-14-79** (10.85 g) was then solubilised in 160

mL de-ionised H_2O and transferred into a 2 L separating funnel. The crude extract then underwent a succession of liquid-liquid partitioning using 160 mL each of Hex, EtOAc and *n*-BuOH to obtain fractions **79a** (H_2O, 4.85 g), **79b** (Hex, 1.78 g), **79c** (EtOAc, 2.86 g) and **79d** (*n*-BuOH, 1.77 g). Each fraction was partially dried *in vacuo*, diluted with sufficient amounts of HPLC-grade H_2O, frozen at -80 °C and then lyophilized. 100g of dry Diaion® HP-20 resin was transferred into a 500 mL beaker to which sufficient amounts of MeOH were added to cover the resin bed by 5 cm. The resin was gently stirred for 1 min and allowed to stand for 15 min after which the MeOH was decanted and replaced with de-ionized H_2O. The mixture was then stirred and allowed to stand for 10 min before it was carefully packed into an open column of diameter 30mm to a resin height of 12.5cm. Fraction **79d** (1.77 g) was then applied to the column and eluted using a series of solvents (200 mL each) in decreasing polarity to yield fractions **82a** (H_2O/MeOH, 7:3, n.d.), **82b** (H_2O/MeOH, 5:5, 270.8 mg), **82c** (H_2O/MeOH, 3:7, 216.3 mg), **82d** (100% MeOH, 144 mg), **82e** (100% EtOH, 5 mg) and **82f** (100% EtOAc, 15.8 mg). After lyophilisation, 160 mg of fraction **82c** was solubilized in 2 mL MeOH, applied onto an open column of diameter 20mm pre-packed with 12 g of Sephadex® LH-20 gel in de-ionized H_2O (swelling ratio; 1 g = 4 mL) and eluted with 50% MeOH. 10 mL fractions were collected and dried to afford sub-fractions **99a – 99l**. Sub-fractions **99g** – **99l** were combined to afford compound **3.17** (26.7 mg) as a yellow amorphous powder.

3.8 Physical data and spectral constants for compound 3.17

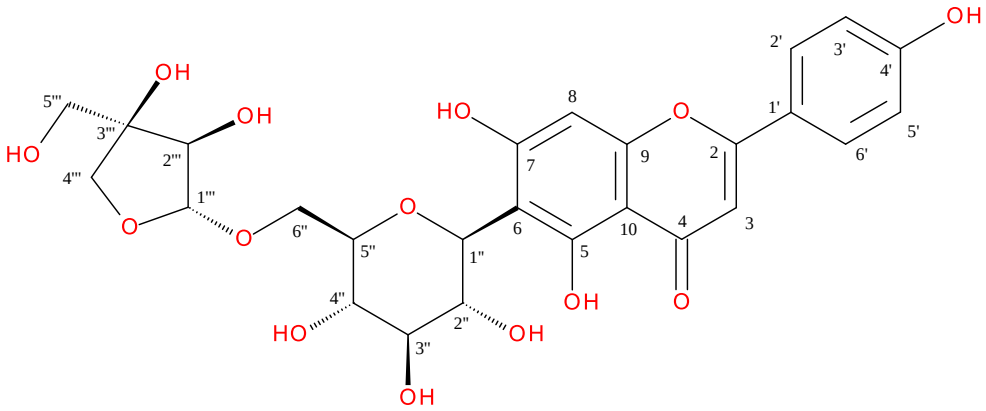

6″-*O*-α-apio-D-furanosylisovitexin (altissimin):

*6-C-[-apio-α-D-furanosyl-(1→6)-β-glucopyranosyl]-4', 5, 7-trihydroxyflavone (**3.17**)*

Yellow amorphous powder (Mp 174 – 178 °C); CD (*c* 0.03, MeOH): $[\Theta]_{235}$ -73 320, $[\Theta]_{271}$ +70 500, $[\Theta]_{300}$ +16 920, $[\Theta]_{345}$ +23 500; UV (MeOH) (log *ε*) λ_{max} 272 (2.40), 333 (2.45); FTIR (KBr) ν_{max}/cm^{-1}: 3338.91 (-OH), 1649.89 (C=O), 1608.89 (Ar), 833.27; HRESI-MS *m/z* (rel. int.): 565.15 $[M+H]^+$ (100), 433 $[M+H-132]^+$ (calcd for $C_{26}H_{28}O_{14}$, 565.15); ^{1}H NMR (CD_3OD, 400 MHz): δ ppm 3.51 (1H, H-3″), 3.56 (1H, H-4″), 3.56 (1H, H-5″), 3.61 (*s*, 2H, H-5‴), 3.94 (*s*, 1H, H-2‴), 3.79 - 4.00 (2H, H-4‴), 3.75 – 4.02 (2H, H-6″), 4.08 (1H, H-2″), 4.93 (*d*, *J* = 10.2 Hz, 1H, H-1″), 5.00 (*d*, *J* = 2.5 Hz, 1H, H-1‴), 6.55 (*s*, 1H, H-8), 6.64 (*s*, 1H, H-3), 6.96 (*d*, *J* = 7.9, 2H, H-3′, H-5′), 7.88 (*d*, *J* = 8.0 Hz, 2H, H-2′, H-6′); ^{13}C NMR (CD_3OD, 100 MHz): δ ppm 65.63 (C-5‴), 68.95 (C-6″), 71.65 (C-4″), 72.86 (C-2″), 75.00 (C-4‴), 75.45 (C-1″), 78.02 (C-2‴), 79.9 (C-3″), 80.51 (C-3‴), 81.26 (C-5″), 95.49 (C-8), 103.92 (C-3), 105.23 (C-10), 109.00 (C-6), 111.09 (C-1‴), 117.06 (C-3′, C-5′), 123.17 (C-1′), 129.48 (C-2′, C-6′), 158.77 (C-9), 161.88 (C-5), 162.80 (C-4′), 164.84 (C-7), 166.25 (C-2), 184.09 (C-4).

References

Aires, A., Fernandes, C., Carvalho, R., Bennett, R.N., Saavedra, M.J., & Rosa, E.A.S. 2011. Seasonal Effects on Bioactive Compounds and Antioxidant Capacity of Six Economically Important Brassica Vegetables., 16, (8)

APG II 2003. An update of the Angiosperm Phylogeny Group classification for the orders and families of flowering plants: APG II. *Botanical Journal of the Linnean Society*, 141, (4) 399-436 available from: http://dx.doi.org/10.1046/j.1095-8339.2003.t01-1-00158.x

APG III 2009. An update of the Angiosperm Phylogeny Group classification for the orders and families of flowering plants: APG III. *Botanical Journal of the Linnean Society*, 161, (2) 105-121 available from: http://dx.doi.org/10.1111/j.1095-8339.2009.00996.x

Benet, L.Z., Hosey, C.M., Ursu, O., & Oprea, T.I. 2016. BDDCS, the Rule of 5 and drugability. *Advanced Drug Delivery Reviews*, 101, 89-98 available from: http://www.sciencedirect.com/science/article/pii/S0169409X16301491

Brower, V. 2008. Back to Nature: Extinction of Medicinal Plants Threatens Drug Discovery. *JNCI: Journal of the National Cancer Institute*, 100, (12) 838-839 available from: http://dx.doi.org/10.1093/jnci/djn199

Chase, W.M., Reveal, L.J., & Fay, F.M. 2009. A Subfamilial Classification for the Expanded *Asparagalean* Families *Amaryllidaceae*, *Asparagaceae* and *Xanthorrhoeaceae*. *Botanical Journal of the Linnean Society*, 161, (2) 132-138

Christenhusz, J.M.M. & Byng, W.J. 2016. The Number of Known Plants Species in the World and its Annual Increase. *Phytotaxa*, 261, (3) 201-217

Claus, B.L. & Underwood, D.J. 2002. Discovery informatics: its evolving role in drug discovery. *Drug Discovery Today*, 7, (18) 957-966 available from: http://www.sciencedirect.com/science/article/pii/S1359644602024339

Conservatoire et Jardin Botaniques. African Plant Databases - *Albuca* L. http://www.ville-ge.ch/musinfo/bd/cjb/africa/details.php?langue=an&id=187923 . 2012.
Ref Type: Online Source

Conservatoire et Jardin Botaniques Ville De Genève. *Drimia altissima* (L. f.) Ker Gawl. http://www.ville-ge.ch/musinfo/bd/cjb/africa/details.php?langue=an&id=15450 . 2012.
Ref Type: Online Source

Crouch, N., Williams, V., Edwards, T., & Brueton, V.J. 2010. *Hyacinthaceae: Drimia cooperi in KwaZulu-Natal, and the ethnomedicinal trade*, 40 ed.

Cuyckens, F. & Claeys, M. 2004. Mass Spectrometry in the Structural Analysis of Flavonoids. *Journal of Mass Spectrometry*, 39, (1) 1-15 available from: http://dx.doi.org/10.1002/jms.585

Decker, M. 2011. Hybrid Molecules Incorporating Natural Products: Applications in Cancer Therapy, Neurodegenerative Disorders and Beyond. *Current Medicinal Chemistry*, 18, (10) 1464-1475 available from: http://www.eurekaselect.com/node/73764/article

Deng, Z.L., Du, C.X., Li, X., Hu, B., Kuang, Z.K., Wang, R., Feng, S.Y., Zhang, H.Y., & Kong, D.X. 2013. Exploring the Biologically Relevant Chemical Space for Drug Discovery. *Journal of Chemical Information and Modeling*, 53, (11) 2820-2828 available from: https://doi.org/10.1021/ci400432a

Dobson, C.M. 2004. Chemical space and biology. *Nature*, 432, 824 available from: http://dx.doi.org/10.1038/nature03192

Dressler, S., Schmidt, M., & Zizka, G. African plants - A Photo Guide. www.africanplants.senckenberg.de . 2014. 12-6-2018.
Ref Type: Online Source

Ermias, D., Wendimagegn, M., Melaku, A., & Ingrid, C. 1994. Two Bufadienolides from *Drimia altissima* (*Urginea altissima*). *Bull.Chem.Soc.Ethiop.*, 8, (2) 85-89

Fernandez, M., Renedo, J., Arrupe, T., & Vega, F.A. 1975. *C*-Glycosylflavones in the Bulbs of Squill. *Phytochemistry*, 14, (2) 586 available from: http://www.sciencedirect.com/science/article/pii/0031942275851405

Gaffield, W. 1970. Circular dichroism, optical rotatory dispersion and absolute configuration of flavanones, 3-hydroxyflavanones and their glycosides: Determination of aglycone chirality

in flavanone glycosides. *Tetrahedron*, 26, (17) 4093-4108 available from: http://www.sciencedirect.com/science/article/pii/S0040402001930509

Goldblatt, P., Manning, J., & Forest, F. 2012. *A review of chromosome cytology in Hyacinthaceae subfamilies Urgineoideae and Hyacinthoideae (tribes Hyacintheae, Massonieae, Pseudoprospereae) in sub-Saharan Africa*, 83 ed.

Guantai, M. E. & Chibale, K. 2012, "Natural Product-Based Drug Discovery in Africa: The Need for Integration into Modern Drug Discovery Paradigms," *In Drug Discovery in Africa*, 1 ed. K. Chibale, M. Davies-Coleman, & C. Musimirembwa, eds., Verlag Berlin Heidelberg: Springer, pp. 101-126.

Hahlbrock, K., Ebel, J., Ortmann, R., Sutter, A., Wellmann, E., & Grisebach, H. 1971. Regulation of Enzyme Activities Related to the Biosynthesis of Flavone Glycosides in Cell Suspension Culture of Parsley (*Petroselinum hortense*). *Biochimica et Biophysica Acta (BBA) - General Subjects*, 244, (1) 7-15 available from: http://www.sciencedirect.com/science/article/pii/0304416571901140

Harborne, B. J. & Williams, A. C. 1982, "Flavone and Flavonol Glycosides," *In The Flavonoids - Advances in Research*, J. B. Harborne & T. J. Mabry, eds., Springer Science + Business Media, B. V., pp. 261-312.

Harvey, A.L., Edrada-Ebel, R., & Quinn, R.J. 2015. The re-emergence of natural products for drug discovery in the genomics era. *Nature Reviews Drug Discovery*, 14, 111 available from: http://dx.doi.org/10.1038/nrd4510

Heneczkowski, M., Kopacz, M., Nowak, D., & Kužniar, A. 2001. Infrared spectrum analysis of some flavonoids. *Acta Pol Pharm*, 58, (6) 415-420

Iizuka, M., Warashina, T., & Noro, T. 2001. Bufadienolides and a New Lignan from the Bulbs of *Urginea maritima*. *Chemical and Pharmaceutical Bulletin*, 49, (3) 282-286

Irwin, J.J. & Shoichet, B.K. 2005. ZINC - A Free Database of Commercially Available Compounds for Virtual Screening. *Journal of Chemical Information and Modeling*, 45, (1) 177-182 available from: https://doi.org/10.1021/ci049714+

Iwu, M. M. 2014, "Pharmacognostical Profile of Selected Medicinal Plants - *Drimia altissima*," *In Handbook of African Medicinal Plants*, 2 ed. M. M. Iwu, ed., Florida: CRC Press, pp. 208-209.

Ji, H.F., Li, X.J., & Zhang, H.Y. 2009. Natural products and drug discovery. Can thousands of years of ancient medical knowledge lead us to new and powerful drug combinations in the fight against cancer and dementia? *EMBO Reports*, 10, (3) 194-200 available from: http://www.ncbi.nlm.nih.gov/pmc/articles/PMC2658564/

Katiyar, C., Gupta, A., Kanjilal, S., & Katiyar, S. 2012. Drug Discovery from Plant Sources: An Integrated Approach. *AYU*, 13, (1) 10-19

Kedra, M. & Kedrowa, S. 1968. Clinical evaluation of Proscillaridin A, a glycoside of *Scilla maritima*. *Polski tygodnik lekarski*, 23, (19) 714-716

Kerscher, F. & Franz, G. 1987. *Biosynthesis of Vitexin and Isovitexin: Enzymatic Synthesis of the C-glucosylflavones Vitexin and Isovitexin with an Enzyme Preparation from Fagopyrum esculentum M. Seedlings*, 42 ed.

Khanna, I. 2012. Drug discovery in pharmaceutical industry: productivity challenges and trends. *Drug Discovery Today*, 17, (19) 1088-1102 available from: http://www.sciencedirect.com/science/article/pii/S1359644612001833

Krämer, K. Chemistry's Toughest Total Synthesis Challenge Put On Hold by Lack of Funds. https://www.chemistryworld.com/research/chemistrys-toughest-total-synthesis-challenge-put-on-hold-by-lack-of-funds/8152.article . 2015. The Royal Society of Chemistry.
Ref Type: Online Source

Lahlou, M. 2013. The Success of Natural Products in Drug Discovery. *Pharmacology & Pharmacy*, 4, (3A) 17-31

Leeson, P. 2012. Chemical beauty contest. *Nature*, 481, 455 available from: http://dx.doi.org/10.1038/481455a

Li, J.W.H. & Vederas, J.C. 2009. Drug Discovery and Natural Products: End of an Era or an Endless Frontier? *Science*, 325, (5937) 161 available from: http://science.sciencemag.org/content/325/5937/161.abstract

Lipinski, C.A. 2004. Lead- and drug-like compounds: the rule-of-five revolution. *Drug Discovery Today: Technologies*, 1, (4) 337-341 available from: http://www.sciencedirect.com/science/article/pii/S1740674904000551

Lynch, A.H., Rudall, P.J., & Cutler, D.F. 2006. Leaf Anatomy and Systematics of *Hyacinthaceae*. *Kew Bulletin*, 61, (2) 145-159 available from: http://www.jstor.org/stable/20443254

Mabry, T. J., Markham, K. R., & Thomas, M. B. 1970, "The Ultraviolet Spectra of Flavones and Flavonols," *In The Systematic Identification of Flavonoids*, T. J. Mabry, K. R. Markham, & M. B. Thomas, eds., Spinger-Verlag, pp. 41-57.

Maltese, F., Erkelens, C., Kooy, F.v.d., Choi, Y.H., & Verpoorte, R. 2009. Identification of natural epimeric flavanone glycosides by NMR spectroscopy. *Food Chemistry*, 116, (2) 575-579 available from: http://www.sciencedirect.com/science/article/pii/S0308814609002957

Manning, J., GOLDBLATT, P., & Fay, M. 2003. A Revised Generic Synopsis of *Hyacinthaceae* in Sub-Saharan Africa, Based on Molecular Evidence, Including New Combinations and the New Tribe *Pseudoprospereae*. *Edinburgh Journal of Botany*, 60, (3) 533-568 available from: doi:10.1017/S0960428603000404

Miyakado, M., Kato, T., Ohno, N., & Koshimizu, K. 1975. Alkaloids of *Urginea altissima* and their antimicrobial activity against *Phytophthora capsici*. *Phytochemistry*, 14, (12) 2717 available from: http://www.sciencedirect.com/science/article/pii/0031942275852642

Moharram, F.A., El Dib, R.A.E.M., Marzouk, M.S., El-Shenawy, S.M., & Ibrahim, H.A. 2017. New Apigenin Glycoside, Polyphenolic Constituents, Anti-inflammatory and Hepatoprotective Activities of *Gaillardia grandiflora* and *Gaillardia pulchella* Aerial Parts. *Pharmacognosy Magazine*, 13, (Suppl 2) S244-S249 available from: http://www.ncbi.nlm.nih.gov/pmc/articles/PMC5538161/

Nath, S., Saha, P. S., & Jha, S. 2014, "Medicinal Bulbous Plants: Biology, Phytochemistry and Biotechnology," *In Bulbous Plants Biotechnology*, K. G. Ramawat & J. M. Mérillon, eds., Florida: CRC Press, pp. 338-369.

Nature. Drug Discovery and Development. https://www.nature.com/subjects/drug-discovery-and-development . 2018. Springer Nature.
Ref Type: Online Source

Newman, D.J. & Cragg, G.M. 2012. Natural Products As Sources of New Drugs over the 30 Years from 1981 to 2010. *Journal of Natural Products*, 75, (3) 311-335 available from: https://doi.org/10.1021/np200906s

Newman, D.J. & Cragg, G.M. 2016. Natural Products as Sources of New Drugs from 1981 to 2014. *Journal of Natural Products*, 79, (3) 629-661 available from: https://doi.org/10.1021/acs.jnatprod.5b01055

Pfosser, M. & Speta, F. 1999. Phylogenetics of *Hyacinthaceae* Based on Plastid DNA Sequences. *Annals of the Missouri Botanical Garden*, 86, (4) 852-875 available from: http://www.jstor.org/stable/2666172

Pikulski, M. & Brodbelt, J.S. 2003. Differentiation of Flavonoid Glycoside Isomers by Using Metal Complexation and Electrospray Ionization Mass Spectrometry. *Journal of the American Society for Mass Spectrometry*, 14, (12) 1437-1453 available from: http://www.sciencedirect.com/science/article/pii/S1044030503006056

Pohl, T.S., Crouch, N.R., & Mulholland, D.A. 2000. Southern African *Hyacinthaceae*: Chemistry, Bioactivity and Ethnobotany. *Current Organic Chemistry*, 4, (12) 1287-1324 available from: http://www.eurekaselect.com/node/65656/article

Pohl, T., Koorbanally, C., Crouch, N.R., & Mulholland, D.A. 2001. Bufadienolides from *Drimia robusta* and *Urginea altissima* (*Hyacinthaceae*). *Phytochemistry*, 58, (4) 557-561 available from: http://www.sciencedirect.com/science/article/pii/S0031942201002254

Quattrocchi, U.F.L.S. 2000. *CRC World Dictionary of Plant Names* Florida, CRC Press.

Ramarathnam, N., Osawa, T., Namiki, M., & Kawakishi, S. 1989. Chemical Studies on Novel Rice Hull Antioxidants. 2. Identification of Isovitexin, a *C*-glycosyl flavonoid. *Journal of Agricultural and Food Chemistry*, 37, (2) 316-319 available from: https://doi.org/10.1021/jf00086a009

Reymond, J.L. & Awale, M. 2012. Exploring Chemical Space for Drug Discovery Using the Chemical Universe Database. *ACS Chemical Neuroscience*, 3, (9) 649-657 available from: https://doi.org/10.1021/cn3000422

Scotti, L., Ferreira, E.I., Silva, M.S.d., & Scotti, M.T. 2010. Chemometric Studies on Natural Products as Potential Inhibitors of the NADH Oxidase from Trypanosoma cruzi Using the VolSurf Approach., 15, (10)

Shimada, K., Umezawa, K., Nambara, T., & Morris Kupchan, S. 1979. Isolation and Characterization of Cardiotonic Steroids from the Bulb of *Urginea altissima* Baker. *Chem.Pharm.Bull.*, 12, (27) 3111-3114

Stedje, B. 1987. A revision of the genus *Drimia* (*Hyacinthaceae*) in East Africa. *Nordic Journal of Botany*, 7, (6) 655-666 available from: https://doi.org/10.1111/j.1756-1051.1987.tb02034.x Accessed 5 October 2018.

Stedje, B. 2000, "The Evolutionary Relationships of the Genera *Drimia*, *Thuranthos*, *Bowiea* and *Schizobasis* Discussed in the Light of Morphology and Chloroplast DNA Sequence Data," *In Monocots - Systematics and Evolution*, L. K. Wilson & A. D. Morrison, eds., Victoria: CSIRO, pp. 414-420.

Stedje, B. 2001. *Hyacinthaceae. Bothalia; Vol 31, No 2 (2001)* available from: http://abcjournal.org/index.php/ABC/article/view/519 Accessed 2001.

Takenaka, T. 2001. Classical vs reverse pharmacology in drug discovery. *BJU International*, 88, 7-10 available from: http://dx.doi.org/10.1111/j.1464-410X.2001.00112.x

Tamimi, N.A.M. & Ellis, P. 2009. Drug Development: From Concept to Marketing! *Nephron Clinical Practice*, 113, (3) c125-c131 available from: https://www.karger.com/DOI/10.1159/000232592

Tietze, L.F., Bell, H.P., & Chandrasekhar, S. 2003. Natural Product Hybrids as New Leads for Drug Discovery. *Angewandte Chemie International Edition*, 42, (34) 3996-4028 available from: http://dx.doi.org/10.1002/anie.200200553

Vukics, V. & Guttman, A. 2010. Structural Characterization of Flavonoid Glycosides by Multi-Stage Mass Spectrometry. *Mass Spectrometry Reviews*, 29, (1) 1-16 available from: http://dx.doi.org/10.1002/mas.20212

Wagner, H. 1963, "Infrared Spectroscopy of Flavonoids," *In Methods in Polyphenol Chemistry*, J. B. Pridham, ed., Norwich: Pergamon Press, pp. 37-48.

Williams, V. L., Raimando, D., Crouch, N. R., Brueton, V. J., Cunningham, A. B., Scott-Shaw, C. R., Lötter, M., & Ngwenya, A. M. *Drimia altissima* (L.f.) Ker Gawl. National Assessment: Red List of South African Plants version 2017. http://redlist.sanbi.org/species.php?species=3812-21 . 2016. SANBI.
Ref Type: Online Source

Chapter 4

In vitro Anticancer Activity of *Drimia altissima* Fractions and Isolated Compound against the HeLa Cell Line

4.1 Introduction

Albeit the advantages of natural over synthetic compounds, recent decades have seen a decline in the approval of natural product-based drug candidates due to increased interest in the application of High-Throughput-Screening (HTS) methods to combinatorial synthetic compounds. This challenge to natural products can be circumvented by the merging of conventional natural product drug discovery paradigms with more modern approaches. A good example of such is the screening and bio-activity guided isolation of natural metabolites using High Content Analysis (HCA) equipment, also referred to as cellomics. HCA is a platform of sophisticated equipment and methods which operate by the use of biological applications and informatics software through automated cell-by-cell screening and quantitative analysis in order to investigate temporal and 3-dimentional cellular and sub-cellular activities and functions (Taylor 2007). Since the 1950's, the interpretation of cellular images has played a significant role in the study of disease pathology and diagnosis. HCA technology was developed in 1996 to enable the large-scale screening of cells performed on either microplates or CellChip™ systems (lab-on-chips) for micro and nanotechnology applications (Kenneth et al. 1997).

Conventional microscopy using manual or semi-automated imaging involves long hours of sitting while focusing with high concentration on the different fields of view. This method is tedious, time consuming and results in the analysis of a small number of samples. On the other hand, HCA platforms offers quantitative imaging with the full capacity for high throughput screening within just a few minutes of data acquisition and processing. HCA systems are able to analyse different types of samples from adherent, fixed and live tissue culture cells to beads, tissue slices, whole organisms and micro-organisms. The presence of a large field of view detector in HCA systems allow for whole well imaging at low magnification, an advantage for high statistic cell counting and scoring as well as for the discovery of rare events. HCA has

thus emerged as a key application among the modern methods employed in early drug discovery.

Figure 4.1 The Molecular Devices® Image Xpress Micro XLS Widefield HCA System (Molecular Devices 2018)

There are several manufacturers of HCA systems such as Yokogawa, ThermoFisher, BioTek® and Molecular Devices®. Being the equipment that was used for this study, Molecular Devices® HCA systems will be further discussed. Molecular Devices® HCA systems come either as standard or Micro XLS models. The Micro XLS model (Figure 4.1) is a benchtop automated widefield microscope with the capacity to hold four objectives of 1 - 100x magnification and five filter cubes for multiple wavelength image acquisition. The XLS model operates using a 4.66 megapixels scientific complementary metal-oxide semi-conductor (cMOS) camera with a larger field of view and a solid state light source of excitation ranging from 380 nm (DAPI) to 650 nm (Cy5). The XLS model utilises a high speed laser autofocus with reduced sample photobleaching and phototoxicity, two problematic phenomena that complicated fluorescent molecule observation in early HCA models (Giuliano et al. 2003). Molecular Devices® HCA systems literally have hundreds of automated image application modules (Figure 4.2) such as cell proliferation, cell cycle analysis, multi-wavelength cell scoring, apoptosis, autophagy,

angiogenesis/ endothelial tube formation, cell signalling by translocation etc. (Molecular Devices 2018).

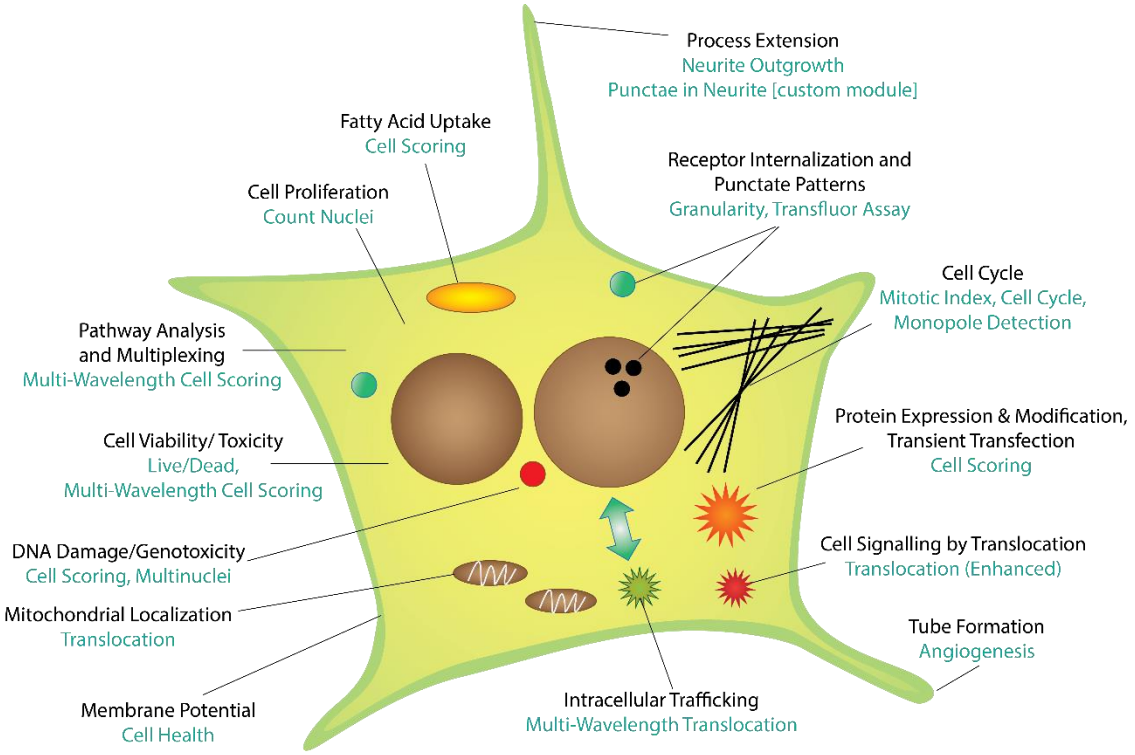

Figure 4.2 Selected application modules used in HCA systems (Adapted from: Molecular Devices 2018)

4.1.1 Basic skill sets for High Content Analysis

There are several basic skill sets required to develop and successfully run experiments on HCA systems. Firstly, biological skills are required in order to identify relevant biological research areas and thereby develop cellular assays that have practical *in vivo* applications (Haney et al. 2015). A sound knowledge on microscopy is also very important. For instance, the choice of light source determines the wavelength to be employed in cellular staining and an understanding of the microscopes objective parameters is important for choosing the sample type to be used, which has a huge influence on the resolution of the acquired images. A firm knowledge on instrumentation is also key in effectively utilising HCA equipment. Unfortunately, most of the practical information needed to successfully run HCA experiments can only be acquired from the manufacturers of the equipment being used. In order to apply information from these manufacturer-provided resources, one needs to have sound knowledge of the equipment's hardware such as laser autofocus, camera exposure time, photomultiplier

tube amplifier gain etc. Understanding instrumentation can also help the researcher to seamlessly integrate HCA systems with other equipment such as automated plate-handling devices for high-throughput screening. Due to the large quantity of data generated by HCA systems, a data analyst may be required for statistical analysis. An information technology expert may also be required for the safe storage and retrieval of HCA generated data. It is important to note that these skills and responsibilities may be shared among a small integrated team, especially in academic institutions were the majority of personnel are research students.

4.1.2 Image acquisition and data management in High Content Analysis systems

During a typical HCA experiment, plates are introduced into the HCA system for image acquisition and the system is configured based on the experiment to be done. Customization of the experiment is then performed using macros software such as MetaMorph® without the need for a programming language. After image acquisition, the data is sent to a computer system for management (Figure 4.3). An interactive data display allows for the detailed view of single cellular data. Molecular Devices® HCA systems give the option of data mining using their MDCStore solution software. Multi-parametric analysis of the acquired data is then performed through the use of various field or cell-by-cell parameters. The processed results can then be exported to various output channels such as ORACLE®, Microsoft® SQL, text file and Microsoft® Excel® (Molecular Devices 2012).

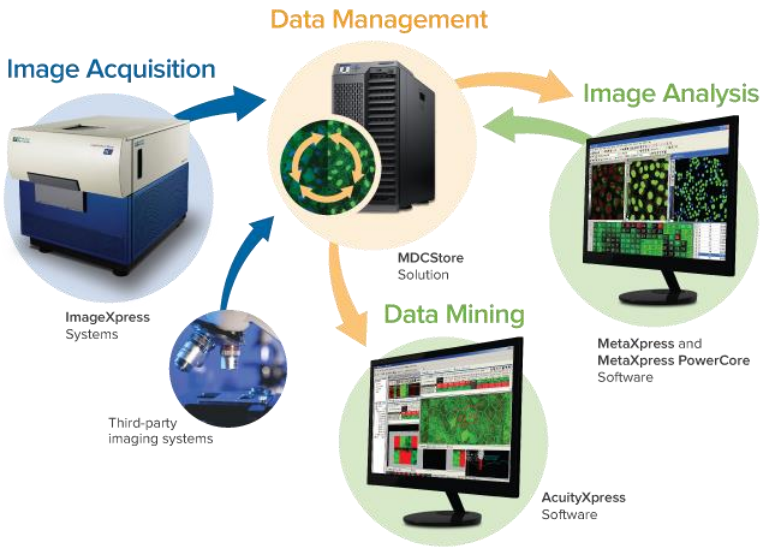

Figure 4.3 Image acquisition and data processing in Molecular Devices® HCA systems (Molecular Devices 2018)

4.1.3 Impact of High Content Analysis on early drug discovery challenges

The key steps involved in early drug discovery include target identification, compound selection and validation, initial screening and lead optimization (Kenneth et al. 1997). At some of these processes, major challenges occur which hinder the rate at which lead drug candidates are discovered. These rate limiting steps are referred to as 'bottlenecks' of early drug discovery (Ekins et al. 2013). The key bottlenecks in early drug discovery are target validation, primary Ultra High Throughput Screening (UHTS), candidate optimization, secondary screening, structural activity relationship studies (SAR) and toxicity evaluation (Figure 4.4). Due to the numerous competitive challenges encountered when identifying potential candidates for drug development, target validation is considered a major bottleneck of early drug discovery (Ilag et al. 2002). During target validation, the causative or functional role of a specific drug target in normal physiology or disease pathology is evaluated through the use of numerous *in vitro* and/or *in vivo* biological assays (Kenneth et al. 1997). The high discovery rate of new drug targets has further raised the target validation input and increased the time required for bio-assay analysis (Thomsen and Gloyn 2017). The three main factors to consider when attempting to improve the output of target validation are; data-handling, productivity and cost reduction. Bio-informatics, proteomics and the use of genomics databases has led to an improvement in the utilisation of data-handling tools (Emilien et al. 2000). To further improve this, HCA systems are now successfully applied to cellular genomics for the discovery of new therapeutic agents. This is because HCA enhances the reliability of cellular and functional genomics by interrogating endogenous markers to determine assay endpoints, normalizing the desired endpoint through meticulous examination of single cells and normalizing multiple endpoints for individual phenotypes, thereby increasing the confidence in candidate gene selection (Heynen-Genel et al. 2012). The high throughput capabilities of HCA systems can also help to improve target validation productivity levels. Due to these properties, HCA systems can be effectively used to eliminate the challenges of target validation, thereby enabling the discovery of new drug discovery targets in various therapeutic areas such as the discovery of new regulators of cell proliferation and the identification of additional components involved in stem cell self-renewal (Zock 2009).

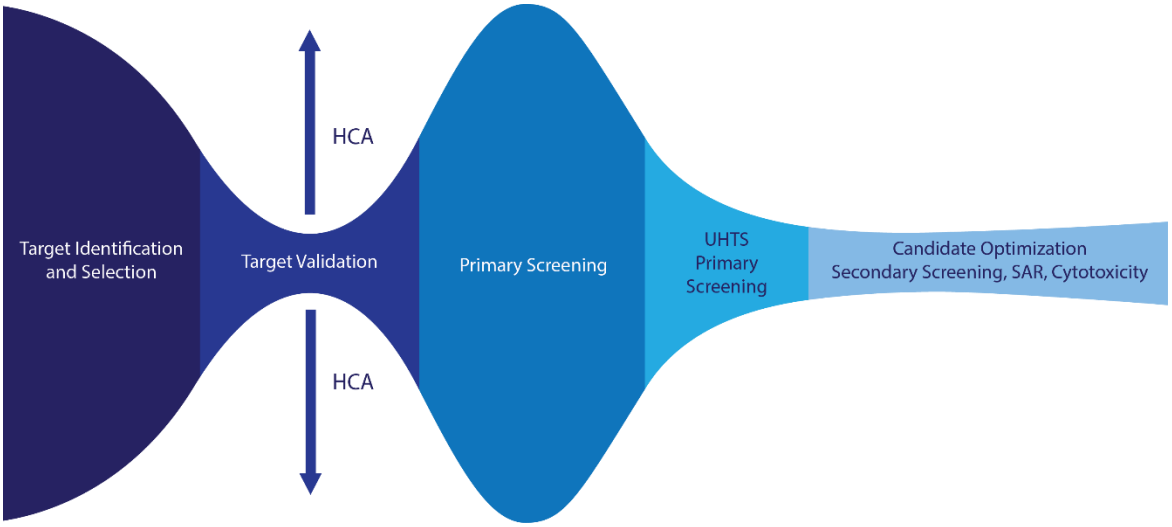

Figure 4.4 Key bottlenecks in early drug discovery (Adapted from: Giuliano et al. 2003)

4.1.4 High Content Analysis in cancer research

Programmed Cell Death (PCD) is a physiological mechanism that works to maintain normal cell proliferation levels and a defence mechanism against infections (Lockshin and Beaulaton 1974; Jorgensen et al. 2017). PCD can be evaded by some disease states to allow for the unwanted and continuous proliferation of cells, which thereby results in the development of malignancies such as cancer (Elmore 2007; Fuchs and Steller 2011). PCD is categorised as apoptosis, autophagy and programmed necrosis (Sun and Peng 2009), each with distinguishable morphological and biochemical features (Ouyang et al. 2012). PCD mechanisms continue to play a significant role in cancer research by aiding the discovery of new pharmacological and genetic modulators of cell death (Alam 2003). Many chemotherapy drugs induce cancer cell death by effecting changes on critical cell cycle signalling pathways (Mills et al. 2018). Application of HCA in cancer research was primarily based on the measurement of PCD. Through quantitative high-resolution biofluorescence imaging, HCA has revolutionized cancer drug discovery by being able to identify chemical entities that are able to alter the phenotypic characteristics of cancerous cells (Chetak et al. 2016). This is because HCA is able to identify morphological and biochemical alterations associated with PCD. In early apoptosis, HCA is able to measure phosphatidylserine "flipping", mitochondrial membrane potential flux, released cytochrome *c* and activation of caspace-3. HCA can also be used to measure membrane permeability and DNA fragmentation in late apoptosis and necrosis, cytoskeletal collapse in late apoptosis and LC3B expression in autophagy.

4.1.5 Advances in natural products research using High Content Analysis

The application of HCA tools to natural products research has produced ground-breaking results. For instance, the application of a High Content Screening (HCS) protocol termed U2nesRELOC to U2OS osteosarcoma cells treated with natural product extracts of microbial origin resulted in the discovery of a novel nuclear export inhibitor, MDN-0105, with an IC_{50} of 3.4 μM (Cautain et al. 2013). Since protein and RNA nucleocytoplasmic transportation plays a key role in the onset and progression of malignancies, the disruption of nuclear export has now been identified as a novel therapeutic approach. HCA of a fungal extract led to the isolation of MDN-0066 (Figure 4.5), a lipodepsipeptide with selective cytotoxicity for Von Hippel-Lindau (VHL) deficient cells, thereby being a potential new treatment for VHL disease and also providing insight into the pathogenesis of the disease (Cautain et al. 2015; Bellomo et al. 2017).

Recently, a new HCA screening platform called "Compound Activity Mapping" (CAM) was developed for the functional annotation of natural product libraries. CAM utilises HCA image based phenotypic screening to accurately predict individual structures and biological activities of plant metabolites from their complex natural product extracts (Kurita and Linington 2015). CAM is highly effective and more efficient than conventional laborious methods in that novel bioactive compounds can be discovered right from the preliminary screening stage. Through CAM, four novel compounds called quinocinnolinomycins A – D (Figure 4.5) were discovered as the first microbial-based natural compounds containing a cinnoline core (Kurita et al. 2015).

HCA is also being used in natural product drug discovery to eliminate bioactive natural compounds with potential adverse effects through the analysis of nuclear morphology. This is because alterations in nuclear area has been identified as a strong marker for potential cytotoxicity, thereby acting as a sensitive endpoint in determining compounds that are likely to fail later on in the drug development process (Martin et al. 2014). Furthermore, the past few decades have seen increased interest in the development of natural product based nanoparticles as novel drug delivery systems due to their increased bio-availability, improved solubility and high target selectivity (Griffin et al. 2018; Khan and Gurav 2018). These "phyto-nanoparticles" have raised serious safety concerns with regards to their impact on human health, hence, the need to adequately evaluate their potential toxicity during early drug discovery (Boczkowski and Hoet 2010; Boraschi et al. 2011). Since HCA has been identified as a universal method for

the characterisation of nanoparticle induced cytotoxicity (Jan et al. 2008; Anguissola et al. 2014), its application in natural product research will significantly increase the number of clinically approved phyto-nanoparticles.

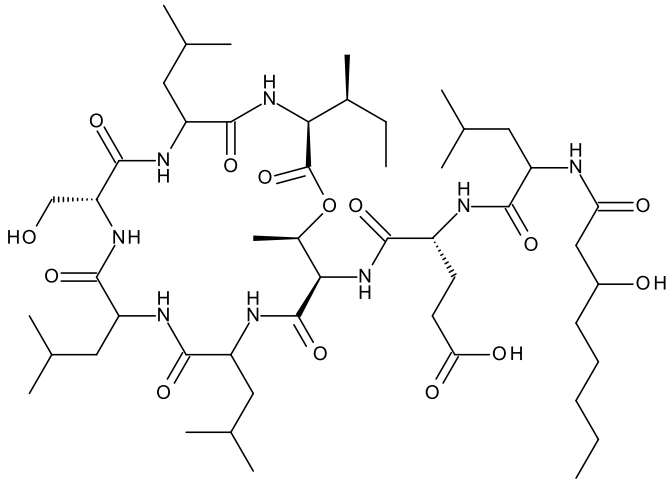

MDN-0066

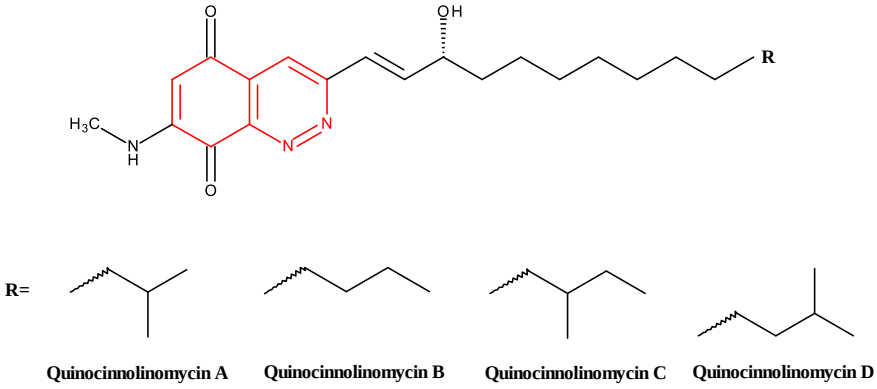

Quinocinnolinomycin A Quinocinnolinomycin B Quinocinnolinomycin C Quinocinnolinomycin D

Figure 4.5 Structures of MDB-0066 (Cautain et al. 2015) and quinocinnolinomycins A – D (Kurita et al. 2015).

The cinnoline moiety is highlighted in red

4.2 Chapter aim

In chapter 3, phytochemical investigation of the methanolic bulb extract of *Drimia altissima* led to the isolation and chemical characterisation of a novel *C*-glucosylflavonoid-*O*-glucoside, compound **3.17**. This chapter provides the bio-activity results which guided the isolation of compound **3.17** through the cytotoxic activity of *D. altissima* partitions and fractions, with

further evaluation of the cytotoxic activity of compound **3.17** against HeLa cervical cancer cells using High Content Analysis (HCA).

4.3 Results and discussion

4.3.1 3-(4,5-dimethylthiazol-2-yl)-2,5-diphenyl tetrazolium bromide (MTT) assay

The potential cytotoxicity of fractions **79a** – **d** and **82b** – **f** were evaluated using a modification of the original MTT assay (Mosmann 1983). From the obtained results (Figure 4.6), fractions **79c** and **79d** exhibited significant anti-proliferative activity at all tested concentrations, with **79d** being slightly more effective. Fractions **79a** and **79b** were less effective, with **79b** showing the least activity at the lowest tested concentration of 0.1 µg/mL. It was based on these results that Fraction **79d** was selected for further bio-assay guided fractionation, which then afforded fractions **82a** – **f** (see Chapter 3, Section 3.5.1). Fractions **82b**, **82c**, **82d** and **82e** exhibited significant anti-proliferative activity at all tested concentrations, with **82c** being the most effective fraction at the lowest tested concentration (Figure 4.7). Fraction **82f** was only effective at 10 µg/mL. After coupling these results with NMR chemical profile comparisons, **82c** was selected for further purification leading to the isolation of compound **3.17**.

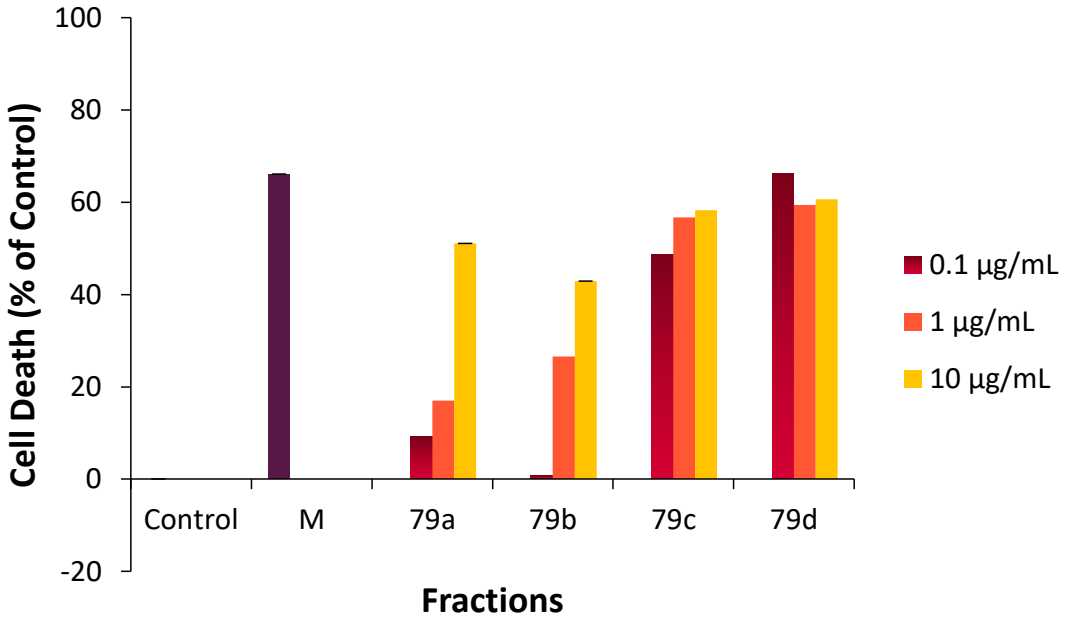

Figure 4.6 MTT assay results after treatment of HeLa cells with fractions **79a** – **d**

Melphalan (M) was used as positive control at 40 µM. Data points represent the mean ± SD of three independent experiments, each performed in quadruplicate

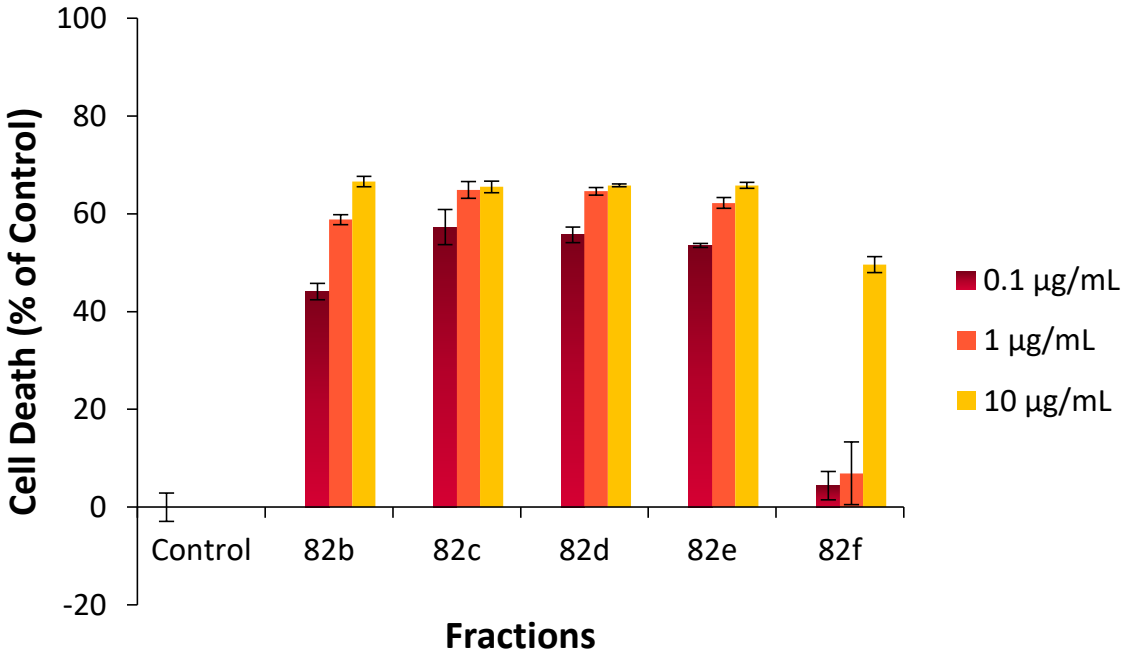

Figure 4.7 MTT assay results after treatment of HeLa cells with fractions **82b** – **f**

Data points represent the mean ± SD of three independent experiments, each performed in quadruplicate

4.3.2 High Content Analysis (HCA)

4.3.2.1 Cytotoxicity - bisBenzamide H 33342 trihydrochloride/ Propidium Iodide (PI)

The bisBenzamide H 33342 trihydrochloride (Hoechst 33342) (Figure 4.8) is a cell permeable nucleic acid stain which acts by binding to the minor groove of deoxyribonucleic acid (DNA) at AT-rich sequences, resulting in a blue-fluorescent stain (Tirino et al. 2016). Hoechst 33342 nucleic acid binding allows for the determination of DNA content in live cells without the need for a fixation agent. In cellular applications, Hoechst 33342 requires excitation by bombardment with either a mercury arc lamp, an argon-ion laser or a 325 nm Helium-Cadmium (He-Cd) laser (Deligeorgiev and Vasilev 2006; Shapiro and Telford 2018). Hoechst 33342 has excitation and emission maxima of 350 nm and 461 nm, respectively (blue-cyan fluorescence). Propidium iodide (PI) (Figure 4.8) is the most commonly used DNA probe. PI is a fluorescent dye which intercalates between bases and stains both DNA and RNA. Specific DNA staining is achieved by enzymatic removal of RNA with a ribonuclease (RNase). PI is commonly used as a nuclear stain in fluorescent microscopy and as a DNA content determinant in cell cycle analyses by flow cytometry. PI has excitation and emission maxima of 535 and 617 nm, respectively (orange to red range of the spectrum). Due to its lack of permeabilization in viable cells, PI is also employed as a viability marker to detect dead cells whose disrupted membranes allow the dye to reach the nucleic acids.

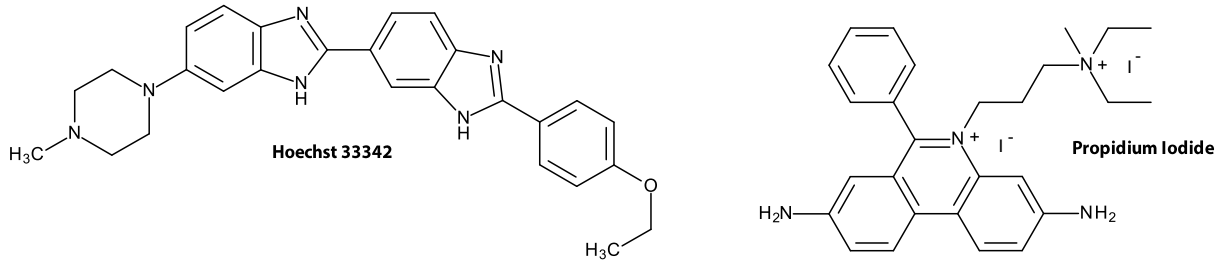

Figure 4.8 Structures for Hoechst 33342 and propidium iodide dyes.

The anti-proliferative activity of partition **79d** and compound **3.17** against HeLa cells was evaluated *via* Hoechst 33342/ PI dual staining with melphalan (40 µM) used as positive control (Figure 4.9A). Images were acquired from 9 sites per well of a treated 96-well plate at 10x objective (Figure 4.9B). Values are reported as the average of 9 sites from each well. From the results obtained after 24 h of treatment, partition **79d** exhibited a dose dependent inhibition of cell proliferation from 0.2 µg/mL onwards (Figure 4.10), with an IC_{50} of ± 0.497 µg/mL (Figure 4.11). At 20 µg/mL, partition **79d** was found to be almost as effective as melphalan. Similarly, compound **3.17** exhibited a dose dependant inhibition of cell proliferation (Figure 4.10), with an IC_{50} of ± 2.44 µM (1.37 µg/mL) (Figure 4.11). At 20 µM, compound **3.17** was found to be more effective than melphalan.

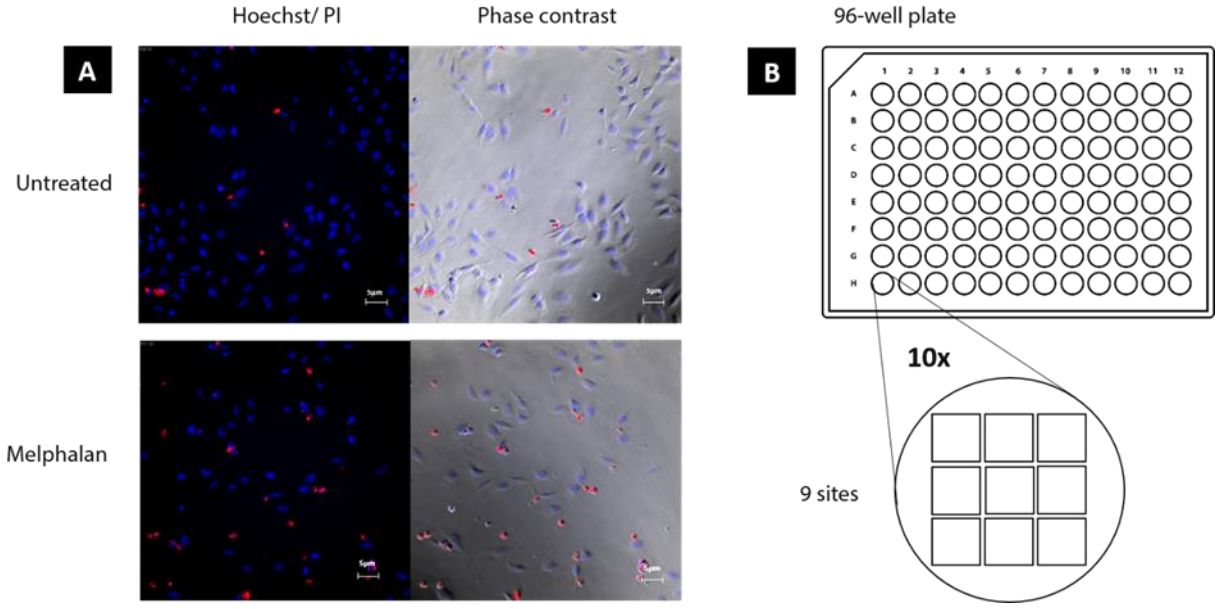

Figure 4.9 (A) Hoechst 33342/ PI dual staining with phase contrast in HeLa cells after a 10x objective, (B) 9 sites per well HCA image acquisition

Blue stains indicate Hoechst/DNA staining of live cells, red stains indicate PI/RNase staining of dead cells.

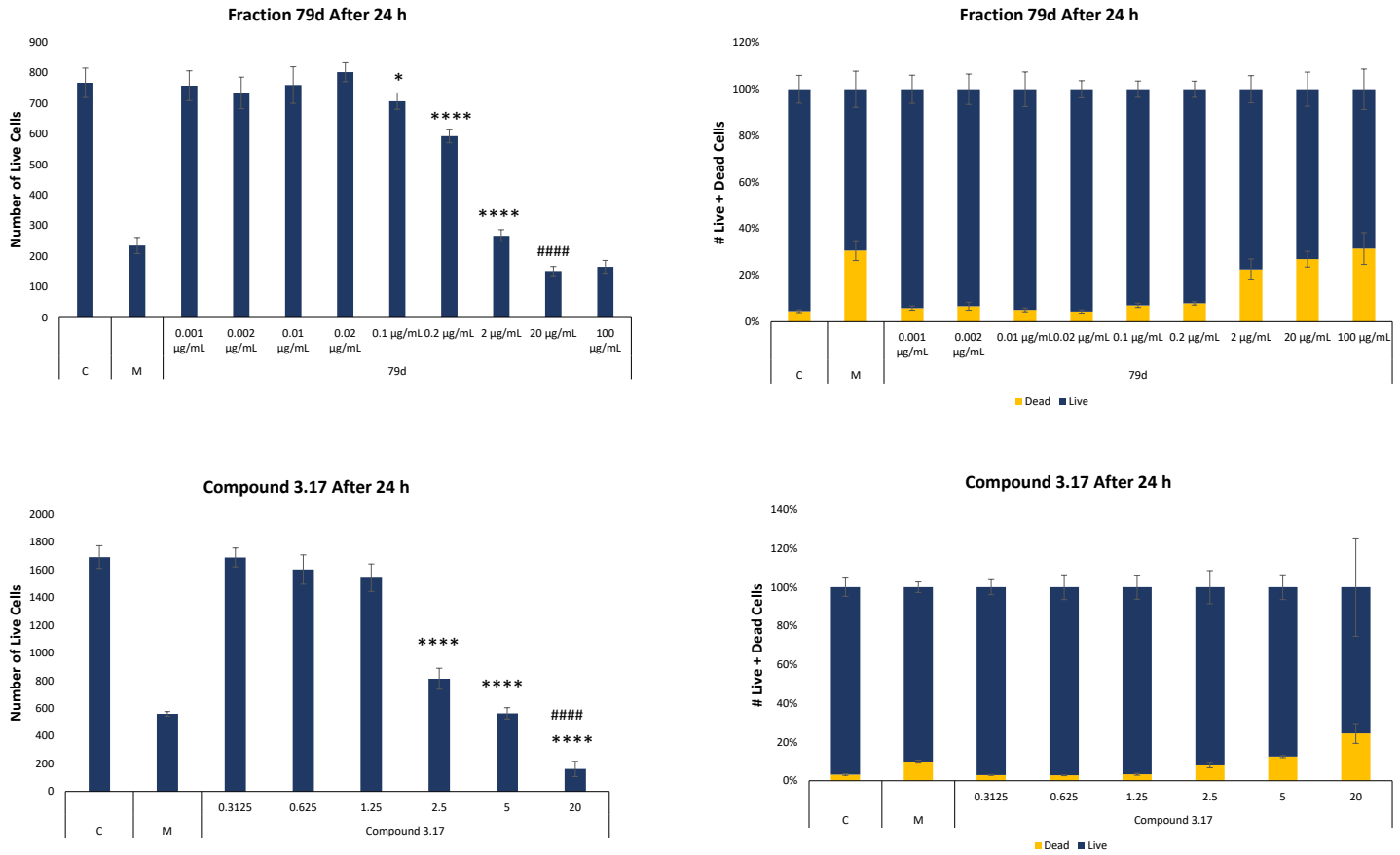

Figure 4.10 Number of live cells per image site (left) and stacked number of live and dead cells (right) after 24 h of treatment with partition **79d** (top) and compound **3.17** (bottom)

Concentrations for partition **79d** and compound **3.17** were measured in µg/mL and µM respectively. Melphalan (M) was used as positive control at 40 µM. Data points represent the mean ± SD of three independent experiments, each performed in quadruplicate. Significance was determined by a two-tailed Student t-test with (****) = p value ≤ 0.0001 compared to untreated control (C). ($^{####}$) = p value ≤ 0.0001 compared to melphalan

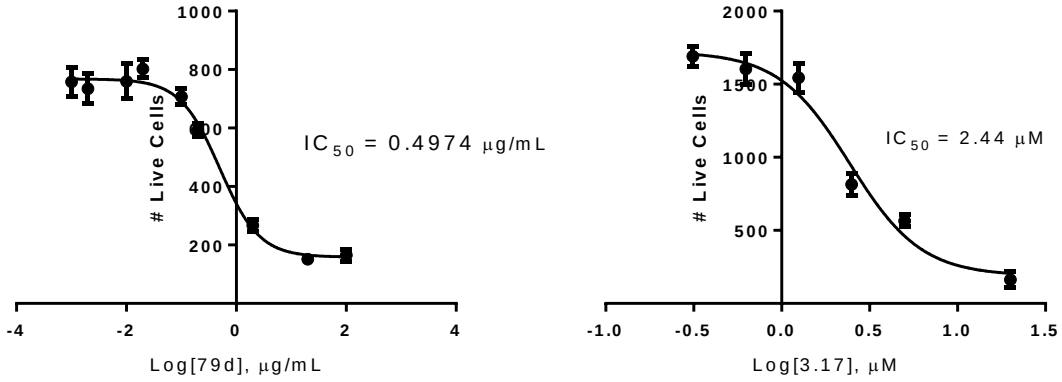

Figure 4.11 Dose response curves for the anti-proliferative activity of partition **79d** (left) and compound **3.17** (right) against HeLa cells after 24 h of treatment

Data points represent the mean ± SD of three independent experiments, each performed in quadruplicate

Besides cell proliferation and mitochondrial area, one of the most sensitive parameters in evaluating cytotoxicity using HCA systems is the measurement of nuclear area (O'Brien et al. 2006). Changes in nuclear area can give an impression of the mechanism of action induced by a cytotoxic agent. For instance, due to the increased DNA content (4N) associated with G_2/ early M phases as well as increased cellular size in necrosis, treatments that cause either G_2/ early M or late S phase cell cycle arrest or necrosis will typically increase the nuclear area of the treated cells. If cell cycle arrest further leads to apoptosis, a consequent reduction in nuclear area can be noticed as a result of nuclear condensation (Sirenko et al. 2014).

After 48 h treatment with partition **79d** and compound **3.17** using melphalan as positive control at 20 and 40 µM respectively, nuclear size was evaluated by the measurement of nuclei area. From the obtained results (Figure 4.12), melphalan caused a reduction in nuclear area at 20 µM and an increase in nuclear area at 40 µM, indicating possible G_2/M cell cycle arrest at the higher dose and induction of apoptosis at the lower dose. Partition **79d** caused a significant increase in nuclei area at 2 µg/ml and a decrease at 20 and 100 µg/mL, suggesting S or G_2/ M cell cycle arrest at the lower concentration and apoptosis induction at the higher concentrations (Figure 4.12A). Compound **3.17** caused an increase in nuclei area at the highest tested concentration of 20 µM, suggesting induction of cell cycle arrest in S, G2 or early M phase (Figure 4.12B).

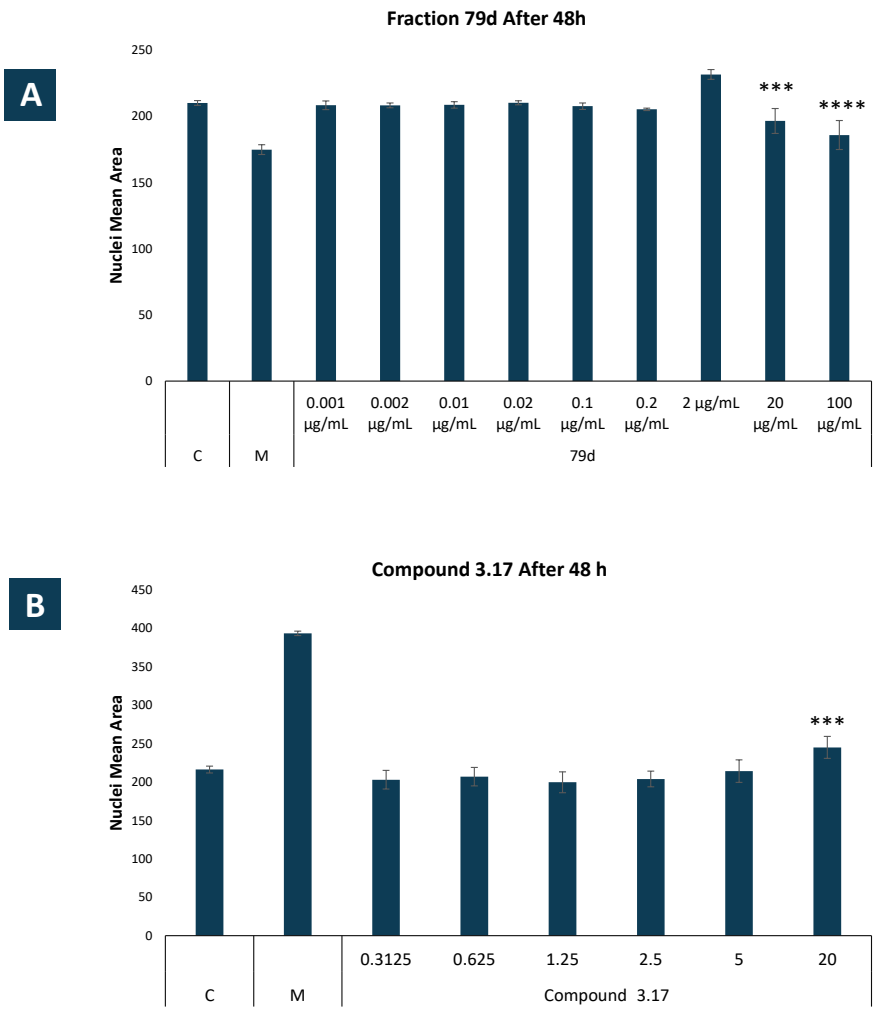

Figure 4.12 Nuclei mean area after 48 h of treatment with partition **79d** (A) and compound **3.17** (B)

Concentrations were measured in µM with melphalan (M) used as positive control at 20 and 40 µM for partition **79d** and compound **3.17** respectively. Data points represent the mean ± SD of three independent experiments, each performed in quadruplicate. Significance was determined by a two-tailed Student t-test with (*) = p value ≤ 0.05, (**) = p value ≤ 0.01, (***) = p value = ≤ 0.001 and (****) = p value ≤ 0.0001 compared to untreated control (C)

4.3.2.2 Cell Cycle Analysis - Hoechst 33342/ Annexin-V-FITC

Cell cycle analysis is a method used to determine the proportion of cells in each phase of the cell cycle (Figure 4.13) for a given cell population based on differences in the content of DNA (Crissman and Tobey 1974). In this method, fluorescent probes are used to measure DNA molecules either by labelling or staining through stoichiometric binding which gives an

equivalent probe-to-DNA quantification (Darzynkiewicz 2010). Generally, these DNA probes are phenanthridiniums in chemical structure which get excited in the ultraviolet spectrum and produce red spectral emissions (Huber et al. 2004). Examples of these DNA fluorescent probes include Hoechst 33342, 1,5-bis{[2-(di-methylamino) ethyl]amino}-4, 8-dihydroxyanthracene-9,10-dione (DRAQ5) and 4′,6-diamidino-2-phenylindole (DAPI) (Martin et al. 2005). The ploidy of a cell is the number of chromosomes that it contains. Cells in G_0 and G_1 have a diploid DNA content (2N) while those in G_2 and M have a tetraploid DNA content (4N). Cells in G_2 and M contain twice the DNA content compared to those in G_0/G_1 because of ploidy implications. The DNA content during S phase lies between these two extremes. If a cytostatic compound caused cell cycle arrest, a cell cycle histogram can be generated to determine whether the arrest is at G_0/G_1, S, G_2 or M based on the percentage of total cells in each phase population. Traditional cell cycle analysis using flow cytometry does not distinguish between G_2 and M. However, HCA-based cell cycle analysis is able to distinguish between G_2, and M as well as between Early M and Late M. This is based on the fluorescence intensity of the dye. Cells in G_2 and early M have large areas, with G_2 cell intensity being lower than that of M phase. In late M phase, each cell exists with two very bright but small nuclei and thereby allowing HCA systems to distinguish between early and late M phases.

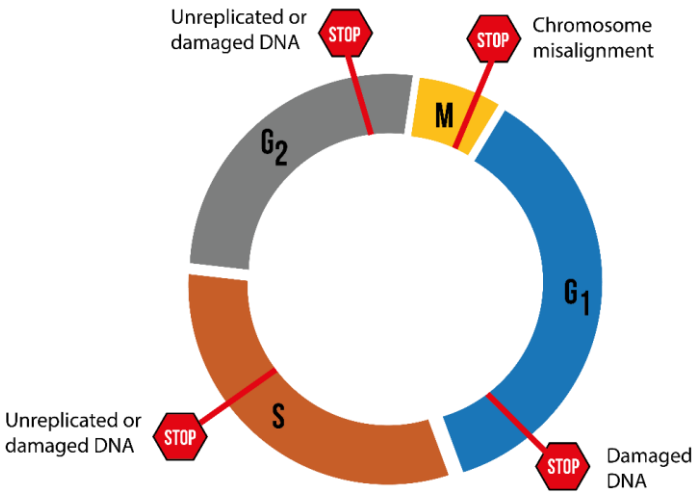

Figure 4.13 Phases of the Cell cycle with key checkpoints (Cooper and Hausman 2007)

Cell cycle analysis of partition **79d** and compound **3.17** was determined via Hoechst 33342/ Annexin-V-fluorescein isothiocyanate (FITC) staining using melphalan at 40 µM as positive control. Apoptotic cells may incorrectly be identified as mitotic cells because of the increased fluorescence intensity. Therefore, it is important to include an apoptosis marker when working with potential apoptosis inducers. From the obtained results, melphalan induced M phase cell cycle arrest as expected. Partition **79d** induced a dose dependent mitotic cell cycle arrest from 0.1 µg/mL onwards, which was characterised by a marked increase in Early M phase and a slight increase in Late M phase cell populations (Figure 4.14).

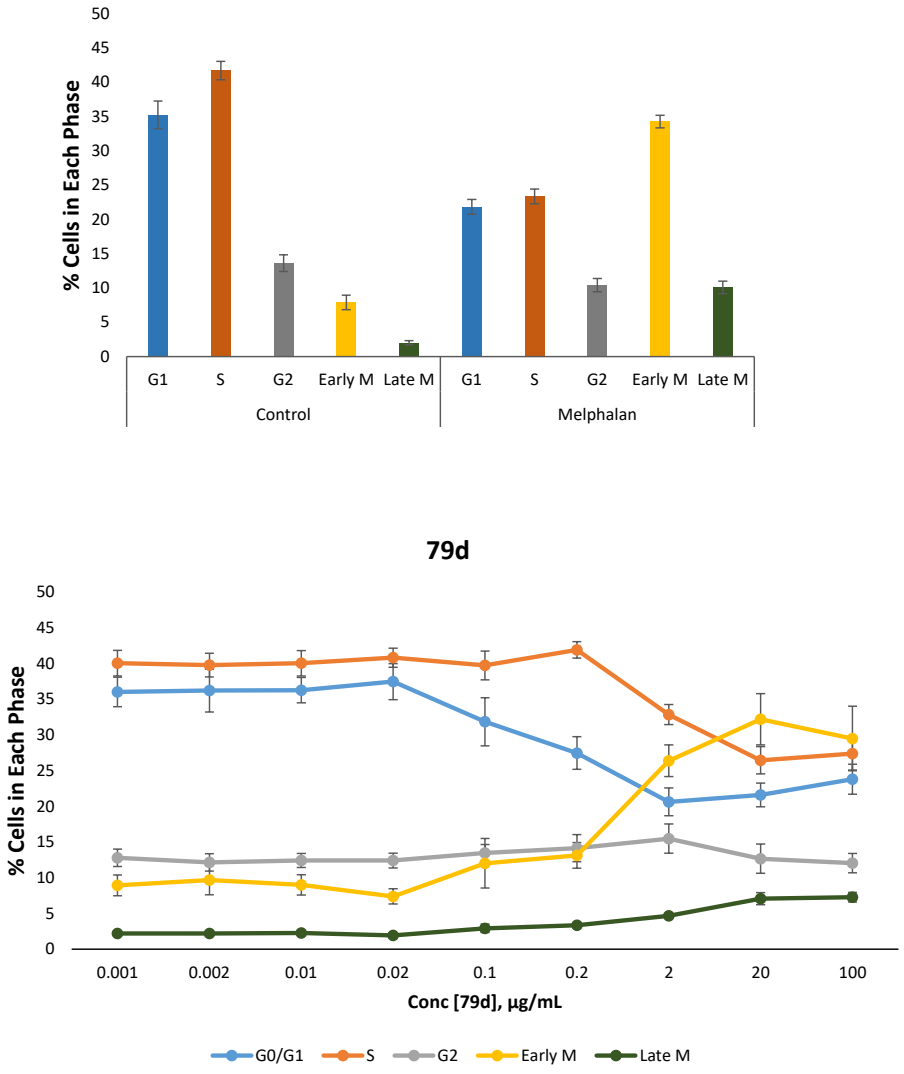

Figure 4.14 Cell Cycle Analysis after 24 h of treatment with partition **79d**

Concentrations were measured in µM with melphalan (40 µM) used as positive control. Data points represent the mean ± SD of three independent experiments performed in quadruplicate

Similar to partition **79d**, compound **3.17** induced a dose dependent mitotic cell cycle arrest exhibited by a marked increase in Early M phase and a slight increase in Late M phase cell populations (Figure 4.15). These results suggested that compound **3.17** is, at least in part, responsible for the anti-proliferative activity of extract **79** and partition **79d** through an induction of M phase cell cycle arrest in HeLa cells.

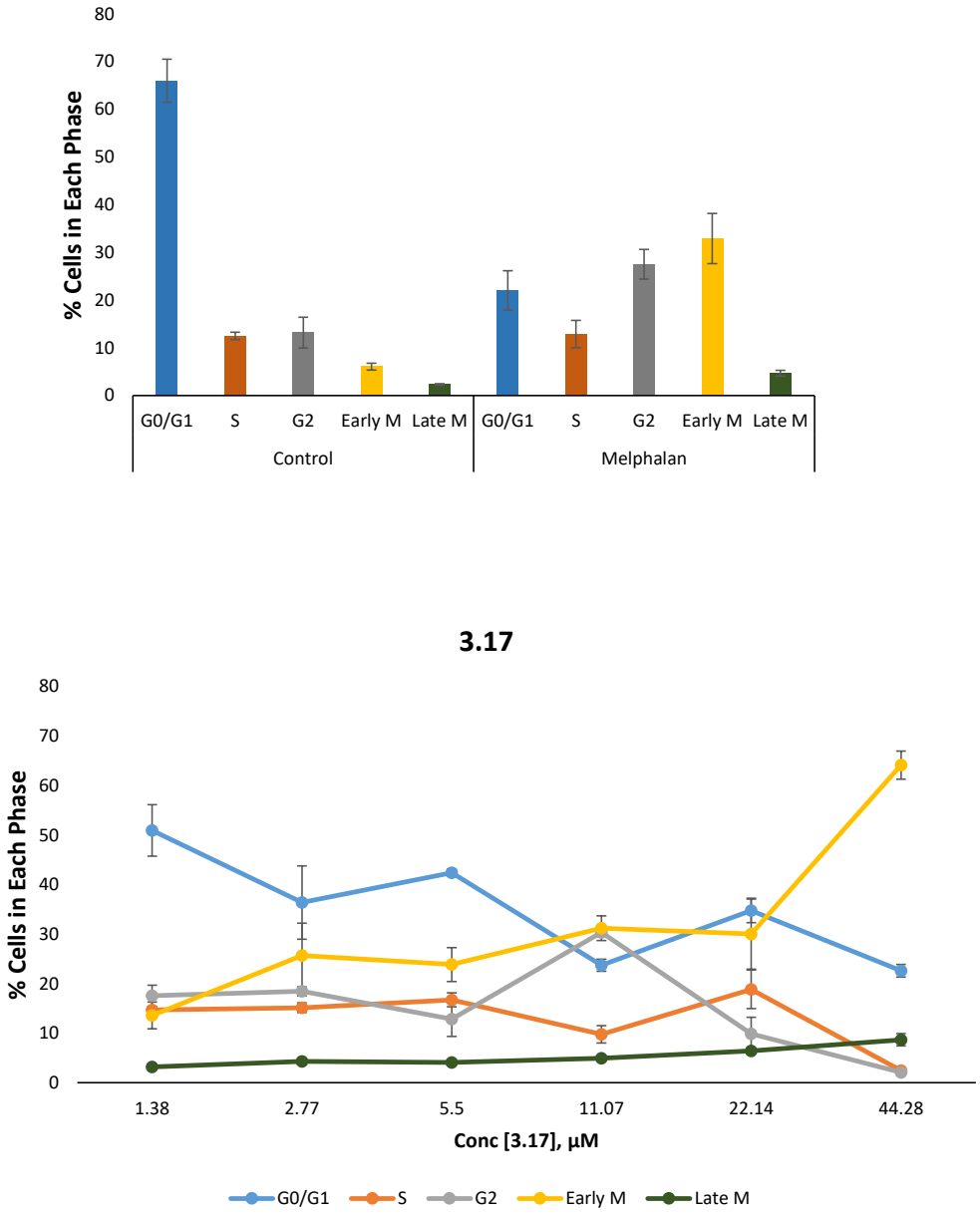

Figure 4.15 Cell Cycle Analysis after 48 h of treatment with compound **3.17**

Concentrations were measured in µM with melphalan (40 µM) used as positive control. Data points represent the mean ± SD of three independent experiments performed in quadruplicate

4.3.2.3 Apoptosis – Hoechst 33342/ Annexin-V-FITC-PI

The characteristics of apoptosis include pyknosis (asymmetric plasma membrane), nuclear and cytoplasmic condensation and DNA fragmentation (Kepp et al. 2011). In the early stages of apoptosis, cells translocate membrane phosphatidylserine (PS) from the internal to the external surfaces of plasma membranes resulting in the exposure of PS to the extracellular space (Segawa and Nagata 2015). Annexin-V, usually conjugated to fluorochromes such as fluorescein isothiocyanate (FITC), is a Ca^{2+} dependent phospholipid binding protein with a high binding affinity for exposed PS. Since exposure of PS in early apoptosis precedes loss of cell membrane integrity in late apoptosis/ necrosis, multiple staining with Hoechst 33342, Annexin-V-FITC and PI can be used to distinguish between live, early apoptotic, late apoptotic/ necrotic and necrotic cells. Ideally, live cells only stain with Hoechst 33342 since they do not expose PS for Annexin-V-FITC binding and PI does not permeate intact cell membranes (Figure 4.16). Early apoptotic cells stain with both Hoechst 33342 and Annexin-V-FITC due to exposed PS while PI is excluded by the presence of intact cell membranes. Late apoptotic/ necrotic cells stain with Hoechst 33342, Annexin-V-FITC and PI resulting from the disruption of cell membranes. Exclusively necrotic cells only stain with Hoechst 33342 and PI since PS is not present for Annexin-V-FITC binding due to loss of membrane integrity.

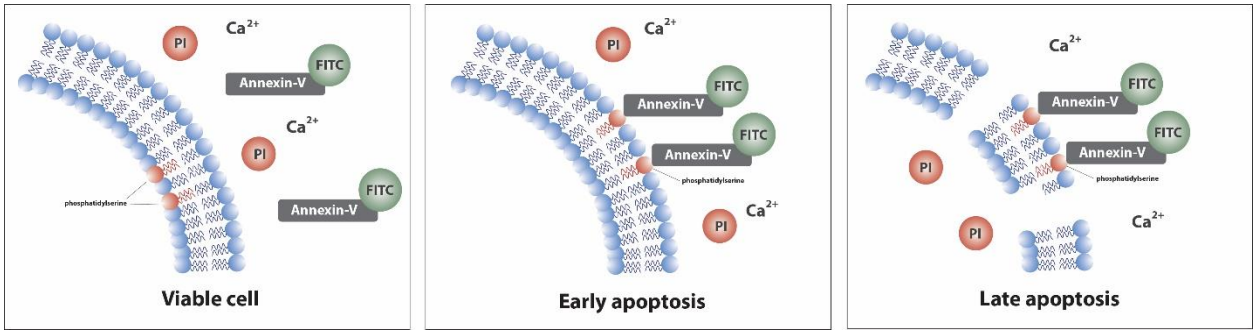

Figure 4.16 An illustration of Annexin-V-FITC-PI staining in viable cells, early apoptosis and late apoptosis (Sawai and Domae 2011)

Multiple staining with Hoechst 33342/ Annexin-V-FITC-PI was employed to determine if compound **3.17** induced apoptosis in HeLa cells at test concentrations of 5.5 and 22.14 µM. This combination of dyes was used to distinguish between viable, early apoptotic and late apoptotic/ necrotic cells as shown below (Figure 4.17).

From the obtained results after 48 h of treatment, 5.5 µM of **3.17** induced 14% apoptosis (Figure 4.19A) and 11.4% late apoptosis/ necrosis (Figure 4.19B). At 22.14 µM, the apoptotic cells increased to 19%, with a corresponding increase in late apoptotic/ necrotic cells (12.6%). These results suggest that the cytotoxic activity of compound **3.17** against HeLa cells involves the induction of apoptosis. The specific apoptotic pathways that are triggered by compound **3.17** in HeLa cells are further investigated and discussed in the next chapter.

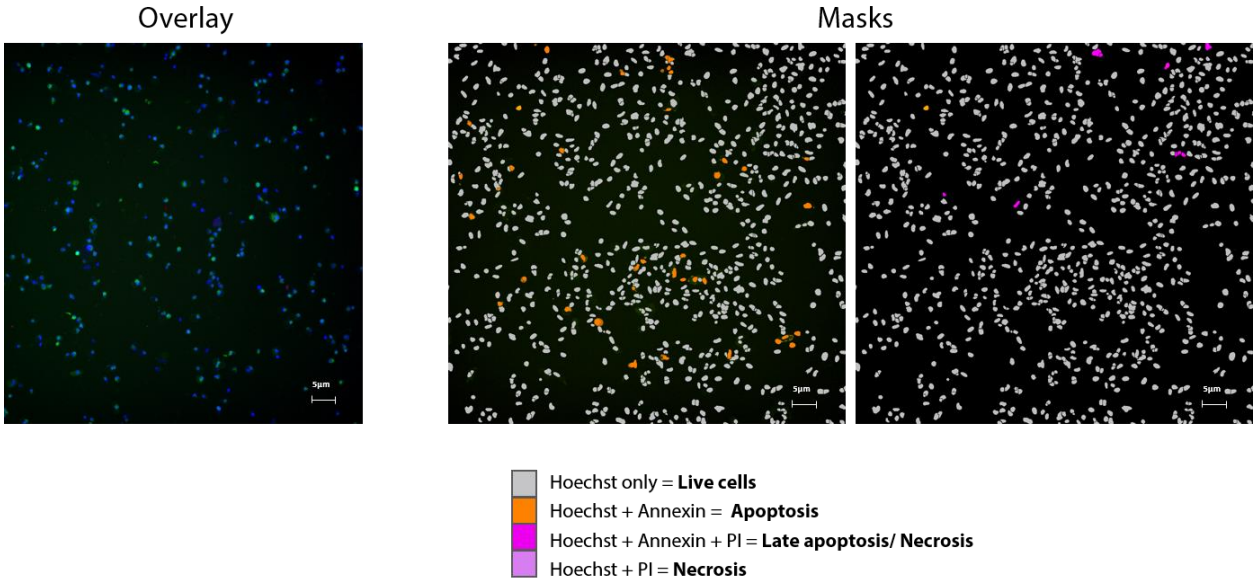

Figure 4.17 HCA acquired image overlay (left) with masks (right) distinguishing between live, apoptotic, late apoptotic/ necrotic and necrotic HeLa cells

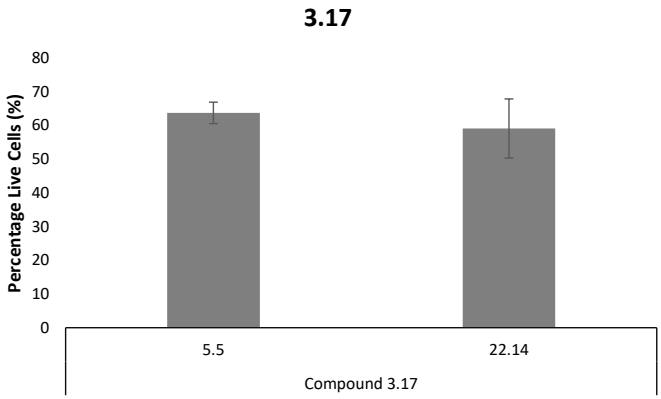

Figure 4.18 Percentage of live HeLa cells after 48 h treatment with compound **3.17**
Concentrations were measured in µM with melphalan (40 µM) used as positive control. Data points represent the mean ± SD of three independent experiments performed in quadruplicate

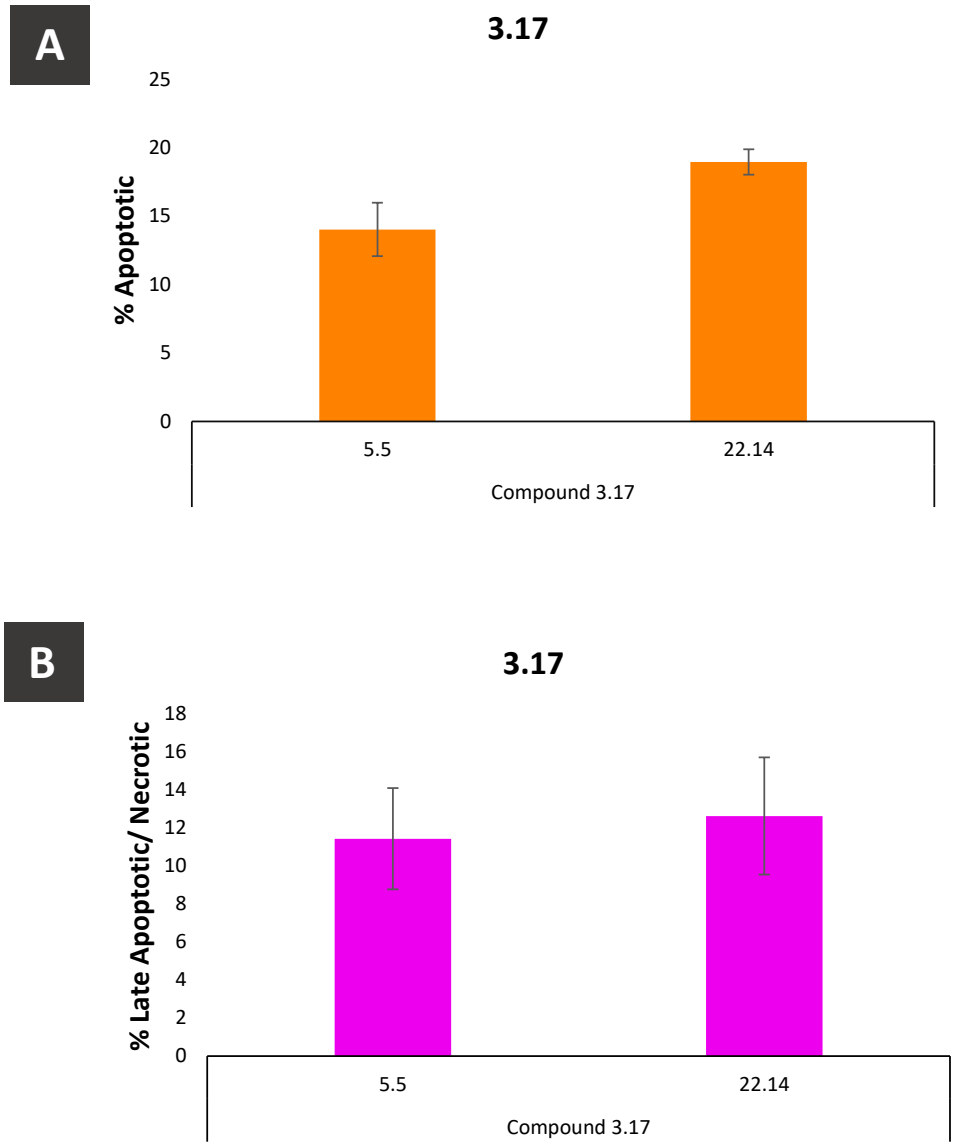

Figure 4.19 Percentage of apoptotic (A) and late apoptotic/necrotic (B) HeLa cells after 48 h treatment with compound **3.17**

Concentrations were measured in µM with melphalan used as positive control. Data points represent the mean ± SD of three independent experiments, each performed in quadruplicate

In Chapter 2, it was established that **79**, the methanolic crude extract of *Drimia altissima* possesses marked anti-proliferative activity against HeLa cells with an IC_{50} of 1.2 µg/mL. Chapter 3 further described the chromatographic separation of **79** into partitions and fractions, which led to the isolation of compound **3.17** from fraction **82c**. In this chapter, the bio-activity results which guided the isolation of compound **3.17** were provided, starting with an evaluation of the cytotoxic activity of partitions **79a** – **d** and fractions **82b** – **f** against HeLa cells using the

MTT assay. This was then followed by an evaluation of the cytotoxic activity of the isolated compound, **3.17**, in comparison with its parent partition, **79d**, against HeLa cells using High Content Analysis (HCA). It was determined from the MTT results that partition **79d** was the most cytotoxic partition after it exhibited significant anti-proliferative activity at all the tested concentrations with 60% cell death (% of control) at 10 µg/mL. Fractions **82b** – **e** showed cytotoxicity profiles similar to that of their parent partition, **79d**, with **82c** being the most effective at 0.1 µg/mL. From the HCA results, both partition **79d** and compound **3.17** showed significant cytotoxicity with IC_{50} values of ± 0.497 µg/mL and ± 2.44 µM (1.37 µg/mL) respectively. Since the IC_{50} of partition **79d** was lower than that of crude extract **79** and compound **3.17**, it is implied that partition **79d** contains other cytotoxic compounds that are yet to be isolated. This can also be seen from the fact that **82c** was not the only cytotoxic fraction from partition **79d**. Thus, **3.17** is one of, if not the main compound, responsible for the anti-proliferative activity of partition **79d**. From cell cycle results, both partition **79d** and compound **3.17** caused a marked increase in Early M phase and a slight increase in Late M phase cell populations after 48 h of treatment. Additionally, compound **3.17** was also found to induce 19% apoptosis at 22.4 µM with only 12.6% late apoptotic/ necrotic cells. It can therefore be summarised that the anti-proliferative activity of the methanolic crude extract of *Drimia altissima* in HeLa cervical cancer cells partly involves the cytotoxic activity of the flavonoid glycoside compound, **3.17**, through its induction of cell cycle arrest at Early M phase and subsequent apoptotic cell death. The mechanisms by which compound **3.17** elicits this anti-proliferative activity is explored in the next chapter.

4.4 Experimental

4.4.1 General experimental procedures

HeLa cervical cancer cells were obtained from Highveld Biological, South Africa and grown in Roswell Park Memorial Institute 1640 (RPMI 1640) medium from GE Healthcare Life Sciences (South Logan, Utah, USA) supplemented with gamma irradiated Fetal Bovine Serum (FBS) from Biowest (South America). Cells were cultured in BioFlow-II Labotec laminar flow cabinets and incubated in a ThermoForma CO_2 incubator. Annexin V-FITC kit was obtained from MACS Miltenyi Biotec (Auburn, USA). 3-(4,5-dimethyl-2-thiazolul)-2,5-diphenyl-2H-tetrazolium bromide (MTT) and Hoechst 33342 were obtained from Sigma (St. Louis, MO, USA).

4.4.2 3-(4,5-dimethylthiazol-2-yl)-2,5-diphenyl tetrazolium bromide (MTT) assay

HeLa cells were seeded into 96-well culture plates at a density of 5 000 cells/well in RPMI 1640 supplemented with 10% fetal bovine serum (FBS) and incubated for 24 h. Partitions **79a** – **d** and fractions **82b** – **f** were added to the cells at 0.1, 1.0 and 10 µg/mL with melphalan used as positive control. The treated cells were incubated for a further 48 h after which the medium was replaced with 100 µL MTT (Sigma®) (0.5 mg/mL in RPMI 1640). After 3 h of incubation at 37 °C, the MTT was aspirated and the purple formazan product dissolved in 100 µL DMSO. The absorbance was measured at 560 nm using a multi-well scanning spectrophotometer (Multiscan MS, Labsystems). All incubation steps were carried out in a 37 °C humidified incubator with 5% CO_2.

4.4.3 High Content Analysis (HCA)

4.4.3.1 Hoechst 33342/ Propidium Iodide (PI) cytotoxicity assay

HCA was used for cytotoxicity screening of partition **79d** and compound **3.17**. HeLa cells were seeded at a density of 5000 cells/well into 96 well culture plates and incubated for 24 h at 36.7 °C in a humidified 5% CO_2 incubator. The cells were treated at different concentrations of the extract, partition and compound. For partition **79d**, cells were treated at 0.001, 0.002, 0.01, 0.02, 0.1, 0.2, 2, 20 and 100 µg/mL. For compound **3.17**, cells were treated at 0.3125, 0.625, 1.25, 2.5, 5 and 20 µM. In each of these experiments, 20 or 40 µM of melphalan was used as positive control. Treatments were incubated for 24 and 48 h at 36.7 °C after which the medium was aspirated and cells washed with PBS containing calcium and magnesium. The cells

underwent Hoechst/PI staining with bisBenzamide H 33342 trihydrochloride (Hoechst 33342) at 5 µg/mL and propridium iodide (PI) at 10 µg/mL. After 15 min incubation at 36.7 °C, cellular images were acquired with a Molecular Devices® ImageXpress Micro XLS Widefield High-Content Analysis System using a DAPI filter for Hoechst 33342 and a Texas Red filter for PI. The acquired images were analysed using the Multiwavelength Cell Scoring analysis module of MetaXpress® High-Content Image Acquisition and Analysis Software.

4.4.3.2 Hoechst 33342/ Annexin V-FITC (Cell Cycle Analysis)

HeLa cells were seeded and treated with partition **79d** and compound **3.17** as above. Cell Cycle Analysis was performed using a Hoechst 33342/ Annexin V-FITC staining mixture prepared by the addition of 50 µL of Annexin V-FITC and 5 µL of Hoechst 33342 to 5 mL PBS (containing 250 µL of Binding Buffer, 20x). The Hoechst 33342/ Annexin V-FITC mixture was used in 50 µL aliquots to stain the cells. The stained cells were incubated for 15 min at room temperature followed by image acquisition with a Molecular Devices® ImageXpress Micro XLS Widefield High-Content Analysis System using a DAPI filter for Hoechst 33342 and a FITC filter for Annexin V-FITC. The acquired images were analysed using the Cell Cycle Analysis module of MetaXpress® High-Content Image Acquisition and Analysis Software.

References

Alam, J.J. 2003. Apoptosis: target for novel drugs. *Trends in Biotechnology*, 21, (11) 479-483 available from: http://dx.doi.org/10.1016/j.tibtech.2003.08.006 Accessed 29 June 2018.

Anguissola, S., Garry, D., Salvati, A., O'Brien, P.J., & Dawson, K.A. 2014. High Content Analysis Provides Mechanistic Insights on the Pathways of Toxicity Induced by Amine-Modified Polystyrene Nanoparticles. *PLOS ONE*, 9, (9) e108025 available from: https://doi.org/10.1371/journal.pone.0108025

Bellomo, F., Medina, D.L., De Leo, E., Panarella, A., & Emma, F. 2017. High-content drug screening for rare diseases. *Journal of Inherited Metabolic Disease*, 40, (4) 601-607

Boczkowski, J. & Hoet, P. 2010. What's new in nanotoxicology? Implications for public health from a brief review of the 2008 literature. *Nanotoxicology*, 4, (1) 1-14 available from: https://doi.org/10.3109/17435390903428844

Boraschi, D., Costantino, L., & Italiani, P. 2011. Interaction of nanoparticles with immunocompetent cells: nanosafety considerations. *Nanomedicine*, 7, (1) 121-131 available from: https://doi.org/10.2217/nnm.11.169 Accessed 17 April 2018.

Cautain, B., de Pedro, N., Murillo Garzón, V., Muñoz de Escalona, M., González Menéndez, V., Tormo, J.R., Martin, J., El Aouad, N., Reyes, F., Asensio, F., Genilloud, O., Vicente, F., & Link, W. 2013. High-Content Screening of Natural Products Reveals Novel Nuclear Export Inhibitors. *Journal of Biomolecular Screening*, 19, (1) 57-65 available from: https://doi.org/10.1177/1087057113501389 Accessed 17 April 2018.

Cautain, B., de Pedro, N., Schulz, C., Pascual, J., da S.Sousa, T., Martin, J., Pérez-Victoria, I., Asensio, F., González, I., Bills, G.F., Reyes, F., Genilloud, O., & Vicente, F. 2015. Identification of the Lipodepsipeptide MDN-0066, a Novel Inhibitor of VHL/HIF Pathway Produced by a New *Pseudomonas* Species. *PLOS ONE*, 10, (5) e0125221 available from: https://doi.org/10.1371/journal.pone.0125221

Chetak, K., Luís, M.S., Luís, A.A., & Jorge, M.S. 2016. High-Content Analysis of Breast Cancer Using Single-Cell Deep Transfer Learning. *Journal of Biomolecular Screening*, 21, (3) 252-259 available from: https://doi.org/10.1177/1087057115623451 Accessed 19 March 2018.

Cooper, M. G. & Hausman, E. R. 2007, "The Cell Cycle - The Eukaryotic Cell Cycle," *In The Cell - A Molecular Approach*, 4 ed. M. G. Cooper & E. R. Hausman, eds., Washington D.C.: ASM Press, pp. 650-656.

Crissman, H.A. & Tobey, R.A. 1974. Cell-Cycle Analysis in 20 Minutes. *Science*, 184, (4143) 1297 available from: http://science.sciencemag.org/content/184/4143/1297.abstract

Darzynkiewicz, Z. 2010. Critical Aspects in Analysis of Cellular DNA Content. *Current protocols in cytometry / editorial board, J.Paul Robinson, managing editor ...[et al.]*, CHAPTER, Unit7 available from: http://www.ncbi.nlm.nih.gov/pmc/articles/PMC2976661/

Deligeorgiev, T. & Vasilev, A. 2006, "Cyanine Dyes as Fluorescent Non-covalent Labels for Nucleic Acid Research," *In Functional Dyes*, Amsterdam: Elsevier Science, pp. 137-183.

Ekins, S., Waller, C.L., Bradley, M.P., Clark, A.M., & Williams, A.J. 2013. Four disruptive strategies for removing drug discovery bottlenecks. *Drug Discovery Today*, 18, (5) 265-271 available from: http://www.sciencedirect.com/science/article/pii/S1359644612003601

Elmore, S. 2007. Apoptosis: A Review of Programmed Cell Death. *Toxicologic Pathology*, 35, (4) 495-516 available from: https://doi.org/10.1080/01926230701320337 Accessed 29 June 2018.

Emilien, G., Ponchon, M., Caldas, C., Isacson, O., & Maloteaux, J.G. 2000. Impact of genomics on drug discovery and clinical medicine. *QJM: An International Journal of Medicine*, 93, (7) 391-423 available from: http://dx.doi.org/10.1093/qjmed/93.7.391

Fuchs, Y. & Steller, H. 2011. Programmed Cell Death in Animal Development and Disease. *Cell*, 147, (4) 742-758 available from: http://www.sciencedirect.com/science/article/pii/S0092867411012839

Giuliano, K.A., Haskins, J.R., & Taylor, D.L. 2003. Advances in High Content Screening for Drug Discovery. *ASSAY and Drug Development Technologies*, 1, (4) 565-577 available from: https://doi.org/10.1089/154065803322302826 Accessed 2 June 2018.

Griffin, S., Masood, M.I., Nasim, M.J., Sarfraz, M., Ebokaiwe, A.P., Sch+ñfer, K.H., Keck, C.M., & Jacob, C. 2018. Natural Nanoparticles: A Particular Matter Inspired by Nature. *Antioxidants*, 7, (1) 3 available from: http://www.ncbi.nlm.nih.gov/pmc/articles/PMC5789313/

Haney, S.A., Bowman, D., & Chakravarty, A. 2015. *An Introduction to High Content Screening: Imaging Technology, Assay Development and Data Analysis in Biology and Drug Discovery* John Wiley & Sons.

Heynen-Genel, S., Pache, L., Chanda, S.K., & Rosen, J. 2012. Functional genomic and high-content screening for target discovery and deconvolution. *Expert Opinion on Drug Discovery*, 7, (10) 955-968 available from: https://doi.org/10.1517/17460441.2012.711311

Huber, R., Amann, N., & Wagenknecht, H.A. 2004. Synthesis of DNA with Phenanthridinium as an Artificial DNA Base. *The Journal of Organic Chemistry*, 69, (3) 744-751 available from: https://doi.org/10.1021/jo0355404

Ilag, L.L., Ng, J.H., Beste, G., & Henning, S.W. 2002. Emerging high-throughput drug target validation technologies. *Drug Discovery Today*, 7, (18) S136-S142 available from: http://www.sciencedirect.com/science/article/pii/S1359644602024297

Jan, E., Byrne, S.J., Cuddihy, M., Davies, A.M., Volkov, Y., GunGÇÖko, Y.K., & Kotov, N.A. 2008. High-Content Screening as a Universal Tool for Fingerprinting of Cytotoxicity of Nanoparticles. *ACS Nano*, 2, (5) 928-938 available from: https://doi.org/10.1021/nn7004393

Jorgensen, I., Rayamajhi, M., & Miao, E.A. 2017. Programmed cell death as a defence against infection. *Nature Reviews Immunology*, 17, 151 available from: http://dx.doi.org/10.1038/nri.2016.147

Kenneth, A.G., Robbin, L.D., Dunlay, R.T., Albert, G., Joanne, M., V, Joseph, Z., George, N.P., & Taylor, D.L. 1997. High-Content Screening: A New Approach to Easing Key Bottlenecks in the Drug Discovery Process. *Journal of Biomolecular Screening*, 2, (4) 249-259

available from: http://journals.sagepub.com/doi/abs/10.1177/108705719700200410 Accessed 20 March 2018.

Kepp, O., Galluzzi, L., Lipinski, M., Yuan, J., & Kroemer, G. 2011. Cell Death Assays for Drug Discovery. *Nature Reviews*, 10, 221-237

Khan, T. & Gurav, P. 2018. PhytoNanotechnology: Enhancing Delivery of Plant Based Anti-cancer Drugs. *Frontiers in Pharmacology*, 8, 1002 available from: https://www.frontiersin.org/article/10.3389/fphar.2017.01002

Kurita, K.L., Glassey, E., & Linington, R.G. 2015. Integration of high-content screening and untargeted metabolomics for comprehensive functional annotation of natural product libraries. *Proceedings of the National Academy of Sciences of the United States of America*, 112, (39) 11999-12004 available from: http://www.ncbi.nlm.nih.gov/pmc/articles/PMC4593099/

Kurita, K.L. & Linington, R.G. 2015. Connecting Phenotype and Chemotype: High-Content Discovery Strategies for Natural Products Research. *Journal of Natural Products*, 78, (3) 587-596 available from: https://doi.org/10.1021/acs.jnatprod.5b00017

Lockshin, R.A. & Beaulaton, J. 1974. Programmed cell death. *Life Sciences*, 15, (9) 1549-1565 available from: http://www.sciencedirect.com/science/article/pii/002432057490321X

Martin, H.L., Adams, M., Higgins, J., Bond, J., Morrison, E.E., Bell, S.M., Warriner, S., Nelson, A., & Tomlinson, D.C. 2014. High-Content, High-Throughput Screening for the Identification of Cytotoxic Compounds Based on Cell Morphology and Cell Proliferation Markers. *PLOS ONE*, 9, (2) e88338 available from: https://doi.org/10.1371/journal.pone.0088338

Martin, R.M., Leonhardt, H., & Cardoso, M.C. 2005. DNA labeling in living cells. *Cytometry Part A*, 67A, (1) 45-52 available from: https://doi.org/10.1002/cyto.a.20172 Accessed 28 June 2018.

Mills, C.C., Kolb, E.A., & Sampson, V.B. 2018. Development of Chemotherapy with Cell-Cycle Inhibitors for Adult and Pediatric Cancer Therapy. *Cancer Research*, 78, (2) 320 available from: http://cancerres.aacrjournals.org/content/78/2/320.abstract

Molecular Devices. MetaXpress Software Cell Cycle Application Module. https://www.moleculardevices.com/sites/default/files/en/assets/data-sheets/dd/img/metaxpress-software-cell-cycle-application-module.pdf . 2012. Sunnyvale, CA 94089 USA.
Ref Type: Online Source

Molecular Devices. ImageXpress Micro XLS Widefield High-Content Analysis System. https://www.moleculardevices.com/products/additional-products/imagexpress-micro-xls-widefield-high-content-analysis-system . 2018.
Ref Type: Online Source

Mosmann, T. 1983. Rapid colorimetric assay for cellular growth and survival: Application to proliferation and cytotoxicity assays. *Journal of Immunological Methods*, 65, 55-63 available from: http://www.sciencedirect.com/science/article/pii/0022175983903034

O'Brien, P., Irwin, W., Diaz, D., Howard-Cofield, E., Krejsa, C.M., Slaughter, M.R., Gao, B., Kaludercic, N., Angeline, A., Bernardi, P., Brain, P., & Hougham, C. 2006. *High concordance of drug-induced human hepatotoxicity with in vitro cytotoxicity measured in a novel cell-based model using high content screening*, 80 ed.

Ouyang, L., Shi, Z., Zhao, S., Wang, F. T., Zhou, T. T., Liu, B., & Bao, J. K. 2012. Programmed cell death pathways in cancer: a review of apoptosis, autophagy and programmed necrosis. *Cell Proliferation*, 45, (6) 487-498 available from: https://doi.org/10.1111/j.1365-2184.2012.00845.x Accessed 29 June 2018.

Sawai, H. & Domae, N. 2011. Discrimination between primary necrosis and apoptosis by necrostatin-1 in Annexin V-positive/propidium iodide-negative cells. *Biochemical and Biophysical Research Communications*, 411, (3) 569-573 available from: http://www.sciencedirect.com/science/article/pii/S0006291X11011995

Segawa, K. & Nagata, S. 2015. An Apoptotic "Eat Me" Signal: Phosphatidylserine Exposure. *Trends in Cell Biology*, 25, (11) 639-650 available from: http://www.sciencedirect.com/science/article/pii/S0962892415001531

Shapiro, H.M. & Telford, W.G. 2018. Lasers for Flow Cytometry: Current and Future Trends. *Current Protocols in Cytometry*, 83, (1) 1 available from: https://doi.org/10.1002/cpcy.30 Accessed 25 June 2018.

Sirenko, O., Hesley, J., Rusyn, I., & Cromwell, E.F. 2014. High-Content Assays for Hepatotoxicity Using Induced Pluripotent Stem Cell-Derived Cells. *ASSAY and Drug Development Technologies*, 12, (1) 43-54 available from: http://www.ncbi.nlm.nih.gov/pmc/articles/PMC3934660/

Sun, Y. & Peng, Z.L. 2009. Programmed cell death and cancer. *Postgraduate Medical Journal*, 85, (1001) 134 available from: http://pmj.bmj.com/content/85/1001/134.abstract

Taylor, D. L. 2007, "Introduction to High Content Screening," *In High Content Screening*, D. L. Taylor, R. J. Haskins, & A. K. iuliano, eds., Totowa, New Jersey: Humana Press, pp. 3-18.

Thomsen, S.K. & Gloyn, A.L. 2017. Human genetics as a model for target validation: finding new therapies for diabetes. *Diabetologia*, 60, (6) 960-970 available from: http://www.ncbi.nlm.nih.gov/pmc/articles/PMC5423999/

Tirino, V., Desiderio, V., Paino, F., & Papaccio, G. 2016, "Cytometry and Pathology," *In Advanced Imaging Techniques in Clinical Pathology*, F. Sacerdoti, A. Giordano, & C. Cavaliere, eds., New York: Humana Press, pp. 65-84.

Zock, J.M. 2009. Applications of High Content Screening in Life Science Research. *Combinatorial Chemistry & High Throughput Screening*, 12, (9) 870-876 available from: http://www.ncbi.nlm.nih.gov/pmc/articles/PMC2841426/

Chapter 5

In vitro Mechanism of Cell Death Induced by 6″-*O*-α-apio-D-furanosylisovitexin (Altissimin) in HeLa Cells

5.1 Introduction

Flavonoids are benzo-γ-pyrone (chromone) derived pigments which are ubiquitous in plants as the largest class of polyphenols. All flavonoids are diphenylpropanes with a C_6-C_3-C_6 carbon framework characterised by the presence of two aromatic rings A and B linked together by three carbon atoms usually presenting as a heterocyclic ring C (Figure 5.1) (Rice-Evans et al. 1996). Based on the position of aromatic ring attachment to the chromone moiety, flavonoids can be broadly classified into flavonoids (2-phenylbenzopyrans) (**5.1**), isoflavonoids (3-benzopyrans) (**5.2**) and neoflavonoids (4-benzopyrans) (**5.3**) (Figure 5.2) (Marais et al. 2006). A fourth class referred to as minor flavonoids consisting of chalcones (**5.4**) and aurones (**5.5**) is often included. Flavonoids can be further categorised into six main subclasses; flavones, flavonols, flavonones, flavanols, anthocyanidins and isoflavones (Ross and Kasum 2002).

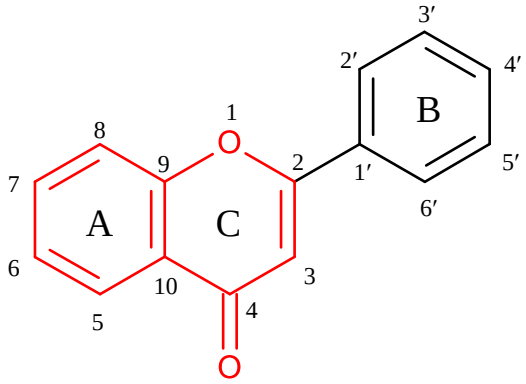

Figure 5.1 Flavonoid scaffold showing aromatic rings A and B, and heterocyclic ring C
The chromone moiety is highlighted in red

In 1979, Dr. Stephen DeFelice coined the term “nutraceuticals” to entail foods or dietary components which possess medicinal and general health benefits through their disease prophylactic and curative effects (DeFelice 1992). Flavonoids are biologically active compounds with various proven nutraceutical benefits (Kaleem and Ahmad 2018). Some of

the nutraceutical benefits associated with the daily intake of flavonoids include antioxidant, antibacterial, antifungal, anti-ulcer, hepatoprotective, cardioprotective, anti-diabetic, anti-inflammatory, and anticancer effects (Tapas et al. 2008). With the isoflavones genistein (**5.6**), daidzein (**5.7**) and equol (**5.8**) (Figure 5.3) being the most extensively studied flavonoids, some safety concerns have been raised concerning the potential risk of uterine hypertrophy, reproductive tract malformations, infertility and estrogen-sensitive cancers due to decreased expression of an estrogen-responsive gene following the consumption of isoflavones in soy products (Harlid et al. 2017). However, the frequently consumed nutraceutical flavonoids (anthocyanins, flavonols, catechins and quercetin) are generally considered to be safe and without adverse effects (Ronis et al. 2018).

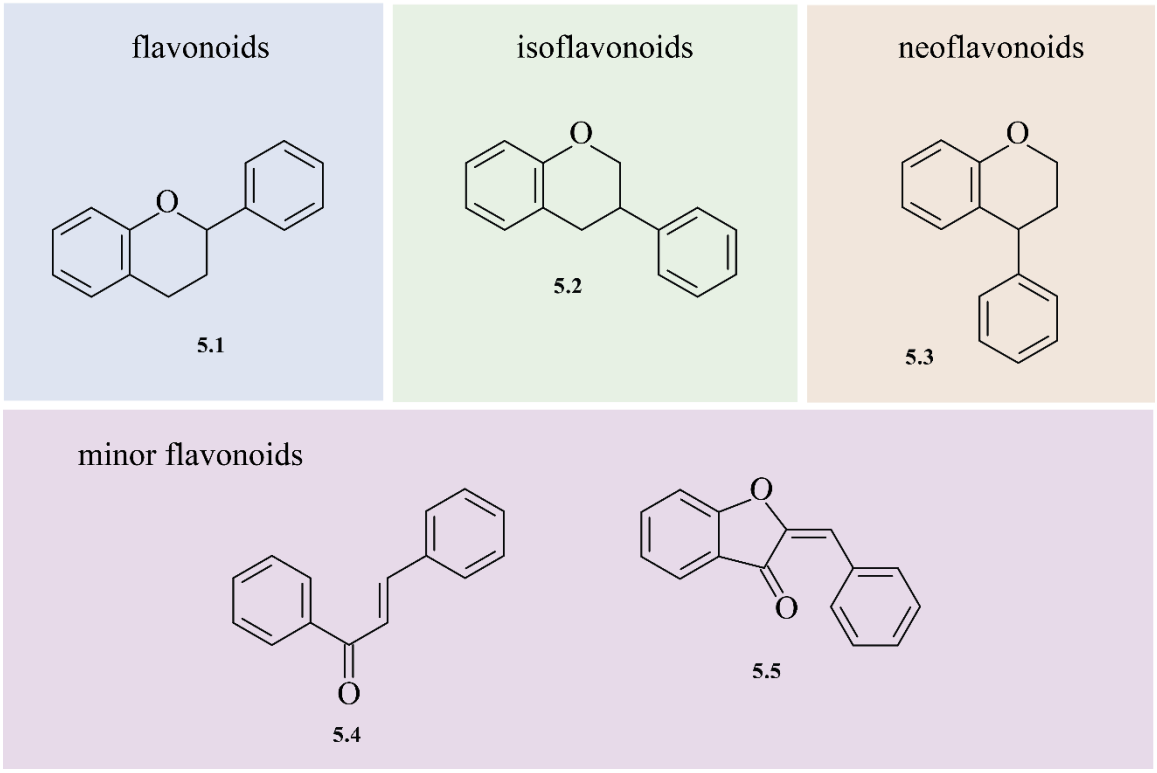

Figure 5.2 Major structural classes for flavonoid compounds (Marais et al. 2006).

There are currently over 5,000 naturally occurring flavonoids which are abundantly sourced from almost all parts of plants (Oyama et al. 2011). The flavonols quercetin (**5.9**), kaempferol (**5.10**) and myricetin (**5.11**) and the flavones apigenin (**5.12**), luteolin (**5.13**) and naringenin (**5.14**) (Figure 5.3) are among the most abundant flavonoids in foods. Some of the food sources for these flavonoids include black rice, vegetables, fruits, berries and red wine for anthocyanins

(Ahmad et al. 2015), parsley, thyme celery and sweet red pepper for flavones, soy beans and legumes for isoflavones (Crozier et al. 2009), onions, broccoli, berries and tea for flavonols and citrus fruits for flavanones (Jung et al. 2006).

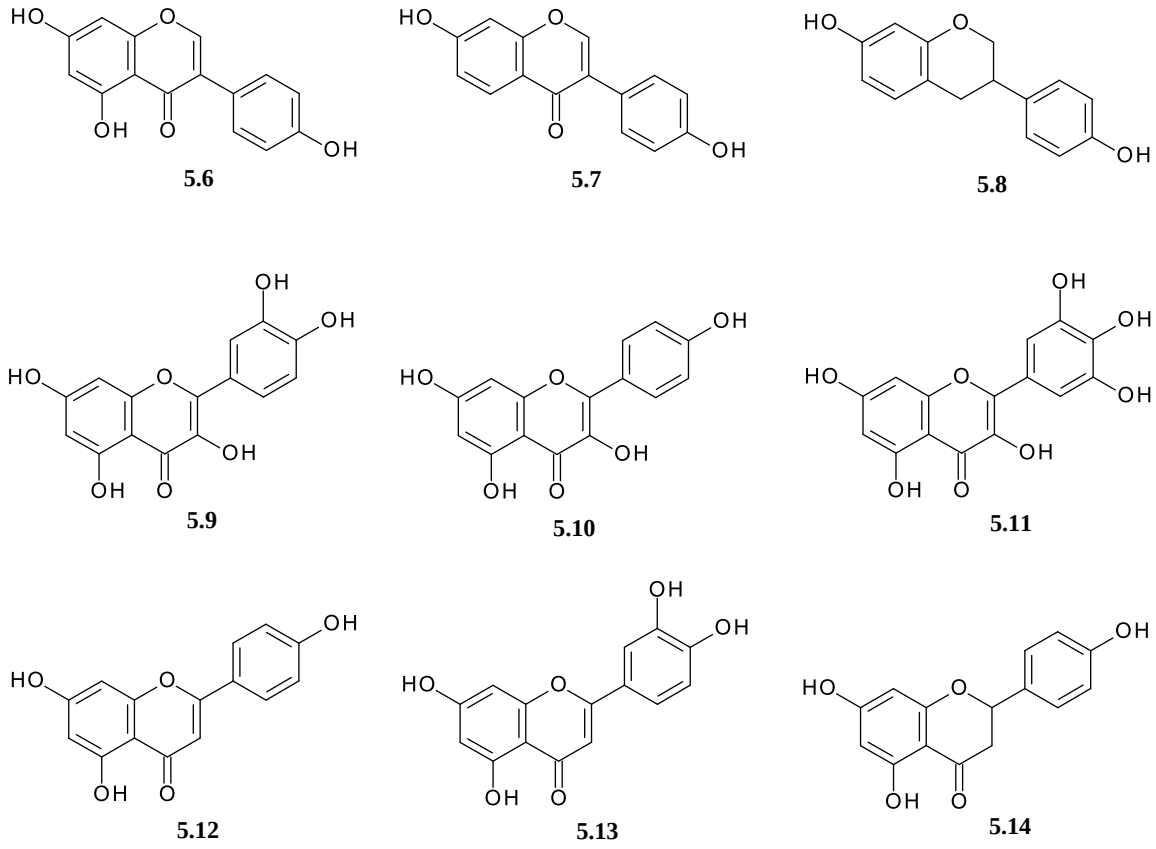

Figure 5.3 Structures for selected natural flavonoids

The daily intake of natural flavonoids has been met with controversy due to some conflicting *in vitro* and *in vivo* scientific reports leading researchers to question whether these compounds have practical human health benefits (Lambert et al. 2007). Others have suggested that daily flavonoid intake is in fact a health risk as it may cause or potentiate various disease states such as hepatotoxicity (chalcones), blood dyscrasias (catechin), allergic dermatitis (catechols), infertility and carcinogenesis (isoflavones) (Galati 2004), or lead to significant drug interactions (Morris and Zhang 2006). It is worth noting that most studies on the total intake of flavonoids have been done in Europe such as the European Prospective Investigation into Cancer and Nutrition (EPIC). A survey discovered that in these European countries (most especially Mediterranean countries, Belgium and Germany) daily flavonoid intake is too low to elicit any therapeutic or adverse effects (Vogiatzoglou et al. 2015). This is despite the fact

that Mediterranean diets are high on flavonoid containing foods such as fruits, vegetables and red wine. This may be explained in that ingested flavonoids as well as their esters, glycosides and polymers are not readily absorbed in their native forms (Manach et al. 2004), thereby significantly reducing bio-availability to sub-therapeutic levels (less than 1% for tea catechins and 20% for quercetin and isoflavones) (Hollman et al. 1995; Lee et al. 1995). It has also been observed that flavonoid concentrations used during *in vitro* and *in vivo* studies are often much higher than the daily human intake (Yang et al. 2001). Additionally, some studies suggest that flavonoids are more effective in *in vitro* than *in vivo* studies due to poor water solubility in the latter (Tan et al. 2012). Certain *in vitro* studies have evaluated entire crude extracts in which flavonoids are deemed to be present without considering single compound isolation. These types of assays provide no further information as to which flavonoids are active or whether other non-flavonoid constituents also contribute to the treatment outcomes. This is important because flavonoids act specifically in that certain flavonoids can significantly reduce the risk of developing a particular disease state in which other flavonoids are without effect. This is evident from the fact that daily intake of apigenin is associated with a reduced risk of ovarian cancer whereas total flavonoid intake is of no effect (Romagnolo and Selmin 2012).

5.2 Anticancer activity of flavonoids

A majority of *in vitro* and *in vivo* studies have shown flavonoids to possess significant anticancer activity through various mechanisms such as steroid hormone modulation, anti-proliferative, chemo-preventive, anti-inflammatory and anti-oxidant effects (Yao et al. 2004). Recently, flavonoids (mostly epigallocatechin gallate) were found to inhibit hepatocellular carcinoma in a murine model through the inhibition of tumour growth, anti-angiogenesis and anti-metastasis (García et al. 2018). In separate meta-analysis studies, the dietary intake of total flavonoids, anthocyanidins, flavones and flavanones reduced the risk of oesophageal cancer (Cui et al. 2016), flavonols and isoflavones reduced the risk of ovarian cancer (Hua et al. 2016), and flavones and flavonols reduced the risk of breast cancer (Hui et al. 2013). Heterogeneous variations in the therapeutic response to flavonoid intake have been noticed, most likely due to agricultural, socio-demographic and lifestyle differences (Romagnolo and Selmin 2012). For instance, dietary flavonoid intake has been found to reduce the risk of gastric cancers in European but not in American and Asian populations (Bo et al. 2016).

5.2.1 Anticancer structure-activity relationship (SAR) studies of flavonoids

In medicinal chemistry, the benzo-γ-pyrone (chromone) moiety found in flavonoid compounds is considered as an important scaffold for developing bioactive compounds of various pharmacological effects (Gaspar et al. 2014). The anticancer activity of flavonoid compounds is influenced by various structural factors such as the number and position of hydroxylation, the presence of the C-4 carbonyl functionality, methoxylation, prenylation, bond unsaturation and glycosylation.

5.2.1.1 Anti-oxidant activity

Due to the important role of free radical-mediated oxidative stress in the development and progression of various cancers through the activation of transcription factors (such as NF-κB, β-catenin/Wnt and p53) and the initiation of inflammatory cascades, compounds possessing anti-oxidant/ free radical scavenging and anti-inflammatory effects have potential anticancer benefits (Reuter et al. 2010). Flavonoids are known to possess strong anti-oxidant properties through the inhibition of free radical generating enzymes, metal ion chelation, radical scavenging, activation of intrinsic anti-oxidant mechanisms, increased elimination of oxidising species and induction of anti-oxidant enzymes (Halliwell 1997; Pietta 2000). In mono-substituted flavonoid B-rings, the presence of a –OH *para*-substituent is vital for anti-oxidant activity, with minimal to no effect observed in *ortho* or *meta* hydroxylation (Scotti et al. 2012). After fast reaction kinetics studies using 2,2′-Azinobis-(3-ethylbenzthiazoline-6-sulfonic acid) (ABTS) radical cation, flavonoids with two or more B-ring –OH substituents such as **5.9**, **5.11** and **5.13** were found to have better anti-oxidant activity than those with one –OH substituent due to an electron donating mechanism leading to the formation of a semi-quinone specie and a subsequent quinine (Scheme 5.1). The anti-oxidant mechanism for flavonoids with C-4′ mono-hydroxylated B-rings (having no potential conjugation with the C-ring due to the absence of a –OH group at C-3) such as apigenin, **5.12**, and naringenin, **5.14**) involve the formation of a phenoxyl radical which can further oxidise glutathione (GSH) to its radical, GS$^{\bullet}$ (Scheme 5.2). Flavonoids with methoxyl-hindered B-rings have strong electron-donating properties through an increased reaction rate and more stable phenoxyl radical formation (Scheme 5.3) (Sekher Pannala et al. 2001).

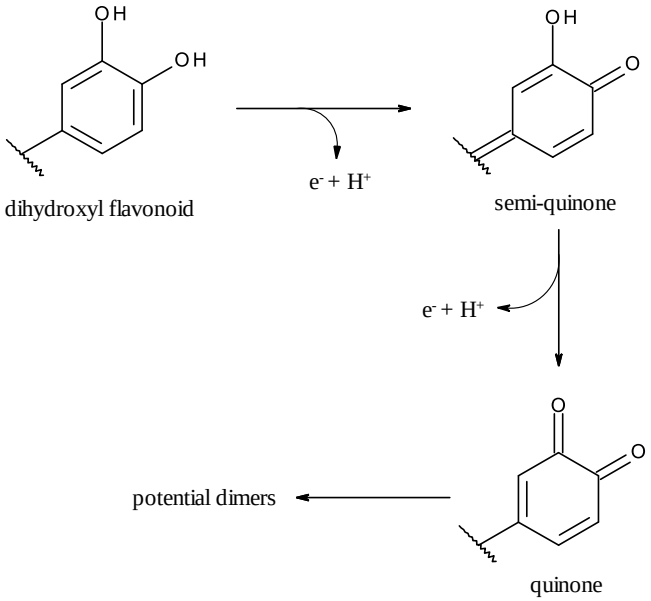

Scheme 5.1 Anti-oxidant mechanism for flavonoids with a dihydroxylated B-ring against ABTS radical cation (Sekher Pannala et al. 2001).

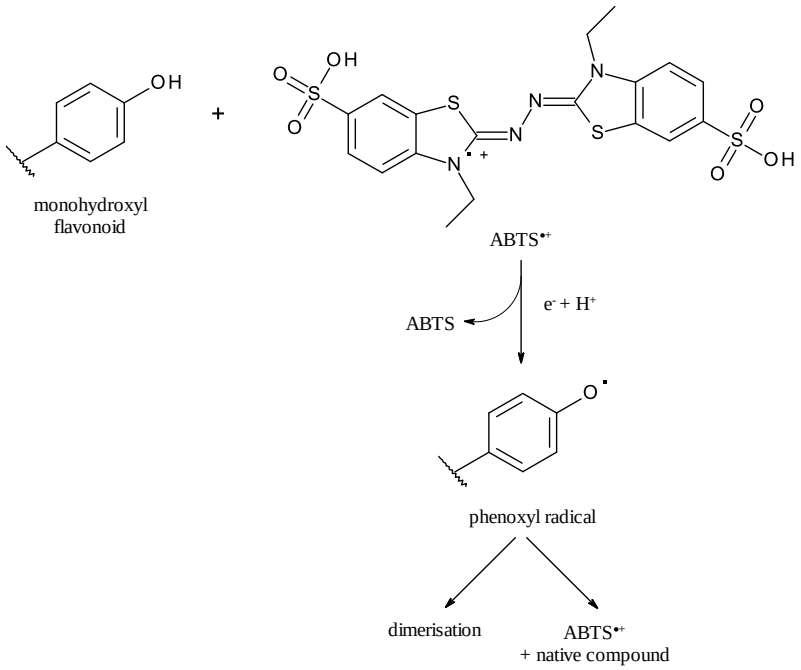

Scheme 5.2 Anti-oxidant mechanism for flavonoids with a monohydroxylated B-ring against ABTS radical cation (Sekher Pannala et al. 2001).

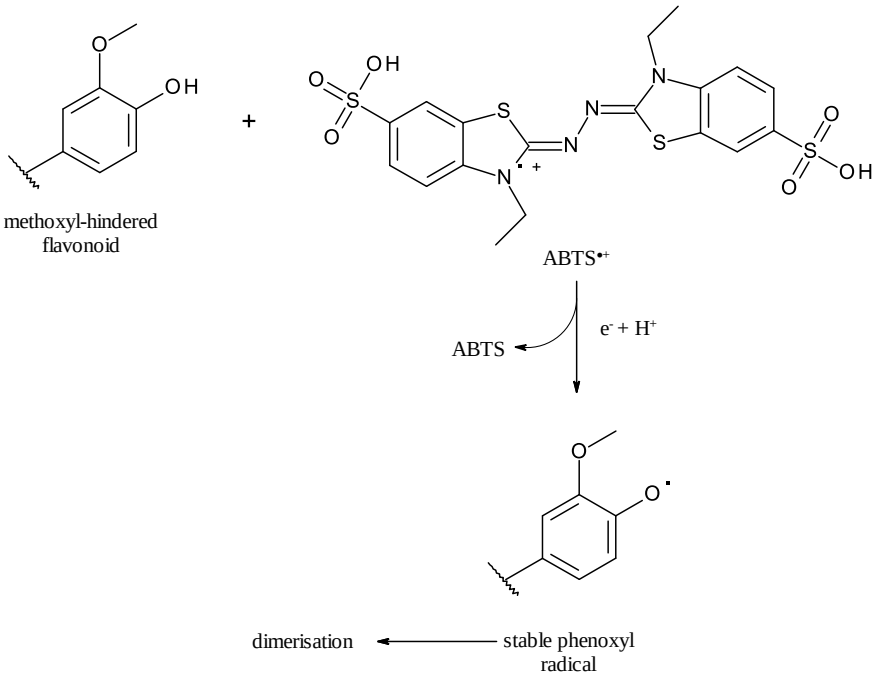

Scheme 5.3 Anti-oxidant mechanism for flavonoids with a methoxyl-hindered B-ring against ABTS radical cation (Sekher Pannala et al. 2001).

The double bond at C2-C3 coupled with the carbonyl functionality at C-4 are also essential for anti-oxidant activity. Hydroxylation at position C-3 (as seen in flavonols) is cardinal while that at positions C-5 and C-7 is of no anti-oxidant benefit (Scotti et al. 2012).

5.2.1.2 Antimutagenic activity

The ability of flavonoids to inhibit carcinogenesis has been previously evaluated through their effects on various environmental pollutants such as nitroarenes and dioxins (Melo et al. 2010). Dioxins transform and translocate arylhydrocarbon receptors (AhR) into the nucleus to facilitate interactions with dioxin-responsible element (DRE), which increases the expression of enzymes that promote carcinogenesis and cancer progression (Ashida 2000). Flavonoids have been found to inhibit dioxin-induced AhR translocation with flavones and flavonols being the most potent followed by flavonones and lastly catechins. Increased hydrophobicity, the presence of a carbonyl functionality at position C-4 and B-ring attachment to position C-2 (flavonones were found to be ineffective) are cardinal for AhR inhibition while glycosylation reduces activity (López-Lázaro 2002). For flavonoid inhibition of nitroarene-induced carcinogenesis, increased polarity and the C-4 carbonyl functionality are essential for activity while the C2-C3 double bond, C-3 B-ring position and C-ring opening are not. Glycosylation

and methylation of phenolic –OH groups were found to significantly reduce this activity (Edenharder and Tang 1997).

5.2.1.3 Inhibition of oncogenic viruses

Oncogenic viruses are known to cause about 15 – 20 % of all human cancers (Luo and Ou 2015), with the common ones including Kaposi's sarcoma (Kaposi's sarcoma herpesvirus - KSHV), Burkitt´s lymphoma (Epstein-Barr virus - EBV), cervical cancer (Human papillomavirus - HPV), hepatic cancers (Hepatitis B - HBV) and adult T-cell leukaemia (Human T-cell lymphotropic virus-1 - HTLV-1) (Chen et al. 2014). Despite the fact that oncogenic viruses are unable to cause cancer by themselves, their ability to infect, but not kill, their host cells results in the establishment of immune response-evading chronic inflammatory disease states which promote DNA damage and cellular mutations (McLaughlin-Drubin and Munger 2008). Several flavonoids and flavonoid derivatives such as the pentaallyl ethers **5.15** and **5.16** (Figure 5.4) have been reported to inhibit the activities of oncogenic viruses (Iwase et al. 2001). For instance, apigenin (**5.12**) was found to inhibit initiation of the EBV lytic cycle by suppressing the immediate-early (IE) gene Zta and Rta promoters (Wu et al. 2017). From SAR studies, the oncogenic virus inhibitory activity of flavones, flavonones and isoflavones against EBV is increased by the presence and number of prenylations, C-3 methoxylation (flavones), 3′,4′ -dihydroxylation (isoflavones) and the presence of allyl groups (Ito et al. 2000; Itoigawa et al. 2002).

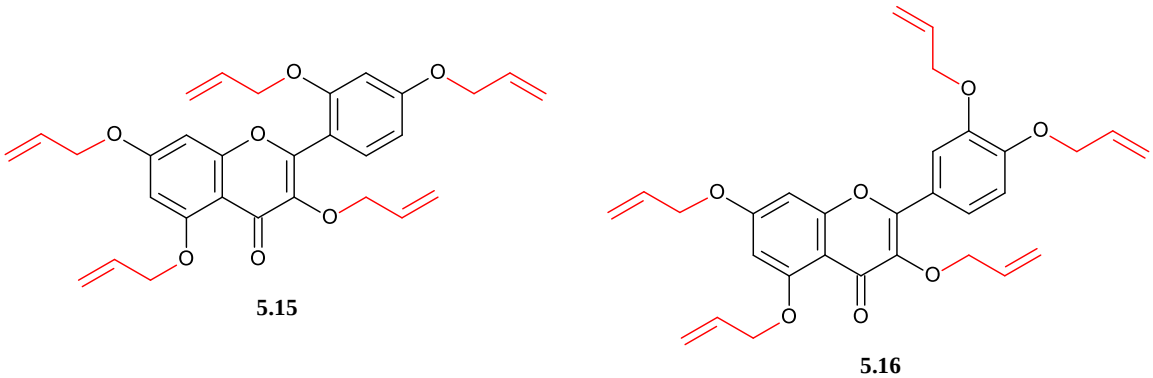

5.15 **5.16**

Figure 5.4 Structures for selected flavonoids with pentaallyl ether substituents
The pentaallyl ether substituents are highlighted in red

5.2.1.4 Anti-proliferative activity

In a study done by Plochmann et al., the cytotoxicity structure-activity relationships of several flavonoids was evaluated (Plochmann et al. 2007). From the obtained results, flavonoids possessing a C2-C3 double bond such as quercetin (**5.9**), apigenin (**5.12**) and luteolin (**5.13**) had increased cytotoxicity (3- to 10-fold) than their molecular counterparts with a single C2-C3 bond (taxifolin, naringenin, eriodictyol), signifying the importance of the double bond for cytotoxic activity. Similarly, the presence of a C-4 carbonyl functionality increased flavonoid cytotoxicity. Taxifolin, a C-4 carbonyl functionalised flavonoid had a 30-fold increased cytotoxicity compared to catechin which has no carbonyl substituent. The presence of a –OH substituent at position C-3 such as in kaempferol, quercetin and taxifolin was associated with a 2- to 10-fold decrease in cytotoxicity. Compared to *meta*, *ortho* –OH substitution of the B-ring resulted in a 3-fold increase in cytotoxicity. Increasing the number of methoxy substituents on flavonoid rings resulted in increased cytotoxicity. This was evident from the fact that 7-methoxy-baicalein (**5.17**) (Figure 5.5) was more cytotoxic than baicalein, cirsimaritin (**5.18**) was more cytotoxic than hispidulin (**5.19**), and hispidulin (**5.19**) was more cytotoxic than scutellarein.

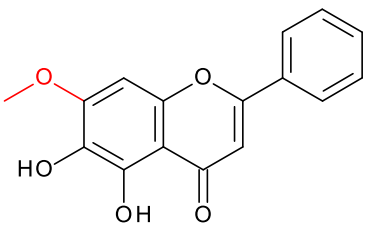

5.17

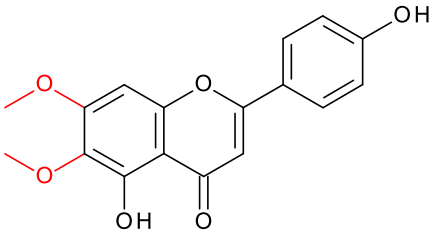

5.18

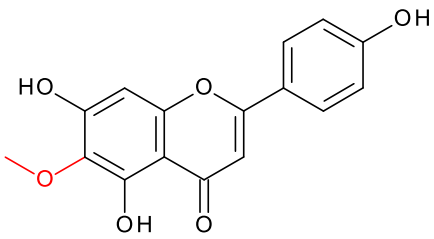

5.19

Figure 5.5 Chemical structures for selected methoxylated flavonoids

The methoxy substituents are highlighted in red

Glucuronidation was also found to increase the cytotoxicity of flavonoids. However, an increase in the number of –OH substituents inversely correlated with cytotoxicity. This was evident from the fact that flavonoids with two -OH substituents showed greater activity than their molecular counterparts with three -OH substituents. The presence of a B-ring was also established as a cardinal feature for flavonoid cytotoxicity.

Prenylation of natural products involves the structural addition of C5 isoprene (dimethylallyl) unit(s) to metabolites through the action of prenyl transferase (Mukai 2018). Naturally occurring prenylated flavonoids mostly have *C*-prenyl groups with a few reported *O*-prenylations. Prenylation has been observed on various positions of the three flavonoid rings with C-8 being the most reported position. The anti-proliferative activity of several flavonoids can be increased through the addition of prenyl substituents. For instance, the prenylation of quercetin at position C-8 (**5.20**) resulted in an increased inhibition of SEK1-JNK1/2 and MEK1/2-ERK1/2 phosphorylation and a stronger inhibition of SEK1 and MEK1 kinases (Hisanaga et al. 2016). Similarly, C-8 prenylation of apigenin and liquritigenin to form licoflavone C (**5.21**) and isobavachin (**5.22**) respectively (Figure 5.6), resulted in an increased cytotoxic activity against MCF7/BOS breast cancer cells (Wang et al. 2006). In H4IIE hepatoma cells, the anti-proliferative activity of **5.21** and **5.22** is mediated via a caspase 3/8 dependent induction of apoptosis (Wätjen et al. 2007). The C-6 prenylated flavonoids, **5.23** and **5.24**, were reported to have anti-proliferative activity against A-549 adenocarcinoma cells with IC_{50} values of 48.6 and 20.2 μg/mL respectively (Yang et al. 2015).

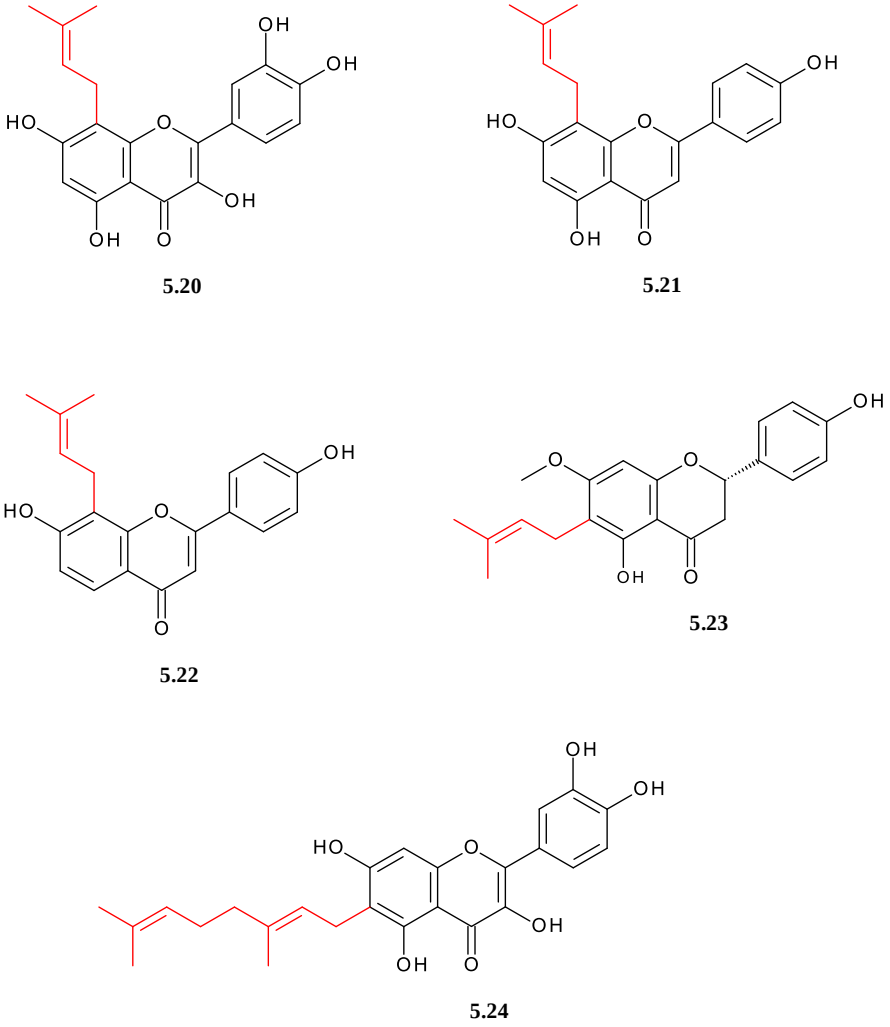

Figure 5.6 Chemical structures for selected C-6 and C-8 prenylated flavonoids

The prenyl substituents are highlighted in red

From an *in vivo* perspective, increasing the number of prenylations enhances the biological activity of flavonoids through a reduction in the rate of excretion by glucuronidation which consequently leads to flavonoid bio-accumulation and increased bio-availability (van de Schans et al. 2015).

5.2.2 Apigenin as a potential scaffold for cancer modulation

The anticancer activity of natural flavonoids has been extensively reported. Among the common flavonoids, apigenin (**5.12**) has been labelled as one of the most promising food-based chemo-preventive agents (Shukla and Gupta 2010). The *in vitro* anti-proliferative activity of apigenin (**5.12**) against various cancer cell lines is well documented and can be broadly

attributed to its ability to induce apoptosis and autophagy as well as its inhibition of carcinogenesis (Table 5.1).

5.2.2.1 Mechanisms for the anti-cancer activity of apigenin

Tumor necrosis factor (TNF)-related apoptosis-inducing ligand (TRAIL), a member of the cytokine superfamily, induces caspace-8 mediated selective apoptosis in various cancer cell lines by binding to death receptors TRAIL-RI (DR4) and TRAIL-RII (DR5). However, TRAIL-based therapies have failed over the past decades due to intrinsic and developed TRAIL-resistance among various cancer cells, poor agonistic activity of existing TRAIL formulations and toxicity concerns (de Miguel et al. 2016). Through p53-independent regulation, apigenin (**5.12**) induced selective DR5 expression in TRAIL-resistant T cell leukemic Jurkat cells *via* proteasome inhibition and thereby restored TRAIL sensitivity (Horinaka et al. 2006). Recently, apigenin-induced TRAIL sensitization in HepG2 and Hep3B human liver carcinoma cells was reported (Kang et al. 2018). The synergism and selectivity of apigenin-TRAIL combinations can therefore be used to develop more potent TRAIL formulations with better safety profiles.

The classical E- and N-cadherins are cell adhesion molecules which play major roles in normal tissue formation. Of particular interest is E-cadherin, an important molecule in the formation of epithelial cells and maintenance of cell-cell adhesions. The control of normal cellular adhesion and motility plays a central role in the prevention of carcinogenesis and tumour invasion (Pecina-Slaus 2003). Therefore, the suppression of E-cadherin expression is a key feature of tumour development and progression. Apigenin (**5.12**) has been reported to increase E-cadherin expression in a prostate cancer model called transgenic adenocarcinoma of the mouse prostate (TRAMP) and in DU145 human prostate cancer cells via the blockade of β-catenin signalling (Hurwitz et al. 2001; Shukla et al. 2007a). This mechanism of apigenin (**5.12**) can be applied to various malignancies such as breast cancer in which cancerous cells avoid the destructive effects of multipolar divisions through centrosome amplification, clustering and loss of E-cadherin (Rhys et al. 2018).

Among several other functions, the enzymes phosphoinositide-3-kinase (PI3K) and protein kinase B (PKB, also known as Akt) play cardinal roles in cell proliferation, motility and survival (Hemmings and Restuccia 2012). The activation of PI3K/PKB leads to an array of

intracellular events which ultimately promote oncogenesis and inhibit apoptotic cell death (Duronio 2008). It is well established that several components involved in the PI3K/PKB activation pathway are genetically altered in many cancers leading to anti-apoptotic events (Amancio 2010; Tang et al. 2018). The PI3K/PKB activation pathway is thus an important therapeutic target for the development of cancer modulating agents. The development of PI3K/PKB inhibitors such as the quercetin derived synthetic compound LY294002 (**5.25**) and the steroidal fungal metabolite wortmannin (**5.26**) (Figure 5.7) for the treatment of cancers has faced safety challenges including cytotoxicity towards normal cells (Polak and Buitenhuis 2012). LY294002 (**5.25**) was also reported to abnormally enhance PKB phosphorylation in gemcitabine (GEM)-resistant pancreatic cancer cells (Wang et al. 2017). In an *in vitro* study, apigenin (**5.12**) was found to induce G_2/M cell cycle arrest and caspase-dependent inhibition of the PI3K/PKB pathway in myeloid human leukemic HL60 cells with an IC_{50} of 40 µM (Ruela-de-Sousa et al. 2010). Apigenin-based compounds can thus be considered as potential candidates for safer PI3K/PKB inhibitors.

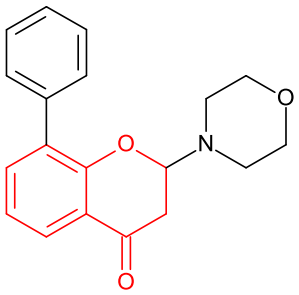

5.25

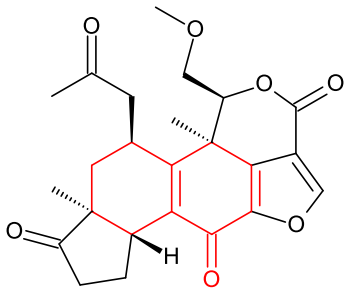

5.26

Figure 5.7 Structures for PI3K/PKB inhibitors, LY294002 (**5.15**) and wortmannin (**5.16**)
The chromone-like moiety is highlighted in red

The ubiquitin/proteasome system is a pathway that handles the degradation of eukaryotic cellular proteins through ubiquitin multimeric 'tagging' that precedes enzymatic proteolysis by the 26S proteasome (Nandi et al. 2006). The 26S proteasome is a large intracellular adenosine 5′-triphosphate–dependent protease that identifies and degrades ubiquitin-tagged proteins (Rajkumar et al. 2005). The proper degradation of eukaryotic cellular proteins by the ubiquitin/proteasome pathway is vital for maintaining a normal cell cycle such that its inhibition results in cell cycle arrest and apoptotic cell death. The deregulation of this

proteasome system causes increased proteolysis of tumour suppressors and oncoproteins with consequent uncontrolled cell proliferation, malignancies and cancer metastasis as is evident in lung, colorectal and breast carcinomas, gliomas and lymphomas (Naujokat and Hoffmann 2002). The first 26S proteasome inhibitor to be approved for the treatment of malignancies was the synthetic compound, bortezomib (**5.27**) (Figure 5.8). However, the use of bortezomib (**5.27**) is limited by its deleterious side effects, intrinsic and acquired drug resistance, significant drug interactions with certain natural products and poor efficacy in solid tumours (Chen et al. 2011). This has warranted an ongoing search for more efficacious and less toxic 26S proteasome inhibitors, possibly from natural sources. Apigenin (**5.12**) was reported to be a potent inhibitor of 26S proteasome after it inhibited the proteasome's chymotrypsin-like, trypsin-like and caspase-like actions at IC_{50} values of 11.5, 20 and 1.5 μM respectively (Li et al. 2016). Other natural proteasome inhibitors include lactacystin (**5.28**), clastol lactacystin β-lactone (**5.29**), (–)-epigallocatechin-3-gallate (EGCG) (**5.30**), genistein (**5.31**) and curcumin (**5.32**) (Figure 5.8) (Yang et al. 2008).

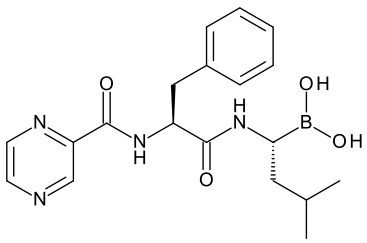

5.27

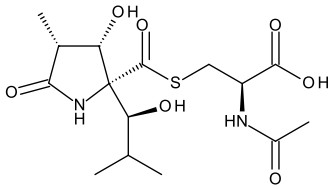

5.28

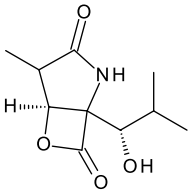

5.29

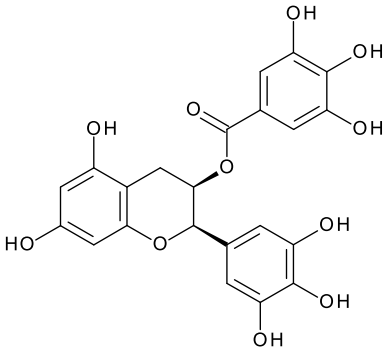

5.30

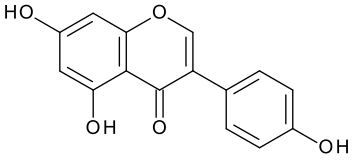

5.31

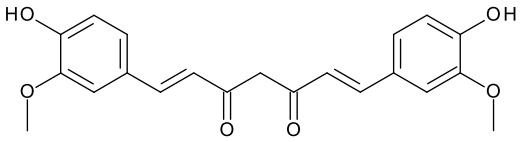

5.32

Figure 5.8 Structures for selected synthetic and natural 26S proteasome inhibitors

Poly (ADP-ribose) polymerase (PARP) is a family of proteins responsible for the routine repair of DNA single strand breaks and base excision repair (BER) through the addition of poly (ADP ribose) polymers and alteration of nuclear proteins (Chaitanya et al. 2010). During attempted DNA repair, activation of PARP leads to the depletion of cellular nicotinamide adenine dinucleotide (NAD) and adenosine triphosphate (ATP) which results in lysis and necrotic cell death (Boulares et al. 1999). The inhibition of PARP through caspase- or cathepsin-mediated enzymatic cleavage results in reduced DNA repair, enhanced cytotoxicity of DNA damaging compounds, telomere shortening and increased apoptosis (Mohan 2009b). The cleavage of PARP by the caspace-3 enzyme is considered as an early apoptotic event. Apigenin (**5.12**) has been reported to induce apoptosis in bladder cancer (RT112) and human chronic myelogenous leukemia (K562) cells through a dose dependent PARP cleavage (Kilani-Jaziri et al. 2012).

Several other natural flavonoids such as quercetin, isoquercetin, naringin, naringenin, hesperetin, hesperidin and rutin, have also been reported to have PARP inhibitory activity (Su et al. 2017).

Oxygen is a fundamental need for all human cells in order for them to grow and perform their normal physiological functions (Costache et al. 2015). Vasculogenesis, which is the *de novo* differentiation of endothelial cell precursors to form vascular systems, is cardinal for tissue perfusion. Maintenance of vasculogenesis is done through the synthesis of vascular systems from pre-existing blood vessels in what is referred to as angiogenesis (Carmeliet and Jain 2000). The process of angiogenesis requires the action of autocrine and paracrine angiogenic growth factors such as vascular endothelial growth factor (VEGF), fibroblast growth factors, tumour necrosis factor-α (TNF-α) and angiogenin (Mohan 2009a). In the absence of sufficient vascular perfusion, the growth of solid tumours is restricted to a size of about 1 – 2 mm owing to the deficiency in oxygen and nutrient supply. Angiogenesis in tumours is dependent on tumour angiogenic factors (TAF) of which VEGF is the most potent (Ferrara and Henzel 1989). Chemical entities which inhibit the VEGF pathway are potential therapeutic agents in the treatment of solid tumours (Adela 2006). A monoclonal antibody called bevacizumab (Avastin®) was the first molecular antibody to be approved by the FDA as a VEGF inhibitor for the treatment of solid tumours in combination with other chemotherapeutics (Ferrara et al. 2005). The fact that bevacizumab is too expensive for cancer patients in low- and medium-income countries (about $21.083 per month of added life and $24,597 per quality-adjusted life month, QALM) has created a desperate need for cheaper alternatives in the treatment of solid tumours (Minion et al. 2015; Gyawali and Iddawela 2017). Apigenin (**5.12**) was among several other flavonoids reported to significantly inhibit VEGF protein secretion in human ovarian cancer cells (OVCAR-3) (IC_{50} = 50 μM) after a 48 hr treatment (Luo et al. 2008). Thus, apigenin-based compounds can have great potential as adjunct therapeutics in the treatment of solid tumours.

The Wnt/wg signal transduction pathways encompass mechanisms that control embryogenic processes such as axis patterning, cell growth, fate and migration, and maintain tissue homeostasis (Logan and Nusse 2004). Wnt/wg signaling causes an increase in the levels of β-catenin which results in the activation of specific target genes during embryogenesis (Morin 1999). Genetic mutations that constitutively activate the Wnt/wg pathways are known to cause

malignancies including colorectal cancers, hair follicle tumours, melanomas, medulloblastomas, hepatocellular carcinomas and leukemia (Clevers 2006). Mutation and consequent deregulation of β-catenin, adenomatous polyposis coli (APC) and scaffold protein Axin signaling play significant roles in the development of these malignancies (Takayama et al. 1996; Hwang et al. 2016). Treatment of DU145 human prostate cancer cells with apigenin (**5.12**) resulted in the inhibition of β-catenin nuclear translocation as well as a decrease in c-Myc and cyclin D1 (Shukla et al. 2007b; Shukla and Gupta 2007).

Epithelial-mesenchymal transition (EMT) is a normal biological process in which polarized epithelial cells are converted to mesenchymal cells through several biochemical alterations which enable them to have, among other properties, increased levels of migration, invasion and resistance to programmed cell death (Kalluri and Weinberg 2009). Transcriptional repressors known as Snail and Slug (or zinc finger proteins SNAI2 and SNAI1 respectively) are responsible for regulating several biological processes including organogenesis, wound healing and the EMT of cancerous cells (Ganesan et al. 2016). Snail and slug mediated EMT increases the metastasis of cancerous cells (Dhasarathy et al. 2011). In a recent study, apigenin (**5.12**) was found to inhibit the snail (not slug) pathway, modulate the levels of EMT markers and reduce invasion and migration in Bel-7402 and PLC/PRF/5 hepatocellular carcinoma cells (Qin et al. 2016).

Apigenin (**5.12**) has also been reported to inhibit pyruvate kinase muscle isozyme M2 (PKM2), an enzyme responsible for catalysing the last step of glycolysis (Xie et al. 2016), in colorectal cancer cell lines HCT116, HT29 and DLD1 (Shan et al. 2017). PKM2 is an important therapeutic target because it is usually deregulated in malignancies through overexpression to meet the high nutrient demand from proliferating cancerous cells (Dong et al. 2016). Other reported anticancer mechanisms of action for apigenin (**5.12**) include mitochondrial redox impairment with inhibition of cancer cell migration and invasion (Erdogan et al. 2016; Souza et al. 2017) and p53 mediated cell cycle arrest and apoptosis (Zheng et al. 2005).

Apart from the induction of apoptosis, apigenin (**5.12**) has also been reported to induce autophagy in various cancer cell lines. Apigenin-induced autophagy was found to be accompanied by G_2/M arrest (*via* inhibition of Cdc25C gene expression) in BCPAP thyroid cancer cells (Zhang et al. 2015), JAK/STAT pathway mediated G_0/G_1 arrest in TF1 erythroleukemic cells (Ruela-de-Sousa et al. 2010), elevated autophagosomal marker LC3-

phosphatidylethanolamine conjugate (LC3-II) in breast (T47D, MDA-MB-231) and colorectal (HCT116) cancer cells (Cao et al. 2013; Lee et al. 2014) and downregulation of casein kinase 2α (CK2α) expression in HeLa sphere-forming cells (SFCs) (Liu et al. 2014). Apigenin (**5.12**) also prevents carcinogenesis through its selective inhibition of AKR1B10 (Figure 5.9), a NADPH-dependent reductase enzyme which is overexpressed in various cancers as a biomarker (Zemanová et al. 2015).

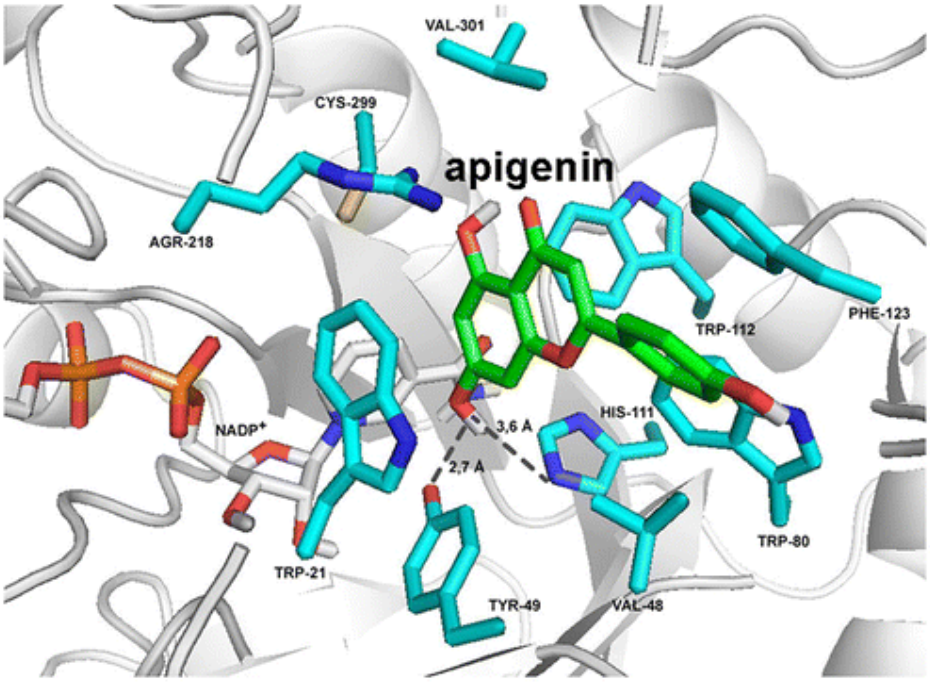

Figure 5.9 Binding of apigenin to the AKR1B10-$NADP^+$ complex (Zemanová et al. 2015). Apigenin is indicated in green, protein residues within 4.0 Å of apigenin are indicated in blue, NADP+ is indicated in white and predicted hydrogen bonding with Tyr49 and His111 is indicated by dashed lines.

Table 5.1 The anticancer activity of apigenin (**5.12**) in various human cancer cell lines

Anticancer Action	Assay	Model	IC_{50}	Signaling Mechanism	Reference
APIGENIN					
Apoptosis	Gene expression	Jurkat	N.D	↑ DR5 expression	Horinaka et al., 2006
	Western blot	DU145 DLD-1	N.D	Sensitizes TRAIL-induced apoptosis	
	in-vivo Longitudinal MRI	TRAMP mice DU145	N.D	↑ E-cadherin	Shukla et al., 2007
	Western blot	DU145	N.D		
	MTT (24 hr)	HL60	40 μM	G2/M arrest, Caspace-dependent ↓ PI3K/PKB	Ruela-de-sousa et al., 2009
	Alamar Blue (72 hr)	HeLa	<20 μM	Inhibits type I IFNs via activation of JAK/STAT pathway through inhibition of 26S proteasome and stabilization of IFNAR1	Li et al., 2016
	MTT (48 hr)	K562 RT112	150μM 28μM	Caspace activation, PARP cleavage	Kalinani-Jaziri et al., 2012
	MTS (24hr)	OVCAR-3	50μM	↓ VEGF expression	Luo et al., 2008
	MTT (48 hr)	LNCaP PC-3	<20μM 20μM	Modulation of MAPK, PI3K-Akt and loss of Cyclin D1 associated Retinoblastoma dephosphorylation	Shukla & Gupta, 2007
	MTT (48 hr)	Bel-7402 PLC/PRF/5	45.60μM 47.16μM	↓ SNAI1 and NF-κB expression, reversed increases in epithelial-mesenchymal transition (EMT) marker levels	Qin et al., 2016
	MTT (24hr)	HCT116 HT29 DLD1	27.9μM 48.2μM 89.5μM	blocks activity and expression of PKM2, selectively inhibits PKM2 expression by blocking β-catenin/c-Myc/PTBP1 signal pathway	Shan et al., 2017

Apoptosis	MTT (48 hr)	HeLa SiHa CaSki C33A	10 μM 72 μM 75 μM 83 μM	mitochondrial redox impairment, ↓ cancer cell migration and invasion	Souza et al., 2017
	MTT (48 hr)	PC3 $CD44^+$ CSCs	13.72μM 13.09μM	↓step cell migration and survival via ↓ PI3K/Akt/NF-κB	Erdogan et al., 2016
	XTT (72 hr)	HeLa	9.8μM	↑ p21/WAF1 protein, ↑ Fas/APO-1 and caspase-3 expression ↑P53 expression	Zheng et al., 2005
Autophagy	MTT (24 hr)	BCPAP	N.D.	p62 G2/M arrest via ↓Cdc25C protein	Zhang et al., 2015
	Electron microscopy	TF1	N.D.	G0/G1 arrest	Ruela-de-sousa et al., 2009
	MTT (48 hr)	T47D MDA-MB-231	N.D.	Apoptosis and autophagy ↑LC3-II	Cao et al., 2013
	MTT (24 hr)	HCT116	>20μM	autophagy ↑LC3-II ↑PARP cleavage	Lee et al., 2014
	MTT (48 hr)	HeLa (SFCs)		↓CK2α expression	Liu et al., 2013
Inhibition of carcinogenesis	MTT (72 hr)	HCT116	EC_{50} = 23.8μM	AKR1B10 non selective inhibitor	Zemanova et al., 2015

N.D. = Not determined

5.3 The influence of *C*-glycosylation on flavonoid *in vivo* biological fate

In flavonoid *C*-glycosides, sugar residues are attached to their aglycones *via* cleavage-resistant C-C bonds usually at positions C-6 and/or C-8. Flavonoid *C*-glycosides have a combination of biological activities from flavonoid aglycones and sugar residues, thereby creating unique and more diverse biological functions than those of *O*- and non-glycosylated flavonoids. Flavonoid *C*-glycosides are categorized into monoglycosides (mono-*C*-glycosylflavonoids) and multiglycosides. Flavonoid *C*-multiglycosides can be further divided into di-*C*-glycosylflavonoids and *C*-glycosylflavonoid-*O*-glycosides (*C*-*O*-glycosides), with the latter having inter-glycosidic bonds via the -OH groups of the *C*-sugars (Cuyckens and Claeys 2004). The most common sugar substituents in flavonoid *C*-glycosides are D-glucopyranose (**5.33**), D-xylopyranose (**5.34**), L-arabinopyranose (**5.35**), L-rhamnopyranose (**5.36**), D-apiose (**5.37**), L-fucopyranose (**5.38**), D-galactopyranosiduronic acid (**5.39**), D-glucopyranosiduronic acid (**5.40**), D-galactopyranose (**5.41**) and D-boivinopyranose (**5.42**) (Figure 5.10) (Zeng et al. 2013).

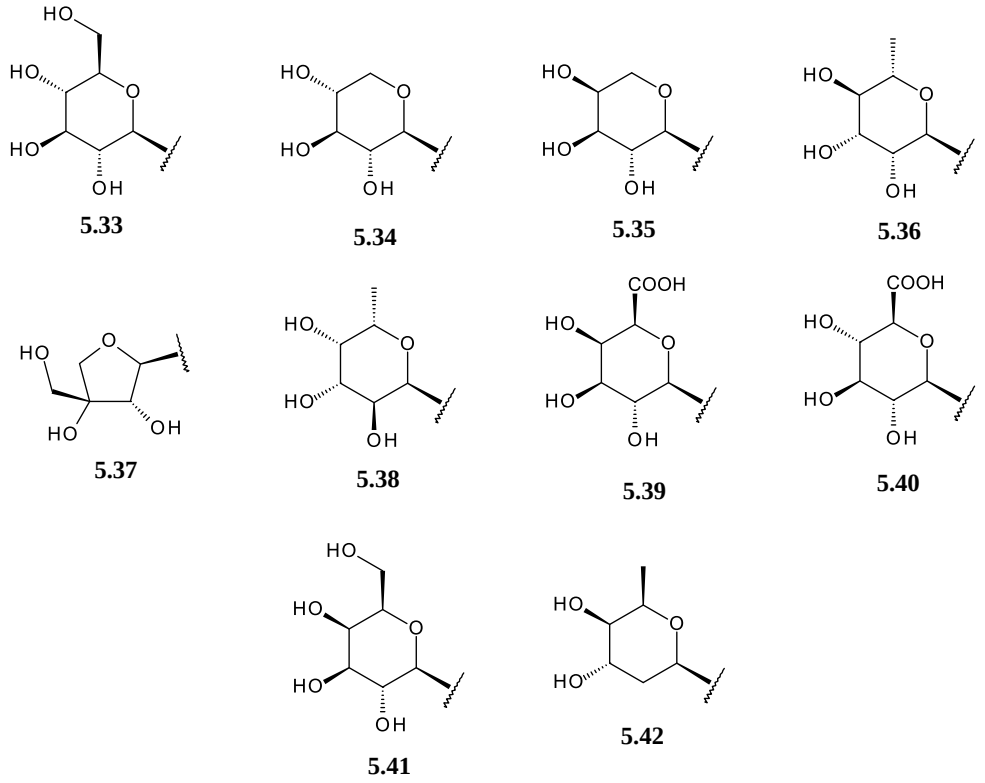

Figure 5.10 Structures for common sugar substituents in flavonoid *C*-glycosides (Zeng et al. 2013).

Together with methylation, hydrogenation and galloylation, glycosylation is a key structural property that increases the chemical stability of flavonoids in blood plasma and *in-vitro* cell culture environments (Xiao and Högger 2015). Flavonoid *C*-glycosides are even more stable than *O*-glycosides and aglycones because their substitution of oxygen with carbon atoms results in increased resistance to β-glucosidase enzyme hydrolysis. (Rawat et al. 2009).

5.3.1 Pharmacokinetic considerations for flavone *C*-glycosides

As a prerequisite to oral absorption, flavonoid *O*-glycosides are deglycosylated in the colon by intestinal microbiota to release the corresponding aglycones. Intestinal microbiota achieve this through the release of *O*-glycosidic bond cleaving enzymes such as α-rhamnosidase, β-glucosidase, endo-β-glucosidase and β-glucuronidase (Yang et al. 2018). *O*-glycosidic bond cleaving is essential for the absorption of flavonoid *O*-glycosides because loss of hydrophilic sugar moieties results in the release of lipophilic aglycones which are then readily absorbed. The absorbed aglycones are then conjugated in the liver to form *O*-glucuronides and *O*-sulfates (Zhang et al. 2007).

In flavone *C*-glycosides, the presence of cleavage-resistant C-C bonds result in deviations from typical flavonoid pharmacokinetics. The major challenge faced by flavone *C*-glycosides is poor intestinal absorption since theoretically, cleavage-resistant *C*-glycosidic bonds do not easily release their aglycones. Despite this, several reports have stated that deglycosylation is not a prerequisite to the intestinal absorption of flavone *C*-glycosides (Courts and Williamson 2009). For instance, after reports of non-absorption in Caco-2 cells (Gouvea et al. 2013), the apigenin *C*-glycoside, vicenin-2 (**5.43**), was later shown to undergo rapid small intestinal absorption in an *in vivo* rat model (Buqui et al. 2015).

The pharmacokinetics of flavone *C*-glycosides vary based on the number of attached glycosides. Flavone *C*-monoglycosides such as vitexin (**5.44**) and isovitexin (**5.45**) are considered to have poor oral absorption with very few metabolite traces in plasma and urine (Xiao et al. 2016). A few intestinal bacteria have been reported to cleave and metabolize flavone-*C*-monoglycosides within 24 h of oral administration. For instance, an isolated *Lachnospiraceae* bacterial strain, CG19-1, completely metabolized vitexin (**5.44**) into 3-(3,4-dihydroxyphenyl)propionic acid and 3-(4-hydroxyphenyl)propionic acid while the intestinal bacterium *Eubacterium cellulosolvens* cleaved isovitexin (**5.45**) and homoorientin (**5.46**) into

their aglycones, apigenin (**5.12**) and luteolin (**5.13**) respectively (Figure 5.11) (Braune and Blaut 2012). The fact that C-C bond cleavage by *Eubacterium cellulosolvens* was observed in C-6 and not C-8 monoglycosides implies that the position of glycosylation (with respect to the –OH substituents at positions C-5 and C-7) and differences in compound transportation may significantly influence the deglycosylation of flavone *C*-monoglycosides (Braune and Blaut 2016). Human intestinal bacterial strains reported to cleave both *C*- and *O*-glycosidic bonds of isoflavones include *Dorea* sp. PUE, *Robinsoniell* sp. CG19-1, *Lactococcus* sp. MRG-IFC-1 and *Enterococcus* sp. MRG-IFC-2, with MRG-IFC-1 and MRG-IFC-2 also able to cleave flavone *O*-glycosides (Kim 2015).

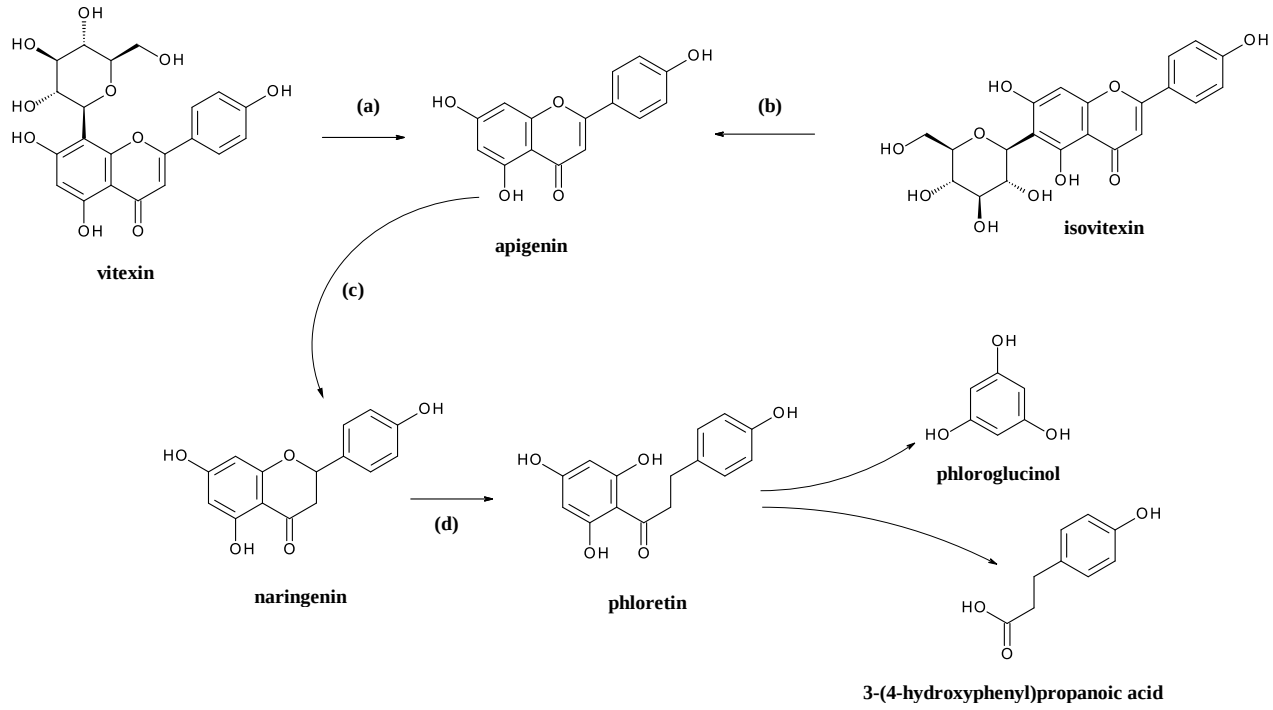

Figure 5.11 Biotransformation of flavone *C*-monoglycosides by human intestinal bacteria (Braune and Blaut 2016)

(a) C-8 deglycosylation by *Lachnospiraceae* bacterial stain, CG19-1 (b) C-6 deglycosylation by *Eubacterium cellulosolvens* (c) hydrogenation (d) ring opening

After oral administration, flavone *C*-multiglycosides are absorption unchanged, received by the liver and taken back to the gut through enterohepatic recirculation. This is followed after by ileal reabsorption of the unchanged and glucuronidated forms into the portal circulation as a sign of bio-availability (Angelino et al. 2013). With regards to flavone-*C*-*O*-diglycosides, sampling of the portal vein after caecal administration of vitexin-2-*O*-xyloside (**5.47**) in rats

resulted in the discovery of reduced forms (possibly with an open flavone C-ring) of the corresponding glucuronidated *C*-monoglycoside (Angelino et al. 2013). This might imply that the deglycosylation of the *O*-sugar in certain flavone-*C*-*O*-diglycosides is performed by intestinal microbiota and/or enterocytes prior to first-pass glucuronidation.

5.3.2 Anticancer activity of selected apigenin *C*-glycosides

The anti-cancer activity of several apigenin *C*- and *C*-*O*-glycosides has been reported. One of the most studied apigenin *C*-glycosides is vitexin (**5.44**), which has a sugar residue attached to the aglycone at position C-8. Vitexin (**5.44**) has been reported to induce apoptosis in U937 human leukaemia cells through the inhibition of Bcl-2 and activation of caspases 3, 7 and 9 (Lee et al. 2012). In another study, vitexin (**5.44**) inhibited the proliferation of hepatocellular carcinoma (HCC) cells and induced apoptotic cell death in HepG2 hepatocellular carcinoma cells *via* the activation of caspases 3, 8 and 9 (Wang et al. 2013). The anticancer mechanism for vitexin (**5.44**) in HepG2 cells involves the inhibition of AKT and ERK1/2 kinase phosphorylation and the activation of FOXO3a, which results in increased expression of apoptosis target gene products such as Bim, TRAIL, DR4 and DR5 (Wang et al. 2013). Vitexin (**5.44**) induced early apoptosis in EC-109 oesophageal cancer cells (An et al. 2015). Vitexin (**5.44**) also induced caspace-3 mediated apoptosis while supressing autophagy in hepatocellular carcinoma (HCC) cell lines SK-Hep1 and Hepa1-6 *via* the JNK MAPK pathway (He et al. 2016). Vitexin (**5.44**) was reported to inhibit cancer angiogenesis, metastasis and invasion in rat pheochromocytoma (PC12) cells through the inhibition of hypoxia inducible factor-1α (HIF-1α) (Jung Choi et al. 2007). The induction of apoptosis and inhibition of human oral cancer cell (OC2) metastasis by vitexin (**5.44**) was elicited *via* the p53 pathway (Yang et al. 2013). Vitexin (**5.44**) induced caspases 7, 8 and 9 mediated apoptosis in MCF-7 human breast adenocarcinoma cells (Mohammed et al. 2014; Czemplik et al. 2016). One of the suggested anticancer mechanisms for vitexin (**5.44**) in HeLa cells is the inhibition of reactive oxygen species (ROS) mediated oxidative damage, increased Bax and decreased Bcl2 expression, leading to caspase 3 dependent apoptosis (Talakatta et al. 2016). Vitexin (**5.44**) also possesses antimutagenic properties through its selective inhibition of AKR1B10, though apigenin (**5.12**) is 3.5 times more potent (Zemanová et al. 2015).

Other apigenin *C*-glycosides such as the monoglycosides isovitexin (**5.45**) (Talakatta et al. 2016), aciculatin (**5.48**) (Lai et al. 2012), 7-de-*O*-methylaciculatin (**5.49**) and 8-*C*-β-D-

boivinopyranosylapigenin (**5.50**) (Shen et al. 2012), and the multiglycoside vitexin-2-*O*-xyloside (**5.47**) (Figure 5.12) (Papi et al. 2013; Salvatore Scarpa et al. 2017), have apoptotic mechanisms that are similar to those of vitexin (**5.44**) (Table 5.2).

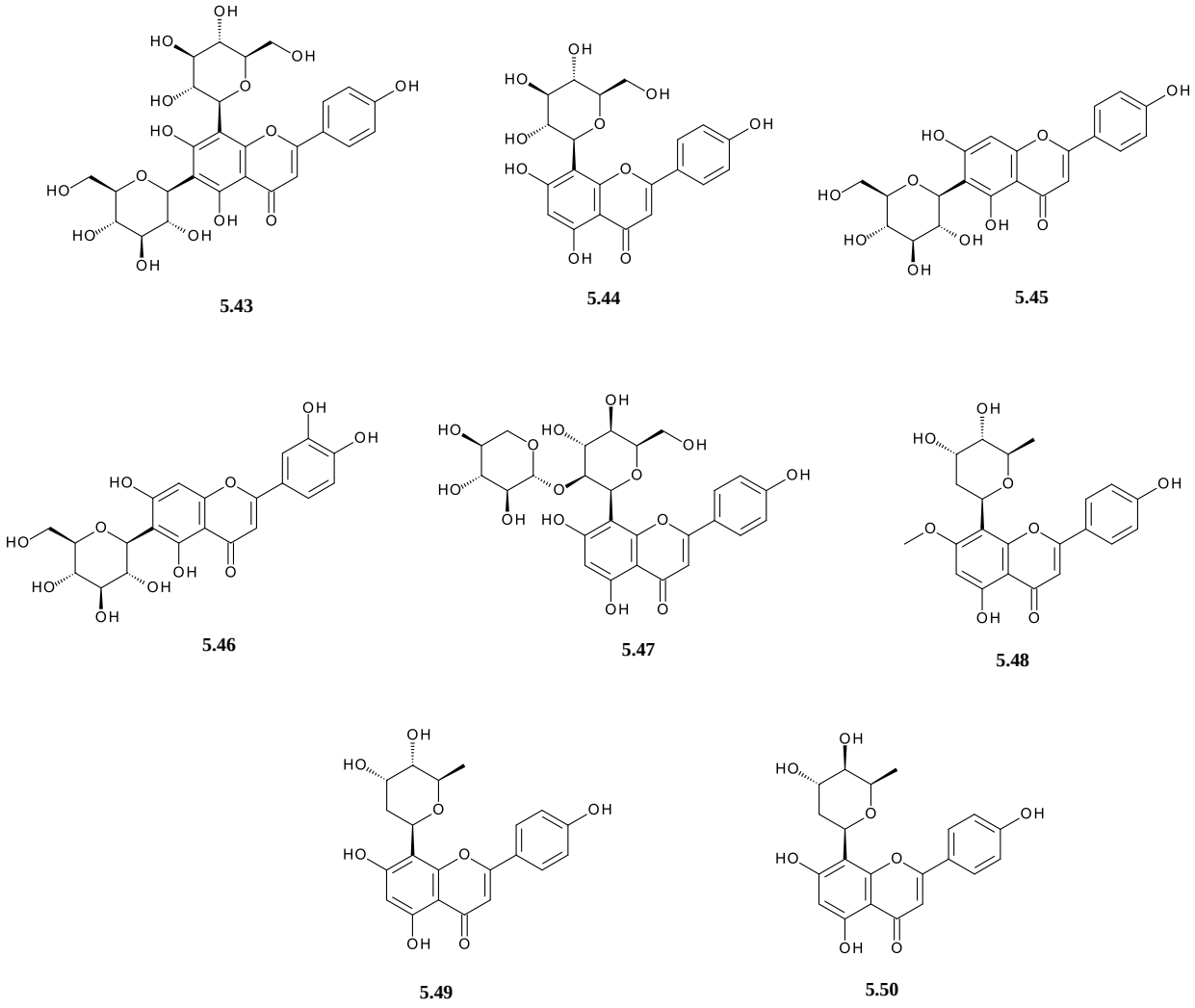

Figure 5.12 Structures for selected apigenin *C*-glycosides

Table 5.2 Anticancer activity of selected apigenin *C*-glycosides in various cancer cell lines

Compound	Anticancer Action	Assay	Model	IC_{50}	Signaling Mechanism	Reference
APIGENIN *C*-GLYCOSIDES						
Vitexin (**5.44**)	**Apoptosis**	MTT (24 hr)	U937	200µM	Inhibition of Bcl-2, ↑caspase-3, 7,9	Lee et al. 2012
		MTT (24 hr)	HCC HepG2	N.D.	inhibition of AKT and ERK1/2 kinase phosphorylation, activation of FOXO3a transcription factor and apoptotic death	Wang et al. 2013
		MTT (72 hr)	EC-109	IC_{20} = 80µM	apoptosis-related gene expression of p53 and bcl-2	An et al. 2015
		MTT (24 hr)	SK-Hep Hepa 1-6	100µM 100µM	apoptosis induction and autophagy suppression via JNK MAPK pathway. ↑Caspase-3, Cleave Caspase-3, ↓Bcl-2	He et al. 2016
		Alamar Blue (24 hr)	OC2	N.D.	↑P53, ↑$P21^{WAFI}$ ↑Bax	Yang et al. 2013
		MTT (48 hr)	MCF-7	Approx: 1.2µg	↑Bax ↑Caspase-7, -8, and -9. ↓mRNA expression of bcl-2	Czemplik et al. 2016
		MTT (48 hr)	HeLa	40 – 50 µg/ml	↓Bcl-2 level with ↑Bax and caspase-3 protein expression	Talakatta et al. 2016
		MTT (48 hr)	HepG2 MCF-7 HCT116	>100µg/ml 50µg/ml 100µg/ml	N.D.	Mohammed et al. 2014
	Antimutagenic	MTT (72 hr)	HCT116	N.D.	AKR1B10 non selective inhibitor	Zemanova et al. 2015
	Anti-metastatic	MTT (24 hr)	PC12 HepG2 HOS	>50µM	↓HIF-1α in PC12 only. Inhibits hypoxia-induced activation of c-jun N-terminal kinase (JNK), but not of extracellular-signal regulated protein kinase (ERK). JNK Pathway	Jung Choi et al. 2007

Isovitexin (**5.45**)	**Apoptosis**	MTT (48 hr)	HeLa	40 – 50 µg/ml	↓Bcl-2 level with ↑Bax and caspase-3 protein expression	Talakatta et al. 2016
Vitexin-2-O-xyloside (**5.47**)	**Apoptosis**	SRB (72 hr)	LoVo CaCo-2 MCF-7 MDA-MB-231	158µg/ml 120µg/ml 235µg/ml 1200µg/ml	Mitochondrial pathway activation of apoptosis elicited by ROS	Papi et al. 2013
		SRB (48 hr)	HepG-2 CaCo-2	71.6µM 50.9µM	↑caspases 9, 8, and 3. ↓BIRC5, HIF1A, and VEGFA	Scarpa et al. 2017
Aciculatin (**5.48**)	**Apoptosis**	Alamar Blue (48 hr)	MCF-7 H460 HT-29 CEM	3.16µM 46.94µM 25.98µM 2.65µM	N.D.	Shen et al. 2012
		MTT (48 hr)	HCT116	N.D.	↑p53 ↑p21 level, dephosphorylation of Rb, ↑PUMA, ↑Caspase-9, -3 ↑PARP	Lai et al. 2012
7-de-O-methyl aciculatin (**5.49**)	**Apoptosis**	Alamar Blue (48 hr)	MCF-7 H460 HT-29 CEM	6.35µM 18.25µM 25.29µM 4.42µM	N.D.	Shen et al. 2012
8-C-β-D-boivino Pyranosyl apigenin (**5.50**)	**Apoptosis**	Alamar Blue (48 hr)	MCF-7 H460 HT-29 CEM	74.98µM 11.96µM 10.0µM 2.58µM	N.D.	Shen et al. 2012

N.D. = Not determined

5.4 Chapter aims

It was discussed in chapter 4 that 6″-*O*-α-apio-D-furanosylisovitexin (altissimin, **3.17**), the flavonoid *C*-multiglycoside that is partly responsible for the cytotoxicity of *Drimia altissima* against HeLa cervical cancer cells, elicits its anti-proliferative activity *via* the induction of Early M phase cell cycle arrest and apoptotic cell death. This chapter further explores the signaling pathways by which altissimin (**3.17**) achieves its anti-proliferative activity and thereby proposes a plausible mechanism of action.

5.5 Results and discussion

5.5.1 Cytotoxicity assay

In Chapter 4, the IC_{50} of compound **3.17** against HeLa cells was determined to be 2.44 µM after a 48 h exposure (Figure 4.11). In this chapter, a fixed concentration of 2.5 µM (representative of the IC_{50}) and an additional two concentrations lower than the IC_{50} were used to investigate the mechanism of action of compound **3.17**. The cytotoxicity of compound **3.17** at these three concentrations against HeLa cells was confirmed through Hoechst 33342/ PI dual staining with melphalan (20 µM) as positive control. Based on results obtained from the analysis of nuclei per site after a 24 and 48 h treatment (Figure 5.13), compound **3.17** induced a dose dependent reduction in cell number, with the highest tested concentration (2.5 µM) eliciting a similar effect to that of melphalan. The untreated control cells doubled in number from 24 to 48 h. Compound **3.17** caused a significant reduction in cell number at 24 h but at 48 h this reduction was much more enhanced and roughly equivalent to the expected 50%.

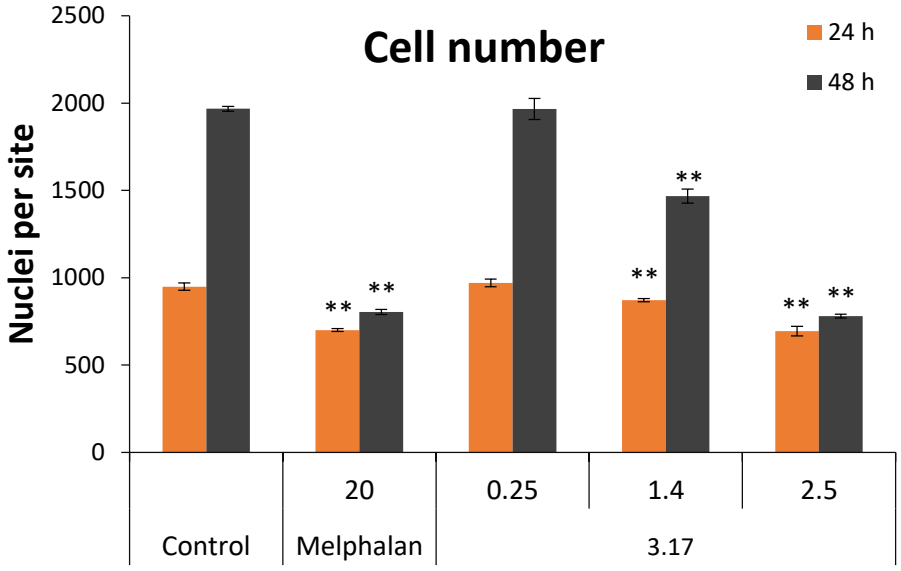

Figure 5.13 Nuclei per site in HeLa cells after 24 and 48 h treatment with compound **3.17**

Concentrations were measured in µM with melphalan (20 µM) used as positive control. Nuclei were stained with Hoechst 33342 and Propidium iodide. Data points represent the mean ± SD of three independent experiments, each performed in quadruplicate. *p<0.05; **p<0.001 compared to control

Nuclear size was also evaluated through the measurement of nuclei area. From the obtained results (Figure 5.14), compound **3.17** caused an increase in nuclear size at 2.5 µM after 48 h of treatment, suggesting S or G_2/M cell cycle arrest.

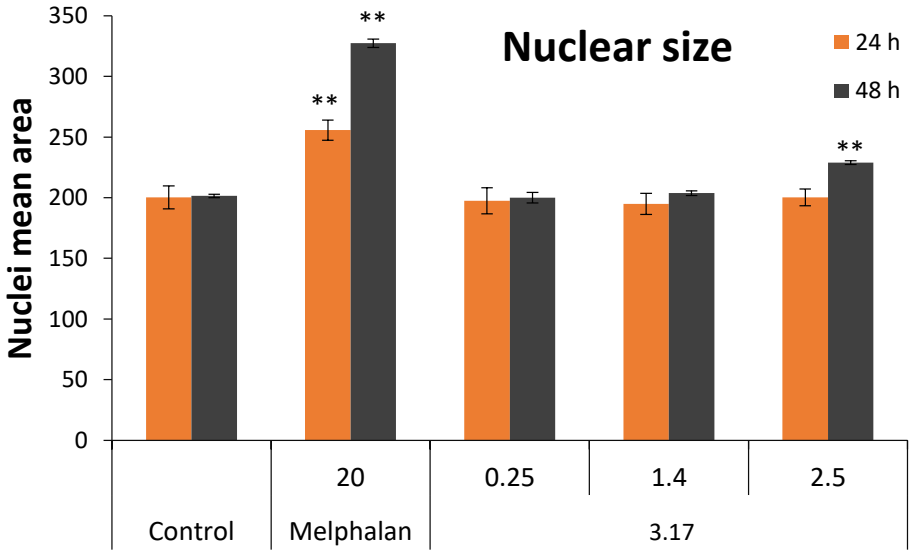

Figure 5.14 Nuclei mean area in HeLa cells after 24 and 48 h treatment with compound **3.17** Concentrations were measured in µM with melphalan (20 µM) used as positive control. Nuclei were stained with Hoechst 33342 and Propidium iodide. Data points represent the mean ± SD of three independent experiments, each performed in quadruplicate. *p<0.05; **p<0.001 compared to control

5.5.2 Cell Cycle Analysis

Anticancer drugs can be cell cycle specific (causing cells to arrest in a specific cell cycle phase) or cell cycle non-specific. Results from Chapter 4 suggested a dose-dependent increase in cells accumulating in early M phase upon exposure to compound **3.17** (Figure 4.15). This experiment was repeated using the IC_{50} of compound **3.17**. Cell cycle analysis of compound **3.17** was determined through Hoechst 33342/ Annexin-V-fluorescein isothiocyanate (FITC) staining using melphalan at 20 µM as positive control. From the obtained results (Figure 5.15), melphalan induced S/G_2 cell cycle arrest. At 2.5 µM, compound **3.17** induced M phase cell cycle arrest which was characterised by a marked increase in Early M phase and a slight increase in Late M phase cell populations. Pie charts were used to present the cell cycle data in this chapter for ease of interpretation.

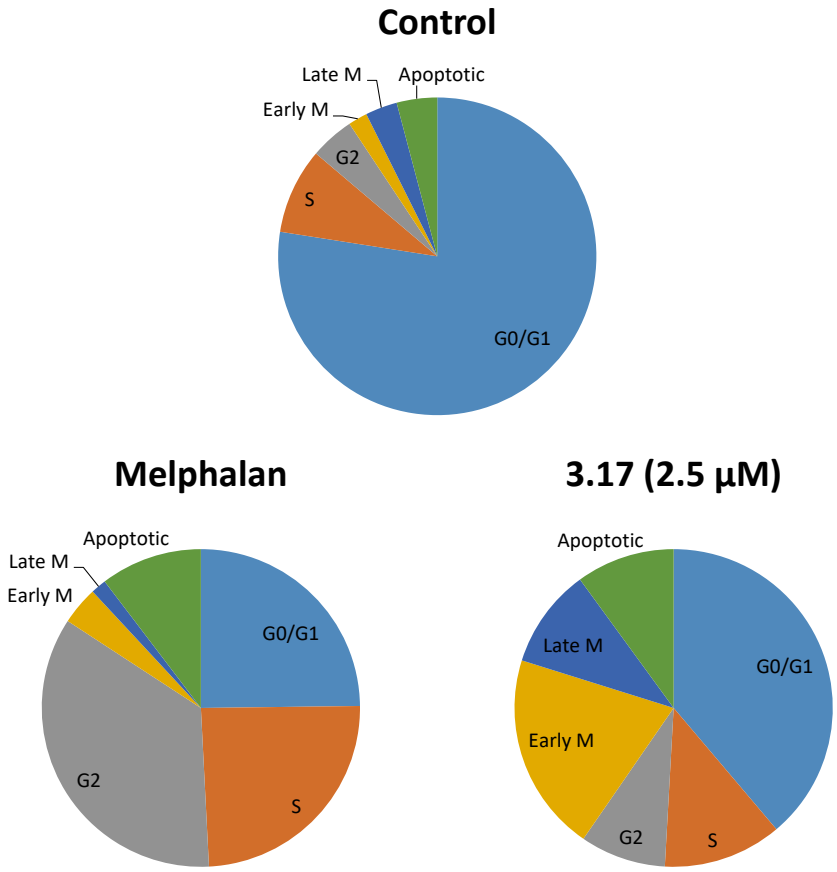

Figure 5.15 Compound **3.17** induces mitotic arrest in HeLa cells after 48 h

Positive control: 20 µM melphalan. Nuclei were stained with NucRed Live 647 and Annexin V-FITC was used as apoptosis marker. Data points represent the mean ± SD of three independent experiments, each performed in quadruplicate.

5.5.3 Mitochondrial membrane potential (MMP)

The mitochondria is considered to play a central role in the induction of apoptotic cell death (Desagher and Martinou 2000). This is because mitochondria centrally regulate the intrinsic apoptotic pathways and are effector-mediators of the extrinsic apoptotic pathways (Cottet-Rousselle et al. 2011). Mitochondria are responsible for maintaining the production of ATP, the mitochondrial membrane potential ($\Delta\Psi m$) or MMP and mitochondrial membrane permeability for release of apoptotic factors into the cytosol (Leist and Nicotera 1997; Kroemer and Reed 2000). The mitochondrial membrane potential ($\Delta\Psi m$) is a part of the transmembrane potential of hydrogen ions which are utilised by cells to generate ATP. Produced by the proton pump Complexes I, III and IV, $\Delta\Psi m$ is a key entity in the energy storage process during

oxidative phosphorylation. The vitality of ΔΨm to cellular health and homeostasis is seen in that sustained changes in ΔΨm may result in reduced cell viability and the onset of various pathological states (Zorova et al. 2018).

The mitochondrial permeability transition pore (mPTP) is a protein channel composed of the voltage-dependent anion channel (VDAC), adenine nucleotide translocase (ANT) and mitochondrial benzodiazepine receptor which is formed in the inner aspects of the mitochondrial membrane during certain pathological conditions (Halestrap et al. 2002). The induction of mPTP leads to increased permeability of apoptotic factors such as cytochrome *c*, apoptosis-inducing factor (AIF) and second mitochondria-derived activator of caspases (Smac/Diablo) (Creagh and Martin 2001). A difference in charge between the mitochondrial matrix and the cytosol causes this "permeability transition" (PT) which may then lead to apoptosis (Ly et al. 2003). The induction of mPTP is regulated by ΔΨm and mitochondrial matrix pH, with a decrease in ΔΨm and a drop in pH below 7.0 both increasing the probability of channel opening (Bernardi et al. 1992; Petronilli et al. 1993). The loss of ΔΨm has been found to be either an early apoptotic event or a result of apoptotic signaling depending on the cell model being used (Ly et al. 2003). Several fluorescent lipophilic cationic dyes are used to detect ΔΨm in cell models, with differences in fluorochrome sensitivity significantly contributing to the accurate determination of changes in ΔΨm. Examples of ΔΨm detection dyes include tetramethylrhodamine methyl ester (TMRM), tetramethylrhodamine ethyl ester (TMRE), Rhodamine 123 (Rhod123), $DiOC_6(3)$ (3,3′- dihexyloxacarbocyanine iodide) and JC-1 (5,5′,6,6′-tetrachloro-1,1′,3,3′- tetraethylbenzimidazolylcarbocyanine iodide) (Sakamuru et al. 2016). The advantages of evaluating ΔΨm using tetramethylrhodamine ester dyes such as TMRE (**5.51**) (Figure 5.16) over other cationic dyes are that they do not interfere with mitochondrial function, their fluorescence quenching is not readily dependent on concentration factors and effects of mitochondrial inhibitors and oxidative phosphorylation uncouplers at submicromolar concentrations can be examined in both isolated and live cell mitochondria (Chazotte 2011).

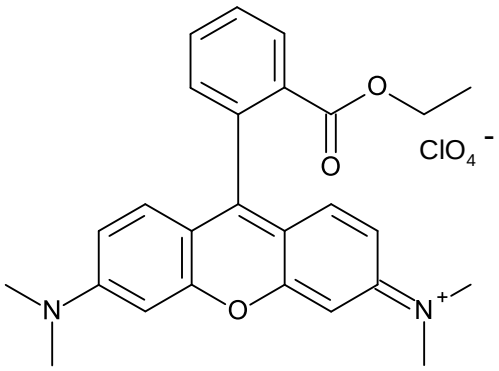

5.51

Figure 5.16 Structure for tetramethylrhodamine ethyl ester (TMRE) dye

Mitochondrial accumulation of ΔΨm detection dyes follows the Nernst equation (below) where E_{cell} is cell potential, $E^{o}{}_{cell}$ is standard cell potential, n is the number of electrons transferred and Q is the reaction quotient. The mitochondrial accumulation of ΔΨm detection dyes is inversely proportional to ΔΨm, with hyperpolarized mitochondria accumulating more dye and depolarized mitochondria accumulating less dye (Perry et al. 2011).

$$E_{cell} = E^{o}{}_{cell} - \frac{0.0592\ \mathrm{V}}{n} \log \mathrm{Q}$$

After 24 and 48 h of treatment with 0.25, 1.4 and 2.5 μM of compound **3.17**, mitochondrial membrane collapse in HeLa cells was determined *via* staining with TMRE and Hoechst 33342 as counterstain. From the acquired images, control cells presented with intense TMRE fluorescence while cells treated with compound **3.17** presented with weak TMRE fluorescence (Figure 5.17). Because apoptotic cells fail to retain TMRE due to the presence of a collapsed ΔΨm, the observed low TMRE fluorescence in cells treated with compound **3.17** was indicative of an apoptotic mitochondrial membrane potential collapse.

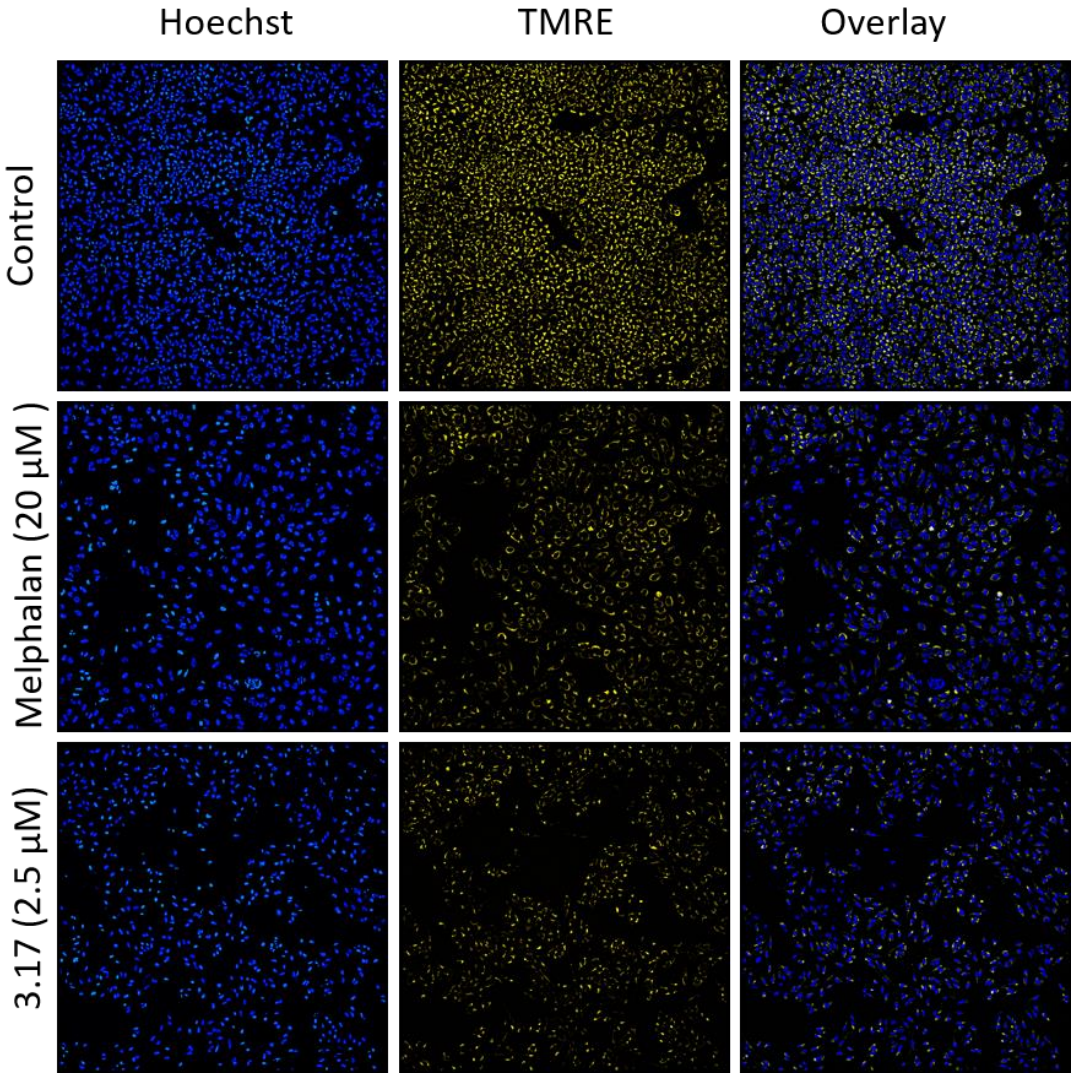

Figure 5.17 HCA acquired images showing mitochondrial membrane depolarisation in HeLa cells after treatment with 2.5 μM of compound **3.17**

Concentrations were measured in μM with melphalan (20 μM) used as positive control. Mitochondria and nuclei were stained with TMRE and Hoechst 33342, respectively.

After HCA of the acquired images, 48 h of treatment with melphalan (20 μM) induced a collapse of the ΔΨm in HeLa cells. Similarly, compound **3.17** significantly collapsed the ΔΨm in HeLa cells at 1.4 and 2.5 μM after 24 and 48 h of treatment (Figure 5.18).

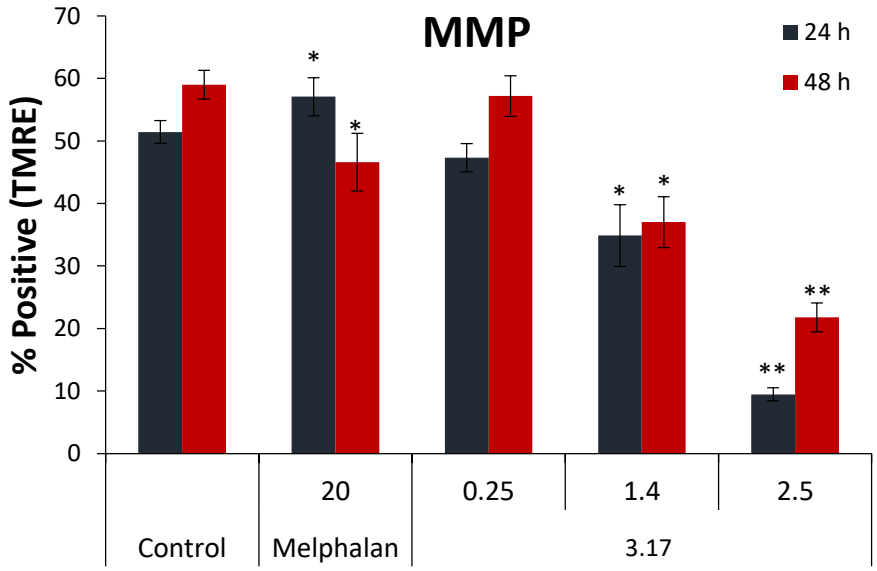

Figure 5.18 Compound **3.17** collapses the mitochondrial membrane potential in HeLa cells after 24 and 48 h

Concentrations were measured in μM with melphalan (20 μM) used as positive control. Mitochondria and nuclei were stained with TMRE and Hoechst 33342, respectively. Data points represent the mean ± SD of three independent experiments, each performed in quadruplicate. *p<0.05; **p<0.001 compared to control

5.5.4 Cleaved caspase -8 and -3 analysis

The caspases (**c**ysteine-**asp**artic prote**ases**, **c**ysteine **asp**art**ases** or **c**ysteine-dependent **asp**artate-directed prote**ases**) are a family of proteases that modulate signaling events which lead to programmed cell death either by apoptosis or pyroptosis *via* apoptotic and inflammatory caspases respectively (Ramirez and Salvesen 2018). Apical caspases of the extrinsic apoptotic pathway, caspases -8 and -10, are monomeric zymogens which are activated through heterodimerization. Caspases -8 and -10 undergo Fas-induced activation at the death-inducing signaling complex (DISC) which is enhanced by the long form $FLIP_L$ (FLICE-like inhibitory protein) at low expression (Salvesen and Walsh 2014). Caspase -8 and $FLIP_L$ form elongations through connections between their N-terminal death effector domains (DEDs), with the short form ($FLIP_S$) not being able to encode caspase activation due to the presence of a stop codon after the DEDs (Dickens et al. 2012). Dimerization of the apical caspases is followed after by cleavage of the N-terminal DEDs and cytosolic release of the activated caspases.

On the other hand, the executioner caspases -3 and -7 exist intracellularly as inactive obligate dimeric zymogens (separated by an interdomain linker) awaiting proteolytic activation *via* cleavage by initiator caspases or by other proteases under specific circumstances (Boatright and Salvesen 2003). Cleavage of the interdomain linker in executioner caspases permits the arrangement of mobile loops which allow for the assembly of the catalytic site. Caspase -3 has been described as a typical hallmark of apoptosis that is required for apoptotic chromatin condensation, DNA fragmentation and blebbing in all cell models (Porter and Jänicke 1999). The activation of caspase -3 consequently leads to the cleavage of downstream death substrates.

As a key feature in the aetiology of cancer, the mutation and deregulation of apoptotic proteins prevents the transmission of pro-apoptotic signals to executioner caspases and thereby gives malignant cells the ability to avert apoptotic cell death. Since the activation of executioner caspases occurs at the final phase of apoptosis, potential anticancer compounds may activate caspases -3 in cancer cells by several mechanisms including DNA damage, increased expression of pro-apoptotic proteins, decreased expression of anti-apoptotic proteins, and direct activation of procaspase -3. PAC-1 (**5.51**) (Figure 5.19) was the first small molecule found to be an allosteric activator of procaspase -3 to caspase -3 (Putt et al. 2006). Other direct activators of procaspase -3 include compound 1541 (**5.52**), compound 42 (**5.53**) and compound 2 (**5.54**) (Wolan et al. 2009; Schipper et al. 2011; Vickers et al. 2013).

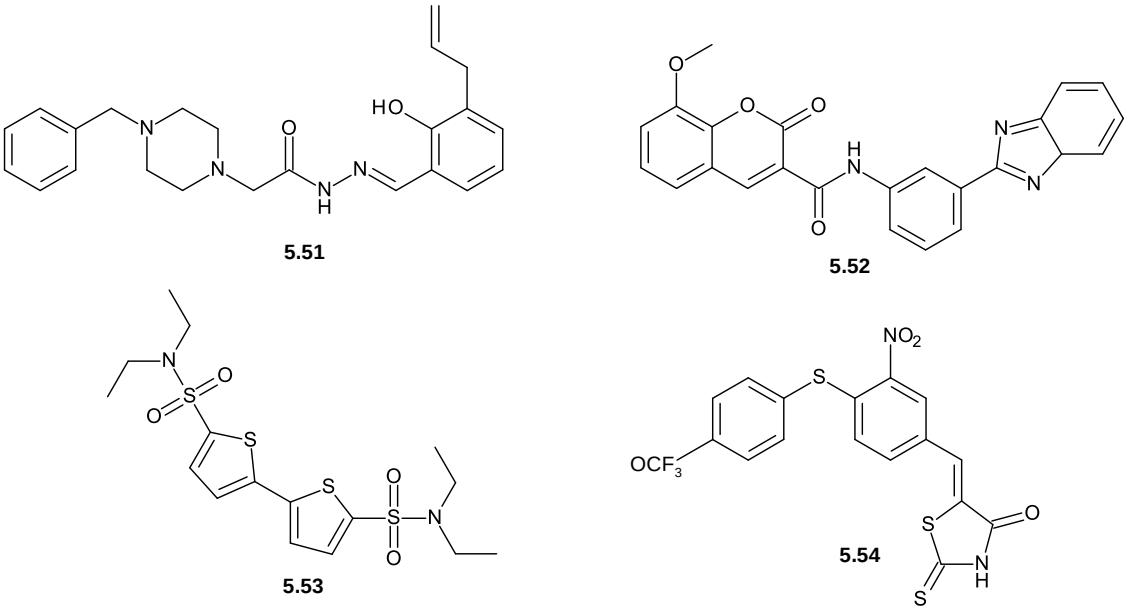

Figure 5.19 Selected direct allosteric activators of procaspase -3 to caspase -3

Caspase activation in HeLa cells was evaluated after 24 and 48 h treatment with compound **3.17** at 0.25, 1.4 and 2.5 μM. From the obtained results (Figure 5.20), compound **3.17** induced significant elevation of cleaved caspase -3 after 48 h (Figure 5.20A) and caspase -8 after 24 h (Figure 5.20B) in HeLa cells, indicating activation of both caspases. The elevation of caspase -8 suggests activation of the extrinsic apoptotic pathway.

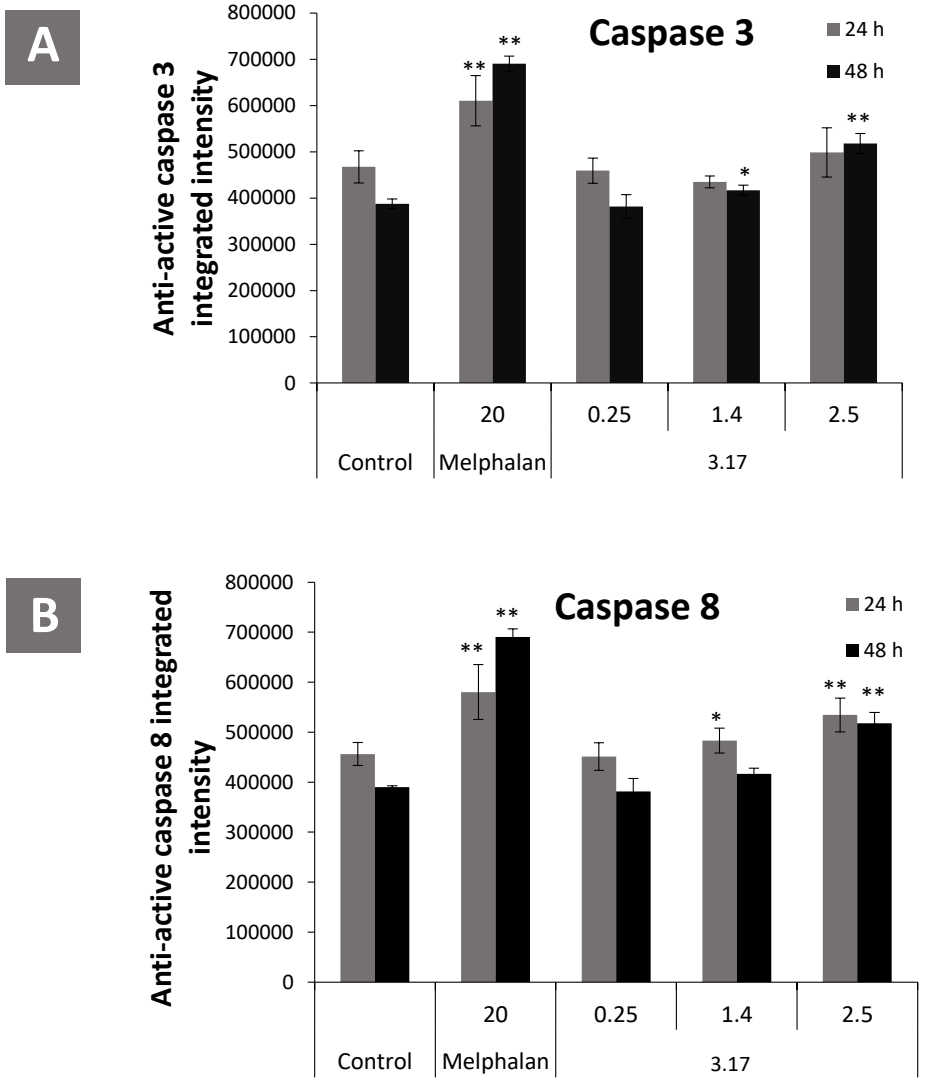

Figure 5.20 Compound **3.17** activates caspases -8 and -3 after 24 and 48 h respectively

Concentrations were measured in μM with melphalan (20 μM) used as positive control. Nuclei were stained with Hoechst 33342 and active caspases with appropriate monoclonal antibodies and Alexa Fluor 488 conjugated secondary antibodies. Data points represent the mean ± SD of three independent experiments, each performed in quadruplicate. *$p<0.05$; **$p<0.001$ compared to control

5.5.5 LysoTracker® Red (autophagy)

Lysosomes are spherical, membrane bound organelles appearing as vesicles containing hydrolytic enzymes for the degradation of biomolecules in eukaryotic cells. Because an acidic environment is optimal for lysosomal proteases, lysosomes have a luminal pH of 4.0 – 6.0 (Yapici et al. 2015). In autophagic cell death, lysosomes fuse with autophagosomes (early autophagic vesicles with neutral pH) to form autolysosomes (late autophagic vesicles with acidic pH) (Figure 5.21) (Nakamura and Yoshimori 2017). Weakly basic amines such as N-{3-[(2,4-Dinitrophenyl)amino]propyl}-N-(3-aminopropyl)methylamine dihydrochloride (DAMP, which has since been discontinued), neutral red and acridine orange and LysoTracker® probes such as LysoTracker® Red and LysoSensor™ are used as lysosomal markers to detect autophagy due to their selective accumulation in autolysosomes (Pierzynska-Mach et al. 2014). Increased cellular staining with these acidotropic probes is indicative of the presence of late autophagic vesicles resulting from the activation of autophagy.

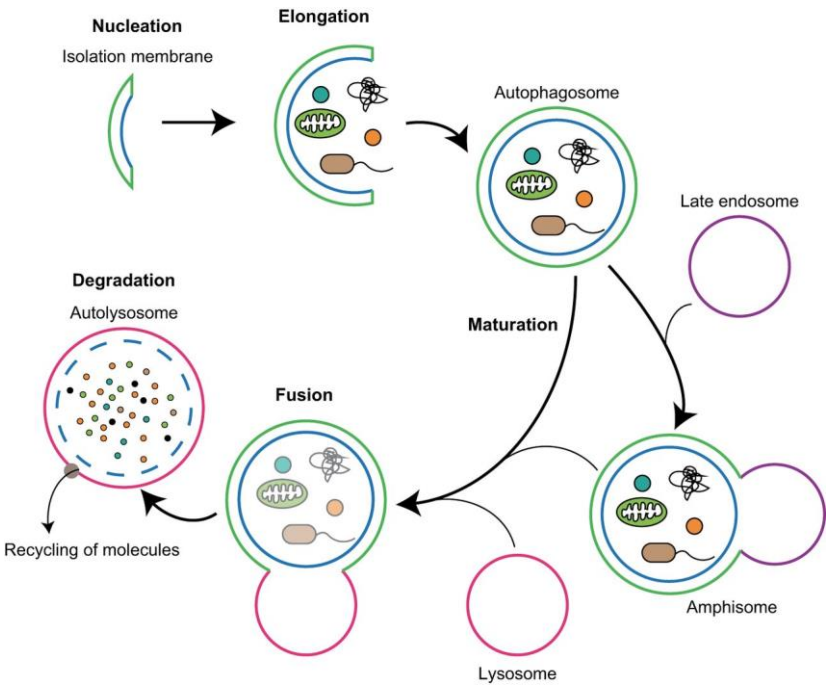

Figure 5.21 An overview of autophagy detailing the biomolecular degradation process

Induced of autophagy leads to the formation of autophagosomes (neutral pH) which fuse with either late endosomes (amphisomes) or lysosomes to form autolysosomes (acidic pH) for the degradation or recycle of biomolecules (Nakamura and Yoshimori 2017)

The activation of autophagy in HeLa cells was evaluated after 24 h treatment with compound **3.17** at 0.25, 1.4 and 2.5 μM. HCA acquired images showed an increase in LysoTracker® Red staining at 2.5 μM of compound **3.17** compared to the control (Figure 5.22). After HCA data analysis, the confirmation of a slight increase in LysoTracker® Red staining at 2.5 μM of compound **3.17** suggested the activation of autophagy (Figure 5.23).

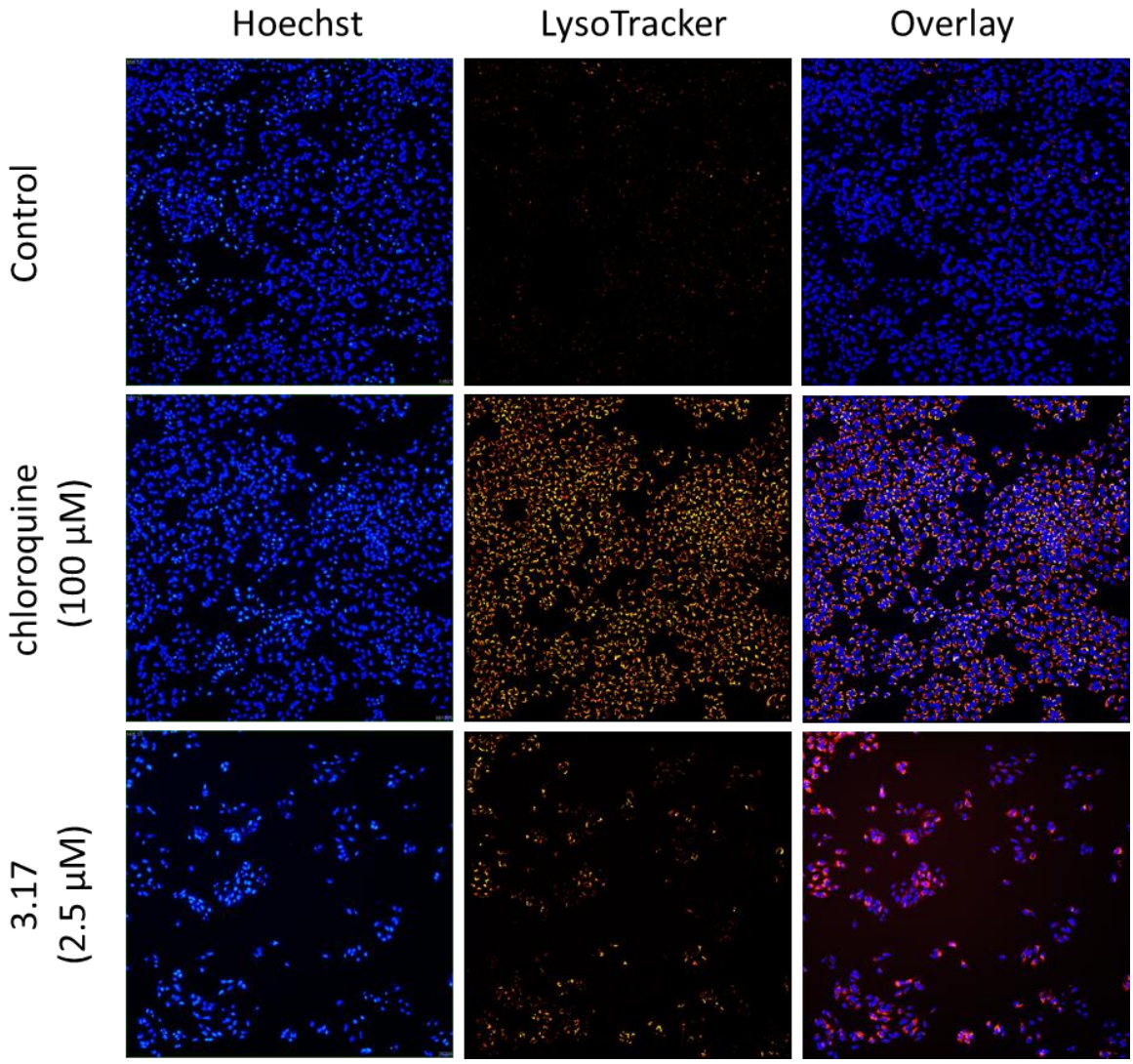

Figure 5.22 HCA acquired images showing increase in LysoTracker® Red staining in HeLa cells after 24 h treatment with 2.5 μM of compound **3.17**.
Concentrations were measured in μM with chloroquine (100 μM) used as positive control

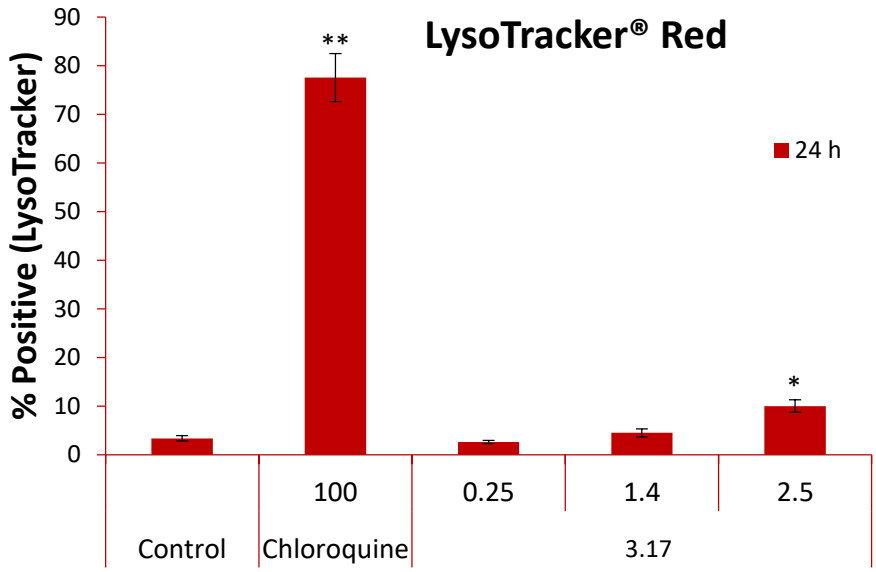

Figure 5.23 Compound **3.17** caused slight increase in LysoTracker® Red staining after 24 h. Concentrations were measured in μM with chloroquine (100 μM) used as positive control. Data points represent the mean ± SD of three independent experiments, each performed in quadruplicate. *p<0.05; **p<0.001 compared to control.

In this chapter, flavonoids are identified as "nutraceuticals" possessing medicinal properties that are ideal for the development of natural product-based therapeutic agents. In particular, flavonoids have shown to possess significant anticancer activity against a wide spectrum of cancers through their various mechanisms. The cancer modulating effects of flavonoids include, but are not limited to, anti-oxidant, anti-inflammatory, antimutagenic, anti-proliferative and inhibition of oncogenic viruses. Some of the structural properties that tend to influence the anticancer activity of flavonoids are hydroxylation, C-4 carbonylation, methoxylation, prenylation, bond unsaturation and glycosylation. Among the different flavonoids, apigenin is highlighted as one of the most promising natural product-based chemotherapeutic agents. Anticancer mechanisms associated with the apigenin scaffold include selective DR5 expression in TRAIL-resistant cancers, increased E-cadherin expression, caspase-dependent PI3K/PKB inhibition, 26S proteasome inhibition, PARP inhibition, VEGF protein inhibition, inhibition of β-catenin nuclear translocation, snail pathway inhibition and the induction of both apoptosis and autophagy. Unfortunately, a major concern with flavonoid therapy is lack of *in vivo* stability due to their susceptibility to β-glucosidase enzyme hydrolysis. Interestingly, the biosynthetic addition of *C*-glycosides to flavonoid aglycones such as apigenin result in the formation of flavonoid *C*-glycosides, a

unique type of compounds with greater *in vivo* stability and more diverse biological functions. Despite concerns of poor absorption, several pharmacokinetic studies have shown flavonoid *C*-glycosides to be sufficiently absorbed after oral administration. Flavonoid *C*-glycosides with anticancer activity include vitexin, isovitexin, aciculatin, 7-de-*O*-methylaciculatin, 8-*C*-β-D-boivinopyranosylapigenin and vitexin-2-*O*-xyloside. The anticancer activity of apigenin *C*-glycosides include the activation of apoptosis and/or autophagy, antimutagenic and anti-metastatic activities.

From the obtained results, compound **3.17**, an apigenin *C*-glycoside, induced a dose dependent anti-proliferative activity against HeLa cells with 2.5 μM of the compound eliciting a similar effect to that of melphalan (20 μM). The anti-proliferative activity of compound **3.17** was then found to involve the induction of M phase cell cycle arrest which was characterised by a marked increase in Early M phase and a slight increase in Late M phase cell populations. On further evaluation, compound **3.17** collapsed the mitochondrial membrane potential (ΔΨm) in HeLa cells, signalling the activation of apoptotic cell death. Induction of both the intrinsic and extrinsic apoptotic pathways by compound **3.17** in HeLa cells was confirmed through the activation of caspases -8 and -3 after 24 h and 48 h respectively. Compound **3.17** also slightly activated autophagic cell death. In summary, the mechanism of cell death elicited by compound **3.17** in HeLa cells involves, to a greater extent, the induction of M phase cell cycle arrest with consequent activation of apoptotic cell death which is evident from annexin V staining, mitochondrial membrane potential (ΔΨm) collapse and activation of caspases -8 and -3. To a lesser extent, compound **3.17** elicits its cytotoxic activity against HeLa cells by activating autophagic cell death.

5.6 Experimental

5.6.1 General experimental procedures

HeLa cervical cancer cells were obtained from Cellonex, South Africa and grown in Roswell Park Memorial Institute 1640 (RPMI 1640) medium from GE Healthcare Life Sciences (South Logan, Utah, USA) supplemented with gamma irradiated Fetal Bovine Serum (FBS) from Biowest (South America). Cells were cultured in BioFlow-II Labotec laminar flow cabinets and incubated in a ThermoForma CO_2 incubator. Annexin V-FITC kit was obtained from MACS Miltenyi Biotec (Auburn, USA).

5.6.2 Hoechst 33342/ Propidium Iodide (PI) cytotoxicity assay

The cytotoxicity of altissimin (**3.17**) against HeLa cells was performed using the Hoechst 33342/ propidium iodide (PI) assay. HeLa cells were seeded into 96 well plates at a density of 5000 cells/well and incubated at 37 °C in a humidified 5% CO_2 incubator for 24 h. The cells were treated with compound **3.17** at 0.25, 1.375 and 2.5 µM and 20 µM of melphalan was used as positive control. Treatments were incubated at 37 °C for 24 or 48 h after which the medium was aspirated and cells washed with Phosphate-buffered saline (PBS) containing calcium and magnesium. The cells underwent Hoechst/PI staining with bisBenzamide H 33342 trihydrochloride (Hoechst 33342) at 5 µg/mL and propidium iodide (PI) at 10 µg/mL. After incubation at 37 °C for 15 min, cellular images were acquired with a Molecular Devices® ImageXpress Micro XLS Widefield High-Content Analysis System using a DAPI filter for Hoechst 33342 and a Texas Red filter for PI. Acquired images were analysed using the Multiwavelength Cell Scoring analysis module of the MetaXpress® High-Content Image Acquisition and Analysis Software.

5.6.3 Hoechst 33342/ Annexin (Cell Cycle Analysis)

For cell cycle analysis, HeLa cells were seeded and treated with compound **3.17** as above. Treatments were aspirated and cells washed with PBS containing calcium and magnesium. A mixture was prepared by the addition of 50 µL of Annexin V-FITC and 5 µL of Hoechst 33342 to 5 mL PBS containing 250 µL of Binding Buffer (20x). Hoechst 33342/ Annexin staining was then performed using 50 µL aliquots drawn from the prepared mixture. The stained cells were incubated at room temperature for 15 min followed by image acquisition with a Molecular Devices® ImageXpress Micro XLS Widefield High-Content Analysis System using a DAPI

filter for Hoechst 33342 and a FITC filter for Annexin V. Acquired images were analysed using the Cell Cycle analysis module of the MetaXpress® High-Content Image Acquisition and Analysis Software.

5.6.4 Hoechst 33342/ Annexin-PI (Phosphatidylserine translocation)

To determine phosphatidylserine translocation, HeLa cells were seeded and treated with compound **3.17** as in Section 5.6.3 and 10 µg/mL of PI further added after staining with Hoechst 33342 and PI and before cellular imaging. Image acquisition with a Molecular Devices® ImageXpress Micro XLS Widefield High-Content Analysis System was done using DAPI, FITC and Texas Red filters for Hoechst 33342, Annexin V and PI respectively. Acquired images were analysed using the Multiwavelength Cell Scoring analysis module of the MetaXpress® High-Content Image Acquisition and Analysis Software.

5.6.5 TMRE (Mitochondrial Membrane Depolarization)

To determine mitochondrial membrane depolarization, HeLa cells were seeded and treated with compound **3.17** as above. A mixture of 0.05 mM tetramethylrhodamine ethyl ester (TMRE) (50 µL) and 5 µg/mL Hoechst 33342 in 10 mL PBS was prepared. After aspiration of the treatment medium, 100 µL aliquots of the prepared mixture were added to the cells and incubated in the dark at 37 °C for 30 min. Image acquisition with a Molecular Devices® ImageXpress Micro XLS Widefield High-Content Analysis System was done using the DAPI filter for hoechst 33342 and the tetramethylrhodamine (TRITC) filter for TMRE. Acquired images were analysed using the Multiwavelength Cell Scoring analysis module of the MetaXpress® High-Content Image Acquisition and Analysis Software.

5.6.6 Caspase Activation (Caspase -8 and -3)

To determine caspase activation, HeLa cells were seeded and treated with compound **3.17** as above. After aspiration of the treatment medium, cells were fixed and permeabilized by adding 50 µL of 4% formaldehyde and incubating at room temperature for 15 min. To this, 10 µL of PBS containing magnesium and calcium was added and the resulting mixture aspirated. 50 µL of 80% ice cold MeOH was added and the cells incubated at -20 °C for 10 min. For treatment with antibody solution, the MeOH was aspirated and 100 µL of PBS was added. Aspiration of the PBS was followed by the addition of 100 µL of 0.5% Bovine serum albumin (BSA) in PBS as blocking solution and incubation at room temperature for 10 min. After aspiration, 50 µL of

antibody solution containing caspase 3 (dilution factor 1:200) and caspase 8 (dilution factor 1:100) were added and the cells incubated in the dark at 37 °C for 60 min. Cells were washed once with blocking solution followed by addition of 50 µL of the secondary antibody anti-rabbit IgG F(ab′)2 fragment (Alexa fluor® 647 conjugate) (dilution factor 1:500) for 30 min. The cells were washed once with blocking solution followed by the addition of 100 µL of Hoechst 33342 at 5 µg/mL. Image acquisition with a Molecular Devices® ImageXpress Micro XLS Widefield High-Content Analysis System was done using DAPI and Cy5 filters for Hoechst 33342 and Alexa fluor 647 respectively. Acquired images were analysed using the Multiwavelength Cell Scoring analysis module of the MetaXpress® High-Content Image Acquisition and Analysis Software.

5.6.7 Lysotracker® Red (Autophagy)

To determine the induction of autophagy, HeLa cells were seeded and treated with compound **3.17** as above. A mixture of 50 nM Lysotracker® Red (0.5 µL) and 5 µg/mL hoechst 33342 in 10 mL PBS was prepared. After aspiration of the treatment medium, cells were stained by the addition of 100 µL aliquots of the prepared mixture and incubated in the dark at 37 °C for 30 min. Image acquisition with a Molecular Devices® ImageXpress Micro XLS Widefield High-Content Analysis System was done using DAPI and TRITC filters for Hoechst 33342 and TMRE respectively. Acquired images were analysed using the Multiwavelength Cell Scoring analysis module of the MetaXpress® High-Content Image Acquisition and Analysis Software.

References

Adela, R.C. & Lionel, L.B. 2006. VEGF Inhibitors in Cancer Therapy. *Current Pharmaceutical Design*, 12, (3) 387-394 available from: http://www.eurekaselect.com/node/55604/article

Ahmad, A., Kaleem, M., Ahmed, Z., & Shafiq, H. 2015. Therapeutic potential of flavonoids and their mechanism of action against microbial and viral infections - A review. *Food Research International*, 77, 221-235 available from: http://www.sciencedirect.com/science/article/pii/S0963996915300673

Amancio, C. 2010. The PKB/AKT Pathway in Cancer. *Current Pharmaceutical Design*, 16, (1) 34-44 available from: http://www.eurekaselect.com/node/70604/article

An, F.A.N., Wang, S.H.U., Tian, Q.I.N., & Zhu, D.E.N. 2015. Effects of orientin and vitexin from *Trollius chinensis* on the growth and apoptosis of esophageal cancer EC-109 cells. *Oncology Letters*, 10, (4) 2627-2633 available from: http://www.ncbi.nlm.nih.gov/pmc/articles/PMC4580036/

Angelino, D., Berhow, M., Ninfali, P., & Jeffery, E. 2013. *Caecal absorption of vitexin-2-O-xyloside and its aglycone apigenin, in the rat*, 4 ed.

Ashida, H. 2000. Suppressive effects of flavonoids on dioxin toxicity. *BioFactors (Oxford, England)*, 12, (1-4) 201-206 available from: http://europepmc.org/abstract/MED/11216487;https://doi.org/10.1002/biof.5520120132

Bernardi, P., Vassanelli, S., Veronese, P., Colonna, R., Szab+¦, I., & Zoratti, M. 1992. Modulation of the mitochondrial permeability transition pore. Effect of protons and divalent cations. *Journal of Biological Chemistry*, 267, (5) 2934-2939 available from: http://www.jbc.org/content/267/5/2934.abstract

Bo, Y., Sun, J., Wang, M., Ding, J., Lu, Q., & Yuan, L. 2016. Dietary flavonoid intake and the risk of digestive tract cancers: a systematic review and meta-analysis. *Scientific Reports*, 6, 24836 available from: http://www.ncbi.nlm.nih.gov/pmc/articles/PMC4845003/

Boatright, K.M. & Salvesen, G.S. 2003. Mechanisms of caspase activation. *Current Opinion in Cell Biology*, 15, (6) 725-731 available from: http://www.sciencedirect.com/science/article/pii/S0955067403001364

Boulares, A.H., Yakovlev, A.G., Ivanova, V., Stoica, B.A., Wang, G., Iyer, S., & Smulson, M. 1999. Role of Poly(ADP-ribose) Polymerase (PARP) Cleavage in Apoptosis: Caspace 3-Resistant PARP Mutant Increases Rates of Apoptosis in Transfected Cells. *Journal of Biological Chemistry*, 274, (33) 22932-22940 available from: http://www.jbc.org/content/274/33/22932.abstract

Braune, A. & Blaut, M. 2012. *Intestinal Bacterium Eubacterium cellulosolvens Deglycosylates Flavonoid C- and O-Glucosides*, 78 ed.

Braune, A. & Blaut, M. 2016. Bacterial Species Involved in the Conversion of Dietary Flavonoids in the Human Gut. *Gut Microbes*, 7, (3) 216-234 available from: http://www.ncbi.nlm.nih.gov/pmc/articles/PMC4939924/

Buqui, G.A., Sy, S.K.B., Merino-Sanjuán, M., Gouvea, D.R., Nixdorf, S.L., Kimura, E., Derendorf, H., Lopes, N.P., & Diniz, A. 2015. Characterization of intestinal absorption of *C*-glycoside flavonoid vicenin-2 from *Lychnophora ericoides* leafs in rats by nonlinear mixed effects modeling. *Revista Brasileira de Farmacognosia*, 25, (3) 212-218 available from: http://www.sciencedirect.com/science/article/pii/S0102695X15000848

Cao, X., Liu, B., Cao, W., Zhang, W., Zhang, F., Zhao, H., Meng, R., Zhang, L., Ruifang, N., Hao, X., & Zhang, B. 2013. *Autophagy inhibition enhances apigenin-induced apoptosis in human breast cancer cells*, 25 ed.

Carmeliet, P. & Jain, R.K. 2000. Angiogenesis in cancer and other diseases. *Nature*, 407, 249 available from: http://dx.doi.org/10.1038/35025220

Chaitanya, G.V., Alexander, J.S., & Babu, P.P. 2010. PARP-1 cleavage fragments: signatures of cell-death proteases in neurodegeneration. *Cell Communication and Signaling : CCS*, 8, 31 available from: http://www.ncbi.nlm.nih.gov/pmc/articles/PMC3022541/

Chazotte, B. 2011. Labeling Mitochondria with TMRM or TMRE. *Cold Spring Harbor Protocols*, 2011, (7) db available from: http://cshprotocols.cshlp.org/content/2011/7/pdb.prot5641.abstract

Chen, D., Frezza, M., Schmitt, S., Kanwar, J., & Dou, Q.P. 2011. Bortezomib as the First Proteasome Inhibitor Anticancer Drug: Current Status and Future Perspectives. *Current Cancer Drug Targets*, 11, (3) 239-253 available from: http://www.ncbi.nlm.nih.gov/pmc/articles/PMC3306611/

Chen, Y., Williams, V., Filippova, M., Filippov, V., & Duerksen-Hughes, P. 2014. Viral Carcinogenesis: Factors Inducing DNA Damage and Virus Integration. *Cancers*, 6, (4) 2155-2186 available from: http://www.ncbi.nlm.nih.gov/pmc/articles/PMC4276961/

Clevers, H. 2006. Wnt/b-Catenin Signaling in Development and Disease. *Cell*, 127, (3) 469-480 available from: http://www.sciencedirect.com/science/article/pii/S0092867406013444

Costache, M.I., Mihai, I., Sevastita, I., Ene, D., Cornelia, A.C., & Saftoiu, A. 2015. VEGF expression in pancreatic cancer and other malignancies: a review of the literature. *Romanian Journal of Internal Medicine*, 53, (3) 199-208 available from: https://content.sciendo.com/view/journals/rjim/53/3/article-p199.xml

Cottet-Rousselle, C., Ronot, X., Leverve, X., & Mayol, J.F. 2011. Cytometric assessment of mitochondria using fluorescent probes. *Cytometry Part A*, 79A, (6) 405-425 available from: https://doi.org/10.1002/cyto.a.21061 Accessed 22 October 2018.

Courts, F.L. & Williamson, G. 2009. The *C*-glycosyl Flavonoid, Aspalathin, is Absorbed, Methylated and Glucuronidated Intact in Humans. *Molecular Nutrition & Food Research*, 53, (9) 1104-1111 available from: https://doi.org/10.1002/mnfr.200800569 Accessed 1 September 2018.

Creagh, E.M. & Martin, S.J. 2001. Caspases: cellular demolition experts. *Biochemical Society Transactions*, 29, (6) 696 available from: http://www.biochemsoctrans.org/content/29/6/696.abstract

Crozier, A., Jaganath, I.B., & Clifford, M.N. 2009. Dietary phenolics: chemistry, bioavailability and effects on health. *Natural Product Reports*, 26, (8) 1001-1043 available from: http://dx.doi.org/10.1039/B802662A

Cui, L., Liu, X., Tian, Y., Xie, C., Li, Q., Cui, H., & Sun, C. 2016. Flavonoids, Flavonoid Subclasses, and Esophageal Cancer Risk: A Meta-Analysis of Epidemiologic Studies. *Nutrients*, 8, (6) 350 available from: http://www.ncbi.nlm.nih.gov/pmc/articles/PMC4924191/

Cuyckens, F. & Claeys, M. 2004. Mass spectrometry in the structural analysis of flavonoids. *Journal of Mass Spectrometry*, 39, (1) 1-15 available from: http://dx.doi.org/10.1002/jms.585

Czemplik, M., Mierziak, J., Szopa, J., & Kulma, A. 2016. Flavonoid *C*-glucosides Derived from Flax Straw Extracts Reduce Human Breast Cancer Cell Growth *In vitro* and Induce Apoptosis. *Front Pharmacol*, 7, 282 available from: http://europepmc.org/abstract/MED/27630565;http://europepmc.org/articles/PMC5006111?pdf=render;http://europepmc.org/articles/PMC5006111;https://doi.org/10.3389/fphar.2016.00282

de Miguel, D., Lemke, J., Anel, A., Walczak, H., & Martinez-Lostao, L. 2016. Onto better TRAILs for cancer treatment. *Cell Death and Differentiation*, 23, (5) 733-747 available from: http://www.ncbi.nlm.nih.gov/pmc/articles/PMC4832109/

DeFelice, L. S. Nutraceuticals - Opportunities in an Emerging Market. http://www.fimdefelice.org/p2463.html . 1992. Scrip Magazine. 6-7-2018.
Ref Type: Online Source

Desagher, S. & Martinou, J.C. 2000. Mitochondria as the central control point of apoptosis. *Trends in Cell Biology*, 10, (9) 369-377 available from: https://doi.org/10.1016/S0962-8924(00)01803-1 Accessed 19 October 2018.

Dhasarathy, A., Phadke, D., Mav, D., Shah, R.R., & Wade, P.A. 2011. The Transcription Factors Snail and Slug Activate the Transforming Growth Factor-Beta Signaling Pathway in Breast Cancer. *PLOS ONE*, 6, (10) e26514 available from: https://doi.org/10.1371/journal.pone.0026514

Dickens, L.S., Boyd, R.S., Jukes-Jones, R., Hughes, M.A., Robinson, G.L., Fairall, L., Schwabe, J.W., Cain, K., & MacFarlane, M. 2012. A Death Effector Domain Chain DISC Model Reveals a Crucial Role for Caspase-8 Chain Assembly in Mediating Apoptotic Cell Death. *Molecular Cell*, 47, (2) 291-305 available from: http://www.sciencedirect.com/science/article/pii/S1097276512003875

Dong, G.A.O., Mao, Q.I.X., Xia, W.E.N., Xu, Y.O.U., Wang, J.I., Xu, L.I., & Jiang, F.E.N. 2016. PKM2 and cancer: The function of PKM2 beyond glycolysis. *Oncology Letters*, 11, (3) 1980-1986 available from: http://www.ncbi.nlm.nih.gov/pmc/articles/PMC4774429/

Duronio, V. 2008. The life of a cell: apoptosis regulation by the PI3K/PKB pathway. *Biochemical Journal*, 415, (3) 333 available from: http://www.biochemj.org/content/415/3/333.abstract

Edenharder, R. & Tang, X. 1997. Inhibition of the mutagenicity of 2-nitrofluorene, 3-nitrofluoranthene and 1-nitropyrene by flavonoids, coumarins, quinones and other phenolic compounds. *Food and Chemical Toxicology*, 35, (3) 357-372 available from: http://www.sciencedirect.com/science/article/pii/S0278691597001257

Erdogan, S., Doganlar, O., Doganlar, Z.B., Serttas, R., Turkekul, K., Dibirdik, I., & Bilir, A. 2016. The flavonoid apigenin reduces prostate cancer CD44+ stem cell survival and migration through PI3K/Akt/NF-kB signaling. *Life Sciences*, 162, 77-86 available from: http://www.sciencedirect.com/science/article/pii/S0024320516304908

Ferrara, N. & Henzel, W.J. 1989. Pituitary follicular cells secrete a novel heparin-binding growth factor specific for vascular endothelial cells. *Biochemical and Biophysical Research Communications*, 161, (2) 851-858 available from: http://www.sciencedirect.com/science/article/pii/0006291X89926788

Ferrara, N., Hillan, K.J., & Novotny, W. 2005. Bevacizumab (Avastin), a humanized anti-VEGF monoclonal antibody for cancer therapy. *Biochemical and Biophysical Research Communications*, 333, (2) 328-335 available from: http://www.sciencedirect.com/science/article/pii/S0006291X05011344

Galati, G. 2004. *Potential toxicity of flavonoids and other dietary phenolics: significance for their chemopreventive and anticancer properties*, 37 ed.

Ganesan, R., Mallets, E., & Gomez-Cambronero, J. 2016. The transcription factors Slug (SNAI2) and Snail (SNAI1) regulate phospholipase D (PLD) promoter in opposite ways towards cancer cell invasion. *Molecular Oncology*, 10, (5) 663-676 available from: http://www.sciencedirect.com/science/article/pii/S1574789115002422

García, E. R., Gutierrez, E.A., de Melo, F.C.S.A., Novaes, R.M.D., & Gonçalves, R.V. 2018. Flavonoids Effects on Hepatocellular Carcinoma in Murine Models: A Systematic Review. *Evidence-based Complementary and Alternative Medicine : eCAM*, 2018, 6328970 available from: http://www.ncbi.nlm.nih.gov/pmc/articles/PMC5850900/

Gaspar, A., Matos, M.J., Garrido, J., Uriarte, E., & Borges, F. 2014. Chromone: A Valid Scaffold in Medicinal Chemistry. *Chemical Reviews*, 114, (9) 4960-4992 available from: https://doi.org/10.1021/cr400265z

Gouvea, D., Ribeiro, A., hormann, U., Lopes, N., & Butterweck, V. 2013. *Evaluation of Intestinal Permeability of Vicenin-2 and Lychnopholic Acid from Lychnophora salicifolia (Brazilian Arnicão) Using Caco-2 Cells*, 77 ed.

Gyawali, B. & Iddawela, M. 2017. Bevacizumab in Advanced Cervical Cancer: Issues and Challenges for Low- and Middle-Income Countries. *Journal of global oncology*, 3, (2) 93-97 available from: http://www.ncbi.nlm.nih.gov/pmc/articles/PMC5493276/

Halestrap, A.P., McStay, G.P., & Clarke, S.J. 2002. The permeability transition pore complex: another view. *Biochimie*, 84, (2) 153-166 available from: http://www.sciencedirect.com/science/article/pii/S0300908402013755

Halliwell, B. 1997. Antioxidants and Human Disease: A General Introduction. *Nutrition Reviews*, 55, (1) S44-S49 available from: https://doi.org/10.1111/j.1753-4887.1997.tb06100.x Accessed 13 August 2018.

Harlid, S., Adgent, M., Jefferson, W.N., Panduri, V., Umbach, D.M., Xu, Z., Stallings, V.A., Williams, C.J., Rogan, W.J., & Taylor, J.A. 2017. Soy Formula and Epigenetic Modifications: Analysis of Vaginal Epithelial Cells from Infant Girls in the IFED Study. *Environmental*

Health Perspectives, 125, (3) 447-452 available from: http://www.ncbi.nlm.nih.gov/pmc/articles/PMC5332195/

He, J.D., Wang, Z., Li, S.P., Xu, Y.J., Yu, Y., Ding, Y.J., Yu, W.L., Zhang, R.X., Zhang, H.M., & Du, H.Y. 2016. Vitexin suppresses autophagy to induce apoptosis in hepatocellular carcinoma via activation of the JNK signaling pathway. *Oncotarget*, 7, (51) 84520-84532 available from: http://www.ncbi.nlm.nih.gov/pmc/articles/PMC5356678/

Hemmings, B.A. & Restuccia, D.F. 2012. PI3K-PKB/Akt Pathway. *Cold Spring Harbor Perspectives in Biology*, 4, (9) a011189 available from: http://www.ncbi.nlm.nih.gov/pmc/articles/PMC3428770/

Hisanaga, A., Mukai, R., Sakao, K., Terao, J., & Hou, D.X. 2016. *Anti-inflammatory effects and molecular mechanisms of 8-prenyl quercetin*, 60 ed.

Hollman, P.C., de Vries, J.H., van Leeuwen, S.D., Mengelers, M.J., & Katan, M.B. 1995. Absorption of dietary quercetin glycosides and quercetin in healthy ileostomy volunteers. *The American Journal of Clinical Nutrition*, 62, (6) 1276-1282 available from: http://dx.doi.org/10.1093/ajcn/62.6.1276

Horinaka, M., Yoshida, T., Shiraishi, T., Nakata, S., Wakada, M., & Sakai, T. 2006. The dietary flavonoid apigenin sensitizes malignant tumor cells to tumor necrosis factor-related apoptosis-inducing ligand. *Molecular Cancer Therapeutics*, 5, (4) 945 available from: http://mct.aacrjournals.org/content/5/4/945.abstract

Hua, X., Yu, L., You, R., Yang, Y., Liao, J., Chen, D., & Yu, L. 2016. Association among Dietary Flavonoids, Flavonoid Subclasses and Ovarian Cancer Risk: A Meta-Analysis. *PLOS ONE*, 11, (3) e0151134 available from: https://doi.org/10.1371/journal.pone.0151134

Hui, C., Qi, X., Qianyong, Z., Xiaoli, P., Jundong, Z., & Mantian, M. 2013. Flavonoids, Flavonoid Subclasses and Breast Cancer Risk: A Meta-Analysis of Epidemiologic Studies. *PLOS ONE*, 8, (1) e54318 available from: https://doi.org/10.1371/journal.pone.0054318

Hurwitz, A.A., Foster, B.A., Allison, J.P., Greenberg, N.M., & Kwon, E. 2001. The TRAMP Mouse as a Model for Prostate Cancer. *Current Protocols in Immunology*, 45, (1) 20 available from: https://doi.org/10.1002/0471142735.im2005s45 Accessed 18 July 2018.

Hwang, S.Y., Deng, X., Byun, S., Lee, C., Lee, S.J., Suh, H., Zhang, J., Kang, Q., Zhang, T., Westover, K.D., Mandinova, A., & Lee, S.W. 2016. Direct Targeting of b-Catenin by a Small Molecule Stimulates Proteasomal Degradation and Suppresses Oncogenic Wnt/b-Catenin Signaling. *Cell Reports*, 16, (1) 28-36 available from: http://www.sciencedirect.com/science/article/pii/S2211124716306842

Ito, C., Itoigawa, M., Tan, H.T.W., Tokuda, H., Yang Mou, X., Mukainaka, T., Ishikawa, T., Nishino, H., & Furukawa, H. 2000. Anti-tumor-promoting effects of isoflavonoids on Epstein-Barr virus activation and two-stage mouse skin carcinogenesis. *Cancer Letters*, 152, (2) 187-192 available from: http://www.sciencedirect.com/science/article/pii/S0304383500003311

Itoigawa, M., Ito, C., Ju-ichi, M., Nobukuni, T., Ichiishi, E., Tokuda, H., Nishino, H., & Furukawa, H. 2002. Cancer chemopreventive activity of flavanones on Epstein-Barr virus activation and two-stage mouse skin carcinogenesis. *Cancer Letters*, 176, (1) 25-29 available from: http://www.sciencedirect.com/science/article/pii/S0304383501007406

Iwase, Y., Takemura, Y., Ju-ichi, M., Mukainaka, T., Ichiishi, E., Ito, C., Furukawa, H., Yano, M., Tokuda, H., & Nishino, H. 2001. Inhibitory effect of flavonoid derivatives on Epstein-Barr virus activation and two-stage carcinogenesis of skin tumors. *Cancer Letters*, 173, (2) 105-109 available from: http://www.sciencedirect.com/science/article/pii/S0304383501006152

Jung Choi, H., Eun, J., Geul Kim, B., Kim, S., Jeon, H., & Soh, Y. 2007. *Vitexin, an HIF-1a inhibitor, has anti-metastatic potential in PC12 cells*, 22 ed.

Jung, U.J., Lee, M.K., Park, Y.B., Kang, M.A., & Choi, M.S. 2006. Effect of citrus flavonoids on lipid metabolism and glucose-regulating enzyme mRNA levels in type-2 diabetic mice. *The International Journal of Biochemistry & Cell Biology*, 38, (7) 1134-1145 available from: http://www.sciencedirect.com/science/article/pii/S1357272505004103

Kaleem, M. & Ahmad, A. 2018, "Chapter 8 - Flavonoids as Nutraceuticals," *In Therapeutic, Probiotic, and Unconventional Foods*, A. M. Grumezescu & A. M. Holban, eds., Academic Press, pp. 137-155.

Kalluri, R. & Weinberg, R.A. 2009. The basics of epithelial-mesenchymal transition. *The Journal of Clinical Investigation*, 119, (6) 1420-1428 available from: http://www.ncbi.nlm.nih.gov/pmc/articles/PMC2689101/

Kang, C.H., Molagoda, I.M.N., Choi, Y.H., Park, C., Moon, D.O., & Kim, G.Y. 2018. Apigenin promotes TRAIL-mediated apoptosis regardless of ROS generation. *Food and Chemical Toxicology*, 111, 623-630 available from: http://www.sciencedirect.com/science/article/pii/S0278691517307597

Kilani-Jaziri, S., Frachet, V., Bhouri, W., Ghedira, K., Chekir-Ghedira, L., & Ronot, X. 2012. Flavones inhibit the proliferation of human tumor cancer cell lines by inducing apoptosis. *Drug and Chemical Toxicology*, 35, (1) 1-10 available from: https://doi.org/10.3109/01480545.2011.564180

Kim, M. 2015. Deglycosylation of isoflavone C-glycosides by newly isolated human intestinal bacteria. *Journal of the science of food and agriculture*, v. 95, (no. 9) 1925-2015

Kroemer, G. & Reed, J.C. 2000. Mitochondrial control of cell death. *Nature Medicine*, 6, 513 available from: http://dx.doi.org/10.1038/74994

Lai, C.Y., Tsai, A.C., Chen, M.C., Chang, L.H., Sun, H.L., Chang, Y.L., Chen, C.C., Teng, C.M., & Pan, S.L. 2012. Aciculatin Induces p53-Dependent Apoptosis via MDM2 Depletion in Human Cancer Cells *In vitro* and *In vivo*. *PLOS ONE*, 7, (8) e42192 available from: https://doi.org/10.1371/journal.pone.0042192

Lambert, J.D., Sang, S., & Yang, C.S. 2007. Possible Controversy over Dietary Polyphenols: Benefits vs Risks. *Chemical Research in Toxicology*, 20, (4) 583-585 available from: https://doi.org/10.1021/tx7000515

Lee, C.Y., Chien, Y.S., Chiu, T.H., Huang, W.W., Lu, C.C., Chiang, J.H., & Yang, J.S. 2012. *Apoptosis triggered by vitexin in U937 human leukemia cells via a mitochondrial signaling pathway*, 28 ed.

Lee, M.J., Wang, Z.Y., Li, H., Chen, L., Sun, Y., Gobbo, S., Balentine, D.A., & Yang, C.S. 1995. Analysis of plasma and urinary tea polyphenols in human subjects. *Cancer Epidemiology*

Biomarkers & Prevention, 4, (4) 393 available from: http://cebp.aacrjournals.org/content/4/4/393.abstract

Lee, Y., Sung, B., Kang, Y.J., Kim, D.H., Jang, J.Y., Hwang, S.Y., Kim, M., Lim, H.S., Yoon, J.H., Chung, H.Y., & Kim, N.D. 2014. Apigenin-induced apoptosis is enhanced by inhibition of autophagy formation in HCT116 human colon cancer cells. *International Journal of Oncology*, 44, (5) 1599-1606 available from: https://app.dimensions.ai/details/publication/pub.1071513429 Accessed 8 August 2018.

Leist, M. & Nicotera, P. 1997. The Shape of Cell Death. *Biochemical and Biophysical Research Communications*, 236, (1) 1-9 available from: http://www.sciencedirect.com/science/article/pii/S0006291X9796890X

Li, S., Yang, L.j., Wang, P., He, Y.j., Huang, J.m., Liu, H.w., Shen, X.f., & Wang, F. 2016. *Dietary apigenin potentiates the inhibitory effect of interferon-a on cancer cell viability through inhibition of 26S proteasome-mediated interferon receptor degradation*, 60 ed.

Liu, J., Cao, X.C., Xiao, Q., & Quan, M.F. 2014. *Apigenin inhibits HeLa sphere-forming cells through inactivation of casein kinase 2a*, 11 ed.

Logan, C.Y. & Nusse, R. 2004. The Wnt Signaling Pathway in Development and Disease. *Annual Review of Cell and Developmental Biology*, 20, (1) 781-810 available from: https://doi.org/10.1146/annurev.cellbio.20.010403.113126 Accessed 31 July 2018.

López-Lázaro, M. Flavonoids as Anticancer Agents: Structure-Activity Relationship Study. Current Medicinal Chemistry - Anti-Cancer Agents 2[6], 691-714. 11-1-2002.
Ref Type: Abstract

Luo, G.G. & Ou, J.H.J. 2015. Oncogenic viruses and cancer. *Virologica Sinica*, 30, (2) 83-84 available from: http://www.ncbi.nlm.nih.gov/pmc/articles/PMC4731227/

Luo, H., Jiang, B.H., King, S.M., & Chen, Y.C. 2008. Inhibition of Cell Growth and VEGF Expression in Ovarian Cancer Cells by Flavonoids. *Nutrition and Cancer*, 60, (6) 800-809 available from: https://doi.org/10.1080/01635580802100851

Ly, J.D., Grubb, D.R., & Lawen, A. 2003. The mitochondrial membrane potential (Dym) in apoptosis; an update. *Apoptosis*, 8, (2) 115-128 available from: https://doi.org/10.1023/A:1022945107762

Manach, C., Scalbert, A., Morand, C., Rémésy, C., & Jiménez, L. 2004. Polyphenols: food sources and bioavailability. *The American Journal of Clinical Nutrition*, 79, (5) 727-747 available from: http://dx.doi.org/10.1093/ajcn/79.5.727

Marais, P. J. J., Deavours, B., Dixon, A. R., & Ferreira, D. 2006, "The Stereochemistry of Flavonoids," *In The Science of Flavonoids*, E. Grotewold, ed., Columbus Oho: Springer, pp. 1-46.

McLaughlin-Drubin, M.E. & Munger, K. 2008. Viruses Associated with Human Cancer. *Biochimica et biophysica acta*, 1782, (3) 127-150 available from: http://www.ncbi.nlm.nih.gov/pmc/articles/PMC2267909/

Melo, E.B., Martins, J.P.A., Jorge, T.C.M., Friozi, M.C., & Ferreira, M.M.C. 2010. Multivariate QSAR study on the antimutagenic activity of flavonoids against 3-NFA on Salmonella typhimurium TA98. *European Journal of Medicinal Chemistry*, 45, (10) 4562-4569

Minion, L.E., Bai, J., Monk, B.J., Robin Keller, L., Ramez, E.N., Forde, G.K., Chan, J.K., & Tewari, K.S. 2015. A Markov model to evaluate cost-effectiveness of antiangiogenesis therapy using bevacizumab in advanced cervical cancer. *Gynecologic Oncology*, 137, (3) 490-496 available from: https://doi.org/10.1016/j.ygyno.2015.02.027 Accessed 30 July 2018.

Mohammed, R., Abou Zeid, A.H., El Hawary, S.S., Sleem, A.A., & Ashour, W.E. 2014. *Flavonoid constituents, cytotoxic and antioxidant activities of Gleditsia triacanthos L. Leaves*.

Mohan, C. 2009a, "Angiogenesis: Its Role in Tumor Growth and Metastasis," *In Signal Transduction - A Short Overview of Its Role in Health and Disease*, C. Mohan, ed., San Diego, California: Merck, pp. 87-90.

Mohan, C. 2009b, "Poly(ADP-ribosylation): PARP in DNA Repair and Apoptosis," *In Signal Transduction - A Short Overview of its Role in Health and Disease*, C. Mohan, ed., San Diego, CA: Merck, pp. 49-52.

Morin, P.J. 1999. b-catenin signaling and cancer. *BioEssays*, 21, (12) 1021-1030 available from: https://doi.org/10.1002/(SICI)1521-1878(199912)22:1<1021::AID-BIES6>3.0.CO;2-P Accessed 31 July 2018.

Morris, M.E. & Zhang, S. 2006. Flavonoid-drug interactions: Effects of flavonoids on ABC transporters. *Life Sciences*, 78, (18) 2116-2130 available from: http://www.sciencedirect.com/science/article/pii/S0024320505012385

Mukai, R. 2018. Prenylation enhances the biological activity of dietary flavonoids by altering their bioavailability. *Bioscience, Biotechnology, and Biochemistry*, 82, (2) 207-215 available from: https://doi.org/10.1080/09168451.2017.1415750

Nakamura, S. & Yoshimori, T. 2017. New insights into autophagosome-lysosome fusion. *Journal of Cell Science*, 130, (7) 1209 available from: http://jcs.biologists.org/content/130/7/1209.abstract

Nandi, D., Tahiliani, P., Kumar, A., & Chandu, D. 2006. The ubiquitin-proteasome system. *Journal of Biosciences*, 31, (1) 137-155 available from: https://doi.org/10.1007/BF02705243

Naujokat, C. & Hoffmann, S. 2002. Role and Function of the 26S Proteasome in Proliferation and Apoptosis. *Laboratory Investigation*, 82, 965 available from: http://dx.doi.org/10.1097/01.LAB.0000022226.23741.37

Oyama, K., Yoshida, K., & Tadao, K. 2011. Recent Progress in the Synthesis of Flavonoids: From Monomers to Supra-Complex Molecules. *Current Organic Chemistry*, 15, (15) 2567-2607 available from: http://www.eurekaselect.com/node/74615/article

Papi, A., Farabegoli, F., Iori, R., Orlandi, M., De Nicola, G.R., Bagatta, M., Angelino, D., Gennari, L., & Ninfali, P. 2013. *Vitexin-2-O-xyloside, raphasatin and (-)-epigallocatechin-3-gallate synergistically affect cell growth and apoptosis of colon cancer cells*, 138 ed.

Pecina-Slaus, N. 2003. Tumor suppressor gene E-cadherin and its role in normal and malignant cells. *Cancer Cell International*, 3, 17 available from: http://www.ncbi.nlm.nih.gov/pmc/articles/PMC270068/

Perry, S.W., Norman, J.P., Barbieri, J., Brown, E.B., & Gelbard, H.A. 2011. Mitochondrial membrane potential probes and the proton gradient: a practical usage guide. *BioTechniques*, 50, (2) 98-115 available from: https://doi.org/10.2144/000113610 Accessed 20 October 2018.

Petronilli, V., Cola, C., Massari, S., Colonna, R., & Bernardi, P. 1993. Physiological effectors modify voltage sensing by the cyclosporin A-sensitive permeability transition pore of mitochondria. *Journal of Biological Chemistry*, 268, (29) 21939-21945 available from: http://www.jbc.org/content/268/29/21939.abstract

Pierzynska-Mach, A., Janowski, P.A., & Dobrucki, J.W. 2014. Evaluation of acridine orange, LysoTracker Red, and quinacrine as fluorescent probes for long-term tracking of acidic vesicles. *Cytometry Part A*, 85, (8) 729-737 available from: https://doi.org/10.1002/cyto.a.22495 Accessed 13 November 2018.

Pietta, P.G. 2000. *ChemInform Abstract: Flavonoids as Antioxidants*, 31 ed.

Plochmann, K., Korte, G., Koutsilieri, E., Richling, E., Riederer, P., Rethwilm, A., Schreier, P., & Scheller, C. 2007. Structure-activity relationships of flavonoid-induced cytotoxicity on human leukemia cells. *Archives of Biochemistry and Biophysics*, 460, (1) 1-9 available from: http://www.sciencedirect.com/science/article/pii/S0003986107000690

Polak, R. & Buitenhuis, M. 2012. The PI3K/PKB signaling module as key regulator of hematopoiesis: implications for therapeutic strategies in leukemia. *Blood*, 119, (4) 911 available from: http://www.bloodjournal.org/content/119/4/911.abstract

Porter, A.G. & Jänicke, R.U. 1999. Emerging roles of caspase-3 in apoptosis. *Cell Death and Differentiation*, 6, 99 available from: https://doi.org/10.1038/sj.cdd.4400476

Putt, K.S., Chen, G.W., Pearson, J.M., Sandhorst, J.S., Hoagland, M.S., Kwon, J.T., Hwang, S.K., Jin, H., Churchwell, M.I., Cho, M.H., Doerge, D.R., Helferich, W.G., & Hergenrother, P.J. 2006. Small-molecule activation of procaspase-3 to caspase-3 as a personalized anticancer strategy. *Nature Chemical Biology*, 2, 543 available from: https://doi.org/10.1038/nchembio814

Qin, Y., Zhao, D., Zhou, H.g., Wang, X.h., Zhong, W.l., Chen, S., Gu, W.g., Wang, W., Zhang, C.h., Liu, Y.r., Liu, H.j., Zhang, Q., Guo, Y.q., Sun, T., & Yang, C. 2016. Apigenin inhibits

NF-kB and Snail signaling, EMT and metastasis in human hepatocellular carcinoma. *Oncotarget*, 7, (27) 41421-41431 available from: http://www.ncbi.nlm.nih.gov/pmc/articles/PMC5173069/

Rajkumar, S.V., Richardson, P.G., Hideshima, T., & Anderson, K.C. 2005. Proteasome Inhibition As a Novel Therapeutic Target in Human Cancer. *Journal of Clinical Oncology*, 23, (3) 630-639 available from: https://doi.org/10.1200/JCO.2005.11.030 Accessed 19 July 2018.

Ramirez, M.L.G. & Salvesen, G.S. 2018. A primer on caspase mechanisms. *Seminars in Cell & Developmental Biology*, 82, 79-85 available from: http://www.sciencedirect.com/science/article/pii/S1084952117301088

Rawat, P., Kumar, M., Sharan, K., Chattopadhyay, N., & Maurya, R. 2009. Ulmosides A and B: Flavonoid 6-C-glycosides from *Ulmuswallichiana*, stimulating osteoblast differentiation assessed by alkaline phosphatase. *Bioorganic & Medicinal Chemistry Letters*, 19, (16) 4684-4687 available from: http://www.sciencedirect.com/science/article/pii/S0960894X09009056

Reuter, S., Gupta, S.C., Chaturvedi, M.M., & Aggarwal, B.B. 2010. Oxidative stress, inflammation, and cancer: How are they linked? *Free radical biology & medicine*, 49, (11) 1603-1616 available from: http://www.ncbi.nlm.nih.gov/pmc/articles/PMC2990475/

Rhys, A.D., Monteiro, P., Smith, C., Vaghela, M., Arnandis, T., Kato, T., Leitinger, B., Sahai, E., McAinsh, A., Charras, G., & Godinho, S.A. 2018. Loss of E-cadherin provides tolerance to centrosome amplification in epithelial cancer cells. *The Journal of Cell Biology*, 217, (1) 195 available from: http://jcb.rupress.org/content/217/1/195.abstract

Rice-Evans, C.A., Miller, N.J., & Paganga, G. 1996. Structure-antioxidant activity relationships of flavonoids and phenolic acids. *Free Radical Biology and Medicine*, 20, (7) 933-956 available from: http://www.sciencedirect.com/science/article/pii/0891584995022279

Romagnolo, F. & Selmin, O. 2012. *Flavonoids and Cancer Prevention: A Review of the Evidence*, 31 ed.

Ronis, M.J.J., Pedersen, K.B., & Watt, J. 2018. Adverse Effects of Nutraceuticals and Dietary Supplements. *Annual Review of Pharmacology and Toxicology*, 58, (1) 583-601 available from: https://doi.org/10.1146/annurev-pharmtox-010617-052844 Accessed 6 July 2018.

Ross, J.A. & Kasum, C.M. 2002. Dietary Flavonoids: Bioavailability, Metabolic Effects, and Safety. *Annual Review of Nutrition*, 22, (1) 19-34 available from: https://doi.org/10.1146/annurev.nutr.22.111401.144957 Accessed 13 July 2018.

Ruela-de-Sousa, R.R., Fuhler, G.M., Blom, N., Ferreira, C.V., Aoyama, H., & Peppelenbosch, M.P. 2010. Cytotoxicity of apigenin on leukemia cell lines: implications for prevention and therapy. *Cell Death &Amp; Disease*, 1, e19 available from: http://dx.doi.org/10.1038/cddis.2009.18

Sakamuru, S., Attene-Ramos, M.S., & Xia, M. 2016. Mitochondrial Membrane Potential Assay. *Methods in molecular biology (Clifton, N.J.)*, 1473, 17-22 available from: http://www.ncbi.nlm.nih.gov/pmc/articles/PMC5375165/

Salvatore Scarpa, E., Antonini, E., Palma, F., Mari, M., & Ninfali, P. 2017. Antiproliferative activity of vitexin-2-O-xyloside and avenanthramides on CaCo-2 and HepG2 cancer cells occurs through apoptosis induction and reduction of pro-survival mechanisms. *European Journal of Nutrition*, 57, (4) 1381-1395

Salvesen, G.S. & Walsh, C.M. 2014. Functions of caspase 8: the identified and the mysterious. *Seminars in immunology*, 2014/05/21, (3) 246-252 available from: https://www.ncbi.nlm.nih.gov/pubmed/24856110

Schipper, J.L., MacKenzie, S.H., Sharma, A., & Clark, A.C. 2011. A bifunctional allosteric site in the dimer interface of procaspase-3. *Biophysical chemistry*, 2011/05/25, (1) 100-109 available from: https://www.ncbi.nlm.nih.gov/pubmed/21645959

Scotti, L., Mendonça junior, F.J.B., Moreira, D.R.M.M., da Silva, M.S., Pitta, I.R., & Scotti, M.T. 2012. SAR, QSAR and Docking of Anticancer Flavonoids and Variants: A Review. *Current Topics in Medicinal Chemistry*, 12, (24) 2785-2809 available from: http://www.eurekaselect.com/node/108153/article

Sekher Pannala, A., Chan, T.S., O'Brien, P.J., & Rice-Evans, C.A. 2001. Flavonoid B-Ring Chemistry and Antioxidant Activity: Fast Reaction Kinetics. *Biochemical and Biophysical Research Communications*, 282, (5) 1161-1168 available from: http://www.sciencedirect.com/science/article/pii/S0006291X01947059

Shan, S., Shi, J., Yang, P., Jia, B., Wu, H., Zhang, X., & Li, Z. 2017. Apigenin Restrains Colon Cancer Cell Proliferation via Targeted Blocking of Pyruvate Kinase M2-Dependent Glycolysis. *Journal of Agricultural and Food Chemistry*, 65, (37) 8136-8144 available from: https://doi.org/10.1021/acs.jafc.7b02757

Shen, C.C., Cheng, J.J., Lay, H.L., Wu, S.Y., Ni, C.L., Teng, C.M., & Chen, C.C. 2012. Cytotoxic Apigenin Derivatives from *Chrysopogon aciculatis*. *Journal of Natural Products*, 75, 198-201

Shukla, S. & Gupta, S. 2007. Apigenin-induced Cell Cycle Arrest is Mediated by Modulation of MAPK, PI3K-Akt, and Loss of Cyclin D1 Associated Retinoblastoma Dephosphorylation in Human Prostate Cancer Cells. *Cell Cycle*, 6, (9) 1102-1114 available from: https://doi.org/10.4161/cc.6.9.4146

Shukla, S. & Gupta, S. 2010. Apigenin: A Promising Molecule for Cancer Prevention. *Pharmaceutical research*, 27, (6) 962-978 available from: http://www.ncbi.nlm.nih.gov/pmc/articles/PMC2874462/

Shukla, S., MacLennan, G.T., Flask, C.A., Fu, P., Mishra, A., Resnick, M.I., & Gupta, S. 2007a. Blockade of b-Catenin Signaling by Plant Flavonoid Apigenin Suppresses Prostate Carcinogenesis in TRAMP Mice. *Cancer Research*, 67, (14) 6925 available from: http://cancerres.aacrjournals.org/content/67/14/6925.abstract

Shukla, S., MacLennan, T., Flask, C., Fu, P., Mishra, A., Resnick, I., & Gupta, S. 2007b. *Blockade of -Catenin Signaling by Plant Flavonoid Apigenin Suppresses Prostate Carcinogenesis in TRAMP Mice*, 67 ed.

Souza, R.P., Bonfim-Mendonça, P.d., Gimenes, F., Ratti, B.A., Kaplum, V., Bruschi, M.L., Nakamura, C.V., Silva, S.O., Maria-Engler, S.S., & Consolaro, M.E.L. 2017. Oxidative Stress Triggered by Apigenin Induces Apoptosis in a Comprehensive Panel of Human Cervical Cancer-Derived Cell Lines. *Oxidative Medicine and Cellular Longevity*, 2017, 1512745 available from: http://www.ncbi.nlm.nih.gov/pmc/articles/PMC5278229/

Su, C., Haskins, H.A., Omata, C., Aizawa, Y., & Kato, A.T. 2017. PARP Inhibition by Flavonoids Induced Selective Cell Killing to BRCA2-Deficient Cells., 10, (4)

Takayama, T., Shiozaki, H., Shibamoto, S., Oka, H., Kimura, Y., Tamura, S., Inoue, M., Monden, T., Ito, F., & Monden, M. 1996. Beta-catenin expression in human cancers. *The American Journal of Pathology*, 148, (1) 39-46 available from: http://www.ncbi.nlm.nih.gov/pmc/articles/PMC1861624/

Talakatta, G., Kumar, K., & Prasada rao, U. 2016. *C-Glycosylated flavonoids from black gram husk: Protection against DNA and erythrocytes from oxidative damage and their cytotoxic effect on HeLa cells*, 3 ed.

Tan, B.J., Liu, Y., Chang, K.L., Lim, B.K., & Chiu, G.N. 2012. Perorally active nanomicellar formulation of quercetin in the treatment of lung cancer. *International Journal of Nanomedicine*, 7, 651-661 available from: http://www.ncbi.nlm.nih.gov/pmc/articles/PMC3278229/

Tang, F., Wang, Y., Hemmings, B.A., Rüegg, C., & Xue, G. 2018. PKB/Akt-dependent regulation of inflammation in cancer. *Seminars in Cancer Biology*, 48, 62-69 available from: http://www.sciencedirect.com/science/article/pii/S1044579X17301177

Tapas, D., Sakarkar, D.M., & Kakde, R. 2008. Flavonoids as Nutraceuticals: A Review. *Tropical Journal of Pharmaceutical Research*, 7, (3) 1089-1099

van de Schans, M.G.M., Bovee, T.F.H., Stoopen, G.M., Lorist, M., Gruppen, H., & Vincken, J.P. 2015. Prenylation and Backbone Structure of Flavonoids and Isoflavonoids from Licorice and Hop Influence Their Phase I and II Metabolism. *Journal of Agricultural and Food Chemistry*, 63, (49) 10628-10640 available from: https://doi.org/10.1021/acs.jafc.5b04703

Vickers, C.J., González-Páez, G.E., Umotoy, J.C., Cayanan-Garrett, C., Brown, S.J., & Wolan, D.W. 2013. Small-Molecule Procaspase Activators Identified Using Fluorescence Polarization. *ChemBioChem*, 14, (12) 1419-1422 available from: https://doi.org/10.1002/cbic.201300315 Accessed 7 November 2018.

Vogiatzoglou, A., Mulligan, A.A., Lentjes, M.A.H., Luben, R.N., Spencer, J.P.E., Schroeter, H., Khaw, K.T., & Kuhnle, G.G.C. 2015. Flavonoid Intake in European Adults (18 to 64 Years). *PLOS ONE*, 10, (5) e0128132 available from: https://doi.org/10.1371/journal.pone.0128132

Wang, J.G., Zheng, X.X., Zeng, G.Y., Zhou, Y.J., & Yuan, H. 2013. *Purified vitexin compound 1 induces apoptosis through activation of FOXO3a in hepatocellular carcinoma*, 31 ed.

Wang, Y., Kuramitsu, Y., Baron, B., Kitagawa, T., Tokuda, K., Akada, J., Maehara, S., Maehara, Y., & Nakamura, K. 2017. PI3K inhibitor LY294002, as opposed to wortmannin, enhances AKT phosphorylation in gemcitabine-resistant pancreatic cancer cells. *International Journal of Oncology*, 50, (2) 606-612

Wang, Z.q., Weber, N., Lou, Y.j., & Proksch, P. 2006. Prenylflavonoids as nonsteroidal phytoestrogens and related structure-activity relationships. *ChemMedChem*, 1, (4) 482-488 available from: http://europepmc.org/abstract/MED/16892383;https://doi.org/10.1002/cmdc.200500089

Wätjen, W., Weber, N., Lou, Y., Wang, Z., Chovolou, Y., Kampkötter, A., Kahl, R., & Proksch, P. 2007. Prenylation enhances cytotoxicity of apigenin and liquiritigenin in rat H4IIE hepatoma and C6 glioma cells. *Food and Chemical Toxicology*, 45, (1) 119-124 available from: http://www.sciencedirect.com/science/article/pii/S0278691506002213

Wolan, D.W., Zorn, J.A., Gray, D.C., & Wells, J.A. 2009. Small-molecule activators of a proenzyme. *Science (New York, N.Y.)*, 326, (5954) 853-858 available from: https://www.ncbi.nlm.nih.gov/pubmed/19892984

Wu, C.C., Fang, C.Y., Cheng, Y.J., Hsu, H.Y., Chou, S.P., Huang, S.Y., Tsai, C.H., & Chen, J.Y. 2017. Inhibition of Epstein-Barr virus reactivation by the flavonoid apigenin. *Journal of Biomedical Science*, 24, (1) 2 available from: https://doi.org/10.1186/s12929-016-0313-9

Xiao, J., Capanoglu, E., Jassbi, A.R., & Miron, A. 2016. Advance on the Flavonoid C-glycosides and Health Benefits. *Critical Reviews in Food Science and Nutrition*, 56, (sup1) S29-S45 available from: https://doi.org/10.1080/10408398.2015.1067595

Xiao, J. & Högger, P. 2015. Stability of Dietary Polyphenols under the Cell Culture Conditions: Avoiding Erroneous Conclusions. *Journal of Agricultural and Food Chemistry*, 63, (5) 1547-1557 available from: https://doi.org/10.1021/jf505514d

Xie, M., Yu, Y., Kang, R., Zhu, S., Yang, L., Zeng, L., Sun, X., Yang, M., Billiar, T.R., Wang, H., Cao, L., Jiang, J., & Tang, D. 2016. PKM2-dependent glycolysis promotes NLRP3 and

AIM2 inflammasome activation. *Nature Communications*, 7, 13280 available from: http://dx.doi.org/10.1038/ncomms13280

Yang, B., Liu, H., Yang, J., Gupta, V.K., & Jiang, Y. 2018. New insights on bioactivities and biosynthesis of flavonoid glycosides. *Trends in Food Science & Technology*, 79, 116-124 available from: http://www.sciencedirect.com/science/article/pii/S0924224418301559

Yang, C.S., Landau, J.M., Huang, M.T., & Newmark, H.L. 2001. Inhibition of Carcinogenesis by Dietary Polyphenolic Compounds. *Annual Review of Nutrition*, 21, (1) 381-406 available from: https://doi.org/10.1146/annurev.nutr.21.1.381 Accessed 17 July 2018.

Yang, D.S., Li, Z.L., Peng, W.B., Yang, Y.P., Wang, X., Liu, K.C., Li, X.L., & Xiao, W.L. 2015. Three new prenylated flavonoids from *Macaranga denticulata* and their anticancer effects. *Fitoterapia*, 103, 165-170 available from: http://www.sciencedirect.com/science/article/pii/S0367326X1500091X

Yang, H., Landis-Piwowar, K.R., Chen, D., Milacic, V., & Dou, Q.P. 2008. Natural Compounds with Proteasome Inhibitory Activity for Cancer Prevention and Treatment. *Current protein & peptide science*, 9, (3) 227-239 available from: http://www.ncbi.nlm.nih.gov/pmc/articles/PMC3303152/

Yang, S.H., Liao, P.H., Pan, Y.F., Chen, S.L., Chou, S.S., & Chou, M.Y. 2013. *The Novel p53-Dependent Metastatic and Apoptotic Pathway Induced by Vitexin in Human Oral Cancer OC2 Cells*, 27 ed.

Yao, L.H., Jiang, Y.M., Shi, J., Tomás-Barberán, F., Datta, N., Singanusong, R., & Chen, S. 2004. *Flavonoids in Food and Their Health Benefits*, 59 ed.

Yapici, N.B., Bi, Y., Li, P., Chen, X., Yan, X., Mandalapu, S.R., Faucett, M., Jockusch, S., Ju, J., Gibson, K.M., Pavan, W.J., & Bi, L. 2015. Highly Stable and Sensitive Fluorescent Probes (LysoProbes) for Lysosomal Labeling and Tracking. *Scientific Reports*, 5, 8576 available from: https://doi.org/10.1038/srep08576

Zemanová, L., Hofman, J., Novotna, E., Musilek, K., Lundova, T., Havrankova, J., Hostalkova, A., Chlebek, J., Cahlikova, L., & Wsol, V. 2015. *Flavones Inhibit the Activity of AKR1B10, a Promising Therapeutic Target for Cancer Treatment*, 78 ed.

Zeng, P., Zhang, Y., Pan, C., Jia, Q., Guo, F., Li, Y., Zhu, W., & Chen, K. 2013. Advances in Studying of the Pharmacological Activities and Structure-Activity Relationships of Natural *C*-glycosylflavonoids. *Acta Pharmaceutica Sinica B*, 3, (3) 154-162 available from: http://www.sciencedirect.com/science/article/pii/S2211383513000361

Zhang, L., Cheng, X., Gao, Y., Zheng, J., Xu, Q., Sun, Y., Guan, H., Yu, H., & Sun, Z. 2015. *Apigenin induces autophagic cell death in human papillary thyroid carcinoma BCPAP cells*, 6 ed.

Zhang, L., Zuo, Z., & Lin, G. 2007. Intestinal and Hepatic Glucuronidation of Flavonoids. *Molecular Pharmaceutics*, 4, (6) 833-845 available from: https://doi.org/10.1021/mp700077z

Zheng, P.W., Chiang, L.C., & Lin, C.C. 2005. Apigenin induced apoptosis through p53-dependent pathway in human cervical carcinoma cells. *Life Sciences*, 76, (12) 1367-1379 available from: http://www.sciencedirect.com/science/article/pii/S0024320504009683

Zorova, L.D., Popkov, V.A., Plotnikov, E.Y., Silachev, D.N., Pevzner, I.B., Jankauskas, S.S., Babenko, V.A., Zorov, S.D., Balakireva, A.V., Juhaszova, M., Sollott, S.J., & Zorov, D.B. 2018. Mitochondrial membrane potential. *Analytical Biochemistry*, 552, 50-59 available from: http://www.sciencedirect.com/science/article/pii/S0003269717302932

Chapter 6

Target Prediction and *In silico* Molecular Docking of Altissimin in the Aldose Reductase (hAR, AKR1B1) Binding Site

6.1 Introduction

Proteins control a wide array of biological processes by interacting with small molecules or other proteins that bind to them (Schreiber et al. 2015). Understanding these protein-ligand interactions is of great interest, providing an opportunity to better understand protein and ligand function for further therapeutic intervention (McFedries et al. 2013). The interaction between a protein and ligand is known as molecular recognition, and is defined by a complex combination of several factors such as inter-molecular forces between the protein, ligand and surrounding solvent, variation in conformation between binding partners and the thermodynamics of molecular association (Cleaves 2011). Despite the development of experimental and computational techniques to better understand the specific role of these factors, complete understanding of molecular recognition is still a work in progress. This chapter includes a brief review of the important aspects of computational target prediction and analysis of protein-ligand interactions.

6.2 Computer aided drug design (CADD)

In the past, drug discovery used to be predominantly serendipitous, coincidental and most often a trial and error process, also referred to as forward pharmacology (Kubinyi 1999). In contrast, modern day approaches involve rational drug design which begins with a hypothetical pharmacological effect resulting from the modulation of a particular biological target, also referred to as reverse pharmacology (Todd et al. 2009). Analogous to the Latin terms *in vitro*, *in vivo* and *in situ*, the term *in silico* (Pseudo-Latin for *in silicon*) was coined in 1989 as an expression for computer aided rational drug design (Geris and Vermolen 2014). The term *in silico* was first used by a mathematician named Pedro Miramontes during the workshop "Cellular Automata: Theory and Applications" to characterise biological experiments solely performed in a computer (Parimal et al. 2018). Computer aided drug design (CADD) involves the use of computerised technologies to streamline drug discovery and development, the

utilisation of chemical and biological data about ligands and biological targets to develop new drugs and the development of *in silico* filters to disqualify compounds with undesirable physicochemical properties (Kapetanovic 2008). By acting as a virtual shortcut, CADD technologies significantly reduce the number of ligands to be screened in experimental assays and hence, reduce the cost of research (Sliwoski et al. 2014). The two main disciplines of CADD are ligand-based and structure-based (Figure 6.1).

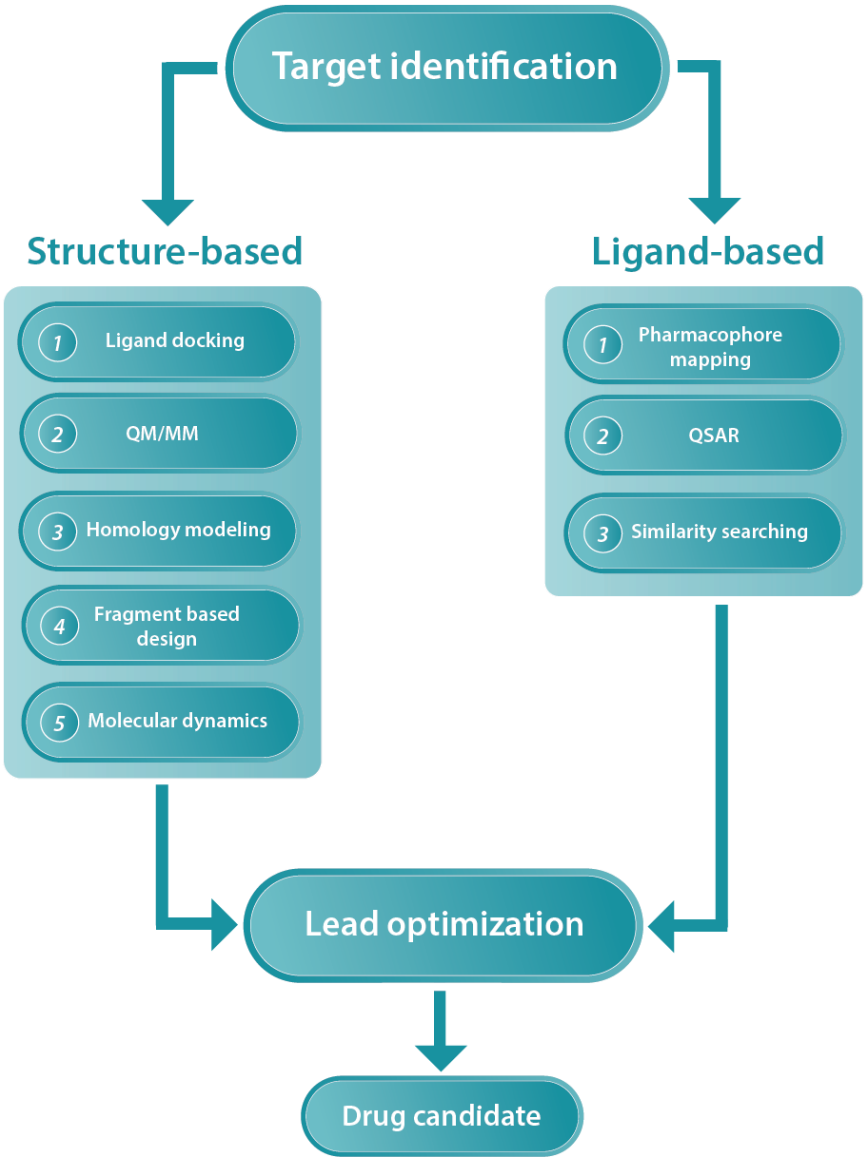

Figure 6.1 An illustration of computer aided drug design (CADD) techniques (Adapted from: Katsila et al. 2016)

6.2.1 Ligand-based CADD

Ligand-based CADD is employed when the structure of the biological target is not properly characterised, as is usually the case with cell surface receptors which are generally difficult to crystallise. Ligand-based CADD employs virtual screening through the molecular docking of large compound libraries (such as the ZINC database) against a target protein to identify compounds that bind to the active site (Irwin et al. 2012). The ligand-based approach heavily relies on the characteristics of bioactive ligands such as physicochemical properties, binding affinities and chemical structure which can be used to develop chemical fingerprints for the identification of similarity hits (Mestres et al. 2006). The ligand-based approach is also employed in the designing of 3D-quantitative structure activity relationship (3D-QSAR) algorithms in which structural and physicochemical descriptors of active and inactive compounds are gathered for use in the prediction of new bioactive compounds (Jitender and Vijay 2010). Recent ligand-based approaches include proteochemometrics modeling (PCM) which combines ligand and protein data into a single predictive model, and polypharmacology modeling which exploits the interaction of single drug molecules to multiple biological targets (Reddy and Zhang 2013; Cortés-Ciriano et al. 2015). Another recent ligand-based method is the similarity ensemble approach (SEA) which is used to predict target proteins for particular compounds of interest.

6.2.1.1 Target protein prediction - Similarity Ensemble Approach (SEA)

Computational target prediction of compounds plays an important role in drug discovery (Katsila et al. 2016). The chemical Similarity Ensemble Approach (SEA) is a promising method which has been successfully applied in many drug-related studies (Wang et al. 2016). This approach considers proteins from a chemocentric point of view, relating them through the chemical similarity of their ligands. The idea is that similar molecules have similar biological profiles and bind similar targets. In 2007, Keiser *et al*. developed the chemical SEA, which relates proteins to one another based on the chemical similarity among their bound ligands (Keiser et al. 2007). Since then, SEA and SEA-like methods have been successfully applied in new target identification for old drugs and natural products (Keiser et al. 2009; Cameron et al. 2013), for side-effect prediction and for the prediction of potential anatomical therapeutic indications (ATCs) of approved drugs (Wu et al. 2013).

6.2.2 Structure-based CADD

With the inception of X-ray crystallography and NMR techniques as utilities for the development of large protein structure depositories such as the protein databank (PDB), increase in the knowledge of biological targets has become the cornerstone of Structure-based CADD (Parasuraman 2012). Through molecular dynamic simulations, a trajectory of protein conformations are rendered over time for the prediction of binding affinities (Hospital et al. 2015). A well-known structure-based approach is homology modeling (also called comparative modeling) which is used when the structure of a biological target is not yet defined. In this case, comparative models are designed as predictors of the protein structure based on structural templates containing similar amino acid sequences (Cavasotto and Phatak 2009). Commonly used homology modeling software include MODELER and SWISS-MODEL (Schwede et al. 2003; Krieger et al. 2005). One of the key structure-based CADD approaches is molecular docking, which is used to predict the preferred orientation of a ligand to its target protein.

6.2.2.1 Molecular docking

Molecular docking is one of the most frequently used methods in structure based drug design because of its ability to predict, with a substantial degree of accuracy, the conformation of small-molecule ligands within the appropriate target binding site (Xuan-Yu et al. 2011). Following the development of the first algorithms in the 1980s, molecular docking became an essential tool in drug discovery (Fabian et al. 2011). For example, investigations involving crucial molecular events, including ligand binding modes and the corresponding intermolecular interactions that stabilize the ligand-receptor complex, can be conveniently performed (Huang and Zou 2010). Furthermore, molecular docking algorithms execute quantitative predictions of binding energetics, providing rankings of docked compounds based on the binding affinity of ligand-receptor complexes (Fabian et al. 2011; Huang and Zou 2010). The identification of the most likely binding conformations require two steps; (i) exploration of a large conformational space representing various potential binding modes; (ii) accurate prediction of the interaction energy associated with each of the predicted binding conformations (Kapetanovic 2008). Molecular docking programs perform these tasks through a cyclic process, in which the ligand conformation is evaluated by specific scoring functions. The commonly used molecular docking software include Autodock (Morris et al. 2009), Autodock Vina (Trott and Olson

2010), Gold (Verdonk et al. 2003), DOCK (Moustakas et al. 2006), GLIDE (Friesner et al. 2006), and SURFLEX (Jain 2003).

6.2.3 Integrating computational approaches to natural product drug discovery

The hallmark of computational drug discovery is what is referred to as 'data mining', a term that was coined by Gasteiger and his colleagues to entail the extraction of knowledge from pre-existing large data repositories for the purpose of generating new information (Hand 2007). In this case, large compound databases are mined using *in silico* techniques from which ideal candidates are selected for further evaluation (Gasteiger et al. 2003). The computational approach is meant to significantly reduce the high costs of drug discovery and development in that experimental efforts are only directed towards promising candidates. An important facet to natural product computational studies is the exploitation of pharmacophoric moieties. In this approach, natural product libraries are screened in search for compounds with specific pharmacophores. Compounds with the desired pharmacophores are then further evaluated based on physicochemical properties that may influence toxicity and pharmacokinetics (absorption distribution, metabolism and excretion or ADME). This approach has proven more effective than random screening by 1700-fold (Doman et al. 2002). In structure-based pharmacophore models a crystalline structure of a target protein with ligand bound to its active site is studied in order to identify pharmacophores that would interact with the target in a similar fashion (Berman et al. 2000). A good example is LigandScout, a software that is used to identify important interaction points between ligands and target proteins (Wolber and Langer 2005).

However, computational natural product drug discovery faces the challenge of limited free access to natural product databases. This has restricted the number of virtual studies conducted on natural product based chemical entities. Computational screening usually requires the input of a large number of synthetic compounds from which about 10 – 30% become successful candidates. Unfortunately, this is difficult to implement with natural products since large numbers of compounds are not easily accessible and only a small quantity of exorbitantly priced secondary metabolites are commercially available. The seamless integration of computational approaches to natural product drug discovery can be achieved through various strategies. One of these strategies begins with the development of a virtual hit using 3D databases of natural compounds followed by the preselection of natural product sources known

to contain the desired metabolites through ethnopharmacology, literature review and resource availability. *In vitro* preliminary screening and direct or bioactivity guided isolation of the desired metabolites is then carried out on the selected natural product sources to obtain the bioactive natural products (Figure 6.2) (Rollinger et al. 2008).

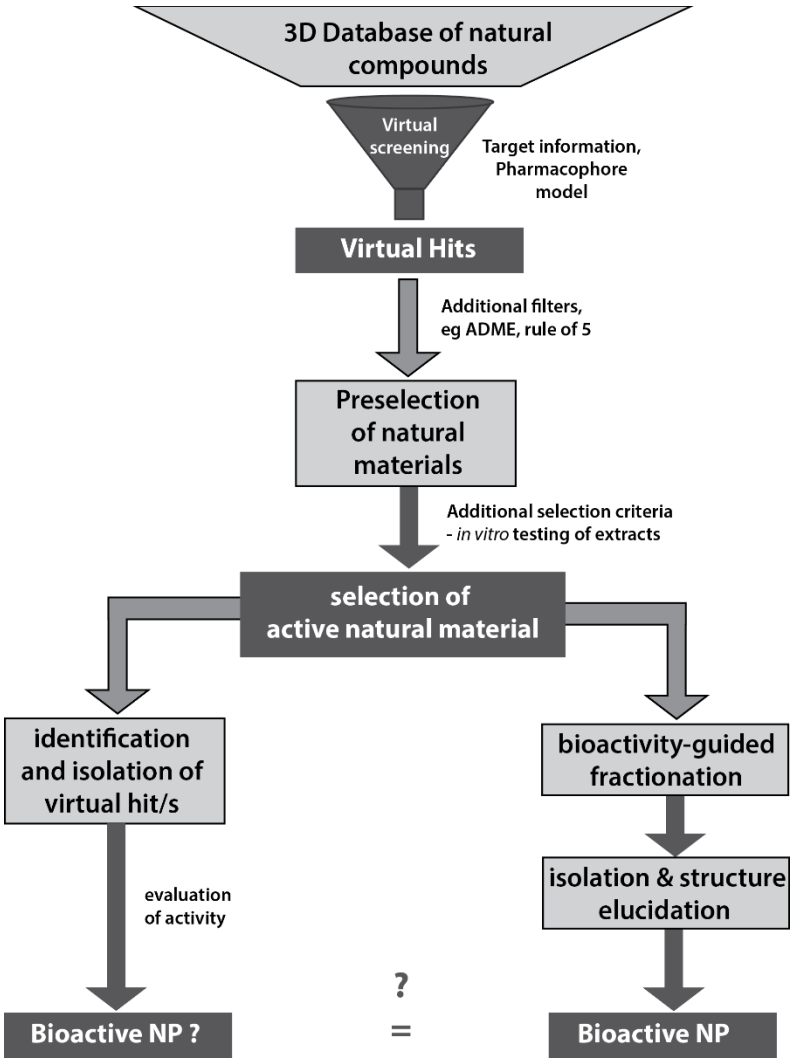

Figure 6.2 Integration of virtual natural product screening and *in vitro* validation methods (Adapted from: Rollinger et al. 2008)

Another approach involves the identification of potential sources of bioactive natural products through ethnomedicinal practices and literature review which are then screened using *in vitro* assays. A virtual database is then created to encompass all the known compounds that have been isolated from the bioactive plant sources. The created natural product database is then virtually screened against a structure based pharmacophore model to identify potentially active pharmacophores followed by the isolation of the virtual hits from the plant sources and

evaluation of bioactivity to identify bioactive natural products. This has been referred to as the *in combo* approach due to its integration of *in silico* and *in vitro* methods (Figure 6.3) (Van De Waterbeemd 2005).

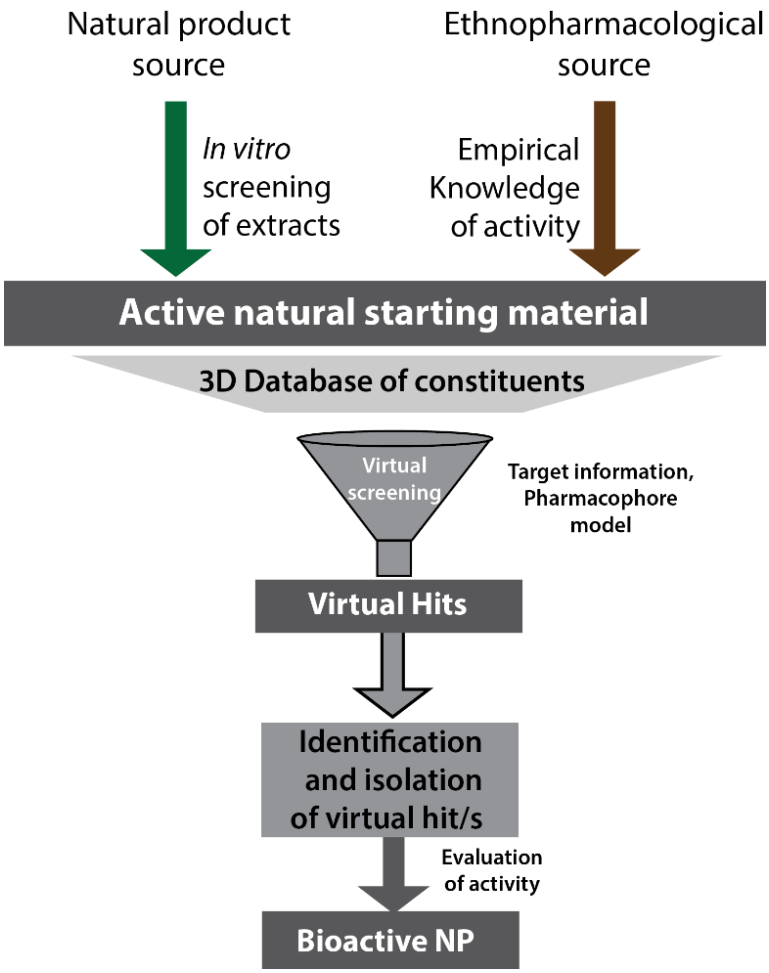

Figure 6.3 The *in combo* approach integrating *in silico* and *in vitro* methods (Adapted from: Rollinger et al. 2008)

One can also start with the virtual screening of a natural compound of unknown biological activity against several biological targets. In this *target fishing* approach, potential target-natural compound interactions are identified followed by the pharmacological evaluation of the interactions to realise bioactive natural products (Figure 6.4) (Nettles et al. 2006).

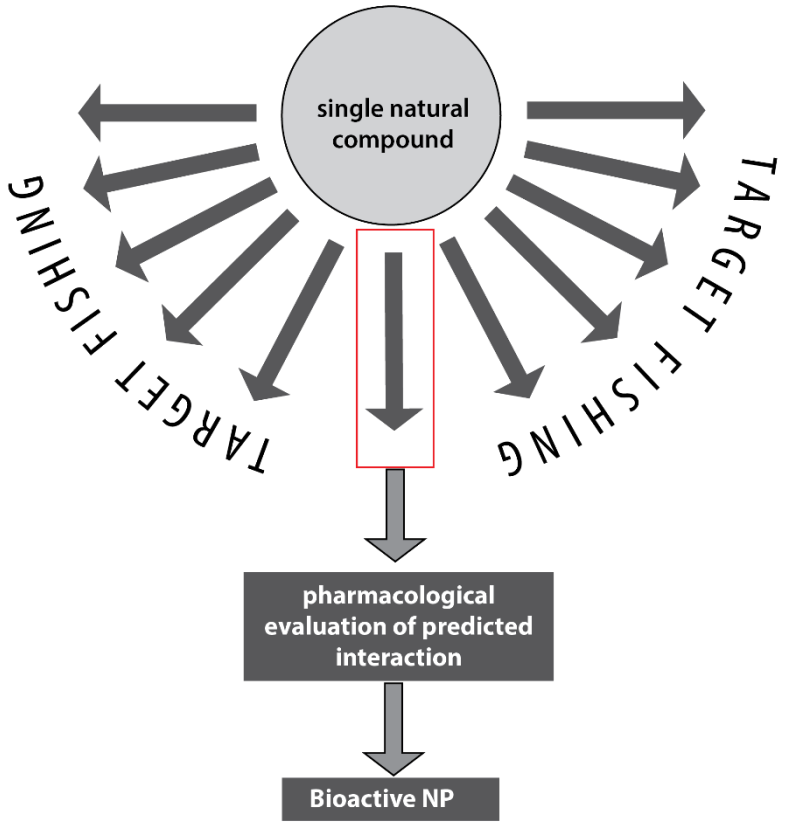

Figure 6.4 The *target fishing* approach to natural product drug discovery (Adapted from: Rollinger et al. 2008)

6.3 Chapter aims

The research in this chapter focuses on the implementation of *in silico* computational techniques to determine potential biological target proteins of 6″-O-α-apio-D-furanosylisovitexin (Altissimin, **3.17**). In addition, molecular docking is utilized to predict ligand-protein interactions. A brief overview and explanation of the aforementioned techniques is given in the introductory section with a detailed description of the *in silico* methodology provided in the experimental section.

6.4 Results and Discussion

6.4.1 SEA target prediction

The results generated by the SEA search server are shown in Table 6.1. Biological targets for altissimin (**3.17**) were ranked based on their respective p-values, Z-scores and max Tc values. Based on these results the most promising protein target for altissimin (**3.17**) was human aldose reductase (hAR). hAR is a NADPH-dependent oxidoreductase that catalyses the reduction of glucose to sorbitol (Brownlee 2001). This is a key reaction in the polyol pathway of glucose metabolism, a process implicated in the long-term complications of diabetes. Hyperglycemia induces overexpression of hAR, leading to an increase in sorbitol concentration, which ultimately causes osmotic imbalance, alterations in membrane permeability, oxidative stress, and finally tissue damage (Srivastava et al. 2005). Accordingly, the enzyme has been extensively studied as a molecular target for the treatment of diabetes complication (Wang et al. 2013).

Table 6.1 SEA search server results for altissimin (**3.17**) target prediction

Rank	Target ID	Name	Description	P-Value	Max Tc	Z-Score
1	ALDR_HUMAN	AKR1B1	Aldose reductase	2.85E-24	0.35	41.8217
2	XDH_HUMAN	XDH	Xanthine dehydrogenase/oxidase	6.76E-23	0.40	39.3527
3	ALDR_RAT	Akr1b1	Aldose reductase	5.44E-20	0.52	34.1355
4	BGLR_RAT	Gusb	Beta-glucuronidase	4.93E-19	0.38	32.4173
5	ULA1_HUMAN	NAE1	NEDD8-activating enzyme E1 regulatory subunit	6.06E-18	0.43	30.4612
6	AMY1_HUMAN	AMY1A; AMY1B; AMY1C	Alpha-amylase 1	6.66E-16	0.43	26.7389
7	CP1B1_HUMAN	CYP1B1	Cytochrome P450 1B1	9.99E-16	0.38	26.4627
8	O96394_LEIAM		Arginase	1.83E-14	0.33	24.212
9	Q965D6_PLAFA	fabG	3-oxoacyl-acyl-carrier protein reductase	6.64E-14	0.35	23.2079
10	PLGF_HUMAN	PGF	Placenta growth factor	2.09E-13	0.31	22.3146
11	IL2_HUMAN	IL2	Interleukin-2	9.91E-12	0.42	19.3056
12	LOX5_RAT	Alox5	Arachidonate 5-lipoxygenase	1.24E-10	0.39	17.3352
13	NMUR2_HUMAN	NMUR2	Neuromedin-U receptor 2	3.99E-10	0.36	16.4234
14	LX15B_RAT	Alox15b	Arachidonate 15-lipoxygenase B	4.03E-10	0.39	16.4172
15	CDK6_HUMAN	CDK6	Cyclin-dependent kinase 6	2.18E-08	0.38	13.306
16	CLK1_MOUSE	Clk1	Dual specificity protein kinase CLK1	2.43E-08	0.31	13.2215
17	CBR1_HUMAN	CBR1	Carbonyl reductase [NADPH] 1	9.34E-08	0.35	12.1702
18	MDR1_HUMAN	ABCB1	Multidrug resistance protein 1	2.08E-07	0.38	11.5457
19	DPO1_THEAQ	polA	DNA polymerase I, thermostable	6.64E-07	0.32	10.6413
20	MRP2_RAT	Abcc2	Canalicular multispecific organic anion transporter 1	7.87E-07	0.41	10.5086

6.4.2 Molecular docking

Molecular docking was performed against hAR for both altissimin (**3.17**) and known ligand 393 (control) (Figure 6.5). Altissimin (**3.17**) and 393 demonstrated high affinities for aldose reductase, with the lowest binding energy observed for altissimin (**3.17**) (Figure 6.6).

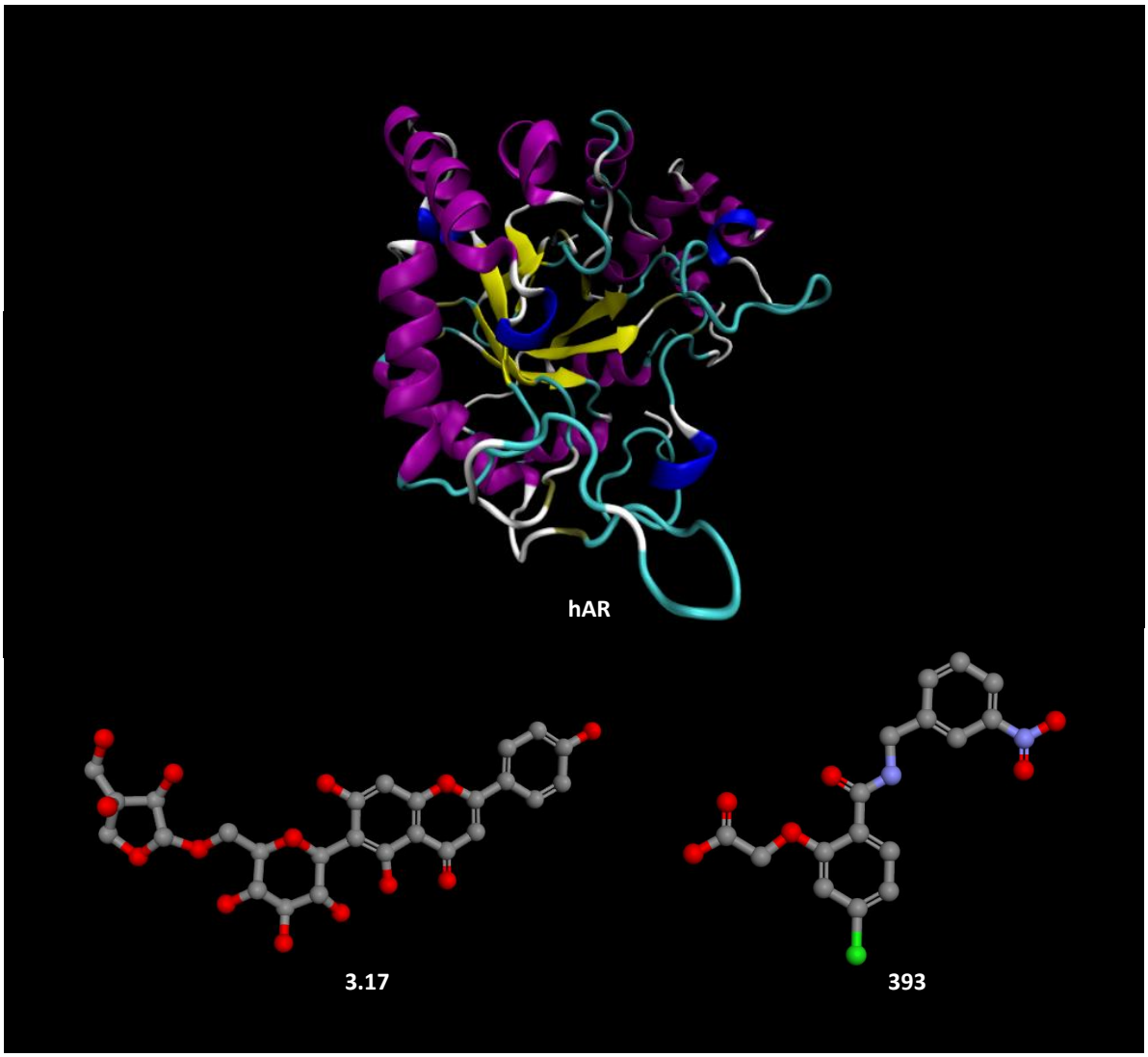

Figure 6.5 3D visualisation of the human aldose reductase (hAR) enzyme (using visual molecular dynamics, VMD), compound **3.17** and known ligand 393 (using BIOVIA's Discovery studio software)

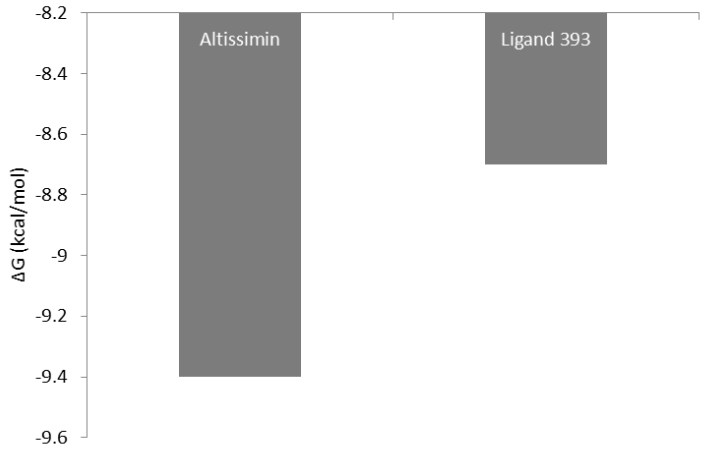

Figure 6.6 Graphical representation of the ΔG free energy binding values for altissimin (**3.17**) (-9.4 kcal/mol) and known ligand 393 (-8.7 kcal/mol) after molecular docking with AutoDock4

6.4.3 Protein-ligand interactions

hAR is a monomeric 36 kDa protein that consists of 315 amino acids and folds into a β/α-TIM-barrel. Eight α-helices and two additional smaller α -helices wrap around eight β-strands. The binding pocket of hAR is located near the C-terminal loop in the barrel core where also the cofactor NADPH is bound. The so-called anionic binding pocket is formed by Tyr 48, His 110, Trp 111, and the nicotinamide moiety of the cofactor. Furthermore, the latter three residues are involved in the catalytic function of hAR.

In the control docking procedure with known ligand 393, the protein-ligand interactions were analysed with LigPlot+ software (Figures 6.7 and 6.8). A total of four hydrogen bonds were observed between the ligand and protein, and involved amino acid residues Tyr48 (2.70 Å), His110 (2.70 Å), Trp111 (2.98 Å) and Leu300 (3.03 Å). Analysis of protein-ligand interactions for altissimin (**3.17**) also witnessed the formation of four hydrogen bonds and involved amino acid residues Lys22 (2.92 Å), Gln50 (3.18 Å), Val48 (2.73 Å) and Leu301 (2.98 Å). The remainder of ligand atoms predominantly forms hydrophobic interactions.

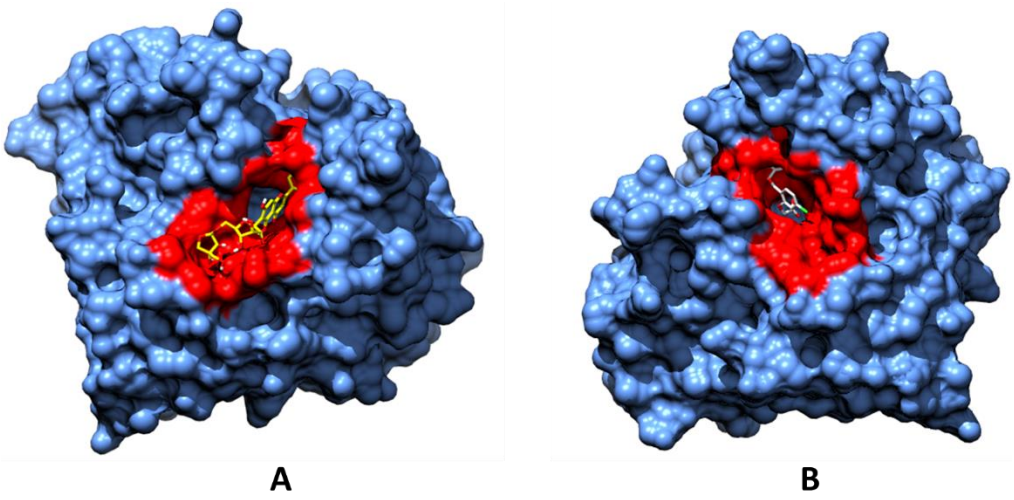

Figure 6.7 Schematic representation of target site bound by ligands; Chimera visualization showing altissimin (**3.17**) (A) and known ligand 393 (B) in the hAR binding pocket

The hAR binding pocket is indicated in red

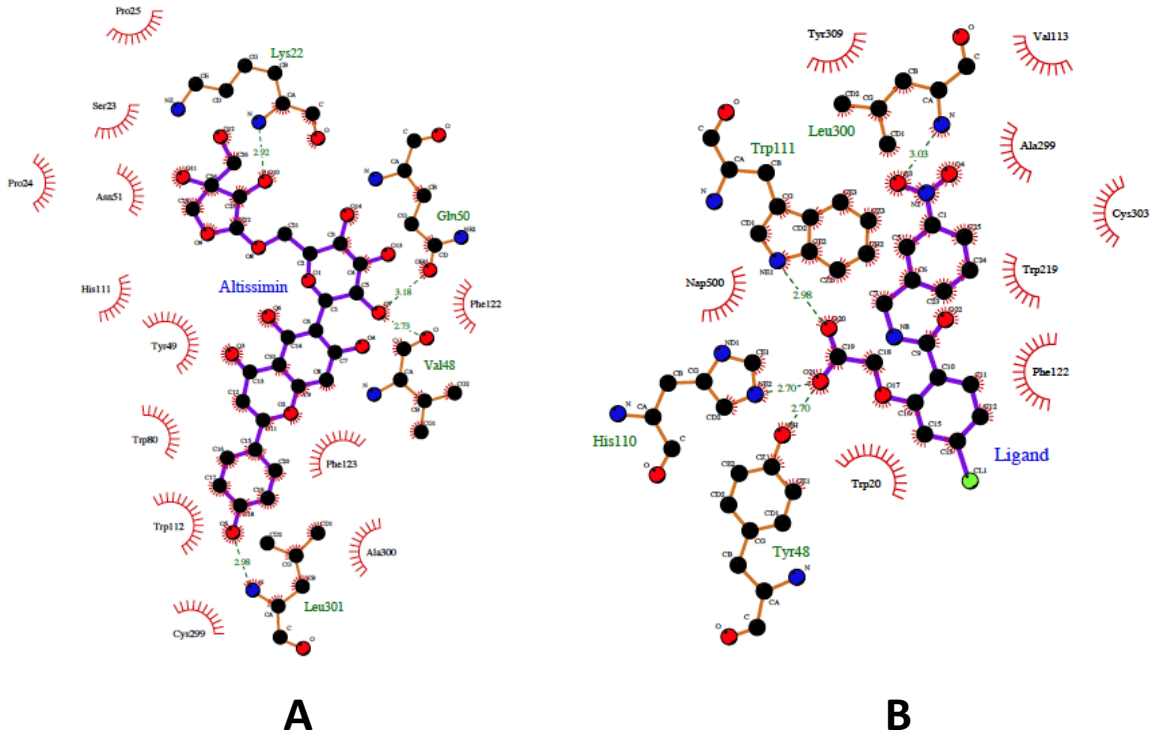

Figure 6.8 Schematic representation of target site bound by ligands; LigPlot+ 2D interaction map showing interacting residues and hydrogen bond for altissimin (**3.17**) (A) and known ligand 393 (B)

From the obtained results, altissimin (**3.17**) showed a high binding affinity (ΔG = -9.4 kcal/mol) for the human aldose reductase (hAR) enzyme. Thus, altissimin (**3.17**) can be considered as a potential aldose reductase inhibitor. However, these *in silico* results require confirmation through further biological testing including *in vitro* biological assays. Besides its involvement in diabetic complications, the human aldose reductase (hAR, AKR1B1) has been found to potentiate various inflammatory conditions such as atherosclerosis, sepsis, uveitis and colorectal cancer (Ramana and Srivastava 2010). Several human malignancies such as hepatic, colorectal, breast, ovarian and cervical cancers have shown overexpression of hAR, thereby giving rationale for the use of aldose reductase inhibitors as modulators of inflammatory cancers (Tammali et al. 2011). For instance, concomitant administration of the aldose reductase inhibitor ethyl 1- benzyl-3-hydroxy-2(5H)-oxopyrrole-4-carboxylate (EBPC) with doxorubicin and cisplatin in HeLa cells was found to enhance the activity of the two chemotherapeutics (Shapiro 2002). Furthermore, the inhibition of aldose reductase has been found to increase the sensitivity of HeLa cells to chemotherapeutic agents through the activation of extracellular signal-regulated kinases (ERK) (Kyoung Lee et al. 2002). These findings warrant the further exploration of aldose reductase inhibitors as potential adjuncts to chemotherapeutic agents. Since increased chemotherapeutic sensitivity translates into reduced therapeutic dosages, hAR inhibitor-chemotherapy combinations may serve the cardinal purpose of reducing the overall cost of cisplatin-based cancer treatments in developing countries.

6.5 Experimental

6.5.1 General experimental

Preparation of compound structure for molecular docking was performed using BIOVIA's Discovery studio software obtained from http://www.3dsbiovia.com/resource-center/downloads/. The Similarity Ensemble Approach (SEA) was performed from the search servers on the website http://sea.bkslab.org/ provided by Shoichet Laboratory, Department of Pharmaceutical Chemistry, University of California, San Francisco (UCSF). Molecular docking of compound was done using AutoDock4 and the Autodock tools suite obtained from http://autodock.scripps.edu/.

6.5.2 Similarity Ensemble Approach (SEA)

The structure file of altissimin (**3.17**) was prepared using BIOVIA's Discovery studio software and exported in MOL format. The structure was converted to the SMILES format using Open BABEL software (O'Boyle et al. 2011), and submitted to the SEA Search Server in order to evaluate potential activities (Keiser et al. 2007). Target proteins were ranked according to their respective Z-scores, max Tc and p-values (Table 1). A threshold of 0.3 for max Tc was adopted and values lower than 0.3 were excluded. The highest overall ranking protein target was identified and selected for subsequent molecular docking studies.

6.5.3 Molecular docking

The 3D structure of aldose reductase was retrieved from the protein data bank (PDB code 3MC5). Molecular docking was performed for both altissimin (**3.17**) and known protein inhibitor 393. All molecular docking experiments were completed using AutoDock4 and the AutoDock tools suite (ADT) (Morris et al. 2009). Molecular docking with AutoDock4 can be broken down into six steps (Figure 6.9). The initial preparation steps 1 and 2 were performed using a custom made python script which incorporated the ADT scripts prepare_receptor4.py and prepare_ligand4.py to convert both the protein model and ligand to required PDBQT format. In preparation for Autogrid4 (step 3), a grid parameter file was defined using the ADT script prepare_gpf4.py. In preparation for the docking run with AutoDock4 (step 6), docking parameters were defined using the ADT script prepare_dpf42.py and user defined parameters passed in TXT file format. Grid box spacing parameter was set to 1 Å and the number of points X = 126, Y = 126, Z = 126. Specific docking parameters were used in docking run; population

= 50, evaluations = 10 million, number of generations = 10 million and the number of runs = 256.

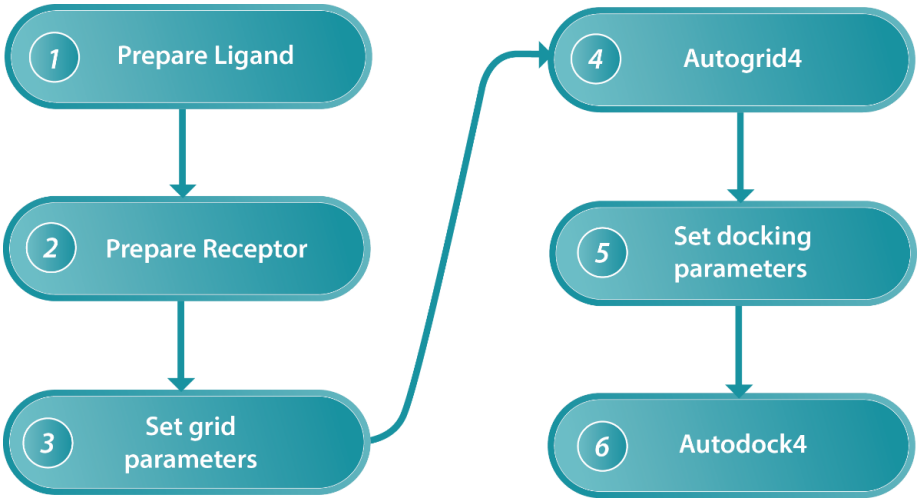

Figure 6.9 Overview of ligand and receptor protein preparation for AutoDock4.

6.5.4 Docking analysis and scoring

Protein docking with AutoDock4 generated a single docking log file (DLG) for screened ligand. The log file was analysed using the write_lowest_energy_ligand.py ADT script and the resulting ligand visually inspected in conjunction with receptor using Chimera molecular viewer software (Pettersen et al. 2004). Ligand-protein interactions were analysed using LigPlot+ software (Laskowski and Swindells 2011). In preparation for LigPlot+, the ligand was written to PDB file format using the ADT scripts write_lowest_energy_ligand.py and pdbqt_to_pdb.py. The ligand PDB was viewed with the respective receptor in Chimera and a PDB file containing the receptor and ligand in complex written.

References

Berman, H.M., Westbrook, J., Feng, Z., Gilliland, G., Bhat, T.N., Weissig, H., Shindyalov, I.N., & Bourne, P.E. 2000. The Protein Data Bank. *Nucleic acids research*, 28, (1) 235-242 available from: https://www.ncbi.nlm.nih.gov/pubmed/10592235

Brownlee, M. 2001. Biochemistry and molecular cell biology of diabetic complications. *Nature*, 414, 813 available from: https://doi.org/10.1038/414813a

Cameron, R.T., Coleman, R.G., Day, J.P., Yalla, K.C., Houslay, M.D., Adams, D.R., Shoichet, B.K., & Baillie, G.S. 2013. Chemical informatics uncovers a new role for moexipril as a novel inhibitor of cAMP phosphodiesterase-4 (PDE4). *Biochemical Pharmacology*, 85, (9) 1297-1305 available from: http://www.sciencedirect.com/science/article/pii/S0006295213001494

Cavasotto, C.N. & Phatak, S.S. 2009. Homology modeling in drug discovery: current trends and applications. *Drug Discovery Today*, 14, (13) 676-683 available from: http://www.sciencedirect.com/science/article/pii/S1359644609001469

Cleaves, H. J. 2011, "Molecular Recognition," *In Encyclopedia of Astrobiology*, M. Gargaud et al., eds., Berlin, Heidelberg: Springer Berlin Heidelberg, pp. 1079-1080.

Cortés-Ciriano, I., Ain, Q.U., Subramanian, V., Lenselink, E.B., Méndez-Lucio, O., IJzerman, A.P., Wohlfahrt, G., Prusis, P., Malliavin, T.E., van Westen, G.J.P., & Bender, A. 2015. Polypharmacology modelling using proteochemometrics (PCM): recent methodological developments, applications to target families, and future prospects. *MedChemComm*, 6, (1) 24-50 available from: http://dx.doi.org/10.1039/C4MD00216D

Doman, T.N., McGovern, S.L., Witherbee, B.J., Kasten, T.P., Kurumbail, R., Stallings, W.C., Connolly, D.T., & Shoichet, B.K. 2002. Molecular Docking and High-Throughput Screening for Novel Inhibitors of Protein Tyrosine Phosphatase-1B. *Journal of Medicinal Chemistry*, 45, (11) 2213-2221 available from: https://doi.org/10.1021/jm010548w

Fabian, L., Thomas, C., Karina, M., Marc, A.G., Adel, N., & Richard, A.H.a.J. 2011. Integrating Virtual Screening and Combinatorial Chemistry for Accelerated Drug Discovery.

Combinatorial Chemistry & High Throughput Screening, 14, (6) 475-487 available from: http://www.eurekaselect.com/node/74234/article

Friesner, R.A., Murphy, R.B., Repasky, M.P., Frye, L.L., Greenwood, J.R., Halgren, T.A., Sanschagrin, P.C., & Mainz, D.T. 2006. Extra Precision Glide: Docking and Scoring Incorporating a Model of Hydrophobic Enclosure for Protein-Ligand Complexes. *Journal of Medicinal Chemistry*, 49, (21) 6177-6196 available from: https://doi.org/10.1021/jm051256o

Gasteiger, J., Teckentrup, A., Terfloth, L., & Spycher, S. 2003. Neural networks as data mining tools in drug design. *Journal of Physical Organic Chemistry*, 16, (4) 232-245 available from: https://doi.org/10.1002/poc.597 Accessed 10 December 2018.

Geris, L. & Vermolen, F.J. 2014. *In silico* cell and tissue science. *In Silico Cell and Tissue Science*, 1, (1) 1 available from: https://doi.org/10.1186/2196-050X-1-1

Hand, D.J. 2007. Principles of Data Mining. *Drug Safety*, 30, (7) 621-622 available from: https://doi.org/10.2165/00002018-200730070-00010

Hospital, A., Goñi, J.R., Orozco, M., & Gelpí, J.L. 2015. Molecular dynamics simulations: advances and applications. *Advances and applications in bioinformatics and chemistry : AABC*, 8, 37-47 available from: https://www.ncbi.nlm.nih.gov/pubmed/26604800

Huang, S.Y. & Zou, X. 2010. Advances and challenges in protein-ligand docking. *International journal of molecular sciences*, 11, (8) 3016-3034 available from: https://www.ncbi.nlm.nih.gov/pubmed/21152288

Irwin, J.J., Sterling, T., Mysinger, M.M., Bolstad, E.S., & Coleman, R.G. 2012. ZINC: A Free Tool to Discover Chemistry for Biology. *Journal of Chemical Information and Modeling*, 52, (7) 1757-1768 available from: https://doi.org/10.1021/ci3001277

Jain, A.N. 2003. Surflex: Fully Automatic Flexible Molecular Docking Using a Molecular Similarity-Based Search Engine. *Journal of Medicinal Chemistry*, 46, (4) 499-511 available from: https://doi.org/10.1021/jm020406h

Jitender, V. & Vijay, M.K.a.E. 2010. 3D-QSAR in Drug Design - A Review. *Current Topics in Medicinal Chemistry*, 10, (1) 95-115 available from: http://www.eurekaselect.com/node/85600/article

Kapetanovic, I.M. 2008. Computer-aided drug discovery and development (CADDD): In silico-chemico-biological approach. *Chemico-Biological Interactions*, 171, (2) 165-176 available from: http://www.sciencedirect.com/science/article/pii/S0009279706003541

Katsila, T., Spyroulias, G.A., Patrinos, G.P., & Matsoukas, M.T. 2016. Computational approaches in target identification and drug discovery. *Computational and Structural Biotechnology Journal*, 14, 177-184 available from: http://www.sciencedirect.com/science/article/pii/S2001037016300058

Keiser, M.J., Roth, B.L., Armbruster, B.N., Ernsberger, P., Irwin, J.J., & Shoichet, B.K. 2007. Relating protein pharmacology by ligand chemistry. *Nature Biotechnology*, 25, 197 available from: https://doi.org/10.1038/nbt1284

Keiser, M.J., Setola, V., Irwin, J.J., Laggner, C., Abbas, A.I., Hufeisen, S.J., Jensen, N.H., Kuijer, M.B., Matos, R.C., Tran, T.B., Whaley, R., Glennon, R.A., Hert, J., Thomas, K.L.H., Edwards, D.D., Shoichet, B.K., & Roth, B.L. 2009. Predicting new molecular targets for known drugs. *Nature*, 462, 175 available from: https://doi.org/10.1038/nature08506

Krieger, E., Nabuurs, S.B., & Vriend, G. 2005. Homology Modeling. available from: https://doi.org/10.1002/0471721204.ch25 Accessed 10 December 2018.

Kubinyi, H. 1999. Chance Favors the Prepared Mind - From Serendipity to Rational Drug Design. *Journal of Receptors and Signal Transduction*, 19, (1-4) 15-39 available from: https://doi.org/10.3109/10799899909036635

Kyoung Lee, E., Regenold, W., & Shapiro, P. 2002. *Inhibition of aldose reductase enhances HeLa cell sensitivity to chemotherapeutic drugs and involves activation of extracellular signal-regulated kinases*, 13 ed.

Laskowski, R.A. & Swindells, M.B. 2011. LigPlot+: Multiple Ligand-Protein Interaction Diagrams for Drug Discovery. *Journal of Chemical Information and Modeling*, 51, (10) 2778-2786 available from: https://doi.org/10.1021/ci200227u

McFedries, A., Schwaid, A., & Saghatelian, A. 2013. Methods for the Elucidation of Protein-Small Molecule Interactions. *Chemistry & Biology*, 20, (5) 667-673 available from: http://www.sciencedirect.com/science/article/pii/S1074552113001646

Mestres, J., Martín-Couce, L., Gregori-Puigjané, E., Cases, M., & Boyer, S. 2006. Ligand-Based Approach to In Silico Pharmacology: Nuclear Receptor Profiling. *Journal of Chemical Information and Modeling*, 46, (6) 2725-2736 available from: https://doi.org/10.1021/ci600300k

Morris, G.M., Huey, R., Lindstrom, W., Sanner, M.F., Belew, R.K., Goodsell, D.S., & Olson, A.J. 2009. AutoDock4 and AutoDockTools4: Automated docking with selective receptor flexibility. *Journal of computational chemistry*, 30, (16) 2785-2791 available from: https://www.ncbi.nlm.nih.gov/pubmed/19399780

Moustakas, D.T., Lang, P.T., Pegg, S., Pettersen, E., Kuntz, I.D., Brooijmans, N., & Rizzo, R.C. 2006. Development and validation of a modular, extensible docking program: DOCK 5. *Journal of Computer-Aided Molecular Design*, 20, (10) 601-619 available from: https://doi.org/10.1007/s10822-006-9060-4

Nettles, J.H., Jenkins, J.L., Bender, A., Deng, Z., Davies, J.W., & Glick, M. 2006. Bridging Chemical and Biological Space:"Target Fishing" Using 2D and 3D Molecular Descriptors. *Journal of Medicinal Chemistry*, 49, (23) 6802-6810 available from: https://doi.org/10.1021/jm060902w

O'Boyle, N.M., Banck, M., James, C.A., Morley, C., Vandermeersch, T., & Hutchison, G.R. 2011. Open Babel: An open chemical toolbox. *Journal of Cheminformatics*, 3, (1) 33 available from: https://doi.org/10.1186/1758-2946-3-33

Parasuraman, S. 2012. Protein data bank. *Journal of pharmacology & pharmacotherapeutics*, 3, (4) 351-352 available from: https://www.ncbi.nlm.nih.gov/pubmed/23326114

Parimal, P.C., Soumyabrata, G., Adip, D., & Somshubhro, P.C. 2018. *A New Kind of Computational Biology* Singapore, Springer.

Pettersen, F., Goddard, D., Huang, C., Couch, G., Greenblatt, M., Meng, E., & Ferrin, E. 2004. *UCSF Chimera - A Visualization System for Exploratory Research and Analysis*, 25 ed.

Ramana, K.V. & Srivastava, S.K. 2010. Aldose reductase: a novel therapeutic target for inflammatory pathologies. *The international journal of biochemistry & cell biology*, 2009/09/22, (1) 17-20 available from: https://www.ncbi.nlm.nih.gov/pubmed/19778627

Reddy, A.S. & Zhang, S. 2013. Polypharmacology: drug discovery for the future. *Expert review of clinical pharmacology*, 6, (1) 41-47 available from: https://www.ncbi.nlm.nih.gov/pubmed/23272792

Rollinger, J. M., Stuppner, H., & Langer, T. 2008, "Virtual screening for the discovery of bioactive natural products," *In Natural Compounds as Drugs Volume I*, F. Petersen & R. Amstutz, eds., Basel: Birkh+ñuser Basel, pp. 211-249.

Schreiber, S.L., Kotz, J.D., Li, M., Aubéy, J., Austin, C.P., Reed, J.C., Rosen, H., White, E.L., Sklar, L.A., Lindsley, C.W., Alexander, B.R., Bittker, J.A., Clemons, P.A., de-Souza, A., Foley, M.A., Palmer, M., Shamji, A.F., Wawer, M.J., McManus, O., Wu, M., Zou, B., Yu, H., Golden, J.E., Schoenen, F.J., Simeonov, A., Jadhav, A., Jackson, M.R., Pinkerton, A.B., Chung, T.D., Griffin, P.R., Cravatt, B.F., Hodder, P.S., Roush, W.R., Roberts, E., Chung, D.H., Jonsson, C.B., Noah, J.W., Severson, W.E., Ananthan, S., Edwards, B., Oprea, T.L., Conn, P.J., Hopkins, C.R., Wood, M.R., Stauffer, S.R., Emmitte, K.A., Brady, L.S., Driscoll, J., Li, I.Y., Loomis, C.R., Margolis, R.N., Michelotti, E., Perry, M.E., Pillai, A., & Yao, Y. 2015. Advancing Biological Understanding and Therapeutics Discovery with Small-Molecule Probes. *Cell*, 161, (6) 1252-1265 available from: http://www.sciencedirect.com/science/article/pii/S0092867415005723

Schwede, T., Kopp, J., Guex, N., & Peitsch, M.C. 2003. SWISS-MODEL: an automated protein homology-modeling server. *Nucleic acids research*, 31, (13) 3381-3385 available from: http://dx.doi.org/10.1093/nar/gkg520

Shapiro, P. 2002. *Mechanistic Basis for Use of Aldose Reductase Inhibitors to Treat Breast Cancer*.

Sliwoski, G., Kothiwale, S., Meiler, J., & Lowe Jr, E. 2014. *Computational Methods in Drug Discovery*, 66 ed.

Srivastava, S.K., Ramana, K.V., & Bhatnagar, A. 2005. Role of Aldose Reductase and Oxidative Damage in Diabetes and the Consequent Potential for Therapeutic Options. *Endocrine Reviews*, 26, (3) 380-392 available from: http://dx.doi.org/10.1210/er.2004-0028

Tammali, R., Srivastava, S.K., & Ramana, K.V. 2011. Targeting aldose reductase for the treatment of cancer. *Current cancer drug targets*, 11, (5) 560-571 available from: https://www.ncbi.nlm.nih.gov/pubmed/21486217

Todd, A., Anderson, R., & Groundwater, P.W. 2009. Rational drug design - Identifying and characterising a target. *Pharmaceutical Journal*, 283, 19-20

Trott, O. & Olson, A.J. 2010. AutoDock Vina: improving the speed and accuracy of docking with a new scoring function, efficient optimization, and multithreading. *Journal of computational chemistry*, 31, (2) 455-461 available from: https://www.ncbi.nlm.nih.gov/pubmed/19499576

Van De Waterbeemd, H. 2005. Which in vitro Screens Guide the Prediction of Oral Absorption and Volume of Distribution? *Basic & Clinical Pharmacology & Toxicology*, 96, (3) 162-166 available from: https://doi.org/10.1111/j.1742-7843.2005.pto960304.x Accessed 10 December 2018.

Verdonk, L., Cole, J., Hartshorn, J., Murray, W., & Taylor, R. 2003. *Improved Protein-ligand docking using GOLD*, 52 ed.

Wang, L., Gu, Q., Zheng, X., Ye, J., Liu, Z., Li, J., Hu, X., Hagler, A., & Xu, J. 2013. Discovery of New Selective Human Aldose Reductase Inhibitors through Virtual Screening Multiple Binding Pocket Conformations. *Journal of Chemical Information and Modeling*, 53, (9) 2409-2422 available from: https://doi.org/10.1021/ci400322j

Wang, Z., Liang, L., Yin, Z., & Lin, J. 2016. Improving chemical similarity ensemble approach in target prediction. *Journal of Cheminformatics*, 8, (1) 20 available from: https://doi.org/10.1186/s13321-016-0130-x

Wolber, G. & Langer, T. 2005. LigandScout: 3-D Pharmacophores Derived from Protein-Bound Ligands and Their Use as Virtual Screening Filters. *Journal of Chemical Information and Modeling*, 45, (1) 160-169 available from: https://doi.org/10.1021/ci049885e

Wu, L., Ai, N., Liu, Y., Wang, Y., & Fan, X. 2013. Relating Anatomical Therapeutic Indications by the Ensemble Similarity of Drug Sets. *Journal of Chemical Information and Modeling*, 53, (8) 2154-2160 available from: https://doi.org/10.1021/ci400155x

Xuan-Yu, M., Hong-Xing, Z., & Mihaly Mezei and Meng Cui 2011. Molecular Docking: A Powerful Approach for Structure-Based Drug Discovery. *Current Computer-Aided Drug Design*, 7, (2) 146-157 available from: http://www.eurekaselect.com/node/74117/article

Chapter 7

Conclusion

This study has demonstrated the anticancer activity of *Drimia altissima* (L.F.) Ker Gawl. against the HeLa cervical cancer cell line and marked the plant genus as a potential source for novel bio-active compounds.

In accordance with the aim of identifying and exploring potential plant sources for novel cytotoxic natural compounds, this research evaluated African traditional claims for the common ethnopharmacological use of the plants *Adansonia digitata*, *Ceiba pentandra*, *Maytenus senegalensis* and *Drimia altissima* as cancer treatments. Preliminary cytotoxicity screening of the selected plants revealed that *Maytenus senegalensis* root extract, **MS-R**, and *Drimia altissima* bulb extract, **DA-B** (**79**), possess significant anti-proliferative activity against HeLa cervical cancer cells with IC_{50} values of 25 and 1.1 μg/mL respectively. Among others, the antimycobacterial, anti-inflammatory and antiplasmodial activity of *M. senegalensis* leaf extracts is well documented (Tahir et al. 1999; da Silva et al. 2011). However, very few studies have embarked on evaluating the anticancer potential of *M. senegalensis* root extracts. This study provides basis for the further phytochemical evaluation of *M. senegalensis* root extracts in order to isolate the metabolites that are responsible for its cytotoxic activity. Unfortunately, this could not be done in this study due to a limitation in biomass quantity. Evaluation of the *D. altissima* bulb extract yielded a cytotoxic *n*-butanol fraction, **79d**, (IC_{50} = 0.497 μg/mL) with greater anti-proliferative activity than the parent extract (**79**) and thus, disclosing the location of the cytotoxic metabolite(s). High Content Analysis (HCA) of **79d** revealed that the partition induces marked early mitotic cell cycle arrest in HeLa cells.

Within the *Asparagaceae* family, *n*-butanol extracts are known for possessing a high saponin content dominated by the presence of bio-active cardenolides, spirostanols and mono or bidesmosidic steroidal glycosides (Mulholland et al. 2013). Previous phytochemical studies on *D. altissima* only resulted in the isolation of several bufadienolides, a class of cardenolides known to be the chemotaxonomic markers of *Urgineeae*, the tribe from whence *D. altissima* emanates. Though bufadienolides are known to possess strong anticancer properties, their narrow therapeutic index and cardiotoxic side effects pose serious safety concerns. Bio-assay

guided fractionation of *n*-butanol fraction **79d** yielded cytotoxic fractions **82b** – **e**, with **82c** being the most effective fraction at the lowest tested concentration (0.1 μg/mL). Despite showing strong cytotoxic activity, fractions **82b**, **82d** and **82e** were not further purified due to lack of time. Future research in the isolation of compounds from these active fractions is highly recommended. Fractionation of **82c** led to the isolation of a novel *C*-glucosylflavonoid-*O*-glucoside, 6-C-[-apio-α-D-furanosyl-(1→6)-β-glucopyranosyl]-4′, 5, 7-trihydroxyflavone (Altissimin, **3.17**). Altissimin (**3.17**) contains a unique arrangement of the glucose and furanose moieties to the apigenin aglycone. This study proposes that the biosynthesis of altissimin (**3.17**) includes the addition of a furanose moiety to the C-6″ –OH by uridine diphosphate-apiose (UDP-apiose) through the enzymatic activity of apiofuranosyltransferase to form a (1→6) *O*-inter-glycosidic linkage between the furanose and the *C*-glucoside. This study reports altissimin (**3.17**) as the first flavonoid to be isolated from *D. altissima*. Unlike the bufadienolides, flavonoids and their *O*-glycosides are generally considered to be safe for human consumption.

Altissimin (**3.17**) exhibited a dose dependant anti-proliferative activity against HeLa cells with an IC_{50} of ± 2.44 μM. The anti-proliferative activity and mechanism of cell death elicited by altissimin (**3.17**) at IC_{50} concentration in HeLa cells was found to involve the induction of M phase cell cycle arrest with consequent activation of apoptotic cell death. Altissimin-induced apoptosis was evident from annexin V staining, increased nuclear size, mitochondrial membrane potential (ΔΨm) collapse and the activation of caspases -8 and -3. The activation of caspase -8 also suggested the induction of extrinsic apoptotic pathways. To a lesser extent, altissimin (**3.17**) induces autophagy in HeLa cells, which was evident from the slight increase in LysoTracker® Red staining. The induction of autophagy by apigenin-type flavonoids is well documented (Ruela-de-Sousa et al. 2010; Cao et al. 2013; Lee et al. 2014; Liu et al. 2014; Zhang et al. 2015), but less observed in flavonoid *C*-mono and diglycosides.

Among the concerns on flavonoid *O*-glycosides is lack of stability in biological systems due to their susceptibility to β-glucosidase enzyme hydrolysis *in vivo* (Yang et al. 2018). On the other hand, flavonoid *C*-glycosides are more stable than *O*-glycosides because of the presence of cleavage resistant C-C bonds. However, due to very few and often conflicting reports, the absorption of flavonoid *C*-glycosides after oral administration has not been fully confirmed. There are even fewer studies on the pharmacokinetic evaluation of flavonoid *C*-diglycosides containing furanose moieties such as altissimin (**3.17**). Future studies will find it beneficial to

investigate the *in vivo* pharmacokinetic properties of altissimin (**3.17**) and other furanose-containing *C*-*O*-diglycosides as a gap that needs urgent filling in the natural product drug development pipeline. The anticancer activity of altissimin (**3.17**) can be further improved through semi-synthetic derivatization including pentaallyl ether substituent additions, methoxylation and prenylation.

Using *in silico* (computational) methods, the human aldose reductase enzyme (hAR, AKR1B1) was identified as a potential biological target for altissimin (**3.17**). Overexpression of hAR is a known feature of inflammatory malignancies, including cervical cancer (Tammali et al. 2011). Compounds with hAR inhibitory activity increase the sensitivity of certain types of cancers to chemotherapeutic agents (Shapiro 2002). These results warrant the confirmation of altissimin (**3.17**) as a potential hAR inhibitor through further *in vitro* and *in vivo* studies. Other virtually determined potential biological targets for altissimin (**3.17**) such as NEDD8-Activating Enzyme E1 regulatory Subunit (NAE1), placenta growth factor (PGF), arachidonate 5-lipoxygenase (Alox5), arachidonate 15-lipoxygenase B (Alox15B), cyclin-dependent kinase 6 (CDK-6) and multidrug resistance protein 1 (ABCB1) are known to play roles in cancer cell proliferation, apoptosis, inflammation and drug resistance. These targets could potentially contribute to the anticancer activity of altissimin (**3.17**).

Thus, it can be concluded that altissimin (**3.17**), a secondary metabolite that is partly responsible for the cytotoxic activity of *D. altissima*, shows promise as a potential anticancer agent, at least, in the management of cervical cancer.

References

Cao, X., Liu, B., Cao, W., Zhang, W., Zhang, F., Zhao, H., Meng, R., Zhang, L., Ruifang, N., Hao, X., & Zhang, B. 2013. *Autophagy inhibition enhances apigenin-induced apoptosis in human breast cancer cells*, 25 ed.

da Silva, G., Taniça, M., Rocha, J., Serrano, R., Gomes, E.T., Sepodes, B., & Silva, O. 2011. *In vivo* anti-inflammatory effect and toxicological screening of *Maytenus heterophylla* and *Maytenus senegalensis* extracts. *Human & Experimental Toxicology*, 30, (7) 693-700 available from: http://het.sagepub.com/content/30/7/693.abstract

Lee, Y., Sung, B., Kang, Y.J., Kim, D.H., Jang, J.Y., Hwang, S.Y., Kim, M., Lim, H.S., Yoon, J.H., Chung, H.Y., & Kim, N.D. 2014. Apigenin-induced apoptosis is enhanced by inhibition of autophagy formation in HCT116 human colon cancer cells. *International Journal of Oncology*, 44, (5) 1599-1606 available from: https://app.dimensions.ai/details/publication/pub.1071513429 Accessed 8 August 2018.

Liu, J., Cao, X.C., Xiao, Q., & Quan, M.F. 2014. *Apigenin inhibits HeLa sphere-forming cells through inactivation of casein kinase 2a*, 11 ed.

Mulholland, D.A., Schwikkard, S.L., & Crouch, N.R. 2013. The Chemistry and Biological Activity of the *Hyacinthaceae*. *Natural Product Reports*, 30, (9) 1165-1210 available from: http://dx.doi.org/10.1039/C3NP70008A

Ruela-de-Sousa, R.R., Fuhler, G.M., Blom, N., Ferreira, C.V., Aoyama, H., & Peppelenbosch, M.P. 2010. Cytotoxicity of apigenin on leukemia cell lines: implications for prevention and therapy. *Cell Death &Amp; Disease*, 1, e19 available from: http://dx.doi.org/10.1038/cddis.2009.18

Shapiro, P. 2002. *Mechanistic Basis for Use of Aldose Reductase Inhibitors to Treat Breast Cancer*.

Tahir, A.E., Satti, G.M.H., & Khalid, S.A. 1999. Antiplasmodial Activity of Selected Sudanese Medicinal Plants with Emphasis on *Maytenus senegalensis* (Lam.) Exell. *Journal of ethnopharmacology*, 64, 227-233

Tammali, R., Srivastava, S.K., & Ramana, K.V. 2011. Targeting aldose reductase for the treatment of cancer. *Current cancer drug targets*, 11, (5) 560-571 available from: https://www.ncbi.nlm.nih.gov/pubmed/21486217

Yang, B., Liu, H., Yang, J., Gupta, V.K., & Jiang, Y. 2018. New insights on bioactivities and biosynthesis of flavonoid glycosides. *Trends in Food Science & Technology*, 79, 116-124 available from: http://www.sciencedirect.com/science/article/pii/S0924224418301559

Zhang, L., Cheng, X., Gao, Y., Zheng, J., Xu, Q., Sun, Y., Guan, H., Yu, H., & Sun, Z. 2015. *Apigenin induces autophagic cell death in human papillary thyroid carcinoma BCPAP cells*, 6 ed.

Appendix I

Nuclear magnetic resonance (NMR) spectra

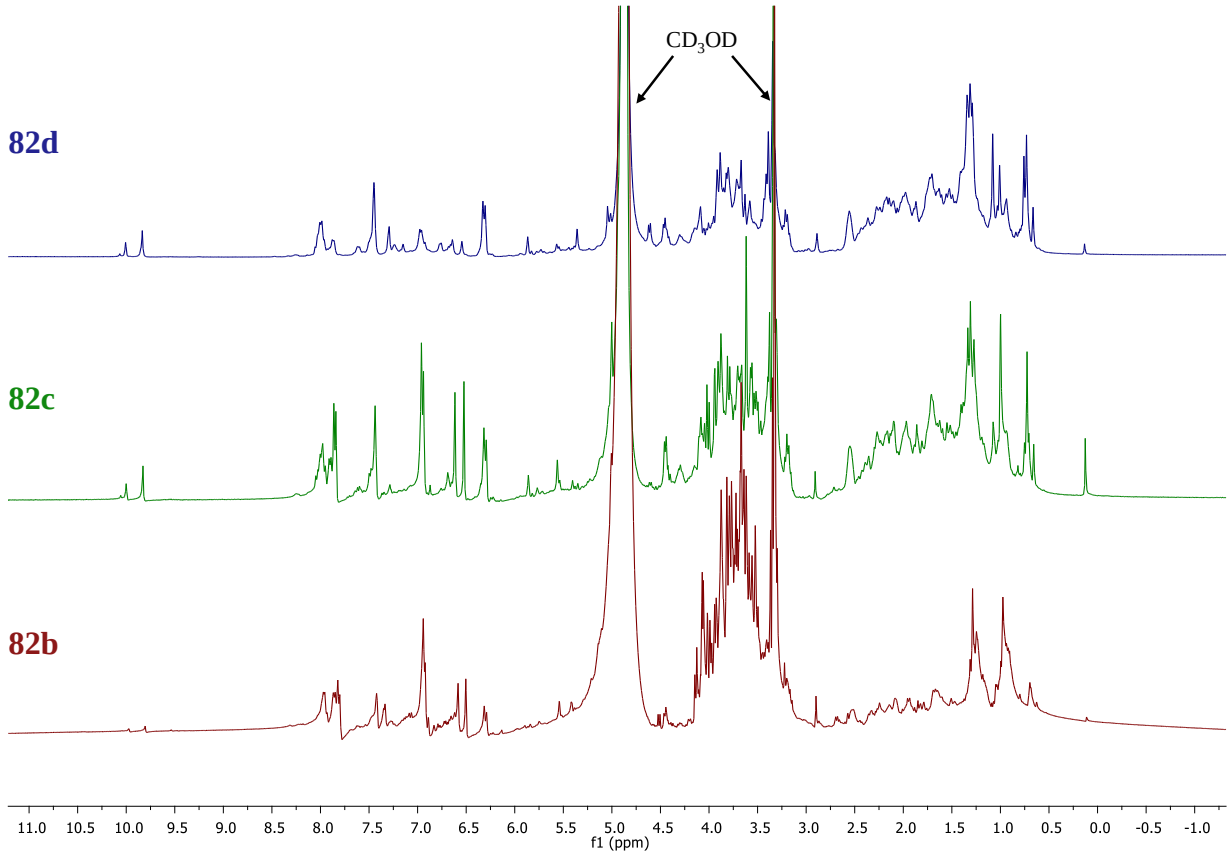

Figure A1.1 ^{1}H NMR spectra (CD_3OD, 400MHz) of fractions **82b**, **82c** and **82d**

Appendix II

LC/MS spectra

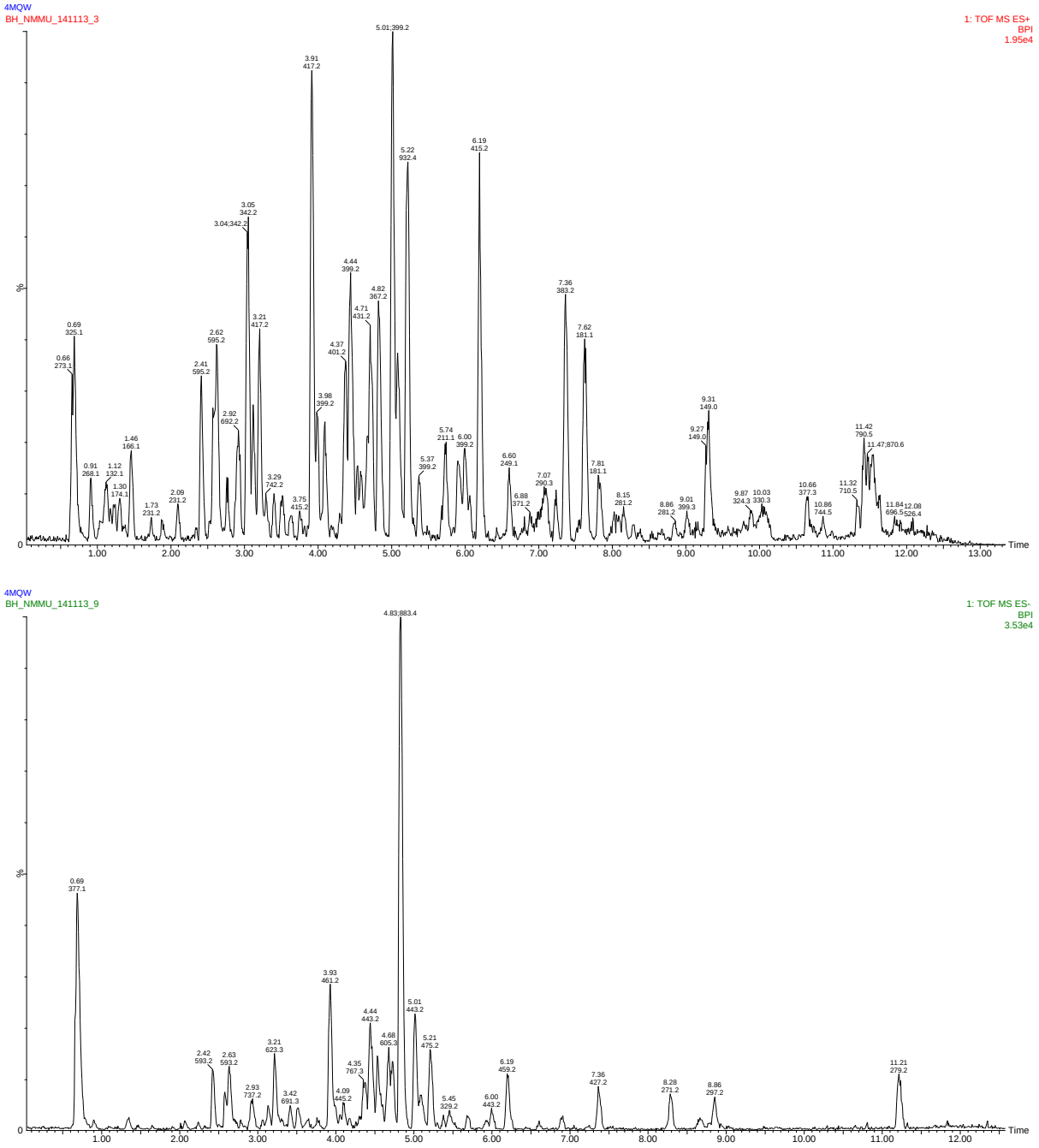

Figure A2.1 LC/ESI-MS spectra of *Drimia altissima* crude extract in positive (top) and negative (bottom) ionization modes

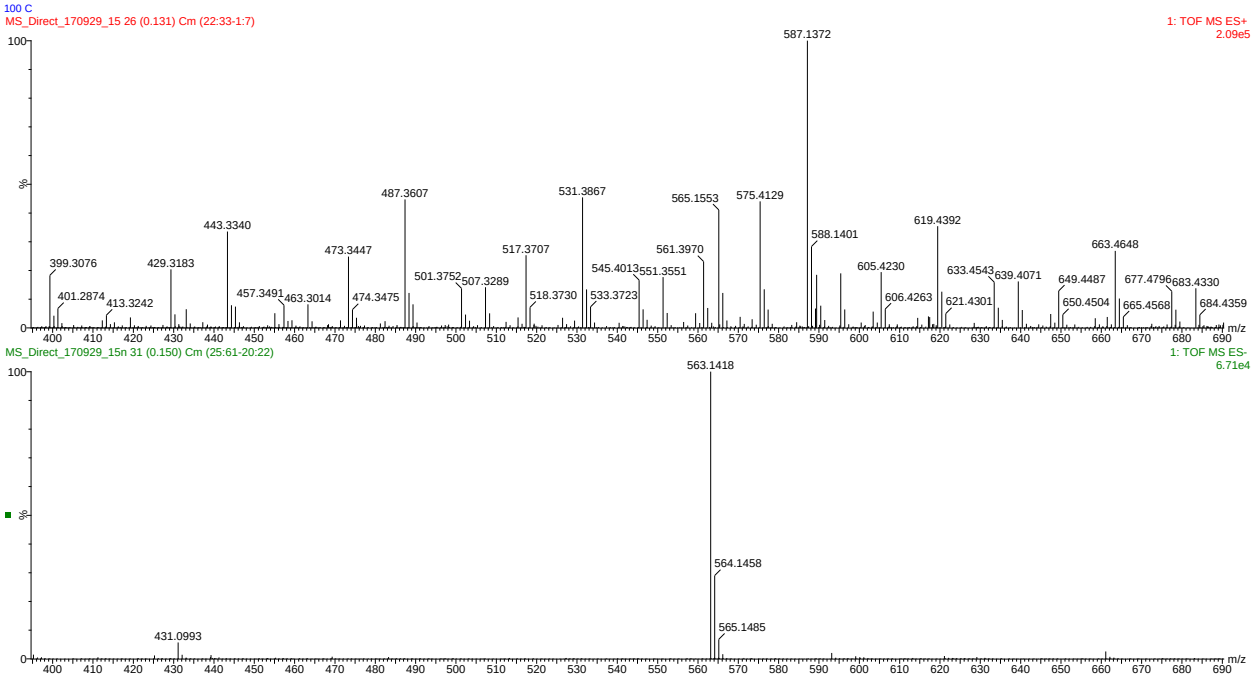

Figure A2.2 LC/ESI-MS spectra of compound **3.17** in positive (top) and negative (bottom) ionization modes

Conference outputs

43rd Federation of European Biochemical Societies (FEBS) Congress, 7 – 21 July 2018, Prague, Czech Republic

Nyambe M, Van de Venter M, Beukes DR, Swanepoel B, Smith N, Hlangothi B. (2018) Anti-cancer activity of a novel flavonoid *C*-apioglucoside from *Drimia altissima* (*Asparagaceae*). Abstract published in FEBS Open Bio Volume 8 Supplement 1: P10-129 page 336.

9th African Laser Centre Student Workshop, 24 – 26 Nov 2016, University of Stellenbosch, South Africa

Nyambe M, Van de Venter M, Swanepoel B. (2016) Evaluation of the Anticancer Potential of *Drimia altissima* using High Content Analysis and Flow Cytometry.

Indigenous Plant Use Forum (IPUF) Conference, 30 June – 3 July 2014, University of the Free State (UFS), Qwa Qwa Campus, Puthaditjaba, South Africa

Nyambe M, Beukes DR, Van de Venter M, Koekemoer T, Goosen L. (2014) Anticancer Potential of the South African Marine Alga *Sargassum heterophyllum*.

Articles prepared/submitted

Accepted:

Isolation and Characterisation of Altissimin: A Novel Cytotoxic Flavonoid *C*-apioglucoside from *Drimia altissima* (*Asparagaceae*)

Mutenta N. Nyambe[a], Denzil R. Beukes[c], Maryna Van De Venter[a] and Buyiswa G. Hlangothi[b]*

[a] Department of Biochemistry and Microbiology, PO Box 7700, Nelson Mandela University, Port Elizabeth 6031, South Africa
[b] Department of Chemistry, PO Box 7700, Nelson Mandela University, Port Elizabeth 6031, South Africa
[c] School of Pharmacy, Private Bag X17, University of the Western Cape, Bellville 7535, South Africa

In preparation:

Anticancer mechanism of compound

Future article:

In silico molecular docking of compound